



## Durham E-Theses

---

*Preparation of polymers by aqueous ring opening metathesis polymerisation and their application to industrial water treatment processes.*

Harrison, David Bryan

### How to cite:

---

Harrison, David Bryan (1990) *Preparation of polymers by aqueous ring opening metathesis polymerisation and their application to industrial water treatment processes.*, Durham theses, Durham University. Available at Durham E-Theses Online: <http://etheses.dur.ac.uk/6075/>

### Use policy

---

The full-text may be used and/or reproduced, and given to third parties in any format or medium, without prior permission or charge, for personal research or study, educational, or not-for-profit purposes provided that:

- a full bibliographic reference is made to the original source
- a [link](#) is made to the metadata record in Durham E-Theses
- the full-text is not changed in any way

The full-text must not be sold in any format or medium without the formal permission of the copyright holders.

Please consult the [full Durham E-Theses policy](#) for further details.

The copyright of this thesis rests with the author.  
No quotation from it should be published without  
his prior written consent and information derived  
from it should be acknowledged.

**PREPARATION OF POLYMERS BY AQUEOUS RING OPENING  
METATHESIS POLYMERISATION, AND THEIR APPLICATION TO  
INDUSTRIAL WATER TREATMENT PROCESSES.**

by

David Bryan Harrison, B.Sc. (Hons.)  
(Graduate society)

A thesis submitted  
for the Degree of Doctor of Philosophy  
to the University of Durham  
1990



21 NOV 1990

## ACKNOWLEDGEMENTS

First and foremost, I would like to thank Professor W.J. Feast for his help, and encouragement throughout my stay in Durham.

Much of the work reported in this thesis relied on obtaining high quality  $^{13}\text{C}$  and  $^1\text{H}$  NMR spectra, and in this respect thanks go to Dr. A.M. Kenwright and Mrs J.M. Say (Interdisciplinary Research Centre in Polymer Science and Technology, University of Durham). I would also like to thank members of the technical staff in Durham, whose help was greatly appreciated; in particular Dr. M. Jones and Mr V.J. McNeilly for the Mass spectra.

Thanks go to my colleagues, in particular, Dr. E. Khosravi-Babadi for many helpful discussions.

I acknowledge funding from the Science and Engineering Research Council, and Ciba-Giegy Industrial Chemicals.

Finally, thanks go to my parents for additional financial support.

## MEMORANDUM

The work reported in this thesis was carried out in the Chemistry Laboratories of the University of Durham, the University of Durham Industrial Research Laboratories, and in the Industrial Chemicals Research Laboratories of Ciba-Geigy Industrial Chemicals, between October 1987 and June 1990. This work has not been submitted for any other degree and is the original work of the author except where acknowledged by references.

Parts of this work have been submitted for publication:

- (i) W.J. Feast and D.B. Harrison, J. Mol. Cat., in Press;
- (ii) W.J. Feast and D.B. Harrison, submitted to Polymer.
- (iii) British Patent application 8919877, September 1989

Aspects of the work have also been presented, as a poster, by the author at the following meeting:

- (i) ISOM 8, University of Bayreuth, FRG, September 1989.

The copyright of this thesis rests with the author. No quotation from it should be published without his prior written consent and information derived from it should be acknowledged.

PREPARATION OF POLYMERS BY AQUEOUS RING OPENING  
METATHESIS POLYMERISATION, AND THEIR APPLICATION TO  
INDUSTRIAL WATER TREATMENT PROCESSES.

by

David Bryan Harrison

---

ABSTRACT

The work described in this thesis was concerned with the synthesis and aqueous Ring Opening Metathesis Polymerisation (ROMP) of some functionalised homo- and heteropolycyclic olefins. The objectives of the work were to explore the range of monomers and catalysts available for the aqueous ROMP reaction, and to assess the application of some of the polymers prepared for the prevention of aragonite precipitation from salt water.

This thesis is divided into seven chapters. In the first chapter the background of industrial water treatment and ROMP is reviewed. Chapter Two gives details of the synthesis and characterisation of some functionalised derivatives of 7-oxabicyclo[2.2.1]hept-2-ene, and bicyclo[2.2.1]hept-2-ene. Chapter Three gives details of the aqueous ROMP of the monomers prepared in chapter Two, and their characterisation. The fourth chapter is concerned with the preparation and characterisation of oligomers via aqueous ROMP. The fifth chapter discusses the observations recorded in chapters Three and Four, and the sixth chapter gives details of the industrial testing of some of the polymers/oligomers. Conclusions, and proposals for future work are made in the final chapter.

## CONTENTS

Acknowledgements	i
Memorandum	ii
Abstract	iii
Introduction	iv
<b>CHAPTER 1: INTRODUCTION</b>	<b>1</b>
<b>1.1 General Introduction</b>	<b>2</b>
<b>1.2 Industrial water treatment applications</b>	<b>3</b>
1.2.1 Petroleum recovery	3
1.2.2 Heat exchangers and boilers	3
<b>1.3 Formation of aragonite and its inhibition</b>	<b>4</b>
1.3.1 Formation of aragonite	4
1.3.2 Commercial products for aragonite scale control	5
1.3.3 Theoretical interaction of polycarboxylates with aragonite	6
<b>1.4 Olefin metathesis</b>	<b>8</b>
1.4.1 Basic theory	8
1.4.2 Development of mechanistic theory	11
1.4.3 Recent advances in mechanistic theory	13
1.4.4 Olefin metathesis in aqueous and ethanolic solution	20
1.4.5 Microstructure of polymers prepared by ROMP	22
<b>1.5 Objectives and methods of this study</b>	<b>26</b>

<b>CHAPTER 2: MONOMER SYNTHESIS AND CHARACTERISATION</b>	<b>29</b>
<b>2.1 Introduction</b>	<b>30</b>
2.1.1 General	30
2.1.2 The Diels-Alder reaction	30
<b>2.2 General Details</b>	<b>31</b>
2.2.1 Reactants	31
2.2.2 Monomer characterisation	32
2.2.3 Computer modelling	32
<b>2.3 Synthesis and characterisation of <i>exo</i>-7-oxabicyclo-</b> <b>[2.2.1]hept-5-ene-2,3-dicarboxy anhydride (I)</b>	<b>32</b>
2.3.1 Synthesis of monomer I	32
2.3.2 Characterisation of monomer I	33
<b>2.4 Synthesis and characterisation of <i>exo,exo</i>-5,6-bis-</b> <b>(hydroxymethyl)-7-oxabicyclo[2.2.1]hept-2-ene (II)</b>	<b>36</b>
2.4.1 Synthesis of monomer II	36
2.4.2 Characterisation of monomer II	37
<b>2.5 Synthesis and characterisation of <i>exo,exo</i>-5,6-bis-</b> <b>(methoxymethyl)-7-oxabicyclo[2.2.1]hept-2-ene (III)</b>	<b>40</b>
2.5.1 Synthesis of monomer III	40
2.5.2 Characterisation of monomer III	41
<b>2.6 Synthesis and characterisation of <i>exo,exo</i>-7-oxabicyclo-</b> <b>[2.2.1]hept-5-ene-2,3-bis(carboxylic acid) (IV)</b>	<b>45</b>
2.6.1 Synthesis of monomer IV	45
2.6.2 Characterisation of monomer IV	45
<b>2.7 Synthesis and characterisation of <i>exo,exo</i>-7-oxabicyclo-</b> <b>[2.2.1]hept-5-ene-2,3-bis(carboxymethyl ester) (V)</b>	<b>48</b>
2.7.1 Synthesis of monomer V	48
2.7.2 Characterisation of monomer V	49

<b>2.8 Synthesis and characterisation of <i>exo</i>-bicyclo-</b>	
<b>[2.2.1]hept-5-ene-2,3-dicarboxy anhydride (VI)</b>	52
2.8.1 Synthesis of monomer VI	52
2.8.2 Characterisation of monomer VI	53
<b>2.9 Synthesis and characterisation of <i>exo,exo</i>-bicyclo-</b>	
<b>[2.2.1]hept-5-ene-2,3-bis(carboxylic acid) (VII)</b>	56
2.9.1 Synthesis of monomer VII	56
2.9.2 Characterisation of monomer VII	57
<b>CHAPTER 3: SYNTHESIS AND CHARACTERISATION OF POLYMERS</b>	60
<b>3.1 Introduction</b>	61
<b>3.2 General Details</b>	61
3.2.1 Reactants	61
3.2.2 Polymer characterisation	61
3.2.3 Computer modelling	62
<b>3.3 Synthesis and characterisation of poly(2,5-</b>	
<b>(3,4-bis(methoxymethyl)furanylene)vinylene) (PIII)</b>	63
3.3.1 Polymer synthesis	63
3.3.2 Catalyst choice	67
3.3.3 Polymer microstructure	68
3.3.4 Computer modelling	84
3.3.5 Conclusions on the microstructure of PIII	89
<b>3.4 Synthesis and characterisation of poly(2,5-</b>	
<b>(3,4-bis(carboxymethyl)furanylene)vinylene) (PV)</b>	89
3.4.1 Polymer synthesis	89
3.4.2 Polymer microstructure	90
3.4.3 Conclusions on the microstructure of PV	96



<b>3.5 Synthesis and characterisation of poly(2,5-</b>	
<b>(3,4-bis(carboxylic acid)furanylene)vinylene) (PIV)</b>	97
3.5.1 Polymer synthesis	97
3.5.2 Catalyst choice	99
3.5.3 Polymer microstructure	100
<b>3.6 Attempted synthesis of poly(2,5-</b>	
<b>(3,4-bis(carboxylic acid)pentylene)vinylene) (PVII)</b>	105
3.6.1 Attempted polymer synthesis	105
3.6.2 Discussion	107
<b>3.7 Synthesis and characterisation of poly(2,5-</b>	
<b>(3,4-bis(hydroxymethyl)furanylene)vinylene) (PII)</b>	109
3.7.1 Polymer synthesis	109
<b>CHAPTER 4: SYNTHESIS AND CHARACTERISATION OF OLIGOMERS</b>	<b>112</b>
<b>4.1 Introduction</b>	<b>113</b>
<b>4.2 General Details</b>	<b>113</b>
4.2.1 Reactants	113
4.2.2 Polymer characterisation	114
<b>4.3 Oligomerisation of monomer III by aqueous ROMP</b>	
<b>using <i>cis</i>-but-2-ene-1,4-diol (VIII) as CTA</b>	<b>115</b>
4.3.1 General considerations	115
4.3.2 ROMP of monomer III in the presence of low concentrations of CTA (VIII)	116
4.3.3 ROMP of monomer III in the presence of high concentrations of CTA (VIII)	118
4.3.4 Oligomer microstructure	119

<b>4.4 Oligomerisation of monomer III by aqueous ROMP</b>	
<b>using <i>cis</i>-1,4-dimethoxybut-2-ene (IX) as CTA</b>	125
4.4.1 Oligomer synthesis	125
4.4.2 Oligomer microstructure	127
<b>4.5 Oligomerisation of monomer IV by aqueous ROMP</b>	
<b>using <i>cis</i>-but-2-ene-1,4-diol (VIII) as CTA</b>	133
4.5.1 Oligomer synthesis	133
4.5.2 Oligomer characterisation	136
<b>4.6 Oligomerisation of monomer IV by aqueous ROMP</b>	
<b>using acrylic acid (X) as CTA</b>	146
4.6.1 Oligomer synthesis	146
4.6.2 Oligomer microstructure	148
<b>4.7 Attempted oligomerisation of monomer IV by</b>	
<b>aqueous ROMP using maleic acid (XI) as CTA</b>	149
4.7.1 Polymer synthesis	149
4.7.2 Polymer microstructure	151
<b>4.8 Attempted ROMP of monomer VII in the presence</b>	
<b>of maleic acid (XI)</b>	152
<b>CHAPTER 5: DISCUSSION</b>	154
<b>5.1 Introduction</b>	155
<b>5.2 Synthesis of high molecular weight polymers</b>	155
5.2.1 Catalyst choice for aqueous ROMP reactions	155
5.2.2 Monomer choice for aqueous ROMP reactions	157
5.2.3 Conclusions	159
<b>5.3 The effect of acyclic olefins on aqueous ROMP</b>	160
5.3.1 Introduction	160

5.3.2	The effect of <b>VIII</b> on the induction period of ROMP reactions	160
5.3.3	The effect of <b>IX</b> on the induction period of ROMP reactions	163
5.3.4	The effect of <b>X</b> on the induction period of ROMP reactions	165
5.3.5	The effect of <b>XI</b> on the induction period of ROMP reactions	168
<b>5.4</b>	<b>Conclusions</b>	<b>169</b>
 <b>CHAPTER 6: APPLICATIONS TESTING OF THE OLIGOMERS PIVb</b>		<b>170</b>
<b>6.1</b>	<b>Introduction</b>	<b>171</b>
<b>6.2</b>	<b>Experimental details</b>	<b>171</b>
6.2.1	Synthesis and characterisation of oligomers	171
6.2.2	Applications test	172
6.2.3	Computer modelling	173
<b>6.3</b>	<b>Results</b>	<b>175</b>
6.3.1	Inhibition of aragonite formation	175
6.3.2	Computer modelling	177
<b>6.4</b>	<b>Discussion</b>	<b>183</b>
<b>6.5</b>	<b>Conclusion</b>	<b>183</b>
 <b>CHAPTER 7: CONCLUSIONS AND PROPOSALS FOR FUTURE WORK</b>		<b>184</b>
<b>7.1</b>	<b>Introduction</b>	<b>185</b>
<b>7.2</b>	<b>Conclusions</b>	<b>185</b>
<b>7.3</b>	<b>Proposals for future work</b>	<b>186</b>

<b>REFERENCES</b>	187
<b>APPENDIX A: <sup>13</sup>C NMR SPECTRA</b>	194
<b>APPENDIX B: INFRARED SPECTRA</b>	202
<b>APPENDIX C: MASS SPECTRA</b>	208
<b>APPENDIX D: ELEMENTAL ANALYSIS</b>	211
<b>APPENDIX E: CONFERENCES/LECTURES ATTENDED</b>	214

CHAPTER 1:  
INTRODUCTION.

## **1.1: General Introduction.**

Heavy industry consumes large quantities of water for manufacturing and processing, the majority of which comes directly from subterranean and surface water reservoirs, or the sea. Such water contains high concentrations of dissolved metal ions and biological material, which can inhibit the smooth operation of the plants. One major industrial problem is the formation of inorganic scales, principally calcium carbonate and barium sulphate, in reservoirs, pipes and equipment.<sup>1</sup> Scale can be removed by flushing with mineral acids, although this procedure is costly both in materials and in the loss of operating time. Pretreatment to remove calcium and barium ions is also prohibitively expensive and, consequently, in-line desalination procedures must be employed.

Desalination products must be carefully matched to the conditions found in each industrial process, and to the salt concentrations of the water feedstocks. Water soluble polymers have been used for many years to prevent or reduce inorganic scaling of metal pipes.<sup>2</sup> The principle function of the polymers is to maintain the water-borne salts in suspension by modification of their crystal growth, and prevent them from adhering to the walls of the equipment. The range of polymers employed for such applications depends primarily on the type of scale formed and its crystal structure; the most efficient materials for the prevention of calcium carbonate scale, polycarboxylic acids, are comparatively ineffective for the prevention of barium sulphate scale.<sup>1</sup>

Preparation of effective polymers for desalination requires a thorough understanding of the desalination mechanism. This in turn requires a knowledge of the type and crystal structure of the scale formed, which can only be established by study of the operating conditions.

---

## **1.2: Industrial water treatment applications.**

### ***1.2.1 Petroleum Recovery:***

Crude oil is a complex mixture of gaseous and liquid hydrocarbons formed by the decomposition of biological material. Oil reservoirs are underground formations of porous sandstone or limestone sandwiched between impermeable rock strata.<sup>3</sup> When the upper stratum is penetrated by a well, the pressure of gas within the reservoir forces the oil to the surface (primary recovery). Thereafter, the well pressure can be raised by injection of water (secondary recovery), or by chemical methods (tertiary recovery).

Large amounts of water are brought to the surface along with the oil during the primary recovery stage.<sup>4</sup> Injection of this water back into the oil reservoir (water-flooding) serves three purposes: (1) it allows recovery of additional oil (secondary recovery); (2) it utilises a potential pollutant; and (3) in some areas it controls land subsidence. Usually the volume of water is insufficient for secondary recovery purposes and must therefore be supplemented by water from other sources, eg. the sea. Blending of the two water sources produces a chemically unstable mixture, from which calcium carbonate and barium sulphate can precipitate; the flood-water must be treated to prevent salt precipitation.<sup>4</sup>

### ***1.2.2 Heat exchangers and boilers:***

Desalination plants, for the preparation of drinking water from sea water are common; sea water is boiled and condensed on the cool water inlet pipes, which act as heat exchangers, preheating the inlet water before it reaches the boiler, and condensing the steam generated by the boiler. Calcium carbonate precipitates both on the heating elements of the boilers and inside the pipes of the heat exchangers; the sea water must be treated to prevent such scale formation.<sup>2</sup>

### 1.3: Formation of aragonite and its inhibition.

#### 1.3.1 *Formation of aragonite:*

Calcium is the most abundant of the alkaline earth metals in the earth's crust (3.55% by weight).<sup>5</sup> As a result of the weathering of calcium bearing rocks, calcium is dissolved as its bicarbonate. Slight changes in the pH<sup>6</sup> or temperature<sup>7</sup> of waters containing calcium bicarbonate will cause precipitation of calcium carbonate (Figure 1.1), which is one of the most common deposits found in plugged oilfield pipes, equipment, and reservoirs.<sup>1</sup>

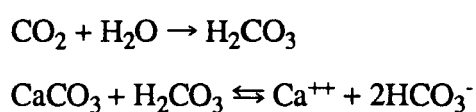
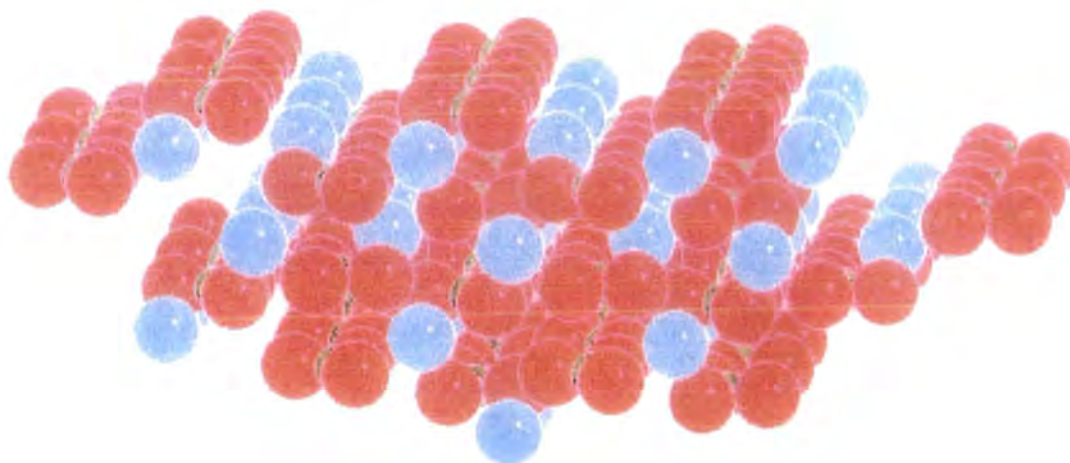


Figure 1.1: Dissolution and precipitation of calcium carbonate.

Calcium carbonate can exist in three pure crystalline forms; calcite, aragonite and vaterite.<sup>8</sup> Vaterite is comparatively rare, but has been found in natural scale deposits;<sup>9</sup> industrial scales consist principally of calcite and aragonite.<sup>10</sup>

The precipitation of pure calcite, pure aragonite or mixtures of the two is strongly temperature dependant; pure calcite is precipitated at 40°C, and pure aragonite (Figure 1.2) above 50°C.<sup>11</sup> The presence of certain metal impurities also favours the preferential formation of aragonite, eg. strontium,<sup>12</sup> barium, zinc, manganese, cobalt and iron.<sup>13</sup> Most of these elements are present in subsurface water or sea water, and operating temperatures in desalination plants are typically above 70°C. Not surprisingly, analysis of scale deposits from desalination plants has indicated that aragonite is the initially formed scale deposit.<sup>14</sup>





Key : Blue = calcium; Red = oxygen ; Green = carbon.

Figure 1.2: Crystal structure of aragonite.<sup>15</sup>

### 1.3.2 Commercial products for aragonite scale control:

Polycarboxylic acids based on homo- and copolymers of acrylic acid and maleic acid are currently used to inhibit the formation of aragonite scale formed in cooling and boiler water during service (Figure 1.3).<sup>2</sup> These are prepared by free radical polymerisations and copolymerisations of maleic anhydride, acrylic acid, vinyl acetate and vinyl chloride.<sup>16</sup> Aragonite antiscalent polymers are typically polyacrylates, produced by free radical polymerisation of acrylic acid or its sodium salt in the presence of chain transfer agents.<sup>16</sup>

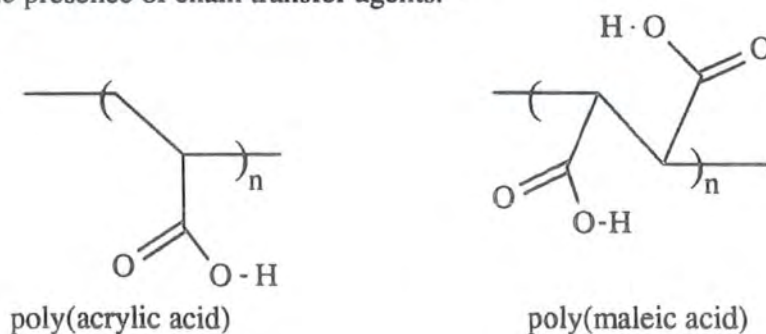


Figure 1.3: Polyacids used for aragonite antiscalents.

Polymers and oligomers of low molecular weight ( $M_n$  1000-5000) appear to be effective for the prevention of aragonite and calcite scale.<sup>2</sup> Polymers of higher molecular weight ( $M_n > 5000$ ) can be used to suspend clays, shales, iron oxides and sulphides in solution.<sup>17</sup>

### 1.3.3 *Theoretical interaction of polycarboxylates with aragonite:*

There are four ways in which polycarboxylates may interact with calcium ions to prevent the formation of scale deposits: (a) complexation; (b) prevention of homogeneous nucleation; (c) crystal surface modification; and (d) prevention of heterogeneous nucleation.

#### a) Complexation:

If the carboxylic acid groups on the polymer strongly complex calcium ions then they are effectively prevented from forming aragonite on the basis of reduced concentration.<sup>18</sup> The problems associated with this method are twofold. Firstly, very high concentrations of polycarboxylates must be used to complex most of the calcium ions, and secondly, the calcium-polymer complexes may be insoluble. Polymers used for complexation are usually of high molecular weight, and are employed in pretreating the water inlet supply.<sup>2</sup>

#### b) Prevention of homogeneous nucleation:

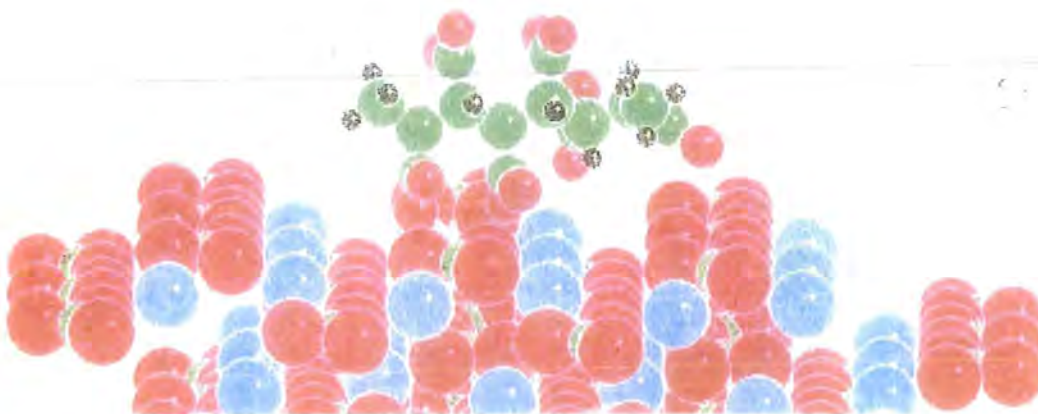
Mass transport of calcium and carbonate ions in solution can result in localised regions of high concentration (supersaturation). Electrostatic attraction draws the ions closer together forming a loose cluster, termed a "*critical nucleus*", which has a greater potential energy than a bulk phase of the same mass. To relieve this thermodynamically unstable position, the critical nucleus can either undergo a phase transformation to become a solid crystal nucleus, or disperse.<sup>19</sup> If

a polycarboxylate enters the supersaturated region, then electrostatic attractions are formed between polymer and calcium ions, and consequently the attractions between calcium ions and carbonate ions are reduced. As a result of this new interaction, the radius of the critical nucleus necessary for phase transformation is increased, and may be both energetically and physically too large to be formed, hence homogeneous nucleation is prevented.<sup>20</sup>

Low molecular weight ( $M_n$  1000-5000) polycarboxylates<sup>17</sup> are used for the prevention of homogeneous nucleation and can be used in low concentrations with respect to the calcium ions present. However such polymers do not necessarily prevent heterogeneous nucleation on the metal surfaces of pipes and other equipment.

c) Crystal surface modification:

This mechanism assumes that nucleation has already occurred. Interaction of the polymer with one of the faces of a growing aragonite crystal can halt the growth on that face (Figure 1.4).



Key : Blue = calcium; Red = oxygen; Green = carbon; Grey = hydrogen.

Figure 1.4: Interaction of polycarboxylate with an aragonite surface.

In solution, crystal growth is an equilibrium between solid and dissolved ions, and a change in the equilibrium may cause the dissolution of the crystal.<sup>19</sup> Thus a crystal nucleus formed in solution may be prevented from growing, redissolved, or grow in a modified form by halting growth at one of its faces.<sup>21</sup> Low molecular weight polyacrylates<sup>2</sup> are used for crystal surface modification; usually polymers suitable for surface modification are also suitable for the prevention of homogeneous nucleation.

d) Prevention of heterogeneous nucleation:

This process requires coating of the heterogeneous surface (eg. steel pipe) with an antiscalent product such as a simple carboxylic or phosphoric acid containing molecule. Polycarboxylates have found little application in this case.

#### 1.4: Olefin metathesis.

##### 1.4.1 *Basic theory:*

For a thorough discussion of the general principles of metathesis the reader is directed to a number of general text books on the subject.<sup>22, 23, 24</sup>

Ring Opening Metathesis Polymerisation (ROMP) was first observed by Anderson and Merckling in the polymerisation of norbornene (Figure 1.5).<sup>25</sup>

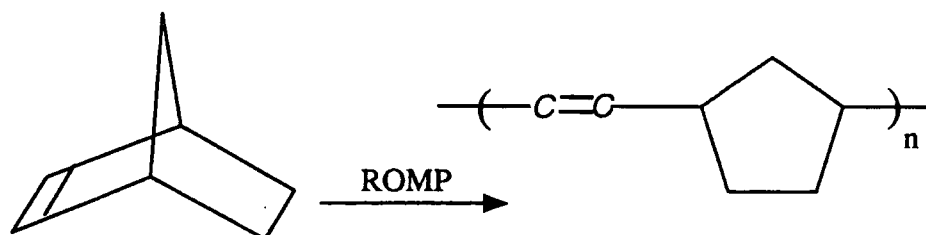


Figure 1.5: ROMP of norbornene.

Calderon noted the similarity between this reaction and the "olefin disproportionation" reaction discovered by Banks and Bailey (Figure 1.6),<sup>26</sup> and used the term "*olefin metathesis*" to describe them both.<sup>27</sup>

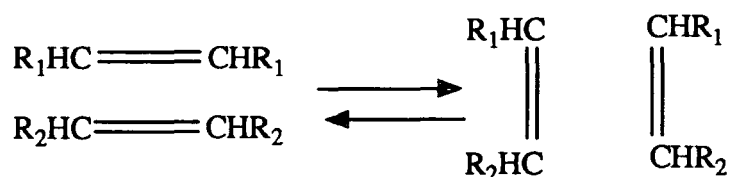


Figure 1.6: The olefin disproportionation reaction.

Since the original discovery, three types of olefin metathesis have been investigated; (a) Exchange (Figure 1.6), (b) Ring Opening Metathesis Polymerisation (ROMP) (Figure 1.5), and (c) degradation/degenerative metathesis.<sup>23</sup> All are now known to proceed via a chain mechanism, with a metal carbene as the chain carrying species.

Unimolecular reactions within the metal carbene complex can cause the deactivation of the catalyst and hence the termination of metathesis. Alternatively, metathesis can be terminated by a Wittig type reaction (Figure 1.7), typically with an oxygen containing molecule, with the formation of an unreactive organometallic compound.<sup>28</sup> The chain growth process can be interrupted by an olefin exchange reaction with an acyclic olefin (chain transfer agent) (Figure 1.8).

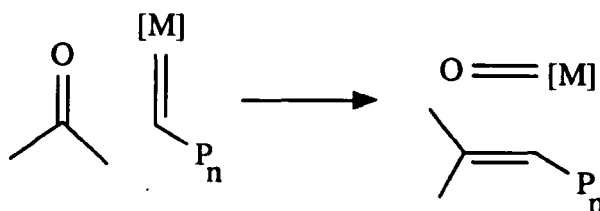


Figure 1.7: Termination of metathesis via a Wittig type reaction.

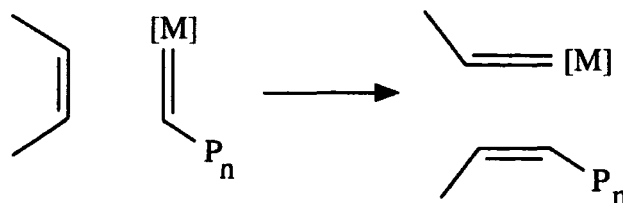


Figure 1.8: Cross-metathesis between a chain propagating species and an acyclic olefin.

The "classical" ROMP reaction is catalysed by a metal carbene generated *in situ* from the halides, oxides or oxyhalides of some of the transition metals (Figure 1.9).

IVA	VA	VIA	VIIA	VIII
Ti	V	Cr		
Zr	Nb	Mo		Ru Rh Pd
Hf	Ta	W	Re	Os Ir Pt

Figure 1.9: Metals active as metathesis catalysts.

In some cases the carbene can be generated directly by reaction of the metal halide with a small proportion of the monomer.<sup>29</sup> Such examples are rare, and it is more usual to use a cocatalyst (eg.  $R_4Sn$ ,  $R = Me$ ,<sup>30,31</sup>  $Ph$ <sup>32</sup>) and/or accelerator (eg.  $H_2O$ ,<sup>30</sup>  $EtOH$ <sup>33</sup>) to aid the generation of the carbene (Figure 1.10). Production of the initiating carbene in these "classical" systems is also dependant on various physical parameters such as temperature,<sup>32</sup> rate of mixing, and concentration;<sup>34</sup> consequently, the reactions are difficult to reproduce.

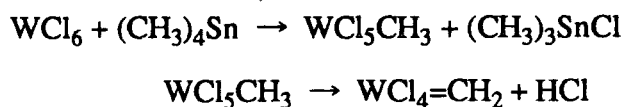


Figure 1.10: Formation of a tungsten carbene in a "classical" catalyst system using a cocatalyst.

Recent advances have led to the preparation of a series of transition metal carbenes by Schrock,<sup>35,36,37</sup> Grubbs<sup>38</sup> and Osborn.<sup>39</sup> These compounds can initiate "living" ROMP of cyclic olefins, enabling mechanistic studies to be performed.

#### 1.4.2 Development of mechanistic theory:

Study of the cross metathesis between cycloalkenes and unsymmetrical linear alkenes led to the proposal by Hérisson and Chauvin that a metal carbene was involved in the metathesis reaction.<sup>40</sup> This concept was supported by using stable Fischer<sup>41,42</sup> and Casey<sup>43-45</sup> carbenes as initiators (Figure 1.11) for the polymerisation of highly strained cyclic olefins.

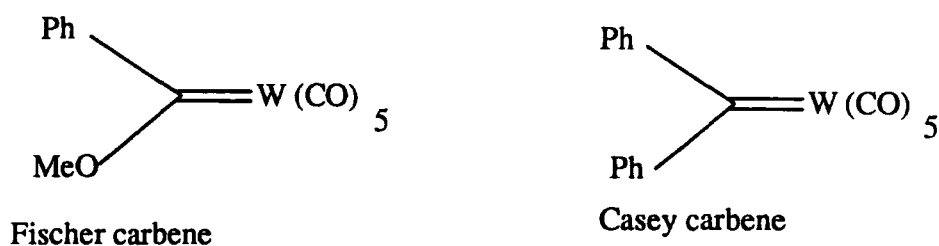


Figure 1.11: Metal carbenes used to initiate metathesis.

The proposed mechanism was assumed to proceed via a transient metallacyclobutane; support for this aspect of the theory was obtained by Grubbs who isolated and determined the structure of a stable complex derived from Tebbé

reagent<sup>46</sup> and norbornene (Figure 1.12), and showed that it could initiate the ROMP of norbornene.<sup>47</sup>

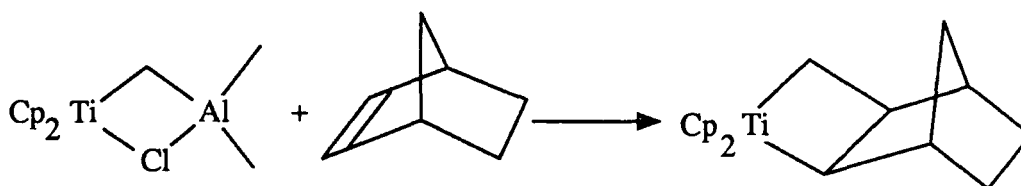


Figure 1.12: Metathesis catalysts derived from Tebbé reagent.

Final confirmation of the theory came from observations of the simultaneous presence, and interconversion, of tungsten carbenes and tungstacyclobutanes during the ROMP of norbornene initiated by the Osborn catalyst (Figure 1.13).<sup>48</sup>

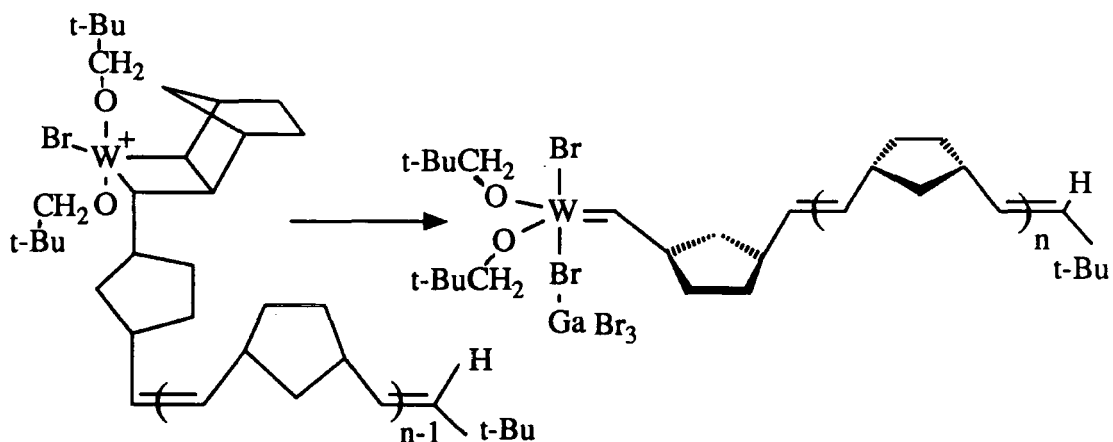


Figure 1.13: Interconversion of metal carbene and metallacyclobutane.

In summary the basic mechanism of productive metathesis involves a [2+2] addition of an olefin to a metal carbene to form a metallacyclobutane.<sup>23</sup> Subsequent rearrangement of the metallacycle followed by its cleavage forms a new carbene and a new olefin.



### 1.4.3 Recent advances in the mechanistic theory:

The metallacycle is initially formed by [2+2] addition of the olefin to the metal carbene. Comparison of the rate of reaction of *cis*-2-pentene with the isostructural tungsten complexes  $W(CH-t-Bu)(NAr)[OCMe(CF_3)_2]_2$  and  $W(CH-t-Bu)(NAr)[O-t-Bu]_2$  shows a turnover rate of  $10^3$  turnovers per minute for the former and 2 per hour for the latter (Figure 1.14), implying that the electrophilicity of the metal carbene is rate determining.<sup>49,50,51</sup>

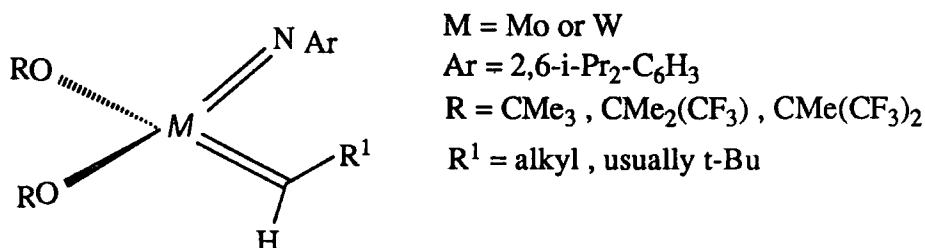


Figure 1.14: Metal carbene initiators prepared by Schrock.

In the case of the metathesis of norbornene or its derivatives, attack is on the *exo* face of the olefin; in the case of a norbornadiene the attack is with the *exo* face of the unsubstituted or less sterically hindered double bond.<sup>52</sup> NMR studies suggest that the first insertion product is solely *trans* (Figure 1.15).<sup>28</sup>

In the case of cyclic olefins, a polymer is formed by cleavage of the metallacycle to form a new metal carbene, followed by attack of another monomer. The rate of initiation and propagation is related to the stability of the metallacycle compared to the carbene. The polydispersity of the polymers is related to the rate of initiation compared to that of propagation. Osborn found that for rates of propagation greater than rates of initiation the polymers produced have a larger molecular weight distribution (MWD) than those prepared with conventional "living" initiators.<sup>54</sup> However the initiator used was shown to be "living" by observation of the downfield hydrogen resonance in  $^1H$  NMR spectrum associated

with the  $\alpha$  hydrogen of the metallacycle, and the ability of the system to make block copolymers.<sup>54</sup>

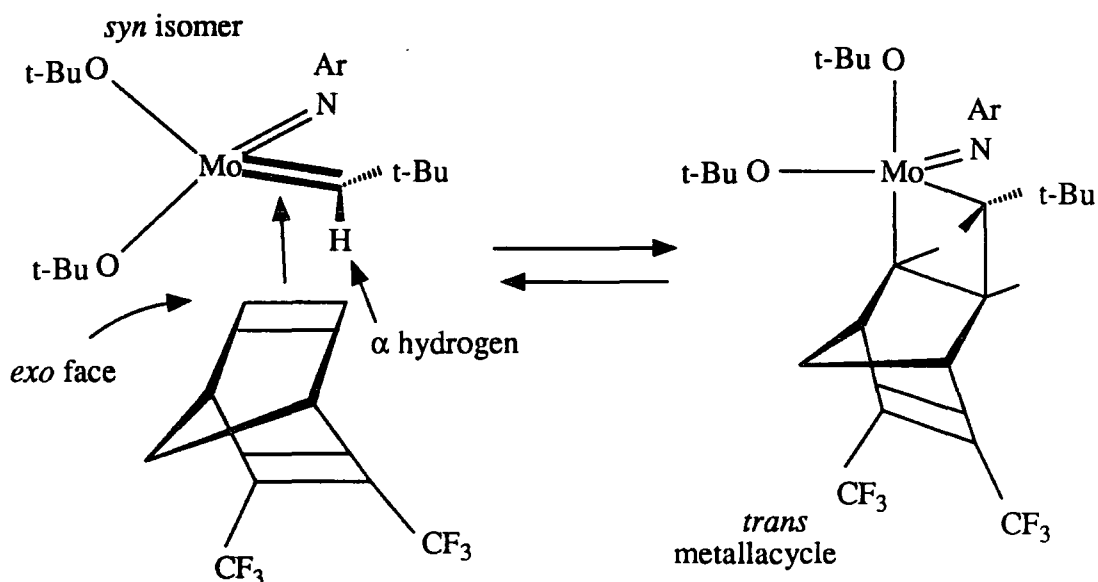


Figure 1.15: Attack on the *exo* face of a norbornadiene derivative to yield a *trans* first insertion product.<sup>53</sup>

Important factors to raise are: (a) how does the substitution on the metallacyclobutane affect the rate of polymerisation ?; (b) what is the effect of the other ligands on the stability of the metallacycle ?; and (c) what rearrangements of core geometry are involved ?.

#### a) Substitution on metallacyclobutanes:

The stability of the metallacyclobutane was shown by Grubbs to be dependant on the degree of substitution of the ring.<sup>47</sup> The difference in initiation and propagation rates is determined by the absence or presence of a bulky polymer chain or alkyl group as a substituent at  $\alpha^1$  on the titanacyclobutane ring (Figure 1.16).

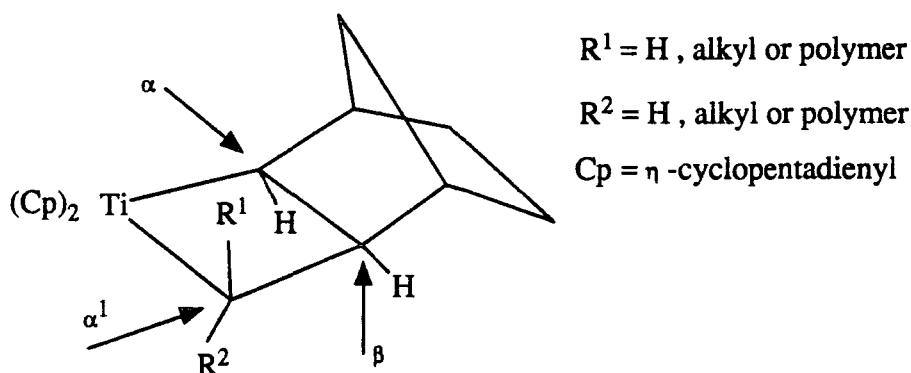


Figure 1.16: Substitution of titanacyclobutanes.

Using titanacycles derived from Tebbe reagent (Figure 1.12), Grubbs demonstrated that the polymerisation of those that were unsubstituted on  $\alpha^1$  proceeded after an induction period that had a first order dependence on monomer concentration. ROMP using titanacycles that have substitution on  $\alpha^1$ , and are hence a model for the propagation step of a polymerisation, proceeded with no induction period and a zero order dependence of rate on monomer concentration. This difference in induction period was reflected in the molecular weight distributions (MWD) of the product polymers; initiators which result in ROMP after an induction period produce polymers with a larger MWD than those which proceed with no induction period.<sup>47</sup>

Similar work using a norbornene monomer was carried out by Schrock with a tantalacyclobutane substituted at  $\alpha^1$ .<sup>35</sup> The polymerisation proceeded with no dependence on the concentration of norbornene monomer, hence the ring opening of the metallacycle was the rate limiting step. An initiation period noted for metallacycles that were unsubstituted on  $\alpha^1$  is again ascribed to the relative stability of the first insertion product compared to the "living" chain carrier for the general propagation step (Figure 1.16).

The carbene complex exists in two forms (rotamers), *syn* and *anti* (Figure

1.17), and cyclic olefins can add to the complex to form *cis* or *trans* metallacycles (Figure 1.15).<sup>53</sup>

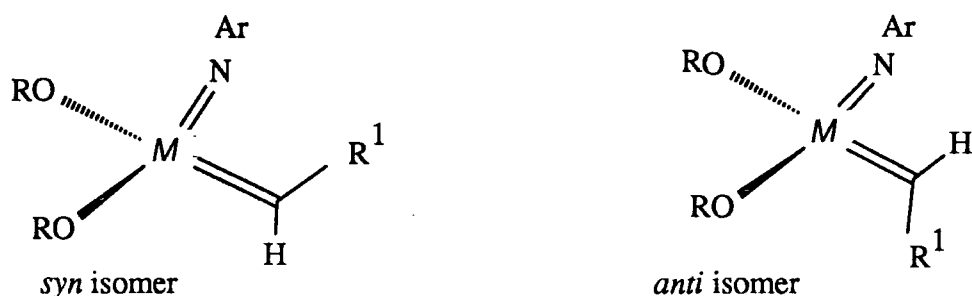


Figure 1.17: Syn and anti carbenes.

*Cis* metallacycles generally ring open much faster than *trans*, supporting the other evidence that *trans* metallacycles are the first insertion product;<sup>55</sup> if *cis* was the major first insertion product then the induction period for the initiation of metallacycles unsubstituted on position  $\alpha^1$  would be small or non-existent. The formation of a *trans* metallacycle from a *syn* rotamer leads to an *anti* first insertion product and formation of a *cis* metallacycle from a *syn* rotamer leads to a *syn* first insertion product. The presence of both rotamers does not rule out the formation of a stereoregular polymer; using Schrock's molybdenum based initiator (Figure 1.14), 2,3-bis(trifluoromethyl)norbornadiene can be polymerised to give a 98% *trans* polymer (living rotamers are observed in the ratio 6:1 *syn:anti*)<sup>53</sup> and 2,3-bis(carbomethoxy)norbornene can be polymerised to give a 90-95% *trans* polymer.<sup>56</sup>

b) Effect of ligands on metallacycle stability:

Grubbs considered the effect of substitution on the cyclopentadienyl rings of initiators derived from Tebbe reagent when they were used for the ROMP of norbornene.<sup>57</sup> The steric bulk of the substituents on the cyclopentadienyl rings can

interfere with the substituents on the  $\beta$  carbon, and destabilise the metallacycle. Thus the rate of propagation of the "cis" form (Figure 1.18) was found to be greater than that of the "trans".

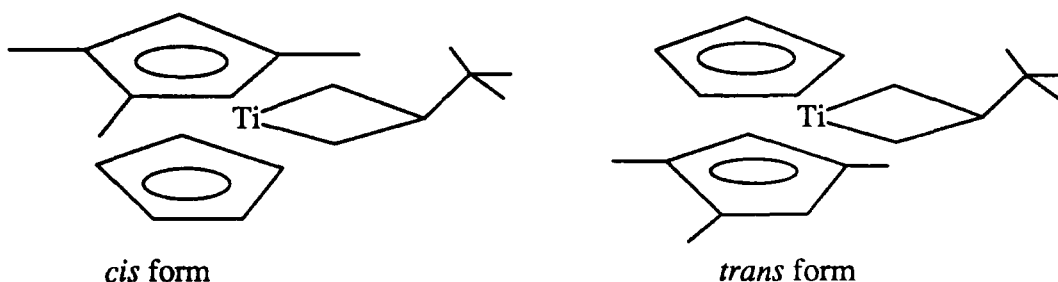


Figure 1.18: Substituted cyclopentadiene rings on a catalyst derived from Tebbe reagent.

For effective ROMP, there must be a low energy barrier for the interconversion of the metallacycle and the metal carbene, and this is dependant on the electron withdrawing effect of the ligands. In the complexes of type  $M(\text{CHR})(\text{NAr})(\text{OR})_2$  ( $M = \text{Mo}$  or  $\text{W}$ ;  $\text{Ar} = 2,6\text{-C}_6\text{H}_3\text{-i-Pr}_2$ ), the activity of the catalyst for a given metal increases significantly in the series  $(\text{R} =) \text{-CMe}_3 < \text{-CMe}_2(\text{CF}_3) < \text{-CMe}(\text{CF}_3)_2$  (Figure 1.14), i.e. rate of metathesis increases as the ligands become more electron withdrawing.<sup>49</sup>

### c) Rearrangements in core geometry during metathesis:

Mechanistic studies<sup>58</sup> using initiators of the Schrock type (Figure 1.14) have recently revealed some of the changes involved in the metal core geometry during the metathesis of simple terminal olefins.<sup>59</sup> The rate of formation, and stability, of the initially observed square pyramidal metallacyclobutane depends on the reaction temperature, solvent, and the alkoxide ligands of the initiator. A number of square pyramidal and trigonal bipyramidal species can be observed when the reaction

temperature and/or ligands are altered (Figure 1.19).

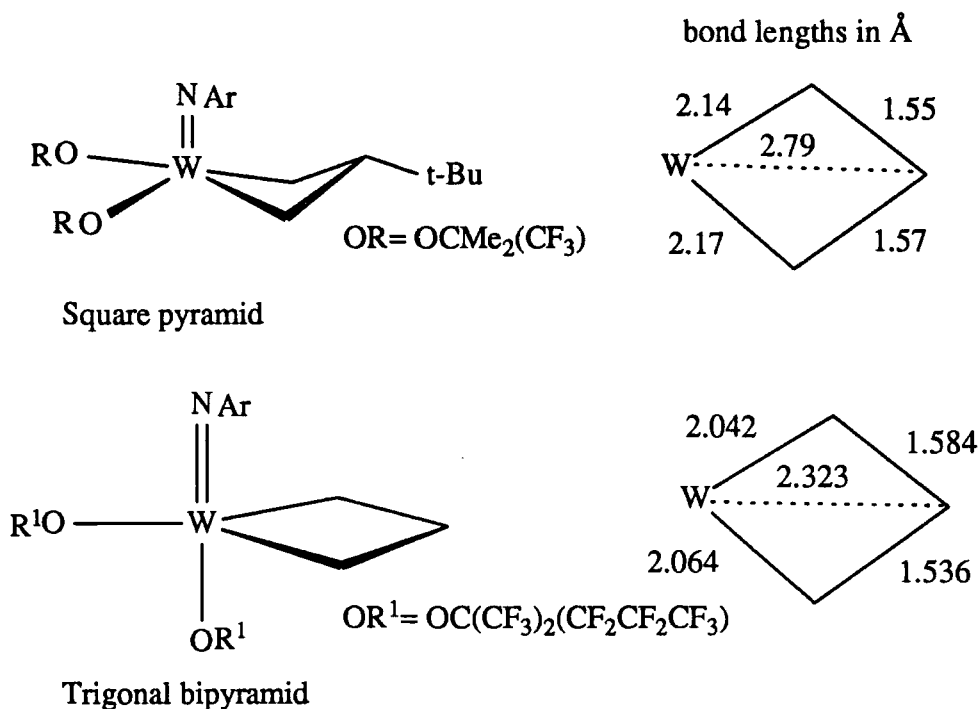


Figure 1.19: Complexes observed in the metathesis of an acyclic olefin.<sup>58</sup>

NMR studies show that these complexes interconvert rapidly compared to the rate of tungstacycle formation and cleavage. When the tungstacycle is substituted on the  $\alpha$  carbon, the geometry of the metallacycle that predominates depends on that substitution. The interconversion of metallacycles is thought to be crucial in productive metathesis reactions, and the mechanism for metathesis of cyclic olefins is therefore postulated to proceed in a similar manner (Figure 1.20).

The mechanism involves attack of the olefin on the carbene on the O/N/C face to yield a trigonal bipyramidal complex. Loss of a new olefin from this complex is not immediately possible. Pseudorotation about the equatorial nitrogen via a square pyramidal intermediate with axial nitrogen results in a new trigonal bipyramid which can now lose the new olefin from an axial position.<sup>60</sup>

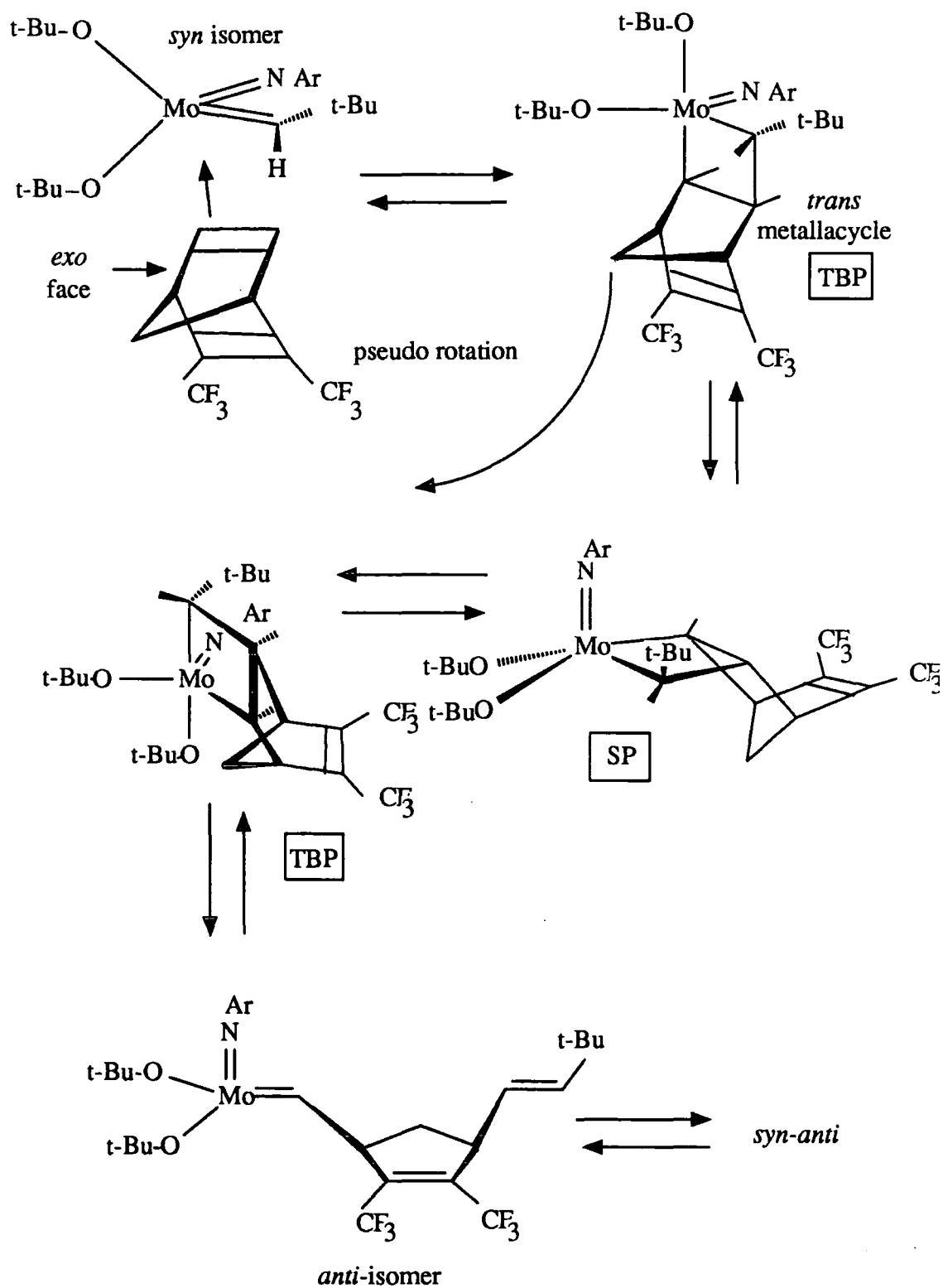


Figure 1.20: Changes in core geometry during metathesis.

The rate of reaction is related to the energy barrier between the trigonal bipyramid and square pyramid forms of the metallacycle. Other pseudorotations are kinetically accessible and are rapidly interconvertible relative to the rate of monomer addition,<sup>58</sup> although they are not thought to be important in ROMP.

#### 1.4.4 Olefin metathesis in aqueous and ethanolic solution:

For effective metathesis, there must be a low energy barrier between metal carbene and metallacyclobutane. Many other reaction paths are also available, and both species can be extremely sensitive to deactivation by solvent and functionalised monomers. The "classical" catalysts derived from tungsten, molybdenum and rhenium are easily destroyed by the presence of oxygen and water in greater than stoichiometric amounts,<sup>23</sup> and some oxygen containing monomers. The carbene initiators made from molybdenum,<sup>36</sup> tungsten,<sup>39</sup> rhenium,<sup>47</sup> titanium,<sup>47</sup> and tantalum<sup>55</sup> are more stable to deactivation by the monomer, but more sensitive to oxygen and water. In both kinds of system the stability of the initiating and chain propagating species depends on steric protection of the unstable carbene, and electronic stabilisation by donation of electron density from the other ligands.<sup>49</sup>

Transition metal carbenes formed *in situ* from group VIII metals are more stable in the presence oxygen containing molecules than their tungsten and molybdenum counterparts.<sup>23</sup> Metathesis catalysts derived from the hydrated chlorides of iridium,<sup>61</sup> osmium<sup>62</sup> ruthenium<sup>63</sup> and rhodium<sup>64</sup> in ethanol are well known. Such catalysts can polymerise a range of functionalised monomers including ester,<sup>65</sup> anhydride<sup>66</sup> and acid<sup>67</sup> derivatives of norbornene. Usually the carbene is formed by direct reaction of a metal halide with the monomer, although in some cases reducing agents have been used as activators.<sup>68,69</sup> The presence of water is tolerated in many of these systems and has been used as a solvent<sup>70</sup> or



co-solvent<sup>68,69</sup> in the ROMP of some homo- and heterocyclic olefins,<sup>71-74</sup> although the exclusion of molecular oxygen is still preferred.<sup>72</sup>

Recently Grubbs has reported the aqueous ROMP of various heteropolycyclic monomers using ruthenium trichloride trihydrate as the precursor to the initiating and chain propagating species (Figure 1.21).<sup>71,72</sup> In water, catalysts derived from iridium and osmium tend to polymerise the same monomers at a much slower rate than ruthenium derived ones,<sup>73</sup> and competitive side reactions are more important. The trend is reversed in ethanol, with iridium initiators being of highest activity.<sup>62</sup> Subsequently the range of functionalised monomers susceptible to aqueous ROMP was expanded to include ester and acid functionalised norbornenes and 7-oxanorbornenes.<sup>75,76,77</sup>

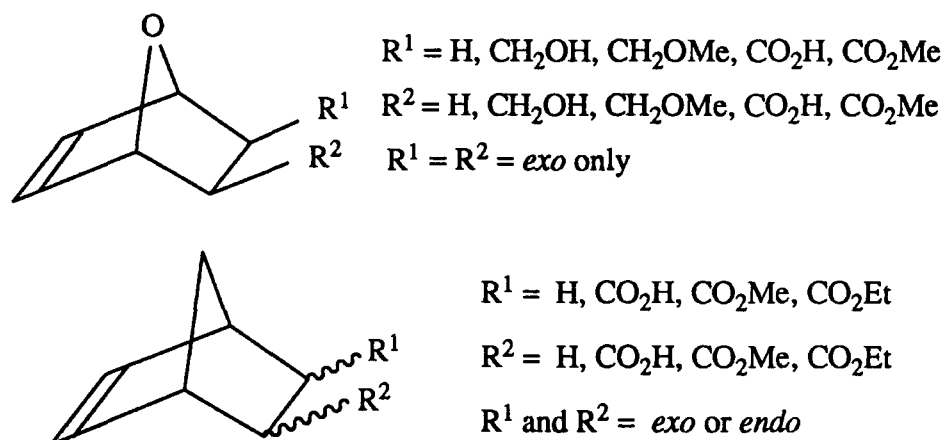


Figure 1.21: Homo- and heteropolycyclic olefins polymerised in pure water or ethanol by ROMP.

ROMP of heterocyclic and heteropolycyclic olefins has traditionally been difficult due to interactions of the hetero atom with the carbene initiator.<sup>78</sup> In addition conventional olefin addition,<sup>63</sup> ether ring opening<sup>75,72</sup>, and copolymerisations with carbon monoxide<sup>79</sup> have been reported as competitive reactions.

### 1.4.5 Microstructure of polymers prepared by ROMP:

The ROMP process is outlined in Figure 1.22, the numbering system depends on the substituents of the monomers and is dealt with later.

There are a number of ways in which the repeat units can be incorporated into the chain. The ultimate microstructure is dependant on four factors: (a) *cis* and *trans* double bonds; (b) head and tail effects; (c) tacticity effects; and (d) sequence effects.<sup>23</sup>

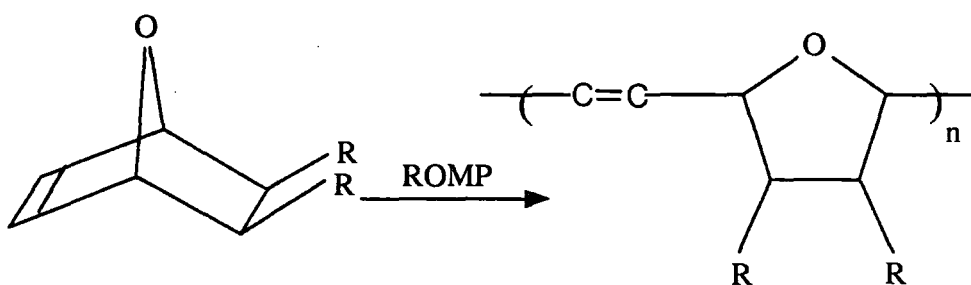


Figure 1.22: ROMP of disubstituted 7-oxanorborene.

#### a) *Cis* and *trans* double bonds:

The backbone of a polymer prepared by ROMP contains unsaturated bonds which can be either *cis* or *trans* (Figure 1.23).

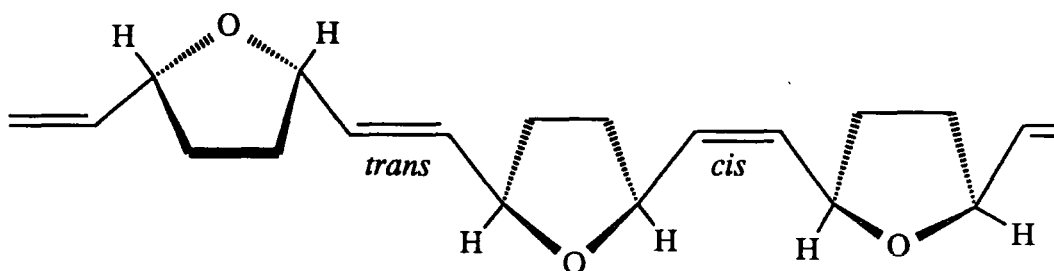


Figure 1.23: *Cis* and *trans* double bonds in poly(2,5(furanylene)vinylene).

Approach of 7-oxabicyclo[2.2.1]hept-2-ene to a carbene of the kind shown in

Figure 1.17 can occur in two different ways, leading to *cis* and *trans* ring opened polymers (Figure 1.24).

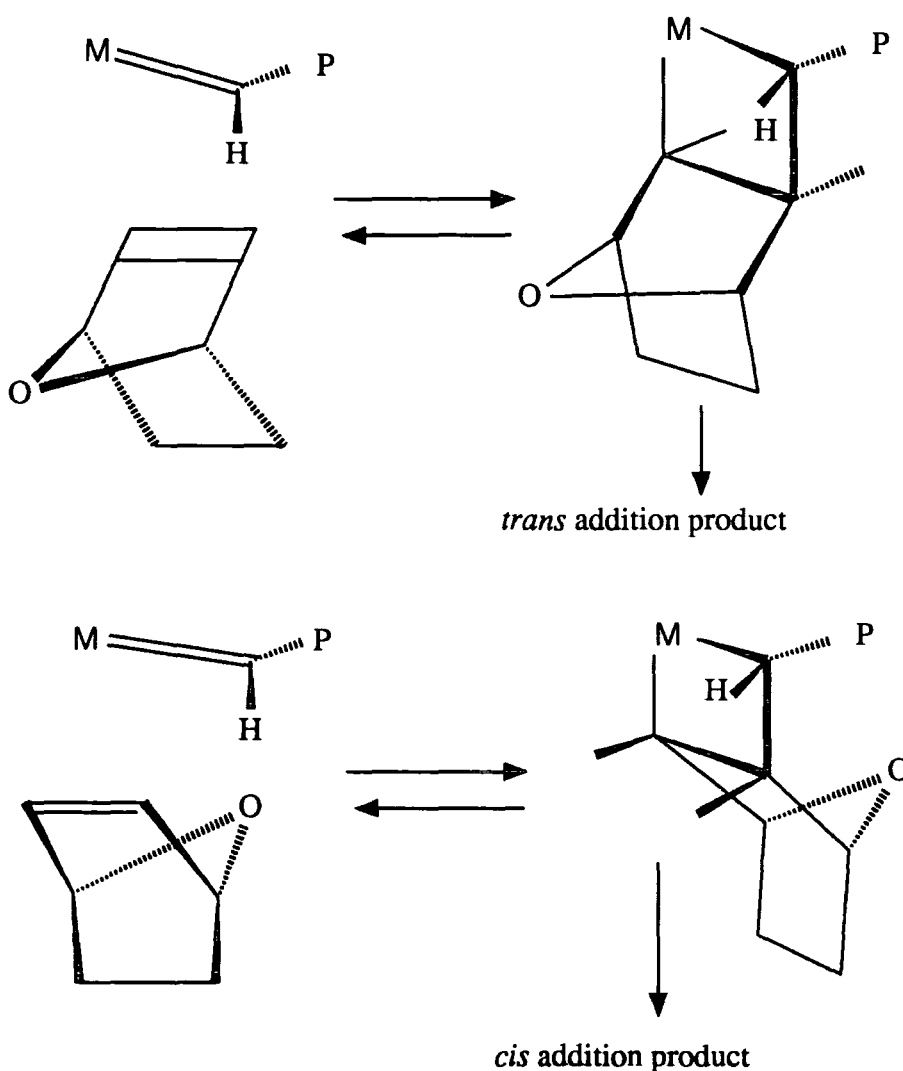


Figure 1.23: Transition steps leading to *cis* and *trans* double bonds.

The double bond content of the polymers prepared by ROMP is denoted by the symbol  $\sigma^c$ , which refers to the proportion of *cis* double bonds in the backbone.<sup>23</sup> Thus for  $\sigma^c = 1.0$  there are only *cis* double bonds and for  $\sigma^c = 0$  there are no *cis* double bonds. This notation is used throughout this thesis.

b) Head and tail effects:

The polymers prepared in this thesis are made from symmetrically substituted 7-oxabicyclo[2.2.1]hept-2-ene monomers. Symmetrical monomers cannot give rise to "head-head" (HH), "head-tail" (HT), or "tail-tail" (TT) addition modes.<sup>24</sup>

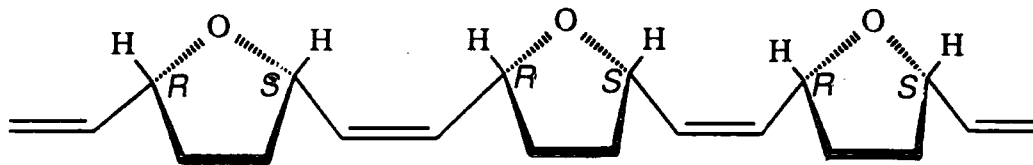
c) Tacticity effects:

The propagating metal carbene can exist in two mirror image forms (Figure 1.17) which may not interconvert rapidly compared to the rate of monomer addition.<sup>53</sup> The monomer can be orientated in two ways when it attacks (Figure 1.24) and therefore four tacticities are available. The allylic carbons on either side of the vinyl bond are chiral and may have opposite chirality, giving meso or m-dyads and isotactic polymer, or have the same chirality giving racemic or r-dyads and syndiotactic polymer. Since the vinylic bonds can either be *cis* or *trans*, there are four possible microstructural arrangements (Figure 1.25).

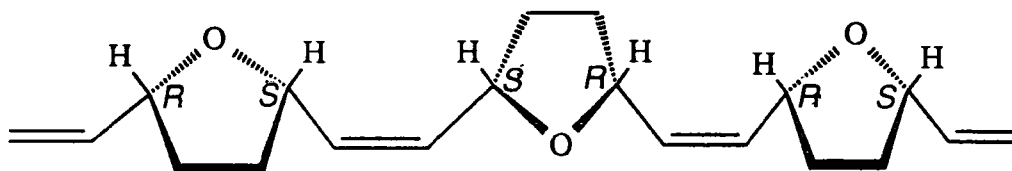
d) Sequence effects:

Generally, for polymers of this type, the sequence effects, or "blockiness" are only observed for  $\sigma^c > 0.5$ . The blockiness is observed in NMR studies as new resonances, distinct from the resonance of non-blocky *cis* or non-blocky *trans*. For polymers with  $\sigma^c < 0.35$  the backbone usually contains a random distribution of *cis* and *trans* double bonds.<sup>80</sup>

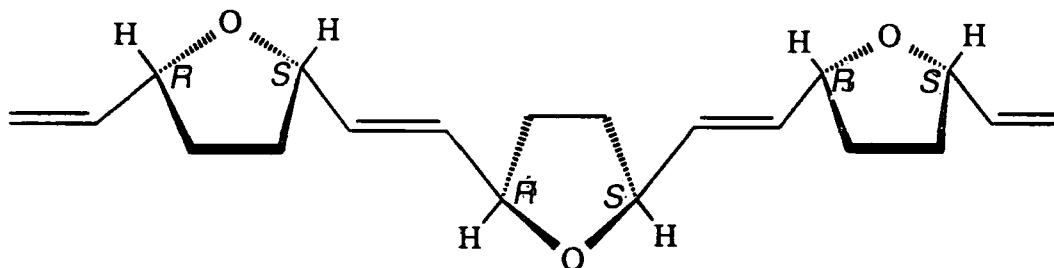
*cis* isotactic, meso or m-dyads.



*cis* syndiotactic, racemic or r-dyads.



*trans* isotactic, meso or m-dyads.



*trans* syndiotactic, racemic or r-dyads.

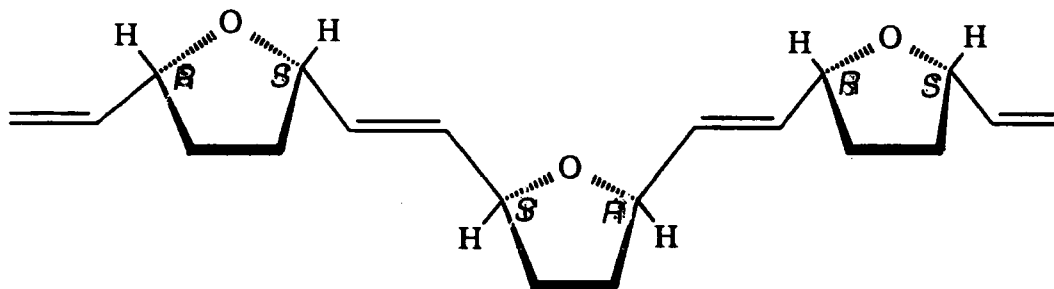


Figure 1.25: The four possible tacticities of poly(2,5(furanylene)vinylene).

### **1.5: Objectives and methods of this study.**

The objectives of the investigation described in this thesis were the synthesis of a variety of functionalised polymers by aqueous ROMP, and the study of their application to aragonite scale control procedures. The approach adopted was to prepare a number of derivatives of 7-oxabicyclo[2.2.1]hept-2-ene and bicyclo[2.2.1]hept-2-ene, and polymerise them via aqueous ROMP. The microstructure of the monomers, oligomers and polymers produced were investigated using  $^1\text{H}$  NMR spectroscopy,  $^{13}\text{C}$  NMR spectroscopy, and infrared spectroscopy. The effectiveness of some of the low molecular weight polymers for the inhibition of aragonite formation was assessed, and correlated to both theoretical models, and polymer microstructure. The monomers shown in Figure 1.26, and polymers shown in Figure 1.27 have been prepared and investigated during the course of this work.

Chapter 2 describes the synthesis and characterisation of the monomers. Chapter 3 is concerned with surveying the monomers that can be polymerised via aqueous ROMP, and surveying the range of transition metal chlorides which are able to form aqueous metathesis initiators *in situ*. In chapter 4, the preparation of oligomers, and the effect of some acyclic olefins on the polymerisation is described. Chapter 5 discusses the results of chapters 3 and 4, and Chapter 6 is concerned with the applications tests, and the theoretical modelling of the inhibition of aragonite formation. Chapter 7 suggests future developments of this work.

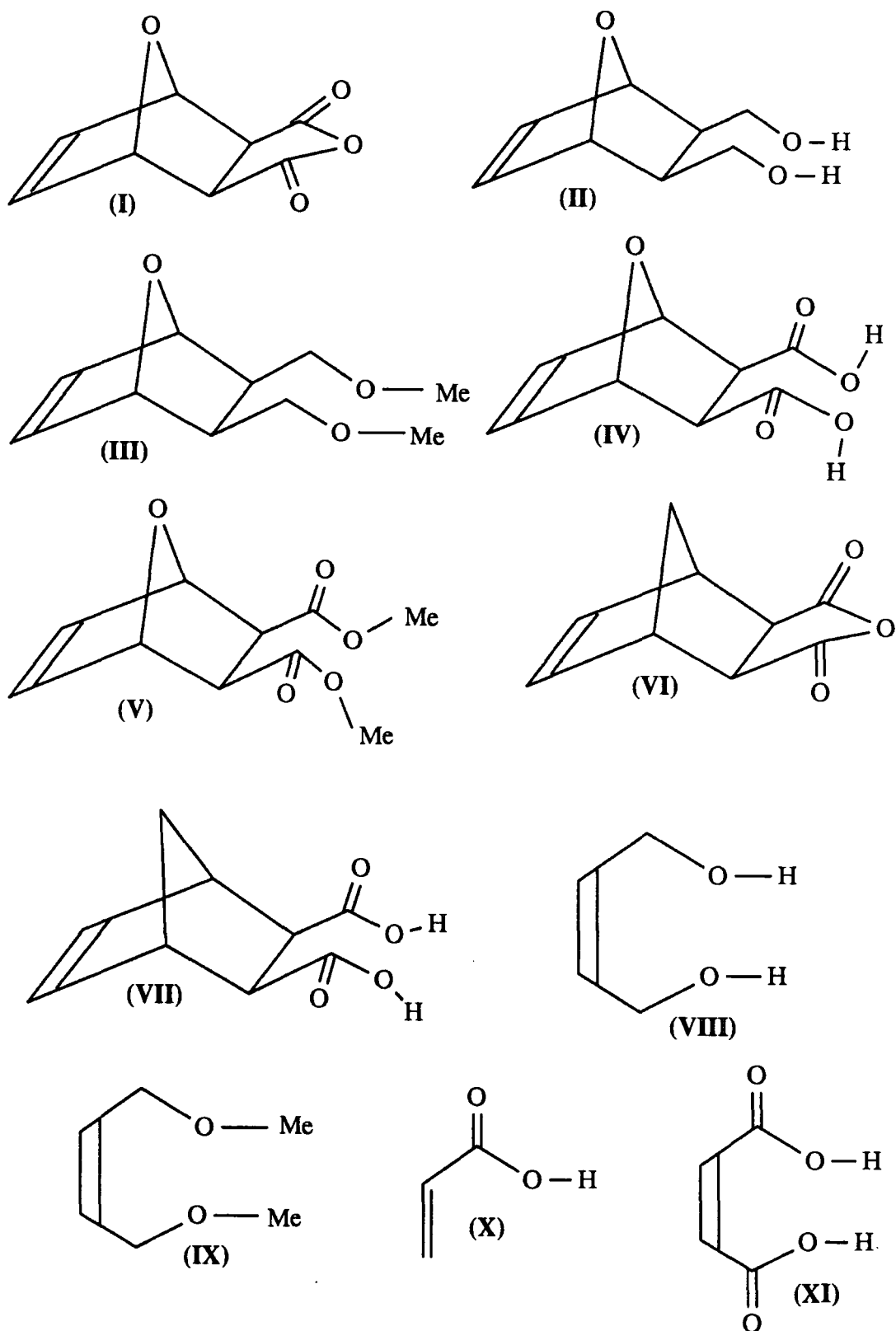


Figure 1.26: Monomers and chain transfer agents used for aqueous ROMP.

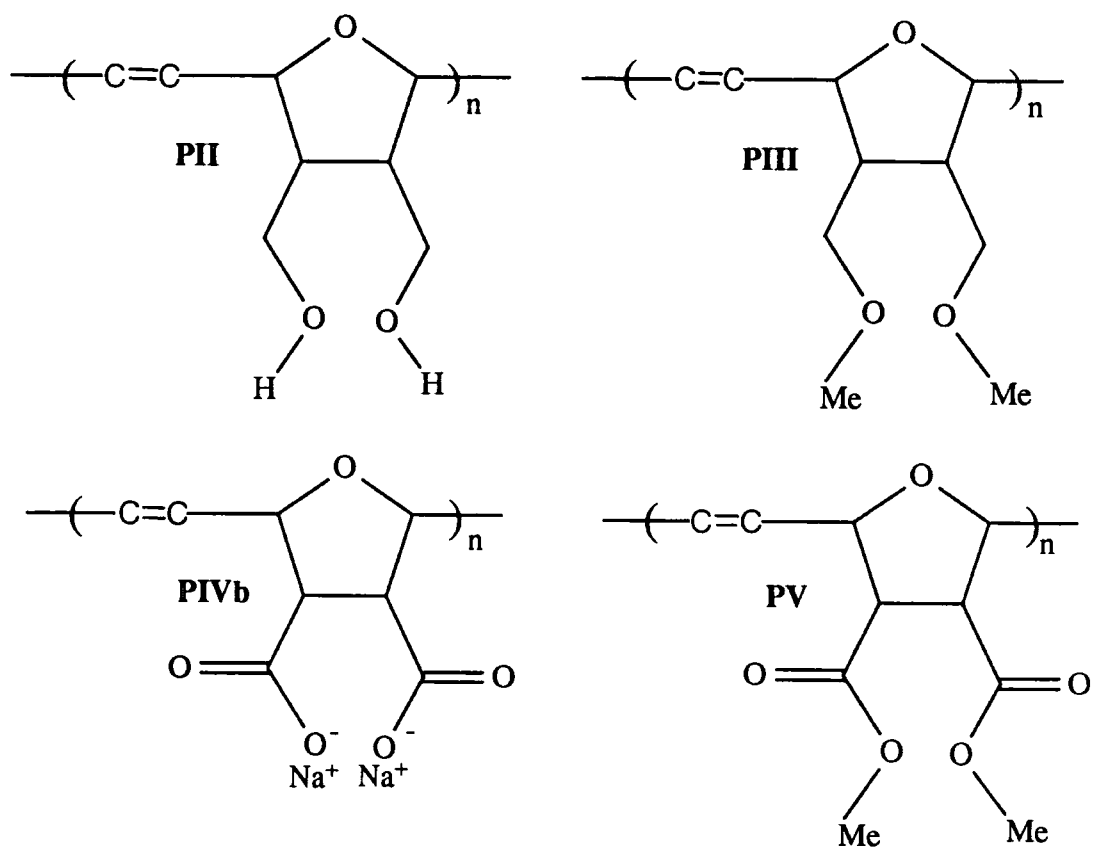


Figure 1.27: Polymers prepared by aqueous ROMP.



CHAPTER 2:  
MONOMER  
SYNTHESIS AND  
CHARACTERISATION.

## 2.1: Introduction.

### 2.1.1 *General:*

The objectives of this chapter are the synthesis and characterisation of a series of functionalised derivatives of 7-oxabicyclo[2.2.1]hept-5-ene and bicyclo[2.2.1]hept-5-ene. The most convenient synthetic route for any of these derivatives was found to involve the formation of the polycyclic ring via a Diels-Alder reaction, followed by derivatisation of the adduct.

### 2.1.2 *The Diels-Alder Reaction:*

The Diels-Alder reaction involves the addition of an olefin or acetylene derivative (dienophile) to a conjugated diene with the formation of a six membered ring (Figure 2.1).<sup>81</sup>

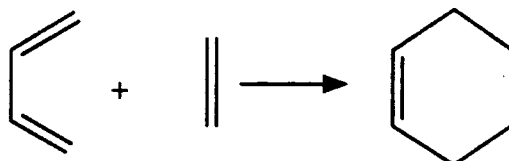


Figure 2.1: The Diels-Alder reaction between a conjugated diene and an olefin.

Effective reaction requires that there are electron withdrawing groups on the dienophile,<sup>82</sup> and electron donating groups on the diene (conventional Diels-Alder), or electron withdrawing groups on the diene and electron donating groups on the dienophile (Diels-Alder with inverse electron demand); the conventional reaction can be accelerated in the presence of Lewis acids.<sup>83</sup> The diene can react only in the *cis* conformation, and therefore cyclic dienes react faster than acyclic dienes; five membered ring dienes are particularly favoured

due to the coplanarity of the double bonds.

With a substituted acyclic dienophile the reaction produces either *exo* or *endo* adducts depending on the conditions (Figure 2.2):<sup>81</sup> the *exo* adduct is the thermodynamically favoured product, and the *endo* adduct is the kinetically favoured product.<sup>84</sup> Careful control of the temperature, pressure and solvent can favour the formation of one adduct over the other. Thus reflux of cyclopentadiene and maleic anhydride in o-dichlorobenzene favours the *exo* adduct,<sup>84</sup> whereas at lower temperature the *endo* adduct is the major product.<sup>85</sup>

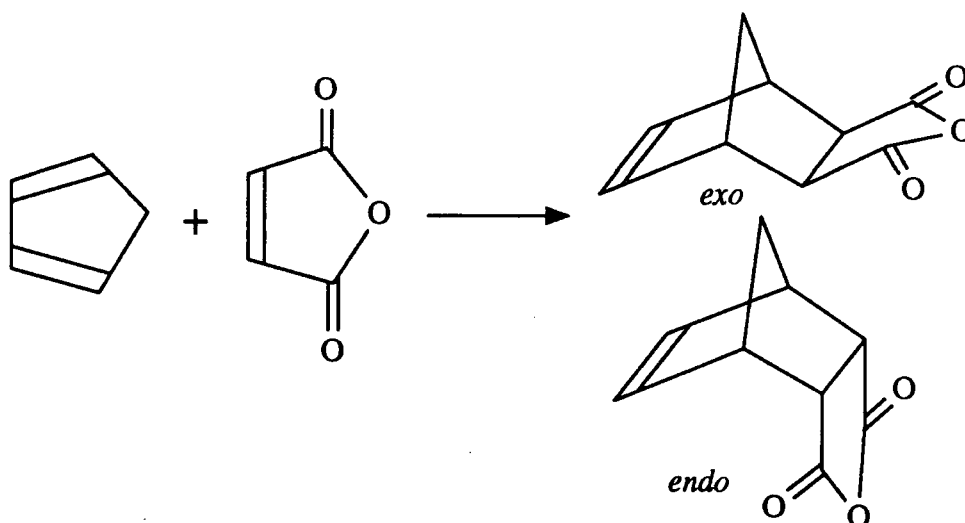


Figure 2.2: Diels-Alder reaction of maleic anhydride and cyclopentadiene to yield *exo* and *endo* adducts.

## 2.2: General Details.

### 2.2.1 *Reactants:*

All reactants and solvents (Aldrich Chemical Co. Ltd.) were used as supplied unless stated otherwise.

### 2.2.2 Monomer characterisation:

All NMR spectra were recorded using either a Varian VXR-400-S NMR spectrometer, operating at 399.952 MHz for  $^1\text{H}$  NMR, and 100.577 MHz for  $^{13}\text{C}$  NMR, or a Bruker AC250 NMR spectrometer, operating at 250.133 MHz for  $^1\text{H}$  NMR, and 62.896 MHz for  $^{13}\text{C}$  NMR. Infrared spectra were recorded with a Nicolet 730 FTIR spectrometer or a Perkin Elmer 577 spectrometer, and Mass spectra were recorded with a VG 7070E mass spectrometer using chemical ionisation from  $\text{NH}_4^+$ .

### 2.2.3 Computer modelling:

Theoretical calculations of the torsion angles in the monomers were made using a transputer based computer modelling system, custom built for Ciba-Geigy Industrial Chemicals. The hardware comprised of 16 INMOS floating point transputers in network with an IBM 80 personal computer, and DIGISOLE BGP64 graphics processing unit. The software, based on the commercial CHEMMOD package, was custom written for Ciba-Geigy by Dr. D.N.J. White<sup>86</sup> at the University of Glasgow, and used Newton-Raphson techniques for the energy minimisation calculations.<sup>87</sup>

## **2.3: Synthesis and characterisation of *exo*-7-oxabicyclo[2.2.1]hept-5-ene-2,3-dicarboxy anhydride (I).**

### 2.3.1 Synthesis of monomer I:

The Diels-Alder reaction between furan and maleic anhydride is shown in Figure 2.3, which also records the numbering system employed.

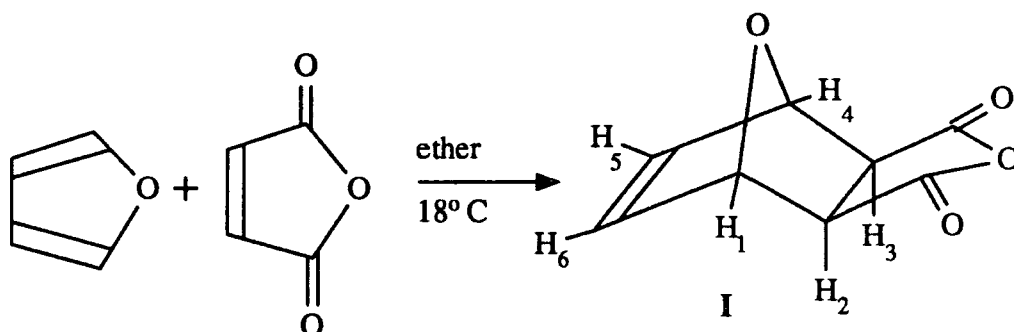


Figure 2.3: Diels-Alder reaction of furan and maleic anhydride to yield monomer I.

The reaction yields both *exo* and *endo* adducts, although the ratio of products depends on the solvent and temperature. The rate constant for the formation of the *endo* adduct in acetonitrile is 500 times greater than that for the *exo* adduct, although the *exo* adduct is 1.9 Kcal.mol<sup>-1</sup> more stable.<sup>88</sup> When the reaction is carried out in diethyl ether at room temperature the *exo* adduct crystallises from solution and is the sole isolated product after two days.<sup>89</sup>

Furan (68g, 1.0 mol) was added to a solution of maleic anhydride (98g, 1.0 mol) in diethyl ether (400 ml) at room temperature and stirred for 12 hours. White crystals began forming after 6 hour; filtration after 48 hours followed by washing with diethyl ether afforded I as a white crystalline product in 69% yield. (m.pt. 125.0°C. Lit.<sup>90</sup> 125.0°C) (Elemental analysis; found: C,57.4%, H,3.5% ; calculated for C<sub>8</sub>H<sub>6</sub>O<sub>4</sub>: C,57.8%, H,3.6%).

### 2.3.2 Characterisation of monomer I:

The <sup>1</sup>H NMR spectrum of monomer I is shown in Figure 2.4, with the chemical shifts recorded in Table 2.1.

Figure 2.4:  $^1\text{H}$  NMR spectrum of *exo*-7-oxabicyclo[2.2.1]hept-5-ene-2,3-dicarboxy anhydride (monomer I) recorded at 399.952 MHz in  $(\text{CD}_3)_2\text{CO}$ .

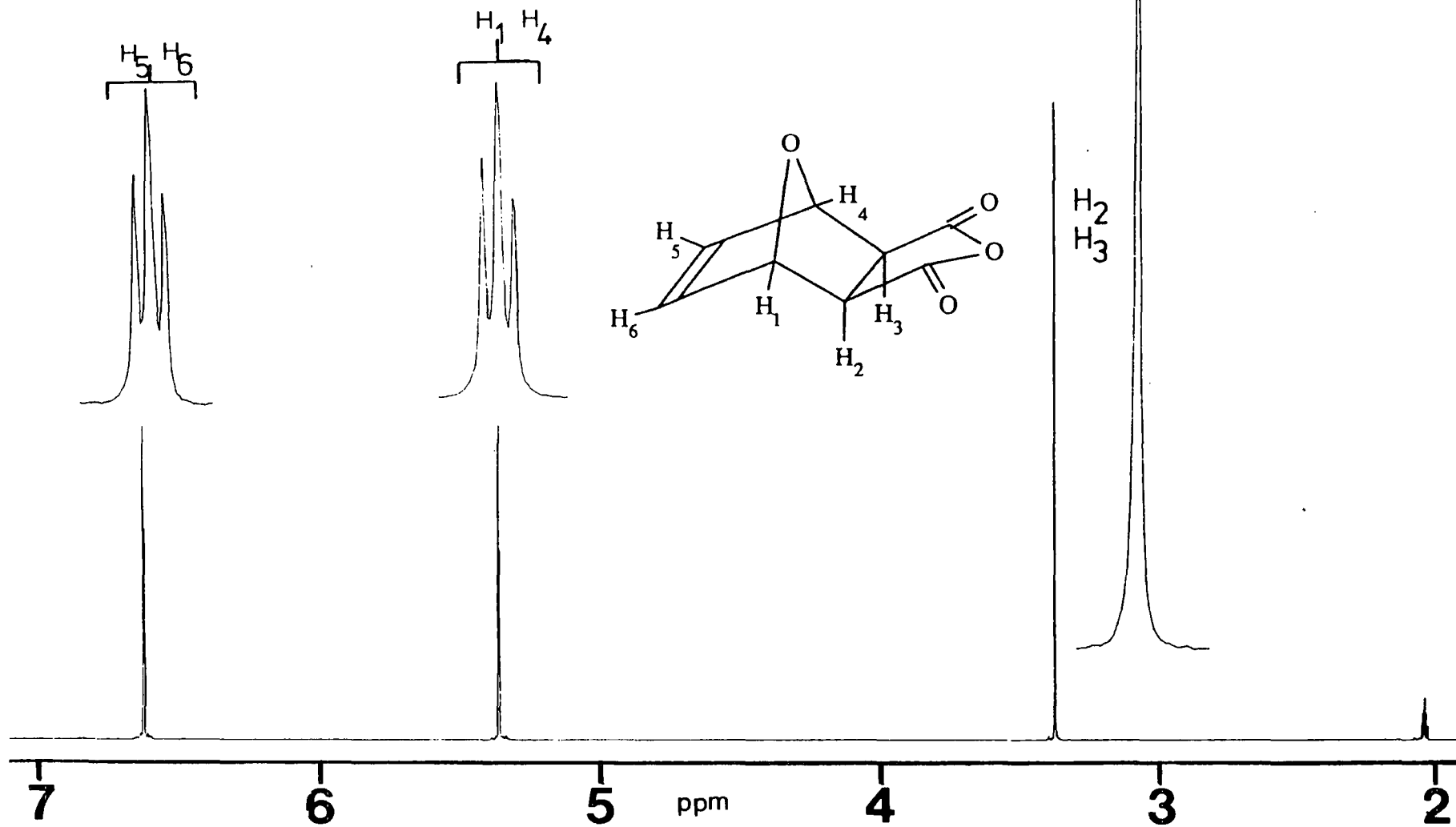
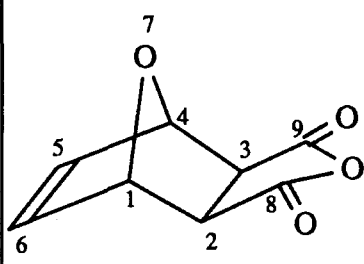


TABLE 2.1: Principal  $^1\text{H}$  NMR spectral parameters<sup>1</sup> for monomer I (399.952 MHz,  $(\text{CD}_3)_2\text{CO}$ ).

Monomer I	shift/ ppm	multiplicity	inte- gral	assign- ment
	6.63	multiplet $J_{6,1} \approx 1.0 \text{ Hz}$ $J_{5,1} \approx 1.0 \text{ Hz}$	2	5, 6
	5.37	multiplet $J_{1,6} \approx 1.0 \text{ Hz}$ $J_{1,5} \approx 1.0 \text{ Hz}$	2	1, 4
	3.37	singlet	2	2, 3

1) with respect to acetone at 2.04 ppm.

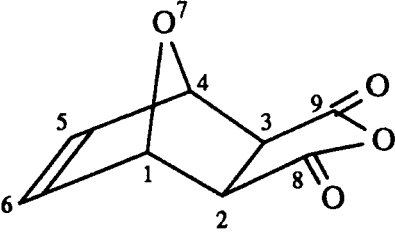
Protons  $\text{H}_1$ ,  $\text{H}_4$ ,  $\text{H}_5$ , and  $\text{H}_6$  form an  $\text{A}_2\text{X}_2$  system with  $J_{5,6} \rightarrow 0$ ,  $J_{1,4} \rightarrow 0$ , and  $J_{1,5} \approx J_{1,6} \approx 1.0 \text{ Hz}$ . The small coupling constants observed are consistent with the torsion angles between the coupled protons, namely  $28.5^\circ$  between  $\text{H}_1$  and  $\text{H}_6$ , and  $50.9^\circ$  between  $\text{H}_1$  and  $\text{H}_5$ .<sup>91</sup>

The proton decoupled  $^{13}\text{C}$  NMR spectrum is consistent with the structure of monomer I, and is shown in appendix A1, with chemical shifts recorded in Table 2.2. The infrared spectrum of monomer I was recorded from a KBr disc (appendix B1), and is consistent with the assigned structure; vinylic C-H stretches at  $3100 \text{ cm}^{-1}$ , allylic C-H stretches at  $3010 \text{ cm}^{-1}$  and  $3000 \text{ cm}^{-1}$ , and anhydride carbonyl stretches at  $1860 \text{ cm}^{-1}$  and  $1780 \text{ cm}^{-1}$ .

The chemical ionisation mass spectrum (appendix C1) contains a base peak at 68 ( $\text{C}_4\text{H}_4\text{O}^+$ ) resulting from a retro Diels-Alder reaction, although no corresponding maleic anhydride peak is observed. The molecular ion peak at 184

(M + NH<sub>4</sub><sup>+</sup>) is of low intensity, which is consistent with the instability of this Diels-Alder adduct. The mass spectrum is consistent with the assigned structure.

TABLE 2.2: Principal <sup>13</sup>C NMR spectral parameters<sup>1</sup> for monomer I (100.577 MHz, (CD<sub>3</sub>)<sub>2</sub>CO).

monomer I	shift / ppm	assignment
	171.91	8, 9
	137.70	5, 6
	83.01	1, 4
	49.87	2, 3

1) with respect to acetone at 29.82 ppm.

#### 2.4: Synthesis and characterisation of

##### exo,exo-5,6-bis(hydroxymethyl)-7-oxabicyclo[2.2.1]hept-2-ene (II).

##### 2.4.1 *Synthesis of monomer II:*

The reduction of monomer I to yield monomer II is shown in Figure 2.5, which also records the numbering system employed. Complete reduction of the anhydride group in monomer I to the diol monomer II can be achieved using LiAlH<sub>4</sub> in THF as the reducing agent;<sup>92</sup> when the reaction is carried out in diethyl ether<sup>93</sup> or using NaBH<sub>4</sub><sup>94</sup> as reducing agent, the anhydride ring is only partially reduced.



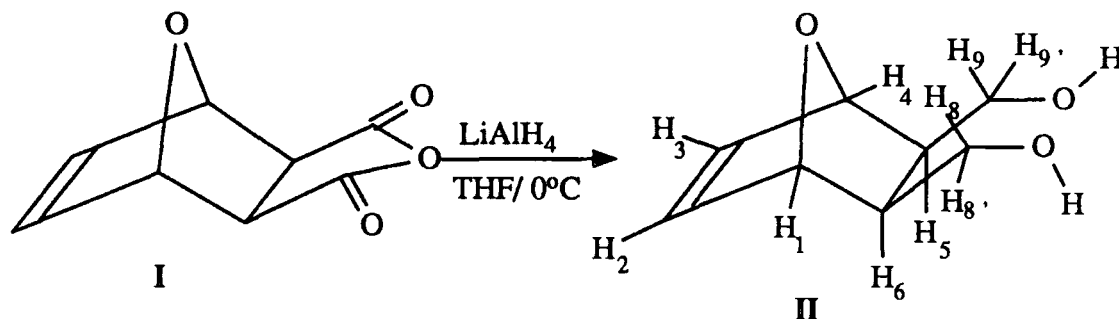


Figure 2.5: Reduction of monomer I to yield monomer II.

Monomer I (9.9g, 60 mmol) in dry THF (160ml) was added over 45 minutes to an ice cooled slurry of  $\text{LiAlH}_4$  (4.6g, 121 mmol) in dry THF (140ml) with stirring under a nitrogen atmosphere.<sup>92</sup> The reaction was allowed to proceed for a further 48 hours at room temperature prior to termination by consecutive additions of water (4.6ml), 15% NaOH (4.6ml) and water (13.8ml).<sup>95</sup> Filtration to remove salt residues followed by evaporation of the solvent yielded the crude product. Purification by extraction into diethyl ether (200ml) with drying over anhydrous  $\text{MgSO}_4$ , followed by removal of solvent in vacuo afforded II as a viscous oil in 70% yield.<sup>92</sup> (Elemental analysis: found: C,61.3%, H,7.5% ; calculated for  $\text{C}_8\text{H}_{12}\text{O}_3$ : C-61.5%, H-7.7%).

#### 2.4.2 Characterisation of monomer II:

The  $^1\text{H}$  NMR spectrum of monomer II is shown in Figure 2.6, with the chemical shifts recorded in Table 2.3. Protons  $\text{H}_1$ ,  $\text{H}_2$ ,  $\text{H}_3$  and  $\text{H}_4$  form an  $\text{A}_2\text{X}_2$  system with  $J_{2,3} \rightarrow 0$ ,  $J_{1,4} \rightarrow 0$ , and  $J_{1,2} \approx J_{1,3} \approx 1.0$  Hz. Proton resonances between 3.85 ppm and 3.50 ppm ( $\text{H}_8$ ,  $\text{H}_8'$ ,  $\text{H}_9$ ,  $\text{H}_9'$ ), and the multiplet centred at 1.81 ppm ( $\text{H}_5$ ,  $\text{H}_6$ ) form two equivalent ABX systems: ( $\text{H}_8$ ,  $\text{H}_8'$  and  $\text{H}_6$ ) and ( $\text{H}_9$ ,  $\text{H}_9'$  and  $\text{H}_5$ ).

Figure 2.6:  $^1\text{H}$  NMR spectrum of *exo,exo*-5,6-bis(hydroxymethyl)-7-oxabicyclo[2.2.1]hept-2-ene (monomer **II**) recorded at 399.952 MHz in  $\text{CDCl}_3$ .

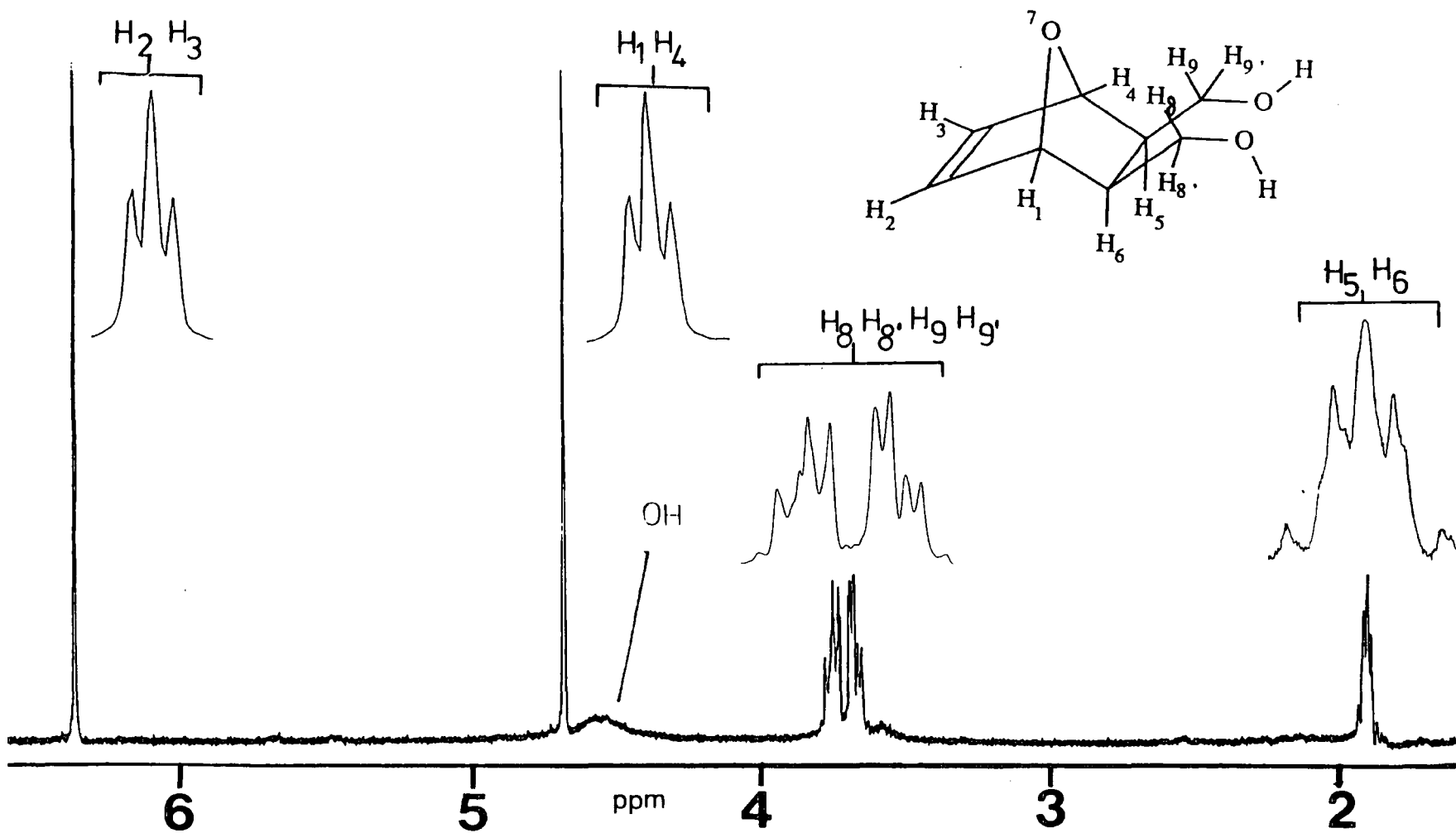
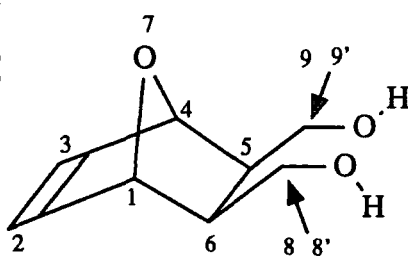


TABLE 2.3: Principal  $^1\text{H}$  NMR spectral parameters<sup>1</sup> for monomer II (399.952 MHz,  $\text{CDCl}_3$ ).

monomer II	shift/ ppm	multiplicity	inte- gral	assign- ment
	6.46	multiplet $J_{2,1} = 1.0 \text{ Hz}$ $J_{3,1} = 1.0 \text{ Hz}$	} 2	2, 3
	4.83	multiplet $J_{1,2} = 1.0 \text{ Hz}$ $J_{1,3} = 1.0 \text{ Hz}$		
	3.85- 3.50	multiplet $\delta_8 = 3.71 \text{ ppm}$ $\delta_{8'} = 3.62 \text{ ppm}$ $\delta_6 = 1.81 \text{ ppm}$	} 4 +	8, 9
	1.81	$J_{8,8'} \approx 10.7 \text{ Hz}$ $J_{8,6} \approx 7.9 \text{ Hz}$ $J_{8',6} \approx 5.4 \text{ Hz}$		

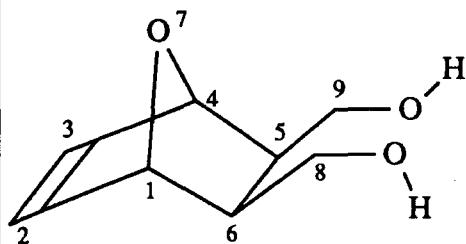
1) with respect to acetone at 7.26 ppm.

The methylene resonances centred at 3.71 ppm ( $\text{H}_8 \equiv \text{H}_9$ ) and 3.62 ppm ( $\text{H}_{8'} \equiv \text{H}_{9'}$ ) couple with each other and with the methine proton centred at 1.81 ppm ( $\text{H}_6 \equiv \text{H}_5$ ) with coupling constants:  $J_{8,8'} \approx 10.7 \text{ Hz}$ ;  $J_{8,6} \approx 7.9 \text{ Hz}$ ; and  $J_{8',6} \approx 5.4 \text{ Hz}$ . This is consistent with the methylene of the hydroxymethyl group being conformationally locked.

The proton decoupled  $^{13}\text{C}$  NMR spectrum is consistent with the structure of monomer II, and is shown in appendix A2, with chemical shifts recorded in Table 2.4. The infrared spectrum of monomer II was recorded from a KBr disc (appendix B2), and is consistent with the assigned structure: hydroxyl O-H stretches at  $3450 \text{ cm}^{-1}$ , alkene C-H stretches at  $2940 \text{ cm}^{-1}$ , and  $2880 \text{ cm}^{-1}$ , and ether

C-O stretches at  $1035\text{cm}^{-1}$ .

TABLE 2.4: Principal  $^{13}\text{C}$  NMR spectral parameters<sup>1</sup> for monomer II (100.577 MHz,  $\text{CDCl}_3$ ).

monomer II	shift/ ppm	assignment
	135.62	2, 3
	81.06	1, 4
	62.46	8, 9
	42.14	5, 6

1) with respect to acetone at 77.44 ppm.

The chemical ionisation mass spectrum (appendix C2) contains a base peak at 68 ( $\text{C}_4\text{H}_4\text{O}^+$ ) resulting from a retro Diels-Alder reaction, although no corresponding but-2-ene-1,4-diol peak is observed. The molecular ions are at 174 ( $\text{M} + \text{NH}_4^+$ ) and 157 ( $\text{M} + \text{H}^+$ ) and are surprisingly intense by comparison with related structures. The mass spectrum is consistent with the assigned structure.

## 2.5: Synthesis and characterisation of

### *exo,exo*-5,6-bis(methoxymethyl)-7-oxabicyclo[2.2.1]hept-2-ene (III).

#### 2.5.1 *Synthesis of monomer III:*

The methylation of monomer II to yield monomer III is shown in Figure 2.7, which also records the numbering system employed.

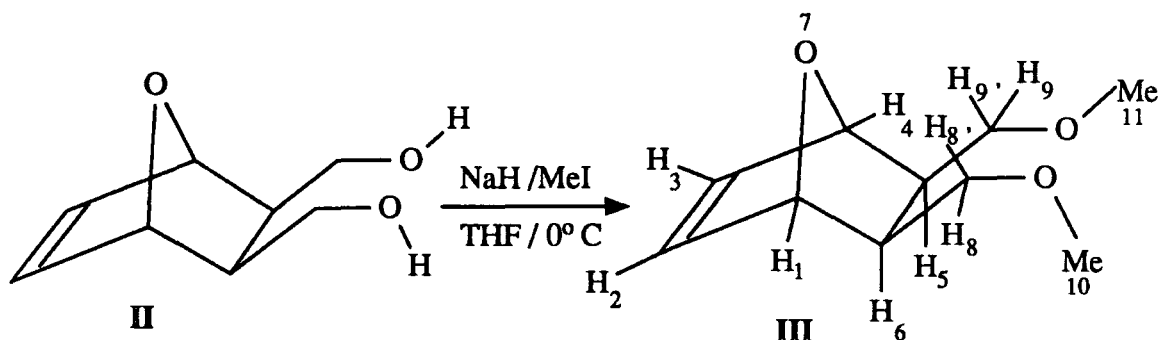


Figure 2.7: Methylation of monomer II to yield monomer III.

CH<sub>3</sub>I (22.5ml, 356 mmol) was added with stirring to a solution of monomer II (6.92g, 44.4 mmol) in dry THF (250ml). The reaction vessel was cooled to 0°C and kept under a nitrogen atmosphere during the further addition of NaH (4.0g, 167 mmol).<sup>96</sup> Filtration of the slurry after 24 hours followed by evaporation of the solvent afforded the product adsorbed onto salt. The solid was taken up into water (20ml) and the product extracted with 3x 200ml diethyl ether. Drying of the combined ether extracts with MgSO<sub>4</sub> followed by evaporation yielded the crude product. Purification by distillation afforded III as a colourless liquid in 85% yield.<sup>72</sup> (b.pt. 68°C @ 3x10<sup>-1</sup> torr) (Elemental analysis; found: C,65.0%, H,8.8% ; calculated for C<sub>10</sub>H<sub>16</sub>O<sub>3</sub>: C,65.2%, H,8.7%)

### 2.5.2 Characterisation of monomer III:

The <sup>1</sup>H NMR spectrum of monomer III is shown in Figure 2.8, with the chemical shifts recorded in Table 2.5. Protons H<sub>1</sub>, H<sub>2</sub>, H<sub>3</sub> and H<sub>4</sub> form an A<sub>2</sub>X<sub>2</sub> system with J<sub>2,3</sub> → 0, J<sub>1,4</sub> → 0, and J<sub>1,2</sub> ≈ J<sub>1,3</sub> ≈ 1.0 Hz. The small coupling constants observed are consistent with the torsion angles between the coupled protons, namely 29.4° between H<sub>1</sub> and H<sub>2</sub>, and 49.8° between H<sub>1</sub> and H<sub>3</sub>.

Figure 2.8:  $^1\text{H}$  NMR spectrum of *exo,exo*-5,6-bis(methoxymethyl)-7-oxabicyclo-[2.2.1]hept-2-ene (monomer **III**) recorded at 399.952 MHz in  $(\text{CD}_3)_2\text{CO}$ .

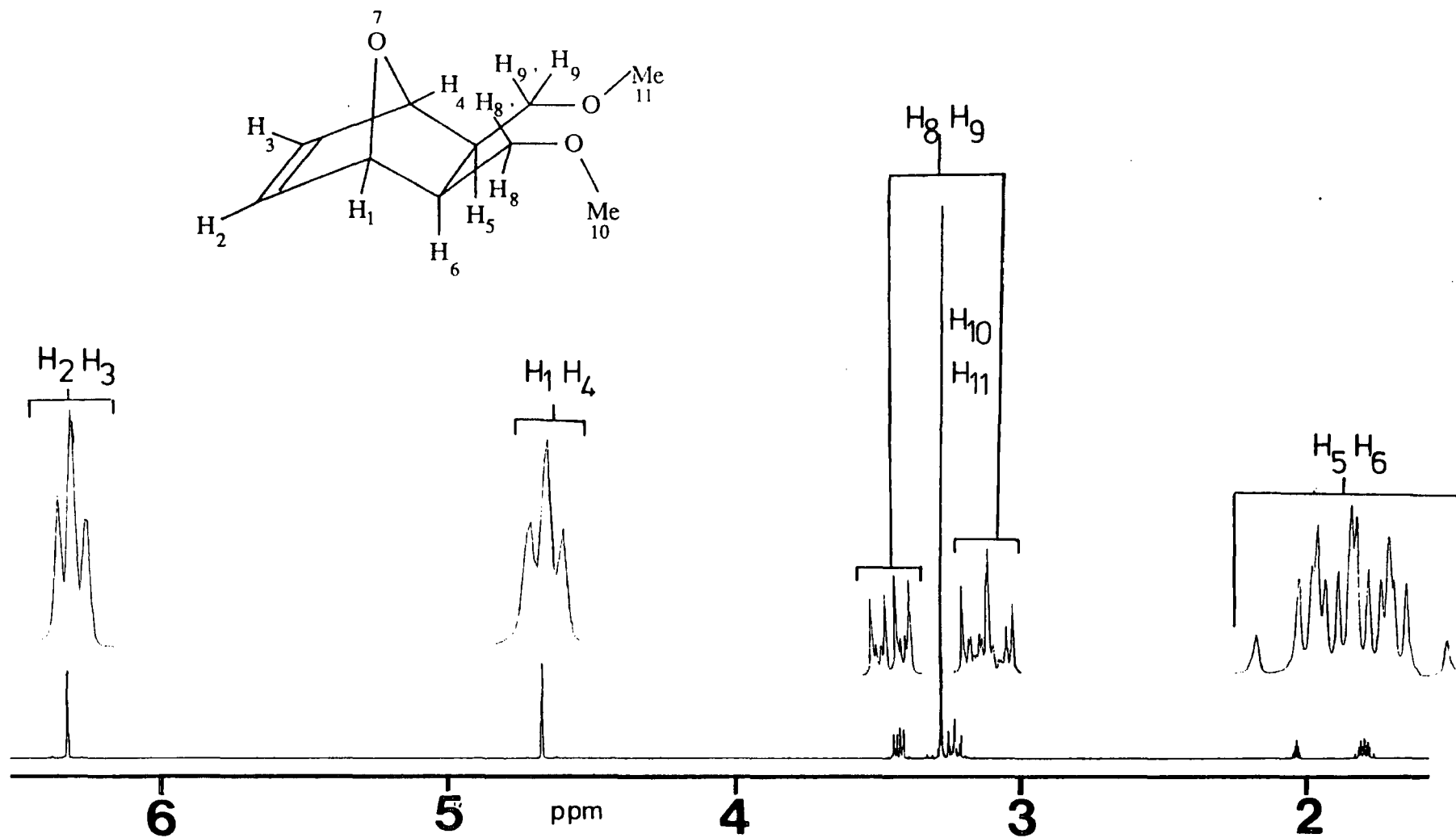
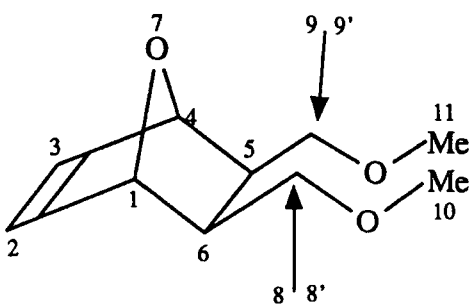


TABLE 2.5: Principal  $^1\text{H}$  NMR spectral parameters<sup>1</sup> for monomer III (399.952 MHz,  $(\text{CD}_3)_2\text{CO}$ ).

monomer III	shift/ ppm	multiplicity	inte- gral	assign- ment
	6.32	multiplet $J_{2,1} \approx 1.0$ Hz $J_{3,1} \approx 1.0$ Hz	2	2, 3
	4.68	multiplet $J_{1,2} \approx 1.0$ Hz $J_{1,3} \approx 1.0$ Hz	2	1, 4
	3.45 - 3.42 and 3.26 - 3.21	2 multiplets  $\delta_8 = 3.44$ ppm $\delta_{8'} = 3.24$ ppm $J_{8,8'} \approx 8.8$ Hz $J_{8,6} \approx 8.8$ Hz $J_{8',6} \approx 5.2$ Hz	4	8, 9
	1.80	multiplet  $\delta_6 = 1.80$ ppm	2	6, 5
	3.28	singlet	6	10, 11

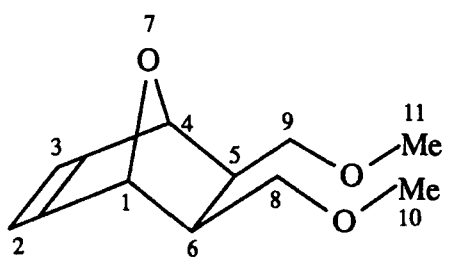
1) with respect to acetone at 2.04 ppm.

Proton resonances between 3.45 and 3.42 ppm ( $\text{H}_8, \text{H}_9$ ), between 3.26 and 3.21 ppm ( $\text{H}_{8'}, \text{H}_{9'}$ ), and the multiplet centred at 1.80 ppm ( $\text{H}_5, \text{H}_6$ ) form two equivalent ABX systems: ( $\text{H}_8, \text{H}_{8'}$  and  $\text{H}_6$ ) and ( $\text{H}_9, \text{H}_{9'}$  and  $\text{H}_5$ ). The methylene resonances centred at 3.44 ppm ( $\text{H}_8 \equiv \text{H}_9$ ) and 3.24 ppm ( $\text{H}_{8'} \equiv \text{H}_{9'}$ ) couple with each other and with the methine proton centred at 1.80 ppm ( $\text{H}_6 \equiv \text{H}_5$ ) with coupling constants:  $J_{8,8'} \approx 8.8$  Hz;  $J_{8,6} \approx 5.4$  Hz; and  $J_{8',6} \approx 8.8$  Hz. This is consistent with the methylene of the methoxymethyl group being conformationally locked. The methyl protons of the methoxymethyl group resonate as a singlet at

3.28 ppm.

The proton decoupled  $^{13}\text{C}$  NMR spectrum is consistent with the structure of monomer **III**, and is shown in appendix A3, with chemical shifts recorded in Table 2.6.

TABLE 2.6: Principal  $^{13}\text{C}$  NMR spectral parameters<sup>1</sup> for monomer **III** (100.577 MHz,  $(\text{CD}_3)_2\text{CO}$ ).

monomer <b>III</b>	shift/ ppm	assignment
	136.26	2, 3
	81.09	1, 4
	72.77	8, 9
	58.72	10, 11
	40.64	5, 6

1) with respect to acetone at 29.82 ppm.

The infrared spectrum of monomer **III** was recorded from a KBr disc (appendix B3), and is consistent with the assigned structure: alkane C-H stretches between  $3000\text{cm}^{-1}$  and  $2800\text{cm}^{-1}$ ; and ether C-O stretches  $1130\text{cm}^{-1}$ , and  $1100\text{cm}^{-1}$ . The chemical ionisation mass spectrum (appendix C3) shows a base peak at 117 ( $\text{C}_6\text{H}_{13}\text{O}_2^+$ ) resulting from a retro Diels-Alder reaction, and a corresponding furan peak at 68 ( $\text{C}_4\text{H}_4\text{O}^+$ ). The molecular ion is observed at 202 ( $\text{M} + \text{NH}_4^+$ ), although this is weak. The mass spectrum is consistent with the assigned structure.



## 2.6: Synthesis and characterisation of

### *exo,exo*-7-oxabicyclo[2.2.1]hept-5-ene-2,3-bis(carboxylic acid) (IV).

#### 2.6.1 *Synthesis of monomer IV:*

The hydrolysis of monomer I to yield monomer IV is shown in Figure 2.9, which also records the numbering system employed.

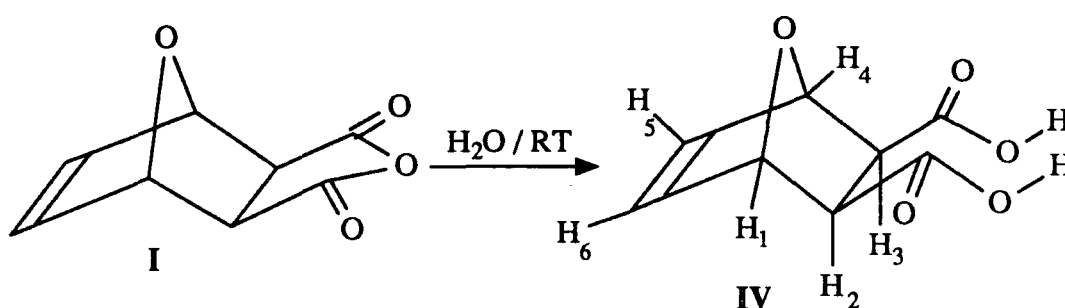


Figure 2.9: Hydrolysis of monomer I to yield monomer IV.

Monomer I (50g, 0.30 mol) was dissolved in distilled water (200ml) with stirring for 4 hours.<sup>97</sup> After 24 hours colourless crystals formed at the bottom of the reaction vessel; the product was filtered after 48 hours to afford IV in 50% yield with respect to monomer I. (m.pt. 133.5°C, Lit.<sup>97</sup> 134.0°C) (Elemental analysis; found: C,52.1%, H-4.1% ; calculated for C<sub>8</sub>H<sub>8</sub>O<sub>5</sub>: C,52.2% H,4.3%).

#### 2.6.2 *Characterisation of monomer IV:*

The <sup>1</sup>H NMR spectrum of monomer IV is shown in Figure 2.10, with the chemical shifts recorded in Table 2.7; all the resonances in the spectrum are broad singlets. The proton decoupled <sup>13</sup>C NMR spectrum is consistent with the structure of monomer IV, and is shown in appendix A4, with chemical shifts recorded in Table 2.8.

Figure 2.10:  $^1\text{H}$  NMR spectrum of *exo,exo*-7-oxabicyclo[2.2.1]hept-5-ene-2,3-bis(carboxylic acid) (monomer IV) recorded at 399.952 MHz in  $\text{D}_2\text{O}$ .

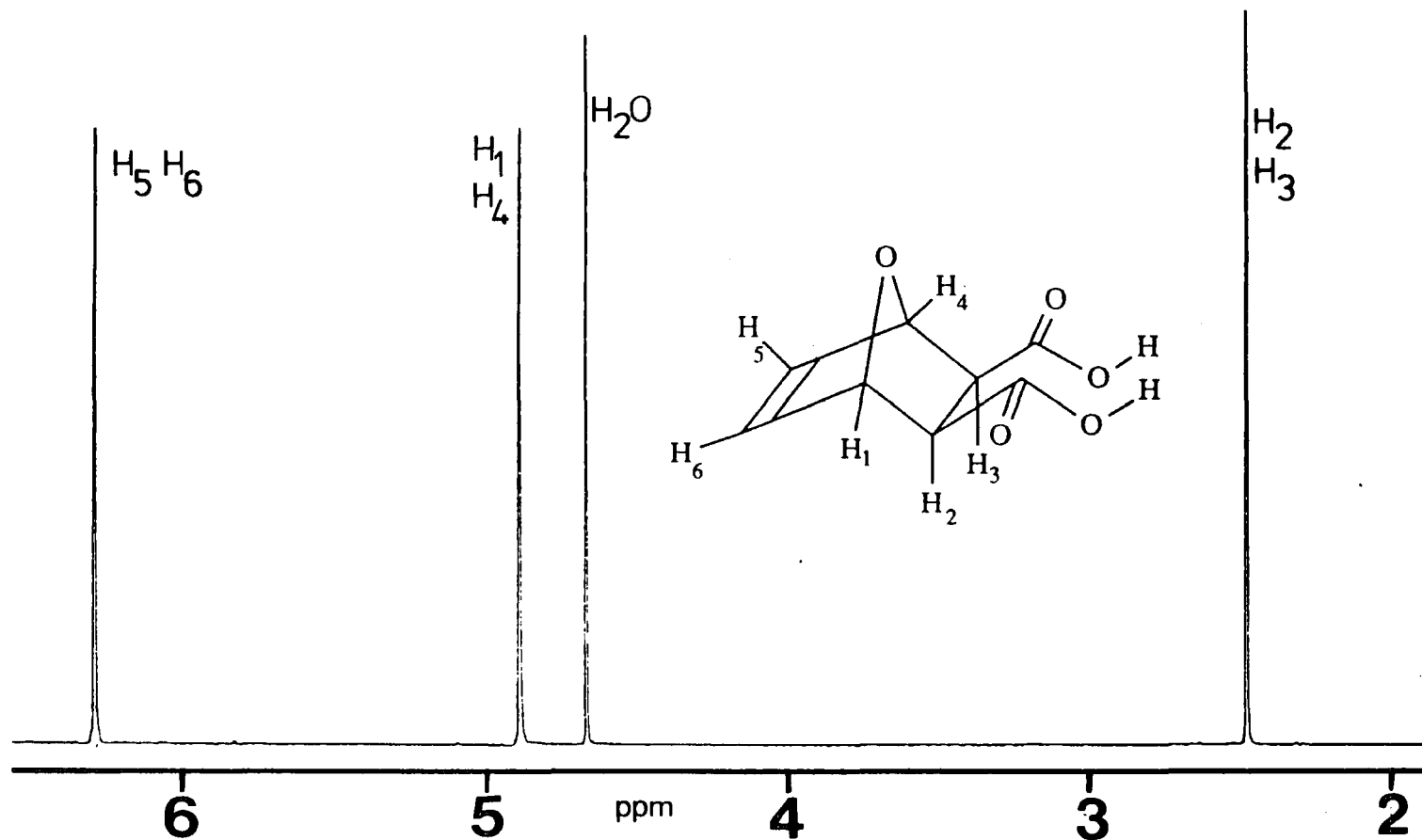
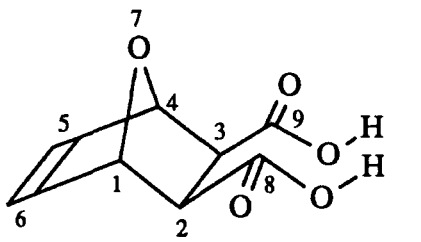
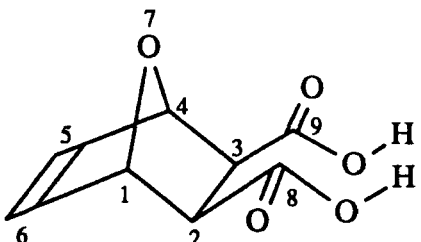


TABLE 2.7: Principal  $^1\text{H}$  NMR spectral parameters<sup>1</sup> for monomer IV (399.952 MHz,  $\text{D}_2\text{O}$ ).

monomer IV	shift/ ppm	multiplicity	inte- gral	assign- ment
	6.29	singlet	2	5, 6
	4.89	singlet	2	1, 4
	2.48	singlet	2	2, 3

1) with respect to water at 4.67 ppm.

TABLE 2.8: Principal  $^{13}\text{C}$  NMR spectral parameters<sup>1</sup> for monomer IV (100.577 MHz,  $\text{D}_2\text{O}$ ).

monomer IV	shifts/ ppm	assignments
	184.49	8, 9
	139.75	5, 6
	84.57	1, 4
	52.61	2, 3

1) with respect to  $(\text{Me}_3\text{Si})\text{CD}_2\text{CD}_2\text{CO}_2\text{Na}$  at 1.70 ppm.

The infrared spectrum of the disodium salt of monomer IV was recorded from a KBr disc (appendix B4), and is consistent with the assigned structure; the carbonyl  $\text{C}=\text{O}$  stretch at  $1680\text{cm}^{-1}$  corresponds to a free carboxylate. The chemical ionisation mass spectrum (appendix C4) contains a base peak at 68 ( $\text{C}_4\text{H}_4\text{O}^+$ ),

corresponding to the retro Diels-Alder product, and a weak molecular ion peak at 202 ( $M + NH_4^+$ ); the mass spectrum is consistent with the assigned structure.

## 2.7: Synthesis and characterisation of

### *exo,exo*-7-oxabicyclo[2.2.1]hept-5-ene-2,3-bis(carboxymethyl ester) (V).

#### 2.7.1 *Synthesis of monomer V:*

**NOTE:** During the synthesis and purification of this monomer the author suffered a severe skin irritation on both hands and forearms. The cause of irritation is still not known. It is suspected that it did not result from contact with the actual monomer, but from contact with some side products, or combinations of materials associated with this synthesis.

The Diels-Alder reaction between furan and dimethyl maleate is shown in Figure 2.11, which also records the numbering system employed.

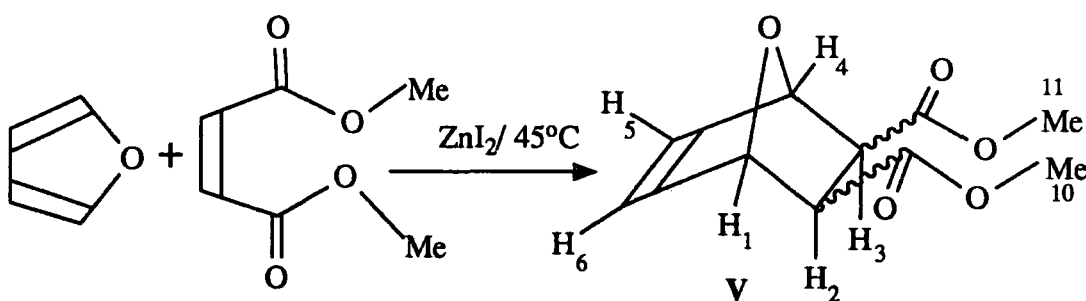


Figure 2.11: The Diels-Alder reaction between furan and dimethyl maleate to yield monomer V.

The reaction is slow at low temperatures and atmospheric pressures, where it can take several months,<sup>98</sup> but proceeds to 90% conversion after eight hours at 15 Kbar and 27°C, with 20% of the product being the *exo* adduct.<sup>99</sup> When zinc iodide

is used as an accelerator at 40°C under normal atmospheric pressure, the reaction affords 50% conversion after two days, with 60% of the product being the *exo* adduct.<sup>100</sup>

Furan (19.6g, 0.29 mol) and dimethyl maleate (28.8g, 0.2 mol) were heated at 45°C in an enclosed vessel under a nitrogen atmosphere in the presence of ZnI<sub>2</sub> (19.1g, 60 mmol).<sup>100</sup> After 48 hours, ethyl acetate (500ml) was added to the product mixture at room temperature, and the resulting slurry was washed with 0.1M sodium thiosulphate (100ml); the organic layer was recovered and dried over anhydrous MgSO<sub>4</sub>. Removal of the solvent by evaporation afforded a mixture of the *exo* isomer, dimethyl maleate, and unidentified coloured by-products; the *endo* isomer decomposed during this work up procedure. The combined products were taken up into dichloromethane (100ml), and decolourised with charcoal. After filtration the brown solution was chromatographed on a neutral alumina column (30mm x 150mm) with dichloromethane as eluent. Evaporation of the solvent yielded white crystals and dimethyl maleate; the crystals were recovered by filtration and recrystallised from dichloromethane to afford **V** in 30% yield. (m.pt. 121.2°C, Lit.<sup>99</sup> 120-121°C) (Elemental analysis; found: C,56.3%, H,5.7% ; calculated for C<sub>10</sub>H<sub>12</sub>O<sub>5</sub>: C,56.6%, H,5.7%)

### 2.7.2 Characterisation of monomer **V**:

The <sup>1</sup>H NMR spectrum of monomer **V** is shown in Figure 2.12, with the chemical shifts recorded in Table 2.9; all the resonances in the spectrum are singlets. The proton decoupled <sup>13</sup>C NMR spectrum is consistent with the structure of monomer **V**, and is shown in appendix A5, with chemical shifts recorded in Table 2.10.

Figure 2.12:  $^1\text{H}$  NMR spectrum of *exo,exo*-7-oxabicyclo[2.2.1]hept-5-ene-2,3-bis(carboxymethyl ester) (monomer V) recorded at 250.133 MHz in  $\text{CDCl}_3$ .

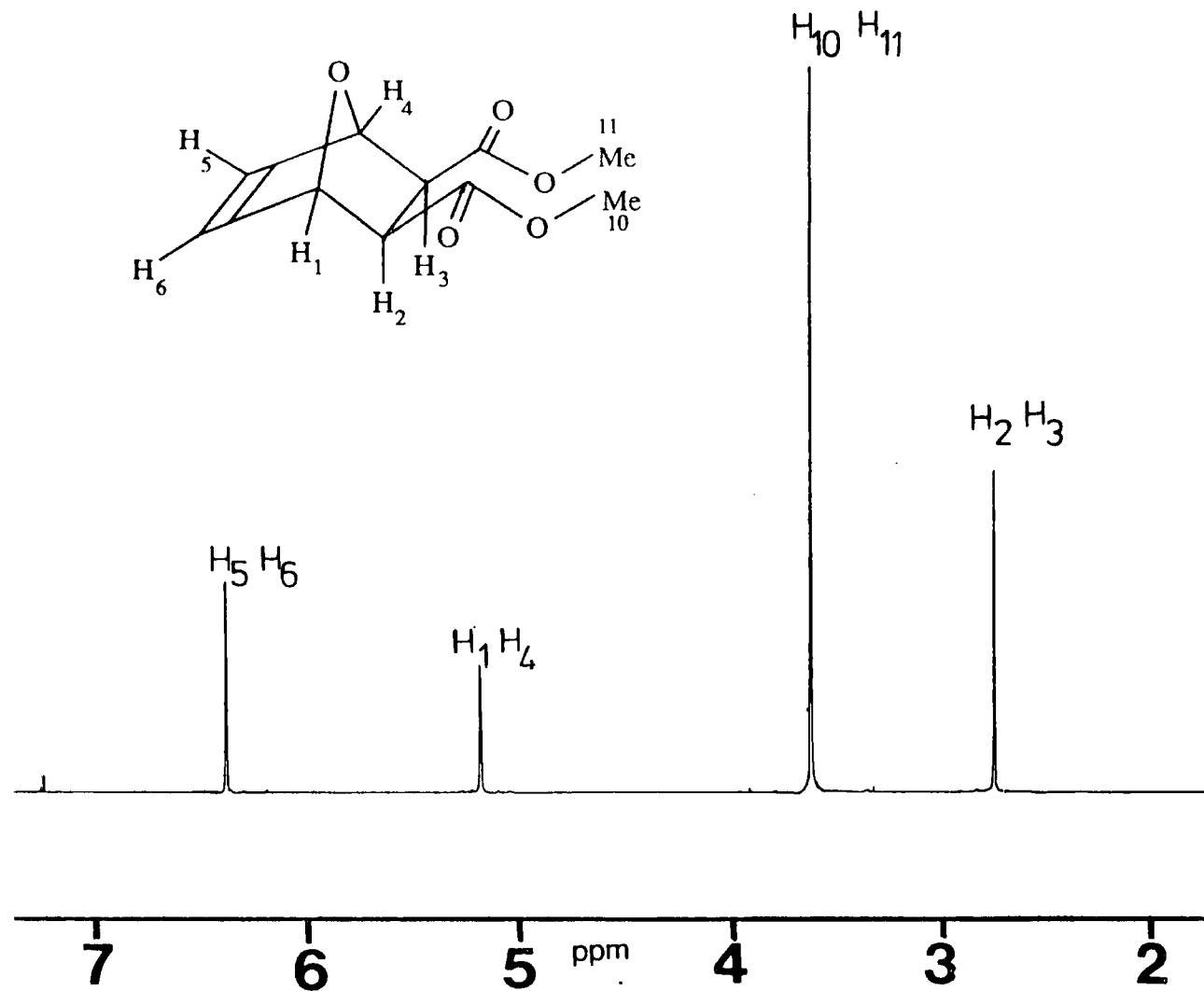
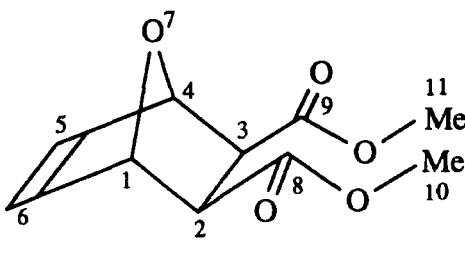
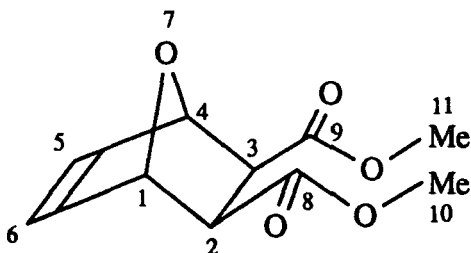


TABLE 2.9: Principal  $^1\text{H}$  NMR spectral parameters<sup>1</sup> for monomer V (250.133 MHz,  $\text{CDCl}_3$ ).

monomer V	shift/ ppm	multiplicity	inte- gral	assign- ment
	6.39	singlet	2	5, 6
	5.19	singlet	2	1, 4
	3.62	singlet	6	10, 11
	2.75	singlet	2	2, 3

1) with respect to chloroform at 7.26 ppm.

TABLE 2.10: Principal  $^{13}\text{C}$  NMR spectral parameters<sup>1</sup> for monomer V (62.896 MHz,  $\text{CDCl}_3$ ).

monomer V	shift/ ppm	assignment
	172.20	8, 9
	136.90	5, 6
	80.72	1, 4
	52.50	10, 11
	47.20	2, 3

1) with respect to chloroform at 77.44 ppm.

The infrared spectrum (appendix B5) of monomer V was recorded from a KBr disc, and is consistent with the assigned structure; carbonyl  $\text{C}=\text{O}$  stretch at

1770 $\text{cm}^{-1}$ , and alkane C-H stretches between 2989 $\text{cm}^{-1}$  and 2845 $\text{cm}^{-1}$ . The chemical ionisation mass spectrum (appendix C5) has a weak molecular ion at 230 ( $M + \text{NH}_4^+$ ) with a base peak at 145 ( $\text{C}_6\text{H}_9\text{O}_4^+$ ) resulting from the retro Diels-Alder reaction.

## 2.8: Synthesis and characterisation of exo-bicyclo[2.2.1]hept-5-ene-2,3-dicarboxy anhydride (VI).

### 2.8.1 *Synthesis of monomer VI:*

The Diels-Alder reaction between cyclopentadiene and maleic anhydride is shown in Figure 2.13, which also records the numbering system employed.

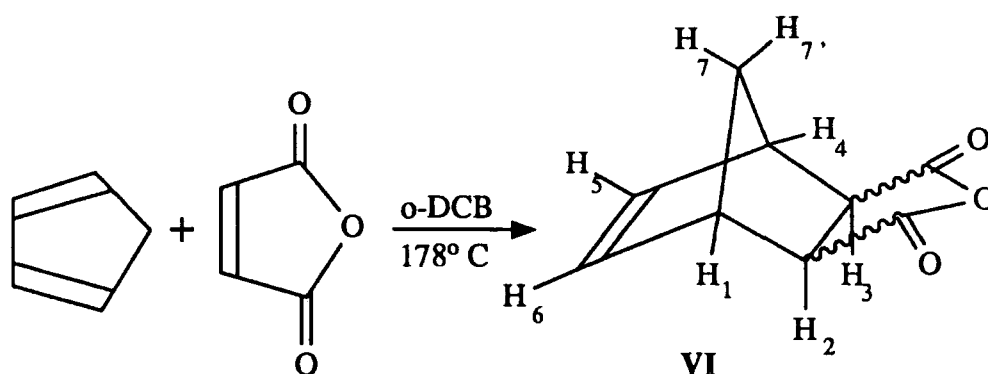


Figure 2.13: Diels-Alder reaction between maleic anhydride and cyclopentadiene to yield monomer VI.

The ratio of *exo* to *endo* adducts produced by this reaction is strongly dependant on the temperature; at room temperature the pure *endo* adduct is formed.<sup>85</sup> When the reaction is performed at 178°C the thermodynamic equilibrium mixture *exo* to *endo* of 55:45 is formed.<sup>85</sup>

Dicyclopentadiene (66g, 0.5 mol) was added dropwise to maleic anhydride



(98g, 1.0 mol) in *o*-dichlorobenzene (200 ml) over a period of two hours. The reflux temperature of 178°C was maintained during the addition, and rose to 184°C after the addition was complete. After a further two hours the reaction mixture was cooled to room temperature and the solid products recovered by filtration. The *exo* adduct has lower solubility in chlorobenzene than the *endo* adduct, and could be isolated by four successive recrystallisations from chlorobenzene to afford VI in 30% yield. Monomer VI was found to be 99.5% pure by NMR spectroscopy. (m.pt 142.5°C, Lit.<sup>85</sup> 143.0°C) (Elemental analysis; found: C,65.6%, H,4.7% ; calculated for C<sub>9</sub>H<sub>8</sub>O<sub>3</sub>: C,65.9%, H,4.9%).

### 2.8.2 Characterisation of monomer VI:

The <sup>1</sup>H NMR spectrum of monomer VI is shown in Figure 2.14, with the chemical shifts recorded in Table 2.11.

Protons H<sub>1</sub>, H<sub>6</sub>, H<sub>5</sub> and H<sub>4</sub> form an A<sub>2</sub>X<sub>2</sub> system with J<sub>5,6</sub> → 0, J<sub>1,4</sub> → 0, and J<sub>1,6</sub> ≈ J<sub>1,5</sub> ≈ 1.7 Hz. The small coupling constants observed are consistent with the torsion angles between the coupled protons, namely 23.7° between H<sub>1</sub> and H<sub>6</sub>, and 42.7° between H<sub>1</sub> and H<sub>5</sub>. The resonances of protons H<sub>1</sub>, H<sub>6</sub>, H<sub>5</sub> and H<sub>4</sub> are further complicated by coupling with the non-equivalent protons H<sub>7</sub> and H<sub>7'</sub>: J<sub>1,7</sub> ≈ 1.5 Hz; J<sub>1,7'</sub> ≈ 0.7 Hz; J<sub>6,7</sub> ≈ 0.8 Hz; J<sub>6,7</sub> → 0.

The bridgehead protons H<sub>7</sub> and H<sub>7'</sub> form an ABq system, which is coupled to protons H<sub>1</sub> (≡ H<sub>4</sub>), H<sub>6</sub> (≡ H<sub>5</sub>), and H<sub>2</sub> (≡ H<sub>3</sub>); δ<sub>7</sub> = 1.62 ppm and δ<sub>7'</sub> = 1.39 ppm, with J<sub>7,7'</sub> ≈ 10.2 Hz, J<sub>7,1</sub> ≈ 1.5 Hz, J<sub>7',1</sub> ≈ 0.7 Hz, J<sub>7',6</sub> ≈ 0.8 Hz, J<sub>7,2</sub> ≈ 1.5 Hz, J<sub>7,6</sub> → 0, J<sub>7',2</sub> → 0.

Figure 2.14:  $^1\text{H}$  NMR spectrum of *exo*-bicyclo[2.2.1]hept-5-ene-2,3-dicarboxy anhydride (monomer VI) recorded at 399.952 MHz in  $\text{CDCl}_3$ .

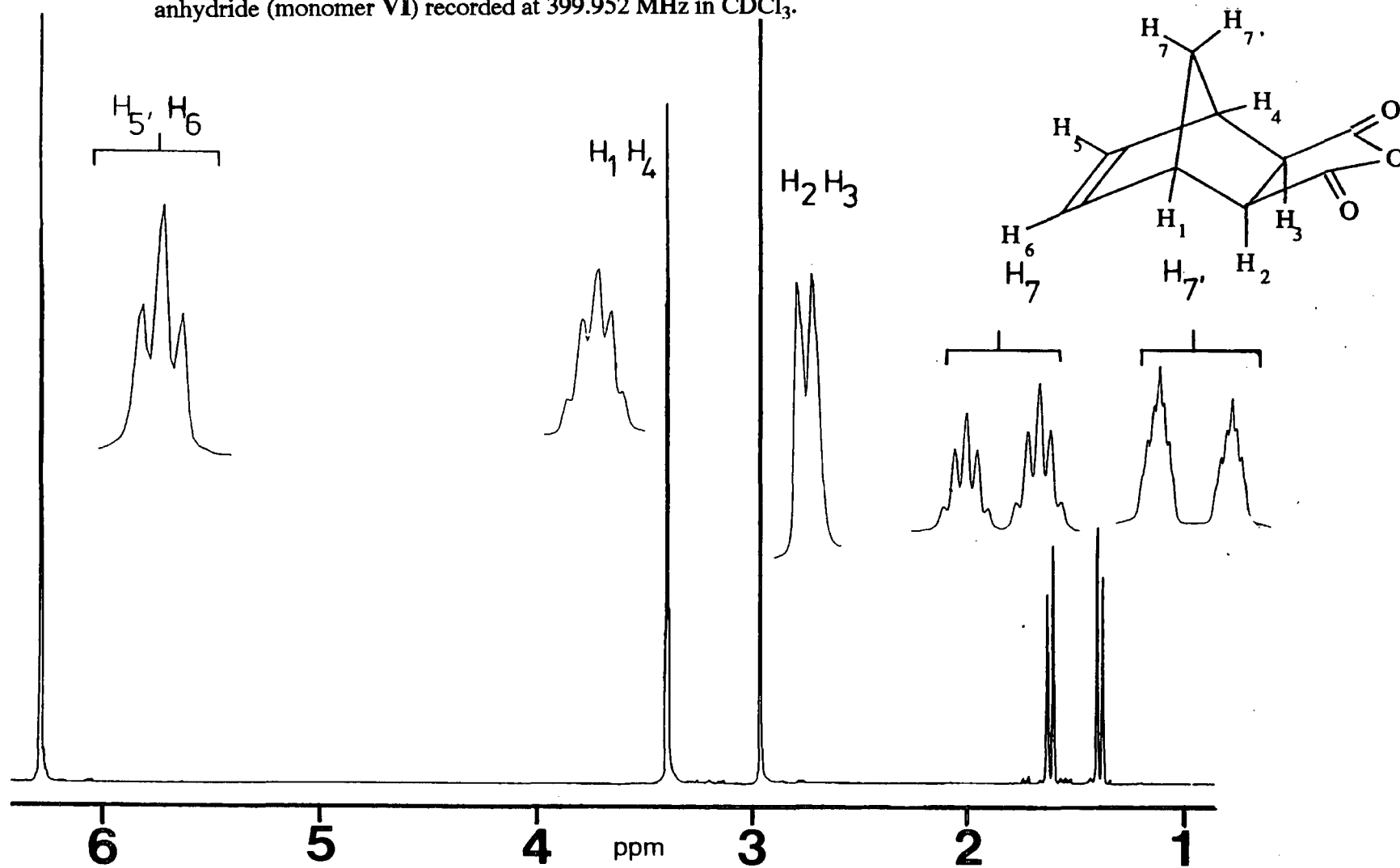
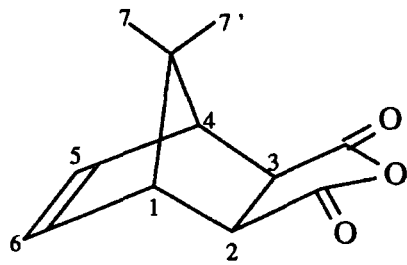


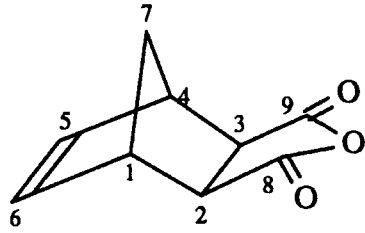
TABLE 2.11: Principal  $^1\text{H}$  NMR spectral parameters<sup>1</sup> for monomer VI (399.952 MHz,  $\text{CDCl}_3$ ).

monomer VI	shift/ ppm	multiplicity	inte- gral	assign- ment
	6.34	multiplet $J_{6,4} \approx 1.7\text{ Hz}$ $J_{6,1} \approx 1.7\text{ Hz}$ $J_{6,7'} \approx 0.8\text{ Hz}$	2	5, 6
	3.46	multiplet $J_{1,6} \approx 1.7\text{ Hz}$ $J_{1,5} \approx 1.7\text{ Hz}$ $J_{1,7} \approx 1.5\text{ Hz}$ $J_{1,7'} \approx 0.7\text{ Hz}$	2	1, 4
	3.02	doublet $J_{2,7} \approx 1.5\text{ Hz}$	2	2, 3
	1.70- 1.65 and	multiplets $\delta_{7'} \approx 1.39\text{ ppm}$	1	7
	1.47- 1.42	$\delta_7 \approx 1.62\text{ ppm}$ $J_{7,7'} = 10.2\text{ Hz}$	1	7'

1) with respect to chloroform at 7.26 ppm.

The proton decoupled  $^{13}\text{C}$  NMR spectrum is consistent with the structure of monomer VI, and is shown in appendix A6, with chemical shifts recorded in Table 2.12. The infrared spectrum (appendix B6) of monomer VI was recorded from a KBr disc, and contains alkane C-H stretches at  $3000\text{cm}^{-1}$ ,  $2970\text{cm}^{-1}$ ,  $2950\text{cm}^{-1}$  and  $2890\text{cm}^{-1}$ , and anhydride C=O stretches at  $1860\text{cm}^{-1}$  and  $1775\text{cm}^{-1}$ . The chemical ionisation mass spectrum (appendix C6) has a strong molecular ion at 182 ( $\text{M} + \text{NH}_4^+$ ), and is consistent with the assigned structure.

TABLE 2.12: Principal  $^{13}\text{C}$  NMR spectral parameters<sup>1</sup> for monomer VI (100.577 MHz,  $\text{CDCl}_3$ ).

monomer VI	shift/ ppm	assignment
	171.57	8, 9
	137.98	5, 6
	48.77	1, 4
	46.89	2, 3
	44.12	7

1) with respect to chloroform at 77.44 ppm.

## 2.9: Synthesis and characterisation of

### exo,exo-bicyclo[2.2.1]hept-5-ene-2,3-bis(carboxylic acid) (VII).

#### 2.9.1 Synthesis of monomer VII:

The hydrolysis of monomer VI to yield monomer VII is shown in Figure 2.15, which also records the numbering system employed.

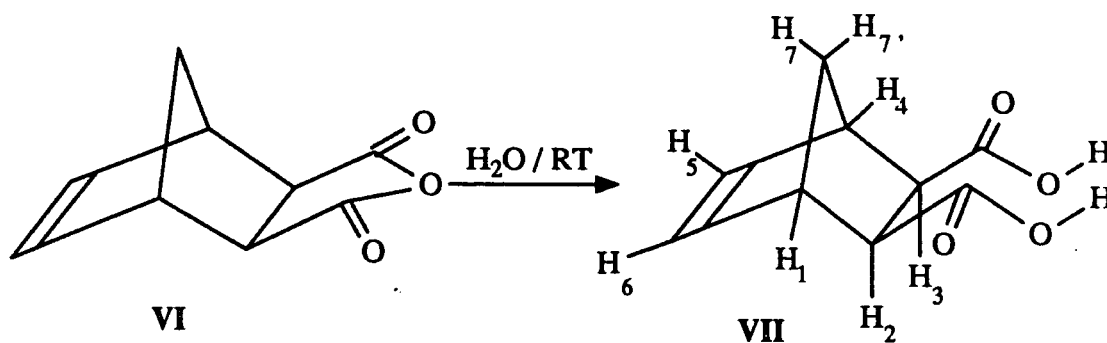


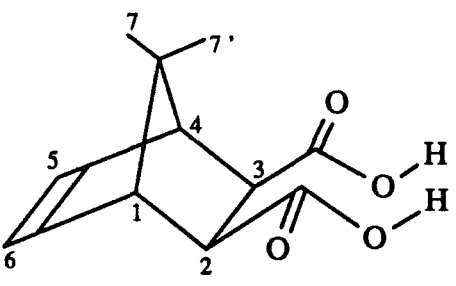
Figure 2.15: Hydrolysis of monomer VI to yield monomer VII.

Monomer VI (50g, 0.28 mol) was dissolved in distilled water (200ml) with stirring for 4 hours. After 24 hours colourless crystals formed at the bottom of the reaction vessel; the product was filtered after 48 hours to afford VII as its monohydrate in 40% yield. (m.pt. 152°C, Lit.<sup>101</sup> 153°C) (Elemental analysis; found; C,53.9%, H,6.2% ; calculated for C<sub>9</sub>H<sub>10</sub>O<sub>4</sub>.H<sub>2</sub>O: C,54.0%, H,6.0%).

### 2.9.2 Characterisation of monomer VII:

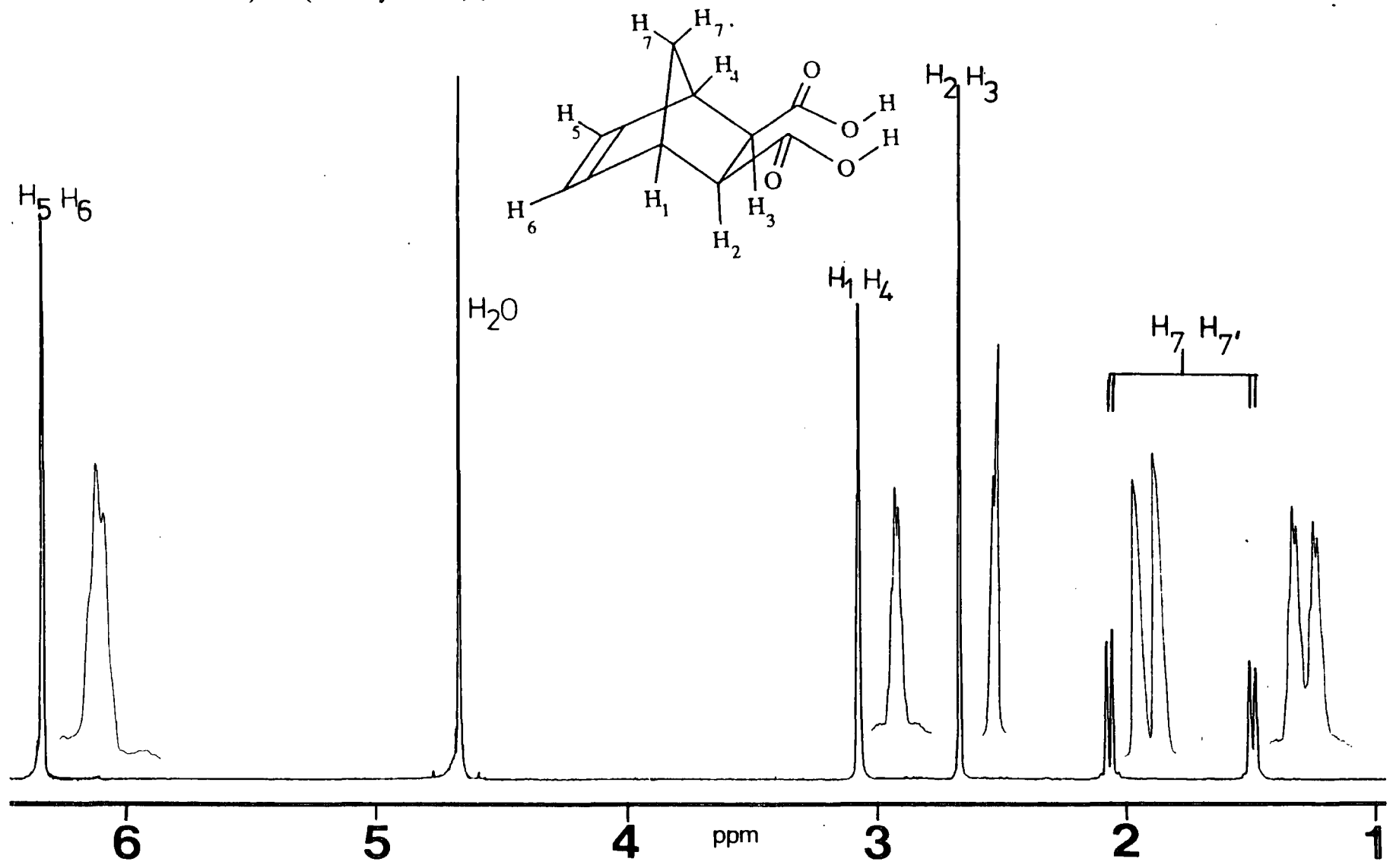
The <sup>1</sup>H NMR spectrum of monomer VII is shown in Figure 2.16, with the chemical shifts recorded in Table 2.13.

TABLE 2.13: Principal <sup>1</sup>H NMR spectral parameters<sup>1</sup> for monomer VII (399.952 MHz, D<sub>2</sub>O).

monomer VII	shift/ ppm	multiplicity	inte- gral	assign- ment	
	6.33	multiplet J <sub>6,1</sub> ≈ 1.6 Hz J <sub>6,4</sub> ≈ 1.6 Hz	2	5, 6	
	3.08	multiplet J <sub>1,6</sub> ≈ 1.6 Hz J <sub>1,5</sub> ≈ 1.6 Hz	2	1, 4	
	2.67	singlet	2	2, 3	
	2.08	multiplet	2	7, 7'	
	2.06	δ <sub>7</sub> ≈ 2.07 ppm			
	1.51	δ <sub>7'</sub> ≈ 1.49 ppm			
1.48	J <sub>7,7'</sub> ≈ 8.5 Hz J <sub>7',6</sub> ≈ 1.5 Hz				

1) with respect to water at 4.67 ppm.

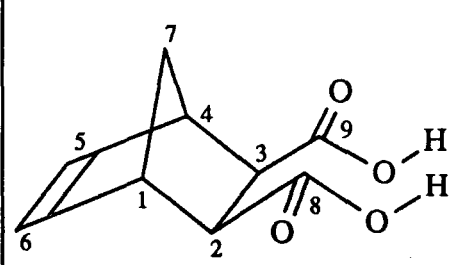
Figure 2.16:  $^1\text{H}$  NMR spectrum of *exo,exo*-bicyclo[2.2.1]hept-5-ene-2,3-bis(carboxylic acid) (monomer VII) recorded at 399.952 MHz in  $\text{D}_2\text{O}$ .



Protons  $H_1$ ,  $H_6$ ,  $H_5$  and  $H_4$  form an  $A_2X_2$  system with  $J_{5,6} \rightarrow 0$ ,  $J_{1,4} \rightarrow 0$ , and  $J_{1,6} \approx J_{1,5} \approx 1.6$  Hz. The bridgehead protons form an ABq system;  $\delta_7 = 2.07$  ppm and  $\delta_{7'} = 1.49$  ppm, with  $J_{7,7'} \approx 8.5$  Hz and  $J_{7',6} \approx 1.5$  Hz.

The proton decoupled  $^{13}\text{C}$  NMR spectrum is consistent with the structure of monomer VII, and is shown in appendix A7, with chemical shifts recorded in Table 2.14.

TABLE 2.14: Principal  $^{13}\text{C}$  NMR spectral parameters<sup>1</sup> for monomer VII (100.577 MHz,  $\text{D}_2\text{O}$ ).

monomer VII	shift/ ppm	assignment
	184.51	8, 9
	142.69	5, 6
	53.22	1, 4
	50.12	2, 3
	49.37	7

1) with respect to  $(\text{Me}_3\text{Si})\text{CD}_2\text{CD}_2\text{CO}_2\text{Na}$  at 1.70 ppm.

The infrared spectrum (appendix B7) recorded from a KBr disc contains a carbonyl stretch at  $1738\text{cm}^{-1}$ , which is consistent with association of carboxylate units. The chemical ionisation mass spectrum (appendix C7) contains a base peak at 200 ( $\text{M} + \text{NH}_4^+$ ), and is consistent with the assigned structure.

**CHAPTER 3:  
SYNTHESIS AND  
CHARACTERISATION  
OF POLYMERS.**



### 3.1: Introduction.

The objectives of the work described in this chapter are the syntheses of high molecular weight polymers via aqueous ROMP, and the characterisation of the products. The attempted ROMP of monomers II, III, IV, V, and VII using various transition metal chlorides as the precursors to the initiating and chain propagating species are described. The initiating species are formed *in situ*, and are not well defined. Each is presumed to contain a metal carbene on the basis of analogy between the structures of the products and those of ROMP polymers formed in well understood processes.<sup>22</sup>

### 3.2: General Details.

#### 3.2.1 *Reactants:*

The aqueous ROMP of the monomers prepared in chapter 2 was attempted in doubly distilled water, and using various transition metal chlorides as the precursors to the initiating and chain propagating species. The transition metal chlorides,  $\text{RuCl}_3 \cdot 3\text{H}_2\text{O}$ ,  $\text{OsCl}_3 \cdot 3\text{H}_2\text{O}$ ,  $\text{IrCl}_3 \cdot 3\text{H}_2\text{O}$ ,  $\text{RhCl}_3 \cdot 3\text{H}_2\text{O}$  and  $\text{PdCl}_2$  (Aldrich Chemical Co. Ltd.), and the solvents (BDH) for the polymer recovery stages, were all used as supplied.

#### 3.2.2 *Polymer characterisation:*

The NMR spectra of the polymers prepared in this chapter were recorded using a Varian VXR-400-S NMR spectrometer, operating at 399.952 MHz for  $^1\text{H}$  NMR, and 100.577 MHz for  $^{13}\text{C}$  NMR. The infrared spectra of the polymers were

recorded with either a Nicolet 730 FTIR or a Perkin Elmer 577 infrared spectrometer.

The molecular weights of water soluble polymers, **PIVb** and **PVIIb**, were assessed by aqueous Gel Permeation Chromatography (GPC) in saline buffer (pH. 6) of composition 0.141 M sodium chloride, 0.008 M sodium phosphate (monobasic) and 0.003 M sodium phosphate (dibasic). The equipment comprised of a Knauer HPLC 64 pump, Rheodyne 7125 injector with 100 $\mu$ l loop, Knauer refractive index detector and PLaquagel P3 30cm column (Polymer Laboratories Ltd.). Molecular weight calculations were made with a Chromatocorder 12 integrator (Quadrant Scientific) calibrated with polyethylene oxide standards (Polymer Laboratories Ltd.). All molecular weight data for polymers **PIVb** and **PVIIb** are expressed in polyethylene oxide equivalent molecular weights.

The molecular weight of THF soluble polymers, **PIII** and **PV**, were assessed by non-aqueous GPC using THF as eluent. The equipment comprised of a Waters model 590 HPLC pump, Waters R401 Refractive Index (RI) detector, Waters U6K injection valve with 200 $\mu$ l injection loop, and a three column set: 5 $\mu$  10<sup>5</sup> $\text{\AA}$  30cm + 5 $\mu$  10<sup>3</sup> $\text{\AA}$  30cm + 5 $\mu$  100 $\text{\AA}$  30cm (Polymer Laboratories Ltd.). Molecular weight calculations were made with a Chromatocorder 12 integrator (Quadrant Scientific) calibrated with polystyrene standards (Polymer Laboratories Ltd.). All molecular weight data for polymers **PIII** and **PV** are expressed in polystyrene equivalent molecular weights.

### 3.2.3 *Computer modelling:*

Theoretical calculations of bond lengths and angles in the polymers were made using a transputer based computer modelling system, custom built for Ciba-Geigy Industrial Chemicals. The hardware comprised of 16 INMOS floating point transputers in network with an IBM 80 personal computer, and DIGISOLE

BGP64 graphics processing unit. The software, based on the commercial CHEMMOD package, was custom written for Ciba-Geigy by Dr. D.N.J. White<sup>86</sup> at the University of Glasgow, and used Newton-Raphson techniques for the energy minimisation calculations.<sup>87</sup>

### 3.3: Synthesis and characterisation of poly(2,5-(3,4-bis(methoxymethyl)furanyl)ene) (PIII).

#### 3.3.1 *Polymer syntheses:*

The ROMP process is outlined in Figure 3.1, which also records the numbering system employed.

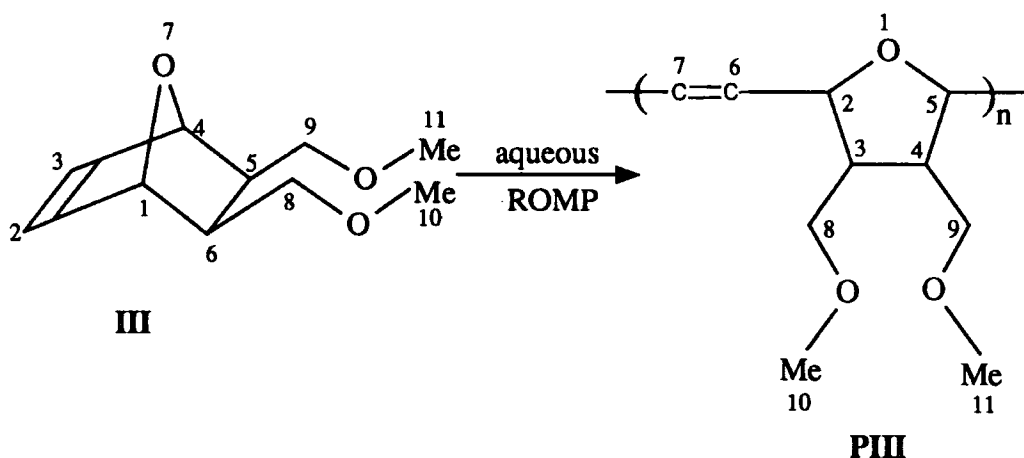


Figure 3.1: Aqueous ROMP of monomer III to yield polymer PIII.

The aqueous ROMP of monomer III was attempted using various transition metal chlorides as the precursors to the initiating and chain propagating species (Table 3.1). In each case, monomer III (1g, 5.4 mmol) was placed in a test tube (13mm I.D.) containing water (3.0 ml), and equipped with a magnetic stirring bar.

The resulting suspension was stirred at  $55\pm 0.1^\circ\text{C}$  under a normal laboratory atmosphere for 30 minutes prior to the addition of an aqueous solution of the metal chloride (3.5 ml of a 0.02g/ml solution). The reaction was allowed to proceed for two days at  $55^\circ\text{C}$ , during which time several colour changes were observed. When  $\text{RuCl}_3\cdot 3\text{H}_2\text{O}$  was used as the precursor to the initiator, the initial brown colour of the solution turned crimson red after two hours, and dark green after four hours; polymer was seen to precipitate after five hours. When  $\text{IrCl}_3\cdot 3\text{H}_2\text{O}$  was used in a similar manner, the initial green solution turned pale brown after nine hours, and dark brown after two days; polymer was seen to precipitate after one day. Finally, when  $\text{OsCl}_3\cdot 3\text{H}_2\text{O}$  was used as the precursor to the initiator, the initial green solution turned brown after one hour, with polymer precipitating after two hours. No colour changes were observed in the polymerisations attempted using either  $\text{RhCl}_3\cdot 3\text{H}_2\text{O}$  or  $\text{PdCl}_2$  as precursors to the initiators, and no polymers were formed.

The solid polymeric products of each reaction were recovered by filtration, and purified by three successive reprecipitations of a magnesium sulphate dried chloroform solution of each polymer into pentane. Product polymers, poly(2,5-(3,4-bis(methoxymethyl)furanylene)vinylene)s, **PIII**, were dried in vacuo ( $5\times 10^{-2}$  Torr, 10 hours) to afford 95% ( $\text{RuCl}_3\cdot 3\text{H}_2\text{O}$ ), 95% ( $\text{OsCl}_3\cdot 3\text{H}_2\text{O}$ ), 2.0% ( $\text{IrCl}_3\cdot \text{H}_2\text{O}$ ), 0% ( $\text{RhCl}_3\cdot 3\text{H}_2\text{O}$ ) and 0% ( $\text{PdCl}_2$ ) conversions. The elemental analyses (appendix D) of each of the polymeric products were consistent with that of the expected product, **PIII**.

For convenience, **PIII-Ru**, **PIII-Os**, and **PIII-Ir** refer to the ROMP polymer prepared by using  $\text{RuCl}_3\cdot 3\text{H}_2\text{O}$ ,  $\text{OsCl}_3\cdot 3\text{H}_2\text{O}$ , and  $\text{IrCl}_3\cdot 3\text{H}_2\text{O}$  as the precursors to the initiating and chain carrying species respectively.

Figure 3.2: GPC Chromatograms recorded in THF for polymers **PIII** prepared using; a)  $\text{RuCl}_3 \cdot 3\text{H}_2\text{O}$ ; b)  $\text{OsCl}_3 \cdot 3\text{H}_2\text{O}$ ; and c)  $\text{IrCl}_3 \cdot 3\text{H}_2\text{O}$  as the precursors to the initiating and chain propagating species.

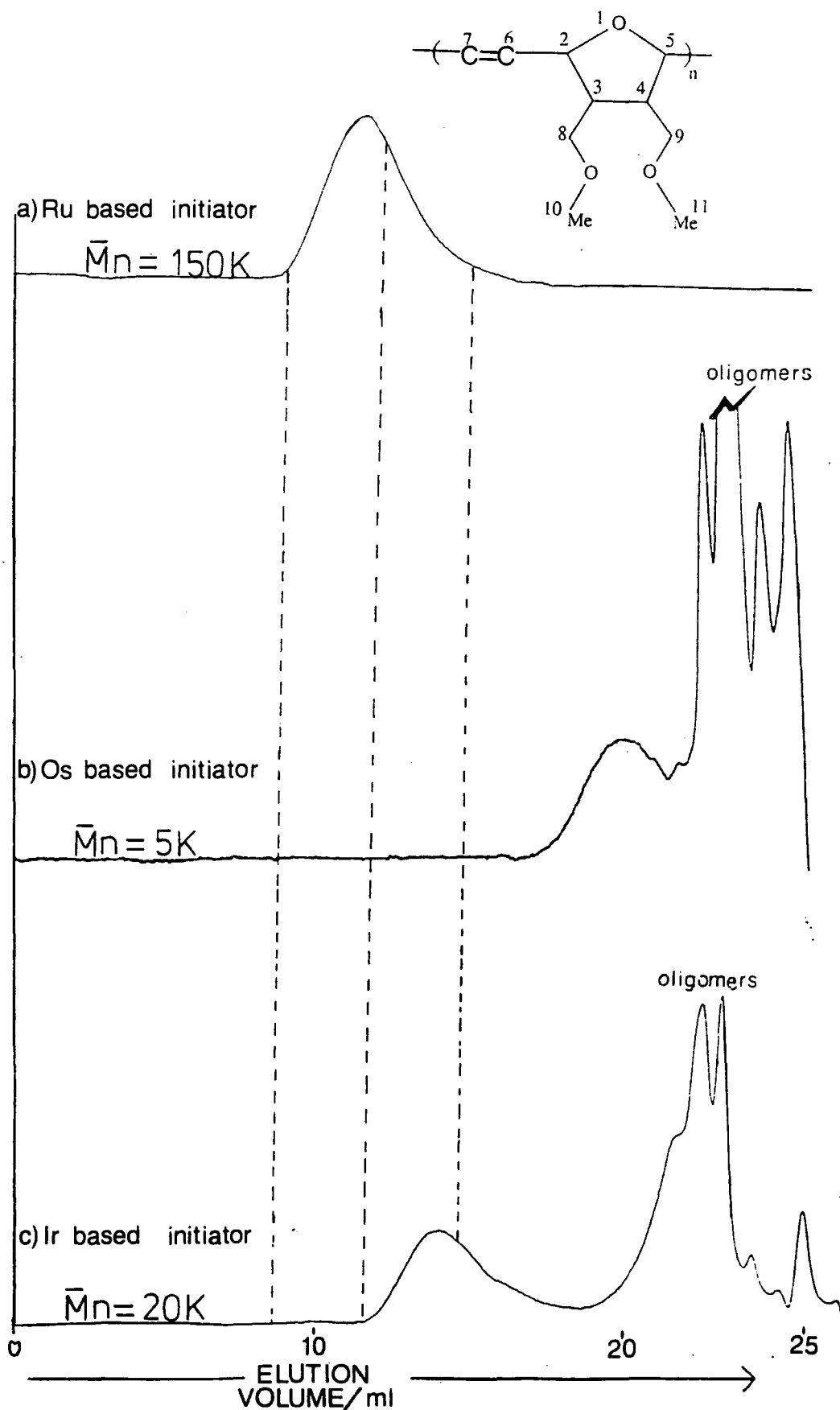


Figure 3.3: Infrared spectra recorded from films cast from acetone of polymers **PIII** prepared using; a)  $\text{RuCl}_3 \cdot 3\text{H}_2\text{O}$ ; b)  $\text{OsCl}_3 \cdot 3\text{H}_2\text{O}$ ; and c)  $\text{IrCl}_3 \cdot 3\text{H}_2\text{O}$  as the precursors to the initiating and chain propagating species.

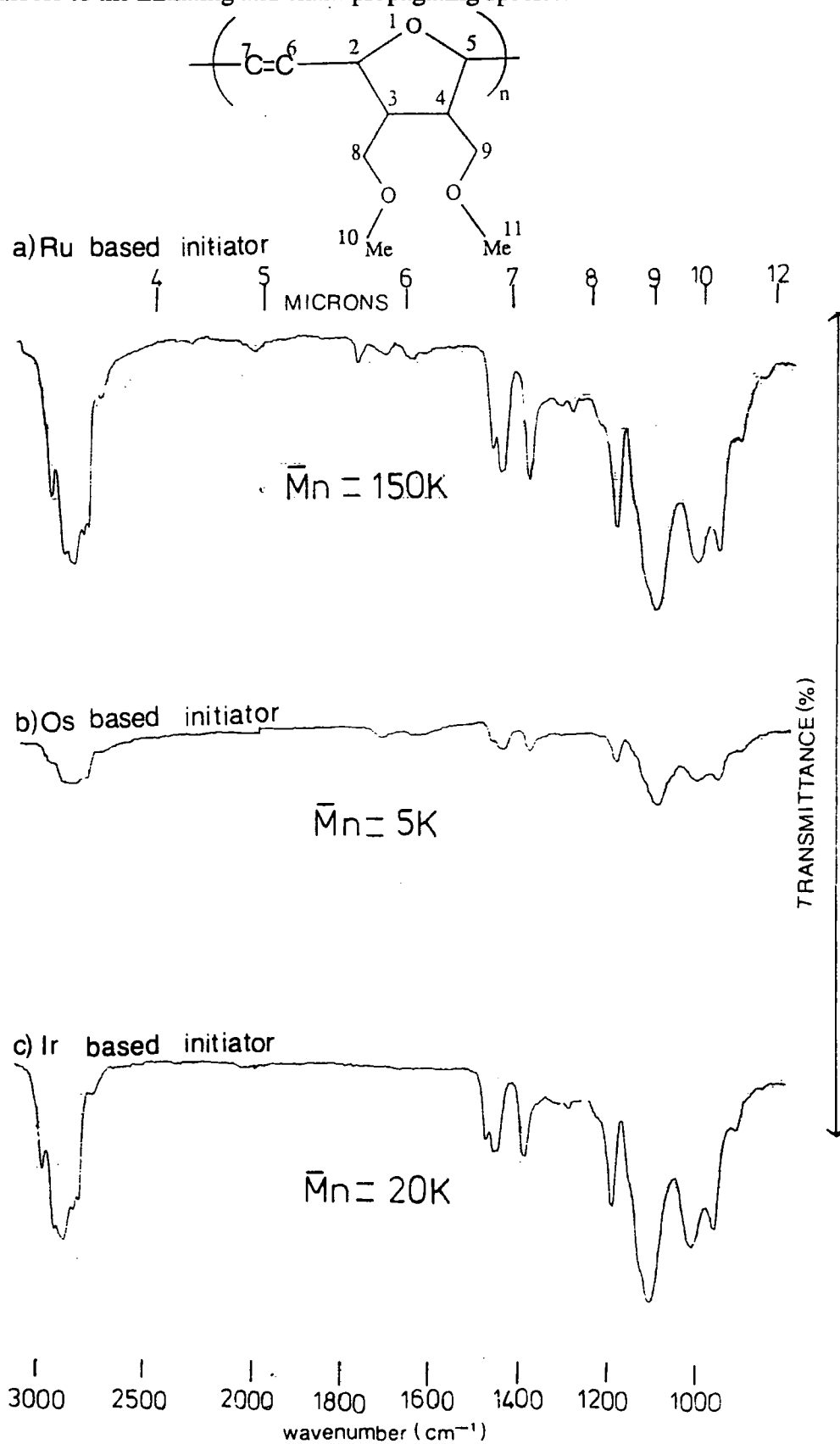


TABLE 3.1: Aqueous ROMP<sup>1</sup> of monomer **III** using various transition metal chlorides as the precursors to the initiating and chain propagating species.

	Transition metal compounds used as precursors to the initiating and chain propagating species				
	RuCl <sub>3</sub> .3H <sub>2</sub> O	OsCl <sub>3</sub> .3H <sub>2</sub> O	IrCl <sub>3</sub> .3H <sub>2</sub> O	RhCl <sub>3</sub> .3H <sub>2</sub> O	PdCl <sub>2</sub>
monomer	1.0g	1.0g	1.0g	1.0g	1.0g
catalyst	0.07g	0.07g	0.07g	0.07g	0.07g
water	6.5ml	6.5ml	6.5ml	6.5ml	6.5ml
temp.	55°C	55°C	55°C	55°C	55°C
yield	95%	95%	2%	0% <sup>2</sup>	0% <sup>2</sup>
Mn	150K	5K	20K	---	---
σ <sup>c</sup> 3	0.40	0.25	0.10	---	---

1) duration of polymerisation was two days unless stated.

2) no polymer formed after one week.

3) determined by <sup>1</sup>H NMR spectroscopy.

### 3.3.2 Catalyst choice:

The aqueous suspension ROMP of monomer **III** was accomplished using RuCl<sub>3</sub>.3H<sub>2</sub>O, OsCl<sub>3</sub>.3H<sub>2</sub>O and IrCl<sub>3</sub>.3H<sub>2</sub>O as the precursors to the initiating and chain propagating species (Table 3.1): under similar reaction conditions RhCl<sub>3</sub>.3H<sub>2</sub>O and PdCl<sub>2</sub> failed to initiate any polymerisation. This observation is consistent with literature reports of the attempted ROMP of norbornene using either palladium or rhodium salts as the precursors to the initiating species, which either yielded no polymer,<sup>64</sup> or the product of a vinyl type polymerisation.<sup>79,63</sup>

Michelotti has suggested that, in ethanol, iridium chlorides have considerably greater metathesis activity than either ruthenium or osmium chlorides for the ROMP of norbornene and some of its derivatives.<sup>62</sup> This trend appears to be

reversed for the aqueous ROMP of monomer **III**; ROMP using initiator(s) derived from  $\text{IrCl}_3 \cdot 3\text{H}_2\text{O}$  proceeded after a longer induction period, and afforded a lower yield, than the ROMP using initiators derived from  $\text{RuCl}_3 \cdot 3\text{H}_2\text{O}$  or  $\text{OsCl}_3 \cdot 3\text{H}_2\text{O}$ .

GPC investigations (Figure 3.2) demonstrate that **PIII-Ru** is a high polymer, whereas both **PIII-Os** and **PIII-Ir** are low molecular weight polymers and oligomers. Infrared spectra (Figure 3.3) were recorded from films of all these samples cast from acetone; they all contain the absorptions of the high polymer described by Grubbs:<sup>71</sup> C-H stretch at 2980, 2920, 2870, 2820, 2800  $\text{cm}^{-1}$ , ether C-O at 1190 and 1100  $\text{cm}^{-1}$ , and other fingerprint absorptions at 1475, 1460 and 1390  $\text{cm}^{-1}$ . Several additional absorptions are present in spectrum of **PIII-Ru** (Figure 3.3a) at 1780, 1720 and 1660  $\text{cm}^{-1}$ , the latter possibly being the alkene C=C stretch, and the former two, the absorptions of impurities; the spectrum of **PIII-Os** contains only the absorptions at 1720 and 1660  $\text{cm}^{-1}$ . Significantly, the spectrum of **PIII-Ir** (Figure 3.3c) contains no such additional absorptions, which suggests that the C=C vinylene stretching modes in this polymer occur without a change in dipole moment. No absorptions due to oligomers or end groups are observed in any of the infrared spectra.

### 3.3.3 Polymer microstructure:

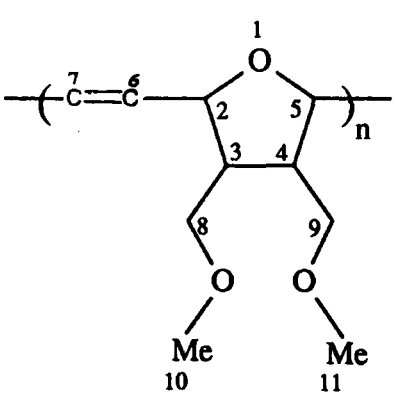
The microstructural analysis of poly(norbornene)s has been discussed in detail,<sup>22</sup> and the analysis established can be applied directly to these heterocyclic analogues. Monomer **III** is symmetrical and therefore cannot give rise to HH, TT or HT addition modes; nevertheless, there are several different ways in which the repeat unit can be incorporated into the polymer chain. The double bonds may be *cis* or *trans*, and the allylic methines on either side of the double bonds are chiral and may have opposite chirality, giving meso- or m-dyads and isotactic polymer, or the same chirality giving racemic- or r-dyads and syndiotactic polymer. Thus,



there are four possible homopolymer microstructures and a variety of other microstructures determined by *cis/trans* and *meso/racemic* dyad sequence effects. The stereochemical constraints in the monomer carried over into the polymer result in *syn* relationships between the pairs of methoxymethyls and vinylic-allylic C-C bonds, and an *anti* relationship between the methoxymethyls and vinylic-allylic bonds.

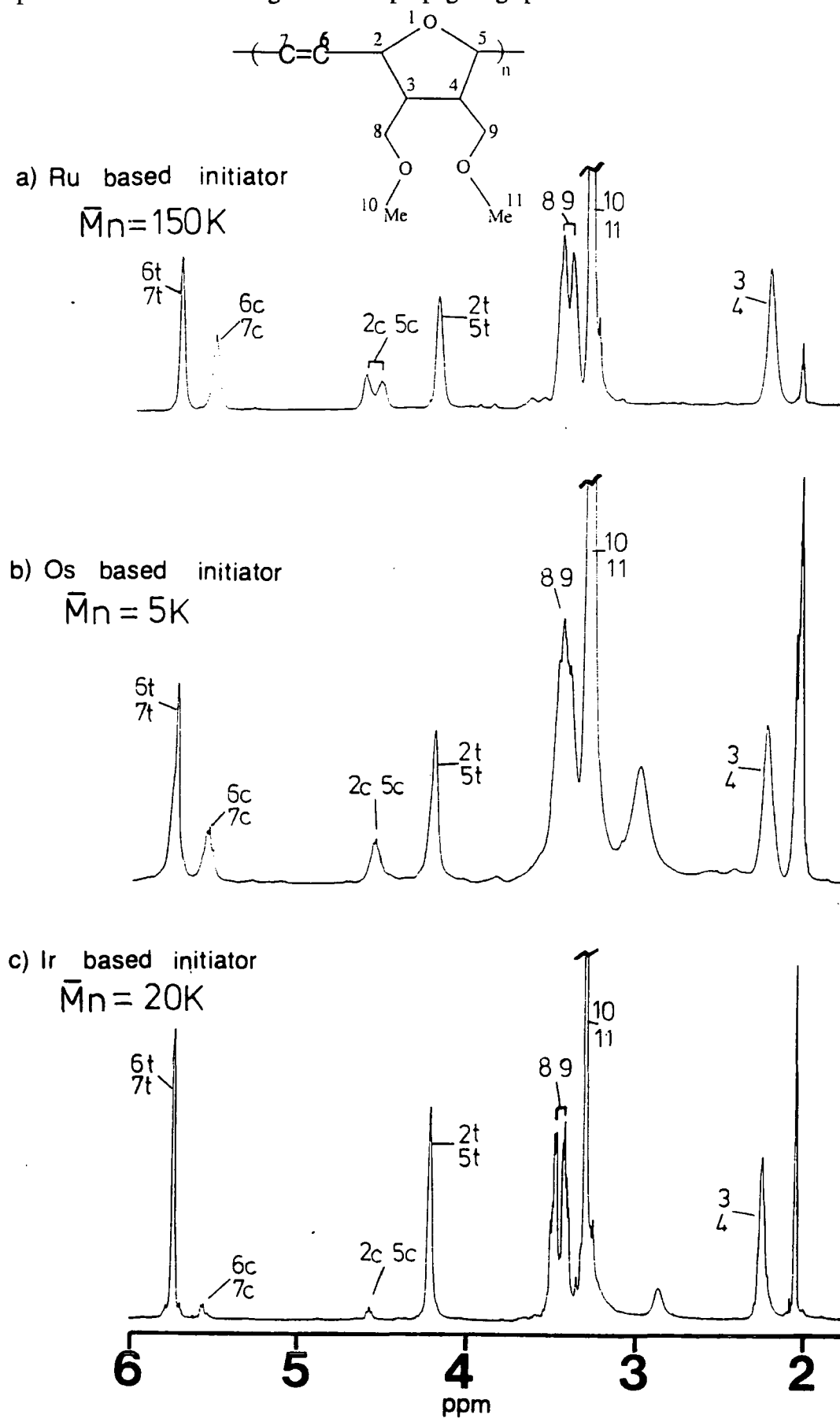
The  $^1\text{H}$  NMR spectra are shown in Figure 3.4 and their assignments, which follow in a straight forward way from the shifts and integrations, are recorded in Table 3.2.

TABLE 3.2: Principal  $^1\text{H}$  NMR spectral parameters<sup>1</sup> of polymer **PIII** (399.952 MHz,  $(\text{CD}_3)_2\text{CO}$ ).

polymer <b>PIII</b>	H at position	chemical shifts /ppm
	6 and 7	5.72 (trans) 5.52 (cis)
	2 and 5	4.63 (c) <sup>2</sup> , 4.54 (c) 4.20 (t) <sup>3</sup>
	8 and 9	3.46, 3.41
	10 and 11	3.29
	3 and 4	2.29

- 1) with respect to acetone at 2.04 ppm.
- 2) "c" refers to a position  $\alpha$  to a *cis* vinylene.
- 3) "t" refers to a position  $\alpha$  to a *trans* vinylene.

Figure 3.4:  $^1\text{H}$  NMR spectra recorded at 399.952 MHz in  $(\text{CD}_3)_2\text{CO}$  of polymers **PIII** prepared using; a)  $\text{RuCl}_3 \cdot 3\text{H}_2\text{O}$ ; b)  $\text{OsCl}_3 \cdot 3\text{H}_2\text{O}$ ; and c)  $\text{IrCl}_3 \cdot 3\text{H}_2\text{O}$  as the precursors to the initiating and chain propagating species.



The  $^1\text{H}$  NMR spectra of polymers **PIII-Ru**, **PIII-Os**, and **PIII-Ir** contain the resonances of the vinylic protons at positions 6 and 7, 5.72 ppm (*trans*) and 5.52 ppm (*cis*) (Figure 3.4). Integration of this region demonstrates that all the polymers **PIII** have predominantly *trans* double bonds,  $\sigma^c = 0.4$  for **PIII-Ru**,  $\sigma^c = 0.25$  for **PIII-Os**, and  $\sigma^c = 0.1$  for **PIII-Ir**. The allylic protons on positions 2 and 5 resonate at 4.20 ppm (adjacent to *trans*) and 4.54 ppm (adjacent to *cis*). In the case of **PIII-Ru** (Figure 3.4a) there is an additional signal at 4.63 ppm due to a *cis*-allylic proton, whereas Grubbs and Novak reported only the higher field *cis*-allylic signal for a polymer prepared in a similar manner.<sup>102,72</sup> Since the inclusion of the lower field signal is necessary to balance the proton integration, it is assumed to be a real part of the spectrum, and is possibly the result of sequence effects in the polymer chain. The spectra of both **PIII-Os** (Figure 3.4b) and **PIII-Ir** (Figure 3.4c) contain only the higher field *cis*-allylic resonance at 4.54 ppm, and are consistent with the spectrum described by Grubbs.<sup>72</sup>

The rest of the  $^1\text{H}$  NMR can be readily interpreted; the methine protons on positions 3 and 4 resonate as a broad singlet at 2.29 ppm; methyl protons on positions 10 and 11 as a narrow singlet at 3.29 ppm; methine protons on positions 8 and 9 as a close pair at 3.46 ppm and 3.41 ppm. Additional resonances are observed at 2.95 ppm in the spectrum of **PIII-Os** (Figure 3.4b), and at 2.90 ppm in the spectrum of **PIII-Ir** (Figure 3.4c). Neither of these resonances can be assigned as high polymer resonances; it is possible that they are the resonances of the end groups, since oligomers are observed in the corresponding GPC chromatograms (Figures 3.2b and 3.2c). However, these signals are too intense for end groups and a more plausible explanation is that they are the resonances of water, present as a contaminant, since no corresponding resonances are observed in the  $^{13}\text{C}$  NMR spectra (see below).

The proton decoupled  $^{13}\text{C}$  NMR spectra are shown in Figure 3.5 and their assignments are recorded in Table 3.3.

Figure 3.5: Proton decoupled  $^{13}\text{C}$  NMR spectra recorded at 100.577 MHz in  $(\text{CD}_3)_2\text{CO}$  of polymers **PIII** prepared using; a)  $\text{RuCl}_3 \cdot 3\text{H}_2\text{O}$ ; b)  $\text{OsCl}_3 \cdot 3\text{H}_2\text{O}$ ; and c)  $\text{IrCl}_3 \cdot 3\text{H}_2\text{O}$  as the precursors to the initiating and chain propagating species.

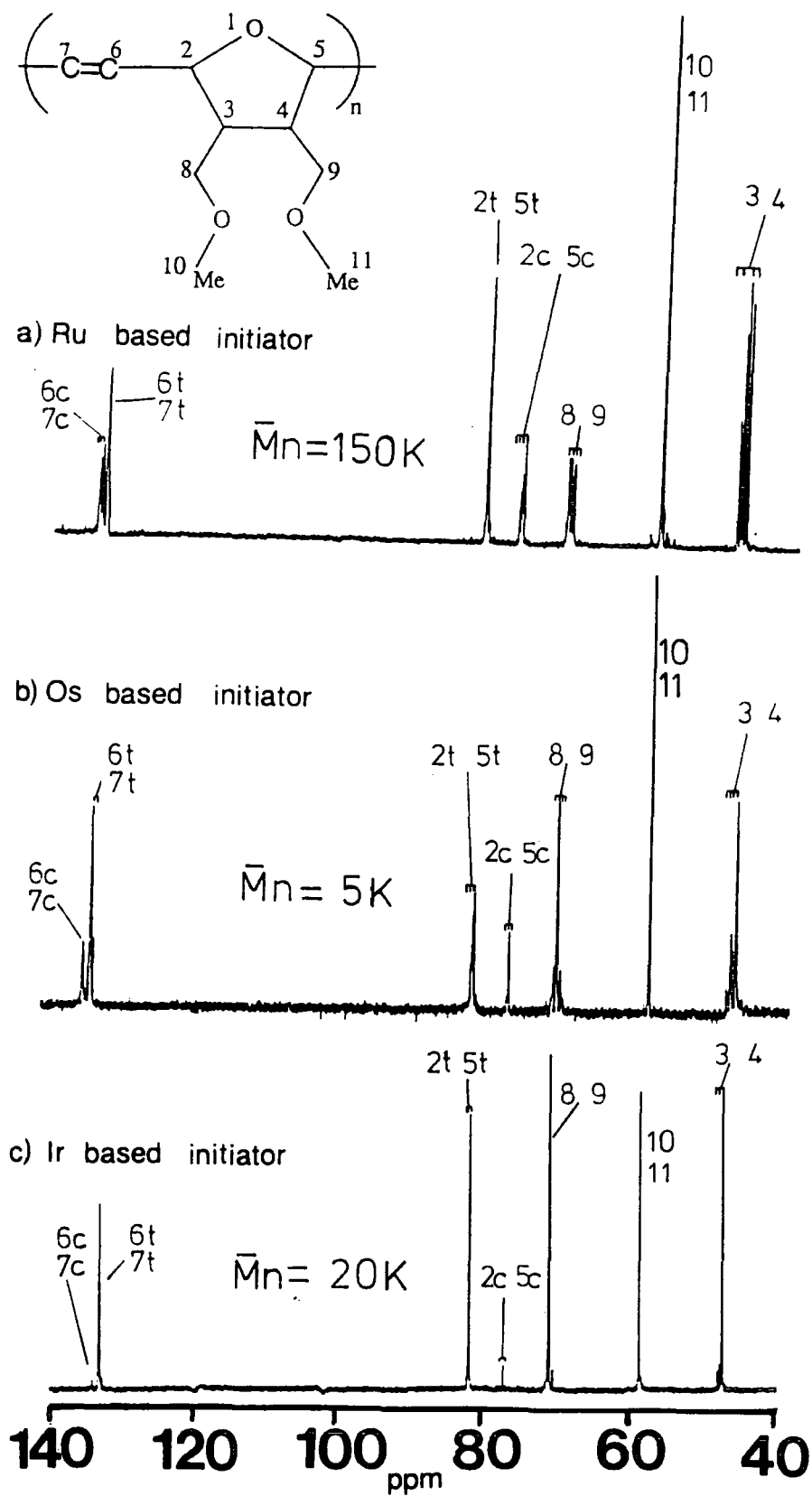
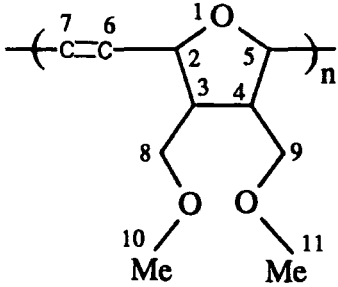


TABLE 3.3: Principal  $^{13}\text{C}$  NMR spectral parameters<sup>1</sup> of polymer **PIII** (100.577 MHz,  $(\text{CD}_3)_2\text{CO}$ ).

				
carbon position	double bond or nearest double bond	PIIRu / ppm	PIIOs / ppm	PIIRr / ppm
6 and 7	<i>cis</i>	134.23	134.25	134.25
	<i>cis</i>	134.11	134.13	
	<i>cis</i>	133.84		
	<i>trans</i>		133.39	
	<i>trans</i>	133.33	133.30	
	<i>trans</i>		133.20	
	<i>trans</i>	133.12	133.13	
	<i>trans</i>	132.97	133.02	
2 and 5	<i>trans</i>			82.40
	<i>trans</i>	82.25	82.24	82.26
	<i>trans</i>	82.08		
	<i>trans</i>	82.03	82.02	82.05
	<i>trans</i>	81.96		
	<i>cis</i>	77.68	77.72	
	<i>cis</i>	77.44		
	<i>cis</i>	77.36	77.38	77.39
3 and 4	<i>cis</i>	77.22		
	<i>cis</i>	48.80		
	<i>cis</i>	48.77	48.76	
	<i>cis</i>	48.34	48.30	48.37
	<i>trans</i>	48.05	48.02	48.10
8 and 9	<i>trans</i>	47.62	47.61	47.69
	<i>trans</i>	71.52		
	<i>trans</i>	71.41	71.37	71.43
	<i>trans</i>	71.29		
	<i>trans</i>	71.15	71.11	71.17
	<i>cis</i>	70.81	70.77	
	<i>cis</i>	70.73		
10 and 11	<i>cis</i>	70.54	70.54	70.59
	<i>cis</i>	70.51		
	<i>cis</i>	58.90	58.90	58.90

1) with respect to acetone at 29.82 ppm.

Proton decoupled  $^{13}\text{C}$  NMR spectra and Attached Proton Test (APT)<sup>103</sup> spectra for polymers **PIII-Ru**, **PIII-Os** and **PIII-Ir** are presented in Figures 3.6, 3.7 and 3.8 respectively. Each polymer spectrum consists of a group of vinylic resonances (135-132 ppm, compared in Figure 3.9, C-6 and C-7), allylic resonances (82.5-77 ppm, compared in Figure 3.10, C-2 and C-5), methine resonances (49-47 ppm, compared in Figure 3.11, C-3 and C-4), methylene resonances (72-70 ppm, compared in Figure 3.12, C-8 and C-9) and methyl resonances (approx. 58.90 ppm).<sup>71</sup> The spectra of **PIII-Ir** are the simplest, and those of **PIII-Ru** are the most complicated.

The spectra of polymers **PIII-Os** and **PIII-Ir** contain no resonances other than those arising from the expected ROMP polymers. This suggests that the additional resonances observed in the  $^1\text{H}$  NMR spectra of these polymers (Figures 3.4b and 3.4c) result from an impurity containing no carbon, possibly water. No end group resonances are observed in the  $^{13}\text{C}$  NMR spectra of either of these polymers, which might be interpreted on the basis that the oligomers observed in the GPC chromatographs (Figure 3.2b and 3.2c) are cyclic, although such a deduction cannot be proved using the evidence of this  $^{13}\text{C}$  NMR data.

A major problem encountered in the assignment of the spectra of polymers of this type is in the determination of tacticity and/or sequence effects.<sup>22</sup> There are four possible assembly modes for polymers prepared by ROMP from symmetrical monomers; *cis* isotactic, *cis* syndiotactic, *trans* isotactic and *trans* syndiotactic (section 1.4.5). Therefore, if more than four resonances are observed for a particular carbon they **must** arise from tacticity **and/or** sequence effects. However, it is not necessarily the case that such structures will result in distinguishable shifts. The methods employed by Ivin to determine the relative effect of sequence and tacticity on chemical shift require the ROMP of unsymmetrical monomers, and his analysis cannot be used in this case since the polymer is prepared from a symmetrical monomer.<sup>104</sup>

Figure 3.6: APT and proton decoupled  $^{13}\text{C}$  NMR spectra recorded at 100.577 MHz in  $(\text{CD}_3)_2\text{CO}$  of polymer **P111** prepared using  $\text{RuCl}_3 \cdot 3\text{H}_2\text{O}$  as the precursor to the initiating and chain propagating species.

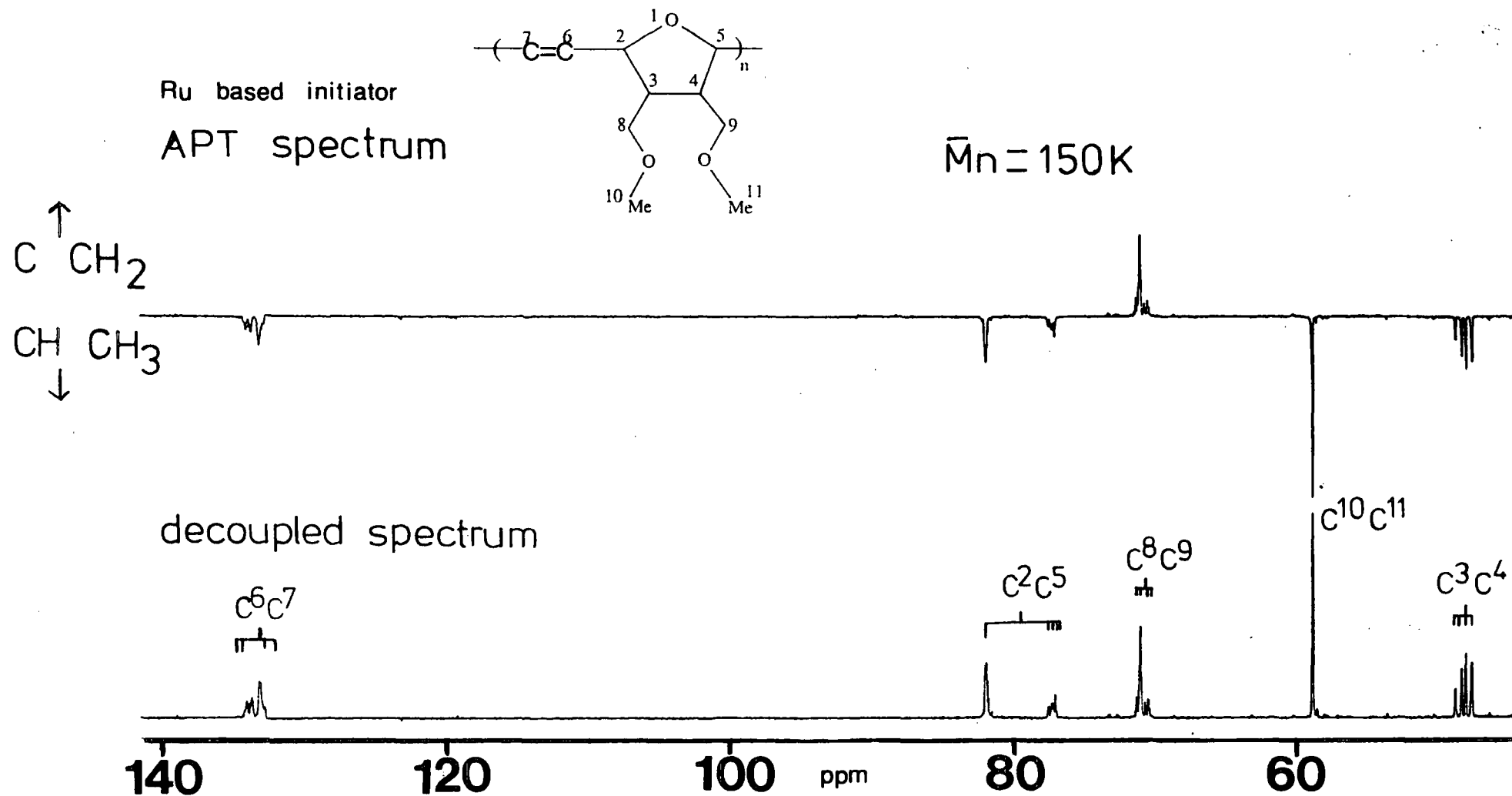


Figure 3.7: APT and proton decoupled  $^{13}\text{C}$  NMR spectra recorded at 100.577 MHz in  $(\text{CD}_3)_2\text{CO}$  of polymer **PIII** prepared using  $\text{OsCl}_3 \cdot 3\text{H}_2\text{O}$  as the precursor to the initiating and chain propagating species.

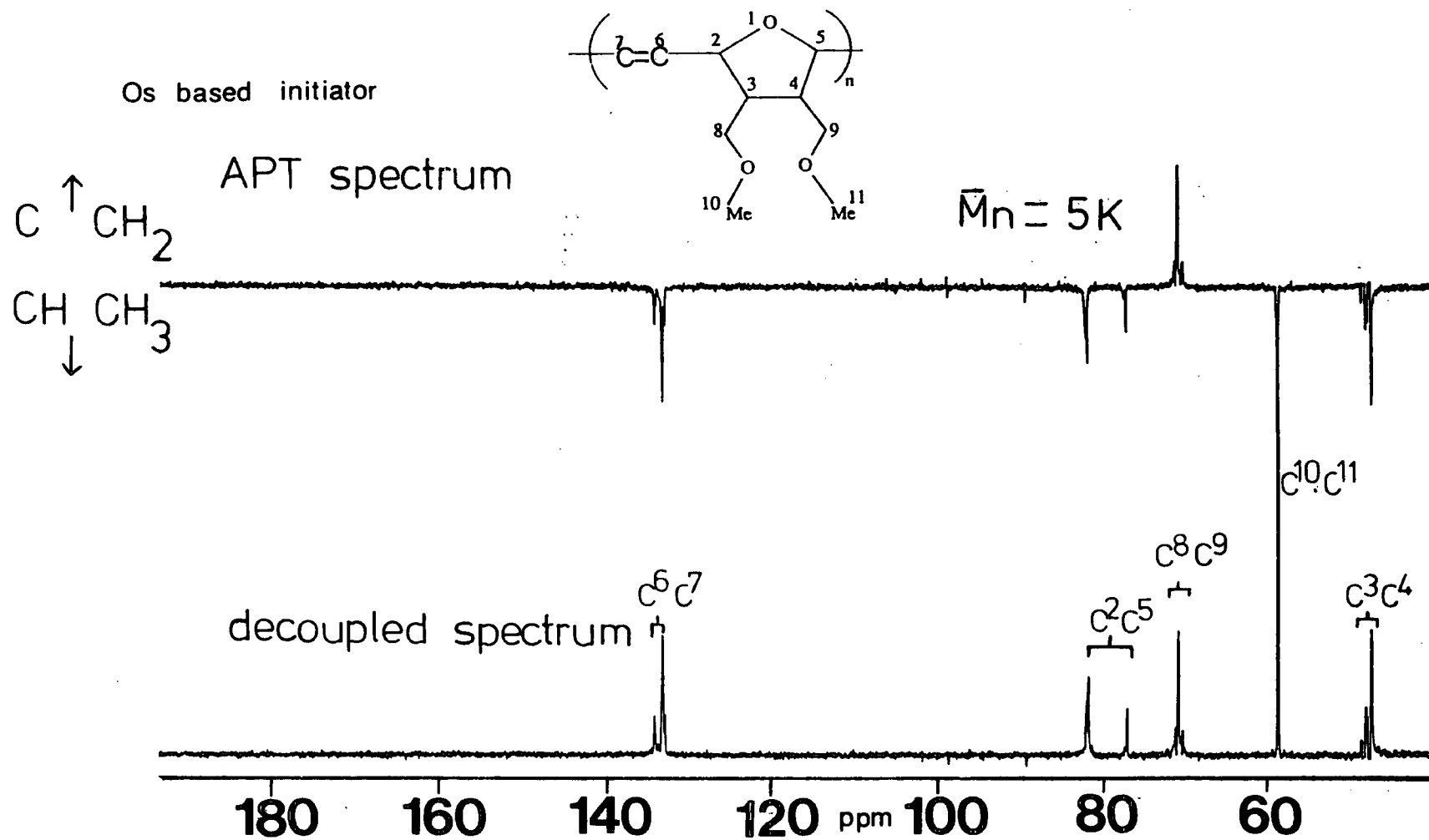




Figure 3.8: APT and proton decoupled  $^{13}\text{C}$  NMR spectra recorded at 100.577 MHz in  $(\text{CD}_3)_2\text{CO}$  of polymer **PIII** prepared using  $\text{IrCl}_3 \cdot 3\text{H}_2\text{O}$  as the precursor to the initiating and chain propagating species.

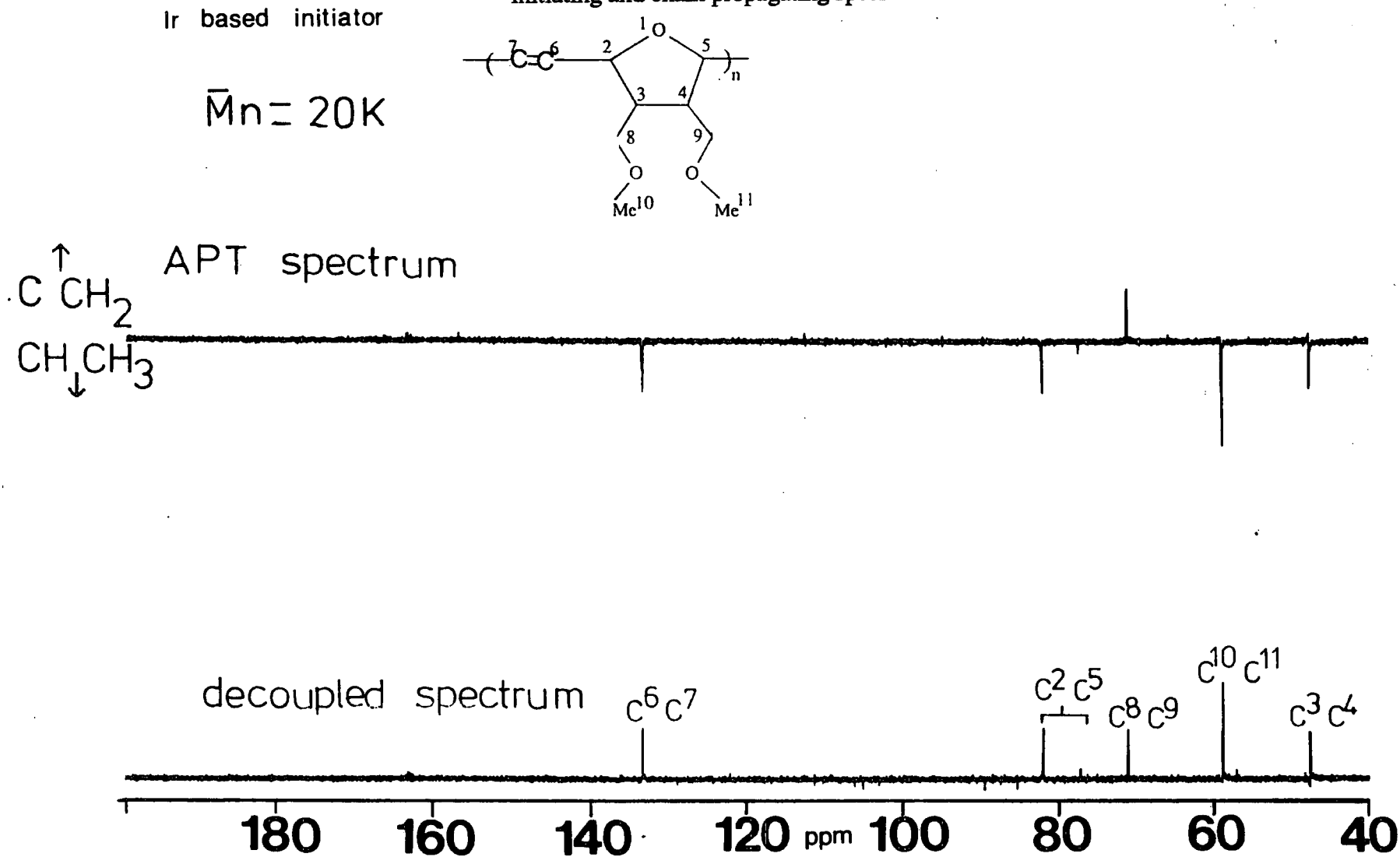


Figure 3.9: Expansion of the proton decoupled  $^{13}\text{C}$  NMR spectra recorded at 100.577 MHz in  $(\text{CD}_3)_2\text{CO}$  of polymers **PIII** prepared using; a)  $\text{RuCl}_3 \cdot 3\text{H}_2\text{O}$ ; b)  $\text{OsCl}_3 \cdot 3\text{H}_2\text{O}$ ; and c)  $\text{IrCl}_3 \cdot 3\text{H}_2\text{O}$  as the precursors to the initiating and chain propagating species: carbons 6 and 7.

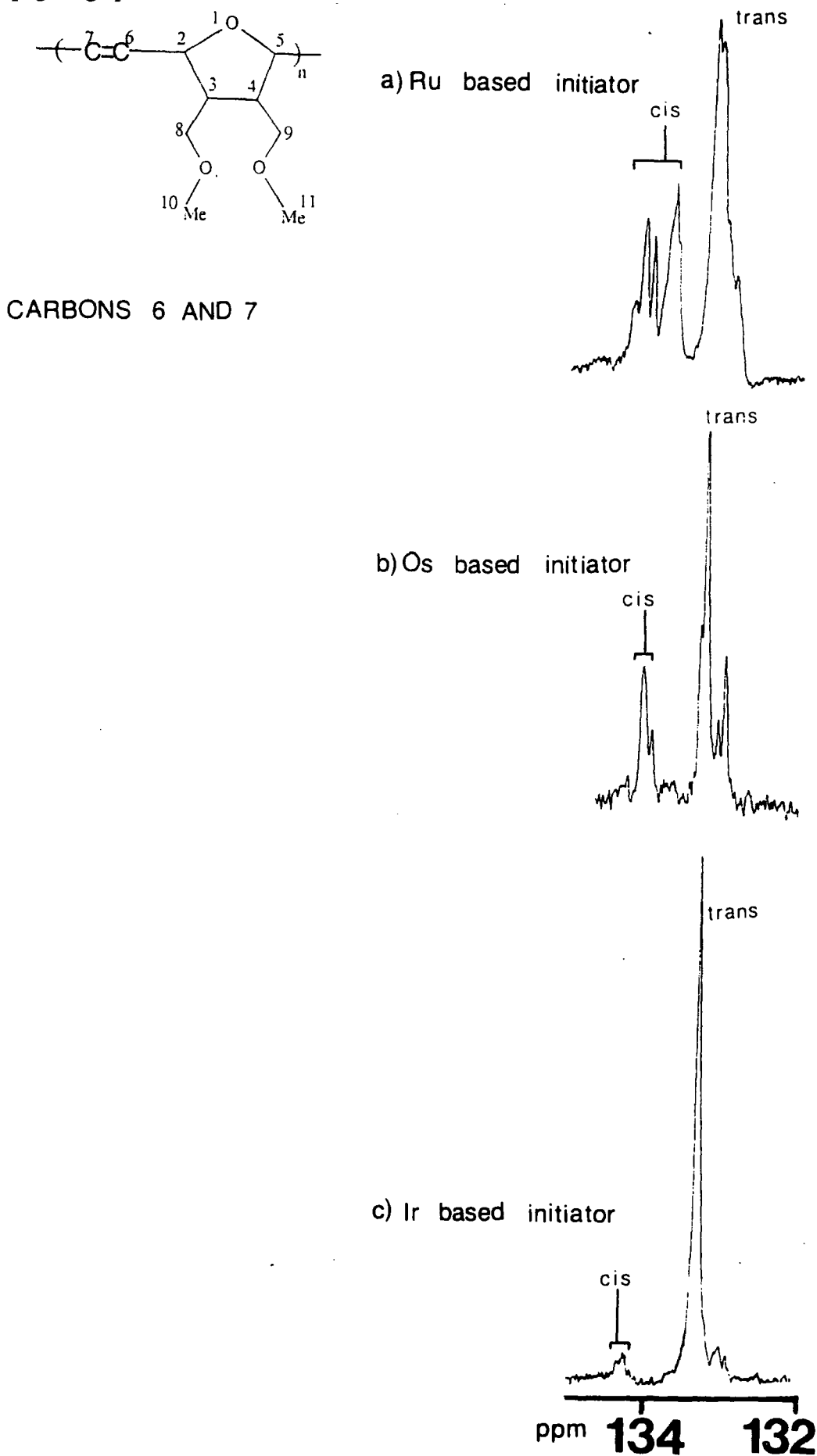


Figure 3.10: Expansion of the proton decoupled  $^{13}\text{C}$  NMR spectra recorded at 100.577 MHz in  $(\text{CD}_3)_2\text{CO}$  of polymers **PIII** prepared using; a)  $\text{RuCl}_3 \cdot 3\text{H}_2\text{O}$ ; b)  $\text{OsCl}_3 \cdot 3\text{H}_2\text{O}$ ; and c)  $\text{IrCl}_3 \cdot 3\text{H}_2\text{O}$  as the precursors to the initiating and chain propagating species: carbons 2 and 5.

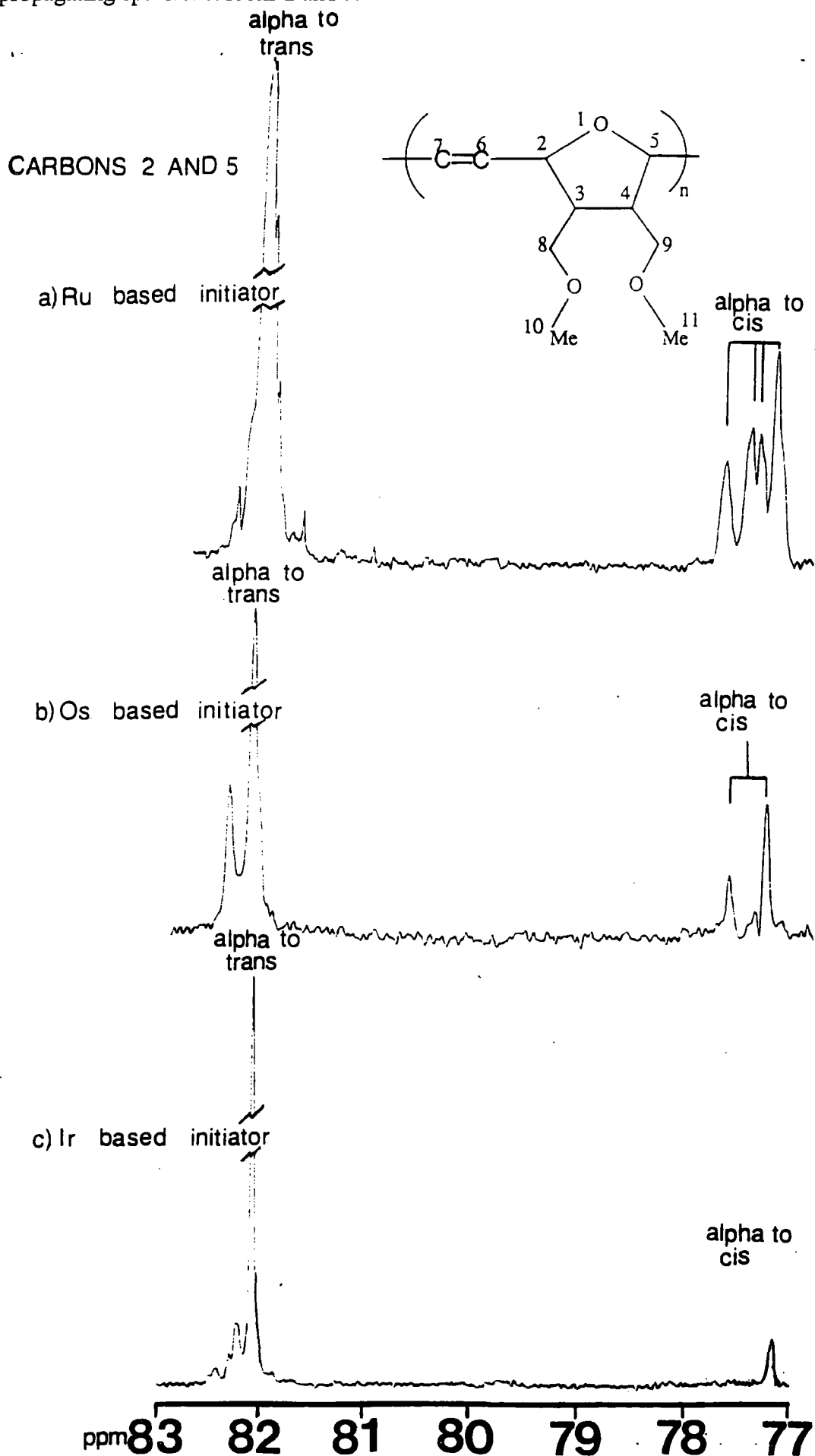
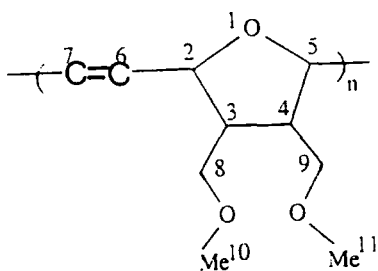


Figure 3.11: Expansion of the proton decoupled  $^{13}\text{C}$  NMR spectra recorded at 100.577 MHz in  $(\text{CD}_3)_2\text{CO}$  of polymers **PIII** prepared using; a)  $\text{RuCl}_3 \cdot 3\text{H}_2\text{O}$ ; b)  $\text{OsCl}_3 \cdot 3\text{H}_2\text{O}$ ; and c)  $\text{IrCl}_3 \cdot 3\text{H}_2\text{O}$  as the precursors to the initiating and chain propagating species: carbons 3 and 4.

CARBONS 3 AND 4

a) Ru based initiator



b) Os based initiator

c) Ir based initiator

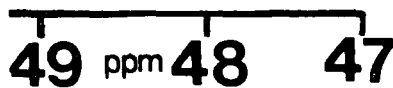
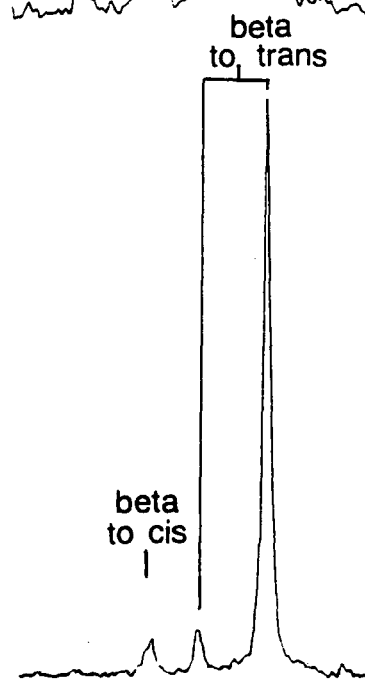
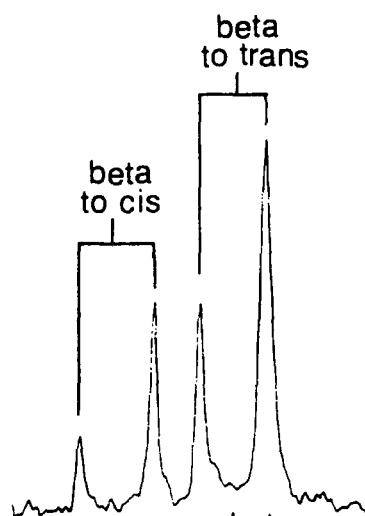
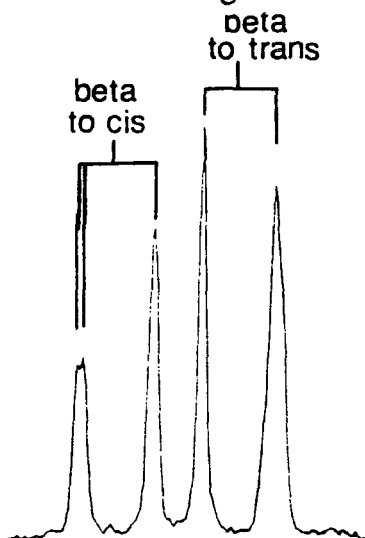
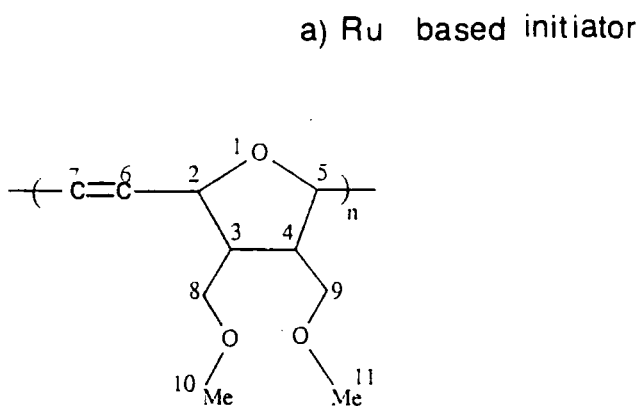


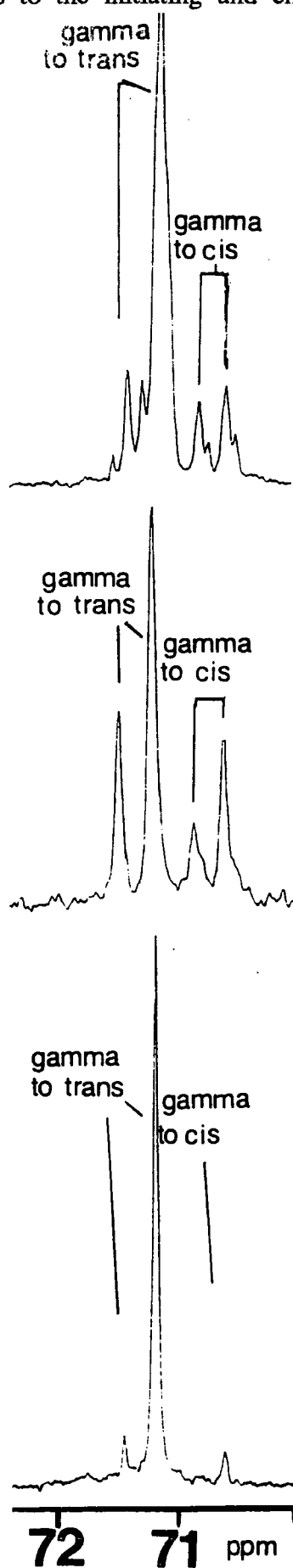
Figure 3.12: Expansion of the proton decoupled  $^{13}\text{C}$  NMR spectra recorded at 100.577 MHz in  $(\text{CD}_3)_2\text{CO}$  of polymers **PIII** prepared using; a)  $\text{RuCl}_3 \cdot 3\text{H}_2\text{O}$ ; b)  $\text{OsCl}_3 \cdot 3\text{H}_2\text{O}$ ; and c)  $\text{IrCl}_3 \cdot 3\text{H}_2\text{O}$  as the precursors to the initiating and chain propagating species: carbons 8 and 9.

CARBONS 8 AND 9



b) Os based initiator

c) Ir based initiator



The expansion of the  $^{13}\text{C}$  NMR spectrum of polymer PIII-Os (Figure 3.9b) contains two resolved resonances resulting from *cis* vinylenes (134.25 and 134.13 ppm), and four resulting from *trans* vinylenes (133.39, 133.30, 133.13 and 133.02 ppm)(Table 3.3). The origin of this multiplicity cannot be unambiguously assigned on the basis of  $^{13}\text{C}$  NMR data in the absence of supporting evidence. If one considers a simple *trans* vinylene carbon, it can exist in a meso or racemic dyad environment (two possible resonances). If the nearest vinylenes influence its shift, three resonances are possible (ctc, ttc  $\equiv$  ctt, and ttt), and if the next nearest ring stereochemistry is important we have more possible environments: mmm, mmm, rmm, rmm, mrr, rrr, rrr, rrr, and rrr. Clearly the number of possible environments for a central *trans* vinylene multiplies considerably in pentad or higher sequences. Since there are four signals for a *trans* vinylene in this spectrum, it is certain that PIII-Os is not tactic, but it is not possible to assign these signals. The corresponding spectrum of PIII-Ru (Figure 3.9a) contains at least six resonances with approximately similar chemical shifts to those observed in the spectrum of PIII-Os, and an additional *cis* vinylene resonance at 133.84 ppm. Again the polymer is not tactic but no unambiguous deductions can be made concerning the detailed assignment of the microstructure. The spectrum of PIII-Ir (Figure 3.9c) contains one *cis* resonance at 134.25 ppm, one major *trans* resonance at 133.30 ppm, and two minor *trans* resonances at 133.20 and 133.12 ppm. This is consistent with a polymer containing predominantly *trans* backbone bonds ( $\sigma^c = 0.1$ ).

The allylic carbons (C-2 and C-5) allow an unambiguous assignment of vinylene content since it is invariably found in polymers of this kind that *cis*-allylic carbon signals occur approximately 5 ppm upfield from those arising from *trans*-allylic carbons (Figure 3.10).<sup>22</sup> The expansion of the proton decoupled  $^{13}\text{C}$  NMR spectrum of polymer PIII-Os in this region (Figure 3.10b) contains at least four resonances, two resulting from carbons adjacent to *trans* double bonds (82.24 and 82.02 ppm), and two resulting from carbons adjacent to *cis* double bonds

(77.72 and 77.38 ppm). In this case it is not possible to determine whether splitting of *cis*- and *trans*-allylic carbons is due to tacticity and/or sequences effects. Note several other minor resonances may be obscured. The corresponding spectrum of **PIII-Ir** (Figure 3.10c) contains only the higher field *cis*-allylic resonance, and is consistent with the spectrum of the vinylic region of the same polymer, which contains only one *cis* resonance (Figure 3.9c). The spectrum of the *trans*-allylic region of **PIII-Ir** (Figure 3.10c) contains one major resonance at 82.05 ppm, and three relatively minor resonances; sequence/tacticity effects must be present. The spectrum of **PIII-Ru** (Figure 3.10a) contains eight resonances, four corresponding to *trans*-allylic carbons, and four to *cis*-allylic carbons. Again, sequence/tacticity effects must be present. Comparison with the corresponding region in the  $^1\text{H}$  NMR spectrum (Figure 3.4a), which contained two *cis*-allylic resonances, reinforces the earlier argument that sequence effects are observed in the spectra of **PIII-Ru**, possibly resulting from blockiness.

The tacticity/sequence effects observed in the spectra of the vinylic and allylic carbons are also observed in the spectra of the methine carbons C-3 and C-4 (Figure 3.11). The spectrum of **PIII-Os** (Figure 3.11b) contains resonances for carbons  $\beta$  to *cis* double bonds at 48.76 and 48.30 ppm, and resonances  $\beta$  to *trans* double bonds at 48.02 and 47.61 ppm. The spectrum of **PIII-Ru** (Figure 3.11a) is somewhat more complicated in the methine region, presumably due to additional sequence effects, and the spectrum of **PIII-Ir** (Figure 3.11c) simpler.

The stereochemical constraints of the polymer backbone affect the chemical environment of the pendant groups, carbons C-8 and C-9 (Figure 3.12). Sequence effects are observed in the spectrum of **PIII-Ru** (Figure 3.12a), and may be present in polymers **PIII-Os** (Figure 3.12b) and **PIII-Ir** (Figure 3.12c), but this cannot be conclusively established.

In summary, the  $^{13}\text{C}$  NMR spectroscopic data indicates the **PIII-Ru** and **PIII-Os** are atactic, and that **PIII-Ir** is highly *trans*, but of uncertain tacticity.

### 3.3.4 Computer modelling of polymer PIII:

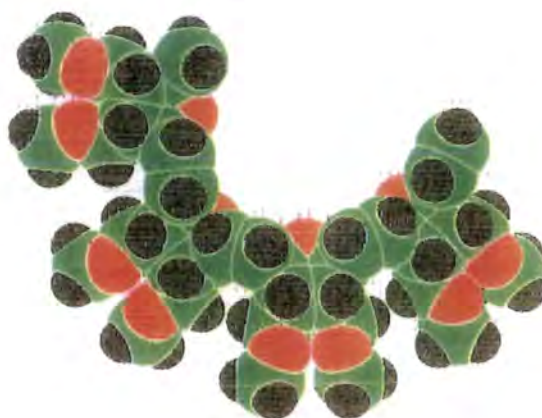
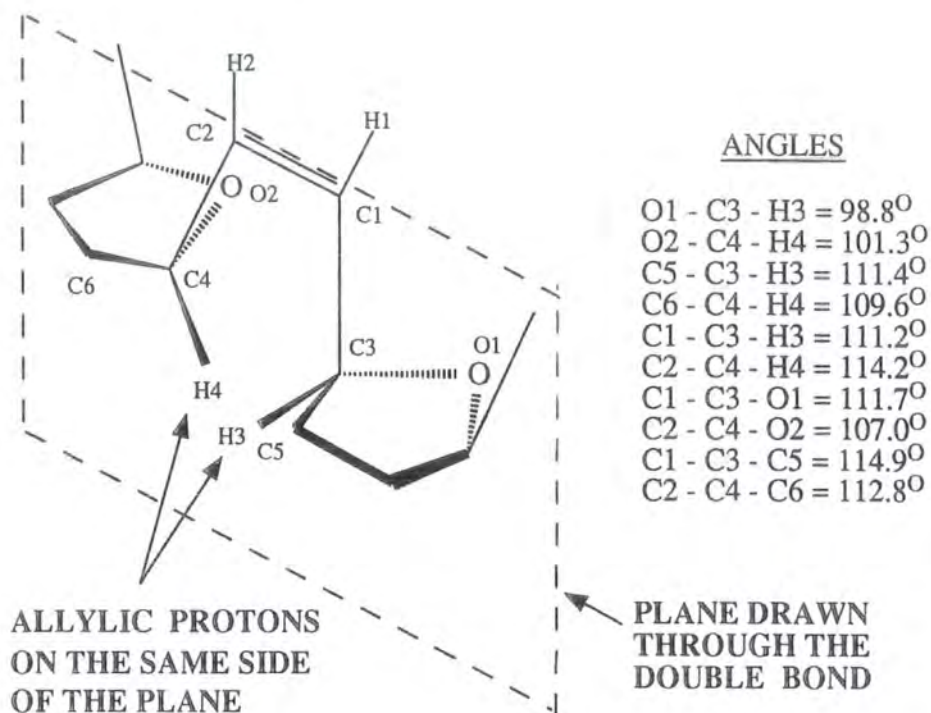
The geometry of the various possible repeat unit structures has been examined using the molecular modelling package developed for Ciba-Geigy Industrial Chemicals.<sup>86</sup> The process involved modelling four tetramer blocks of polymer PIII, each block being of a single tacticity; *cis* isotactic (Figure 3.13), *cis* syndiotactic (Figure 3.14), *trans* syndiotactic (Figure 3.15), and *trans* isotactic (Figure 3.16). The potential energy of each block was calculated as the sum of the bond, Van der Waals, and bond strain energies. The overall potential energy of each model could be altered by moving any of the atoms or bonds; this process eventually leading to a conformation of minimum energy for each block. The bond angles and lengths of each of the four models were measured when the minimum energy conformation was found, although care must be taken in this type of examination since the bonds of a real polymer are not static.

The allylic protons in each of the four possible polymer assembly modes are twisted out of a vertical plane drawn through the axis of the vinylic bond (Figures 3.13, 3.14, 3.15 and 3.16). In the cases of both the *trans* isomers (Figures 3.15 and 3.16) and syndiotactic *cis* isomer (Figure 3.14), the allylic protons on each side of the bond are found on opposite sides of the plane. In these three conformations, the polymer is free to rotate around the vinylic-allylic bond giving an equilibrium resonance with the allylic protons exactly in the plane. In the case of isotactic *cis* isomer (Figure 3.13), both allylic protons are found on the same side of the plane, the side that also contains the polymer side groups. Rotation in this conformation is hindered by the steric bulk of the side groups, the result being that the allylic protons can not easily pass through the plane. Consequently the equilibrium resonance of a *cis* isotactic block has both allylic protons one side of the plane, hence a different environment as compared with non-blocky *cis* isotactic bonds. This modelling study provides a basis for rationalisation of the <sup>1</sup>H NMR spectral analysis presented in section 3.3.3.



Figure 3.13: Isotactic *cis* bond in polymer PIII.

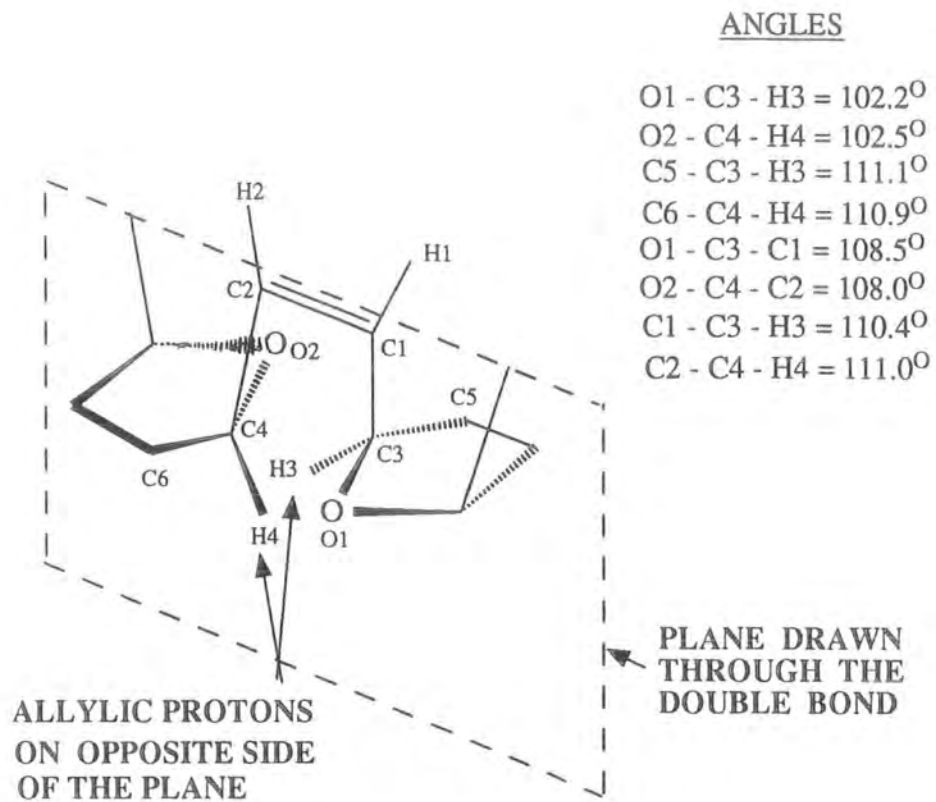
(note: for convenience, side groups are not shown)



KEY: Green = carbon; red = oxygen; Grey = hydrogen.

Figure 3.14: Syndiotactic *cis* bond in polymer PIII.

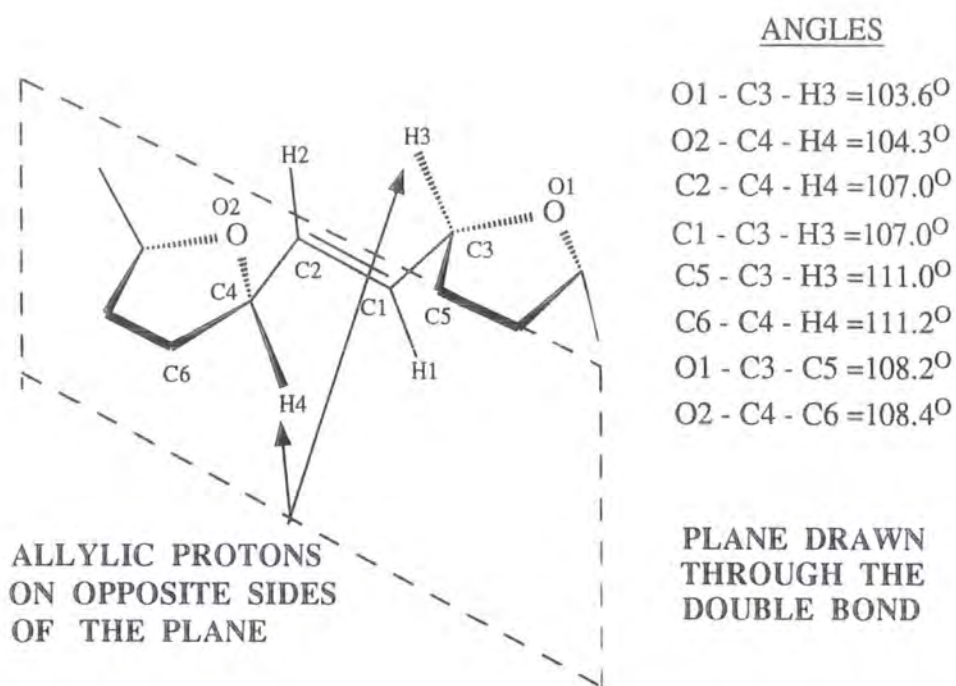
(note: for convenience, side groups are not shown)



**KEY:** Green = carbon; red = oxygen; Grey = hydrogen.

Figure 3.15: Syndiotactic *trans* bond in polymer PIII.

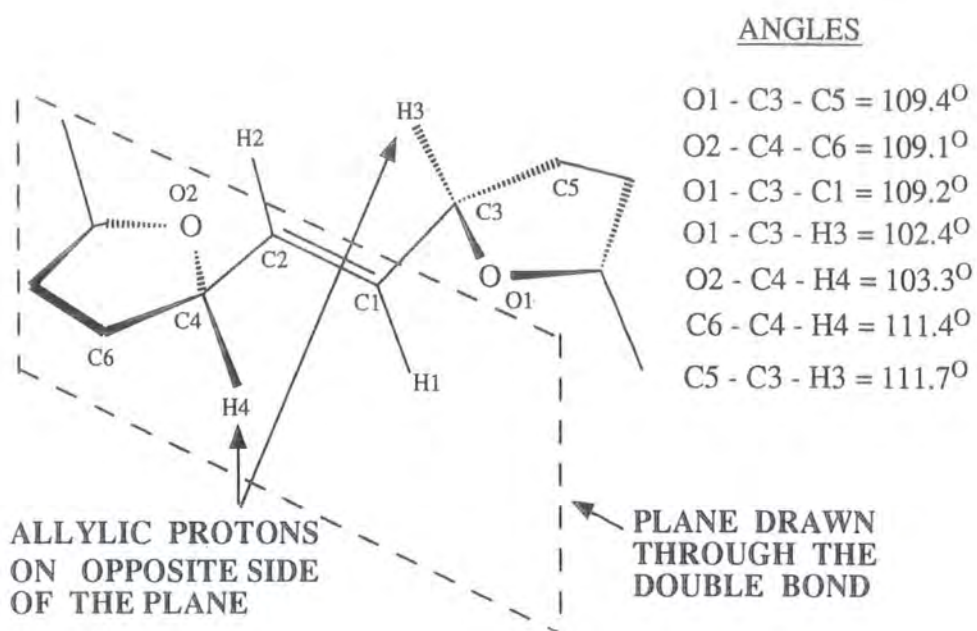
(note: for convenience, side groups are not shown)



**KEY:** Green = carbon; red = oxygen; Grey = hydrogen.

Figure 3.16: Isotactic trans bond in polymer PIII.

(note: for convenience, side groups are not shown)



KEY: Green = carbon; red = oxygen; Grey = hydrogen.

### 3.3.5 Conclusions on the microstructures of *PIII-Ru*, *PIII-Os* and *PIII-Ir*:

The  $^{13}\text{C}$  and  $^1\text{H}$  NMR spectra are self-consistent and reveal sequence/tacticity effects present in all polymers. The effect of sequence on the chemical shifts is particularly strong in the case of **PIII-Ru**, as observed in the spectra of the *cis*-vinylic (Figure 3.9a) and *cis*-allylic (Figure 3.10a) regions. It is possible that one of the *cis*-allylic proton resonances (Figure 3.4a) results from isotactic blocks since in this conformation the rotation of the polymer backbone about the methine carbons 2 and 5 is hindered; the two non blocky *cis* isomers have no such restrictions and experience a different chemical environment to that of the *cis* isotactic blocks (Figures 3.13 and 3.14). The *trans* isomers are free to rotate and are observed in only one environment (Figures 3.15 and 3.16).

### 3.4: Synthesis and characterisation of

#### poly(2,5-(3,4-bis(carboxymethyl)furanylene)vinylene) (PV).

##### 3.4.1 Polymer synthesis:

The ROMP process is outlined in Figure 3.17, which also records the numbering system employed.

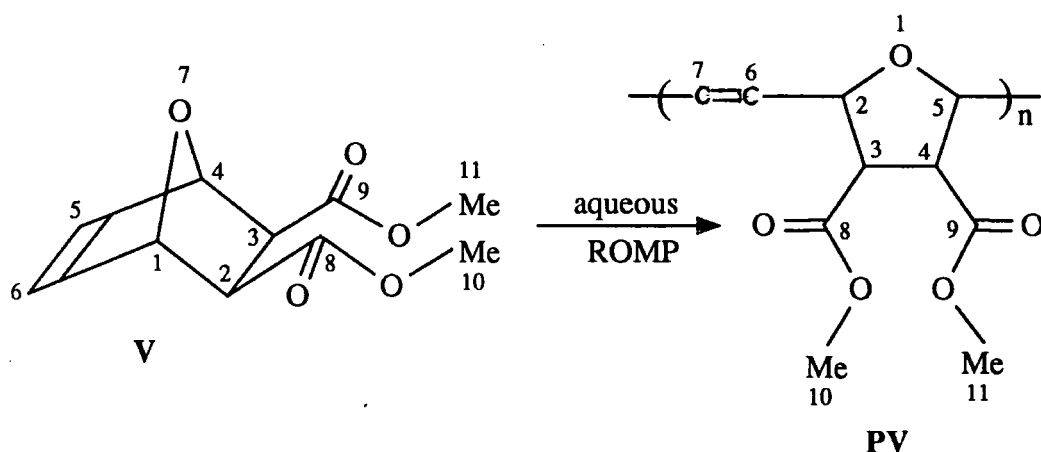


Figure 3.17: Aqueous ROMP of monomer V to yield polymer PV.

The polymerisation of monomer V was attempted only once, since it was suspected of being a toxic substance.

Polymer PV was prepared by placing monomer V (1g, 4.7mmol) in a test tube containing water (3 ml) and equipped with a magnetic stirring bar. The resulting mixture was stirred at  $55\pm 0.1^\circ\text{C}$  under a normal laboratory atmosphere for 30 minutes prior to the addition of an aqueous solution of  $\text{RuCl}_3 \cdot 3\text{H}_2\text{O}$  (3.5 ml of a 0.02g/ml solution). The reaction was allowed to proceed for two days at  $55^\circ\text{C}$ , during which time the colour of the reaction solution changed from brown to crimson red, and finally to green after four hours. The solid polymeric product was recovered by filtration, and purified by three successive reprecipitations of a magnesium sulphate dried chloroform solution of the polymer into diethyl ether. The polymer product, poly(2,5-(3,4-bis(carboxymethyl)furanylene)vinylene), PV, was dried in vacuo ( $5 \times 10^{-3}$  Torr, 4 hours) to afford 60% yield of high polymer ( $M_n = 68\text{K}$ ).

The infrared spectrum of the polymer (Appendix B8) was consistent with the expected structure: C-H stretch at 2990, 2950 2940 and  $2820\text{ cm}^{-1}$  and C=O stretch at  $1765\text{ cm}^{-1}$ ; as was the elemental analysis (found: C,55.8%, H,5.4%, ruthenium->0.1% ; calculated for  $(\text{C}_{10}\text{H}_{12}\text{O}_5)_n$ : C-56.6%, H-5.7%).

### 3.4.2 Polymer microstructure:

The microstructural analysis of polymer PV was made with reference to its analogue, polymer PIII, and the assumptions made in section 3.3 are applied here. The  $^1\text{H}$  NMR spectrum of polymer PV is shown in Figure 3.18 and its assignment, which follows in a straight forward way from the shifts and integrations, is recorded in Table 3.4.

Figure 3.18:  $^1\text{H}$  NMR spectrum recorded at 399.952 MHz in  $(\text{CD}_3)_2\text{CO}$  of polymer PV prepared using  $\text{RuCl}_3 \cdot 3\text{H}_2\text{O}$  as the precursor to the initiating and chain propagating species.

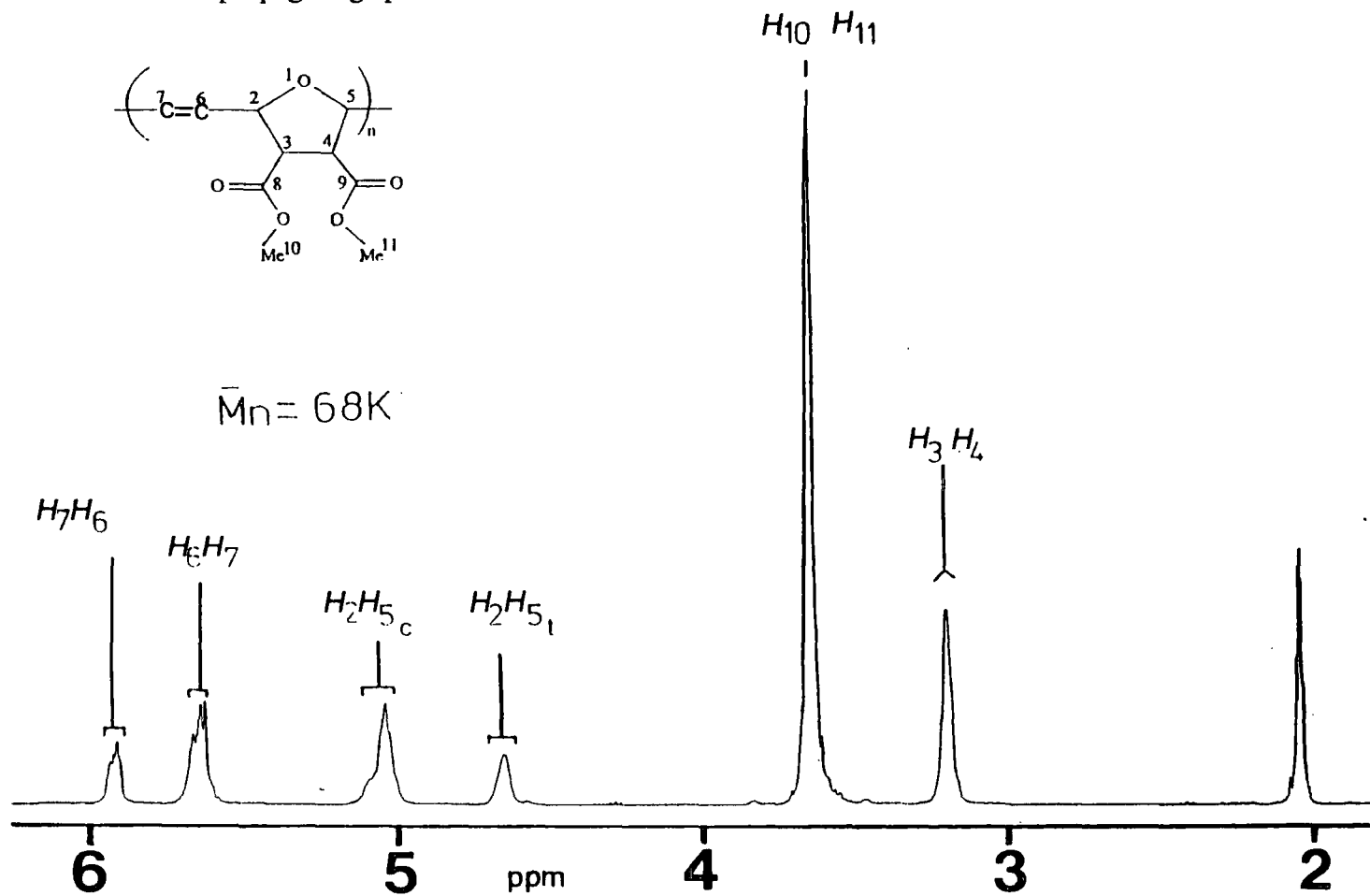
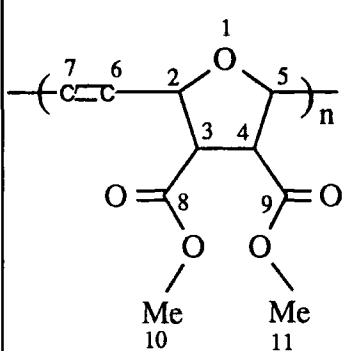


TABLE 3.4: Principal  $^1\text{H}$  NMR spectral parameters<sup>1</sup> of polymer **PV** (399.952 MHz,  $(\text{CD}_3)_2\text{CO}$ ).

polymer <b>PV</b>	H at position	chemical shifts (ppm)
	6 and 7	5.91 ( <i>trans</i> ), 5.63 ( <i>cis</i> )
	2 and 5	5.04 (c) <sup>2</sup> , 4.69 (t) <sup>3</sup>
	10 and 11	3.65
	3 and 4	3.20

- 1) with respect to acetone at 2.04 ppm.
- 2) "c" refers to a position  $\alpha$  to a *cis* vinylene.
- 3) "t" refers to a position  $\alpha$  to a *trans* vinylene.

The  $^1\text{H}$  NMR spectrum of polymer **PV** contains multiple vinylic resonances, corresponding to protons attached to positions 6 and 7, principally at 5.91 ppm (*trans*) and 5.63 ppm (*cis*) (Figure 3.18). Integration of this region provides unambiguous evidence that the polymer contains predominantly *cis* vinylic bonds,  $\sigma^c = 0.6$ . Similar polymers prepared by Rooney via aqueous ROMP of 7-oxa-2,3-bismethoxycarbonylbicyclo[2.2.1]hepta-2,5-diene using  $\text{RuCl}_3 \cdot 3\text{H}_2\text{O}$  as the precursor to the initiator have a lower *cis* content ( $\sigma^c = 0.1$ ).<sup>74</sup>

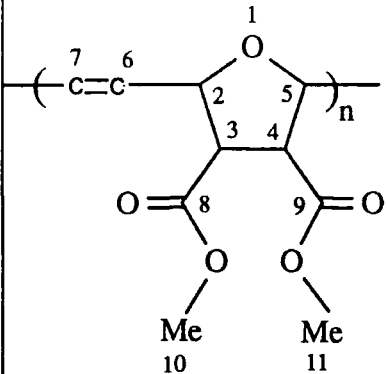
The allylic protons on positions 2 and 5 resonate at 4.69 ppm (adjacent to *trans*) and 5.04 ppm (adjacent to *cis*), both resonances being considerably downfield from the resonances of the corresponding protons in polymer **PIII** (Figure 3.4a). The *cis*-allylic resonance in the  $^1\text{H}$  NMR spectrum of **PV** has a shoulder at low field, but does not show well resolved peaks seen in the spectrum



of **PIII-Ru** (Figure 3.4a), even though polymer **PV** has a greater *cis* content. Presumably there are either no blocks of *cis* isotactic bonds in this polymer, or the effect of blockiness on chemical shift is small. The rest of the spectrum can be readily interpreted; the methine protons on positions 3 and 4 resonate as a singlet at 3.20 ppm and the methyl protons on positions 10 and 11 as a singlet at 3.65 ppm.

The  $^{13}\text{C}$  NMR spectrum of polymer **PV** is shown in Figure 3.19, and its APT spectrum<sup>103</sup> in Figure 3.20; assignments are recorded in Table 3.5.

TABLE 3.5: Principal  $^{13}\text{C}$  NMR spectral parameters<sup>1</sup> of polymer **PV** (100.577 MHz,  $(\text{CD}_3)_2\text{CO}$ ).

polymer <b>PV</b>	C at position	chemical shifts (ppm)
	8 and 9	171.72, 171.58, 171.55
	6 and 7	133.06, 133.00 ( <i>cis</i> ) 132.13 ( <i>trans</i> )
	2 and 5	81.48(t), <sup>2</sup> 81.41(t) 78.28(c), <sup>3</sup> 78.11(c) 78.03(c)
	3 and 4	54.56(c), 52.36(t)
	10 and 11	52.46

1) with respect to acetone at 29.82 ppm.

2) "t" refers to a position  $\alpha$  or  $\beta$  to a *trans* vinylene.

3) "c" refers to a position  $\alpha$  or  $\beta$  to a *cis* vinylene.

Figure 3.19: Proton decoupled  $^{13}\text{C}$  NMR spectrum recorded at 100.577 MHz in  $(\text{CD}_3)_2\text{CO}$  of polymer PV prepared using  $\text{RuCl}_3 \cdot 3\text{H}_2\text{O}$  as the precursor to the initiating and chain propagating species.

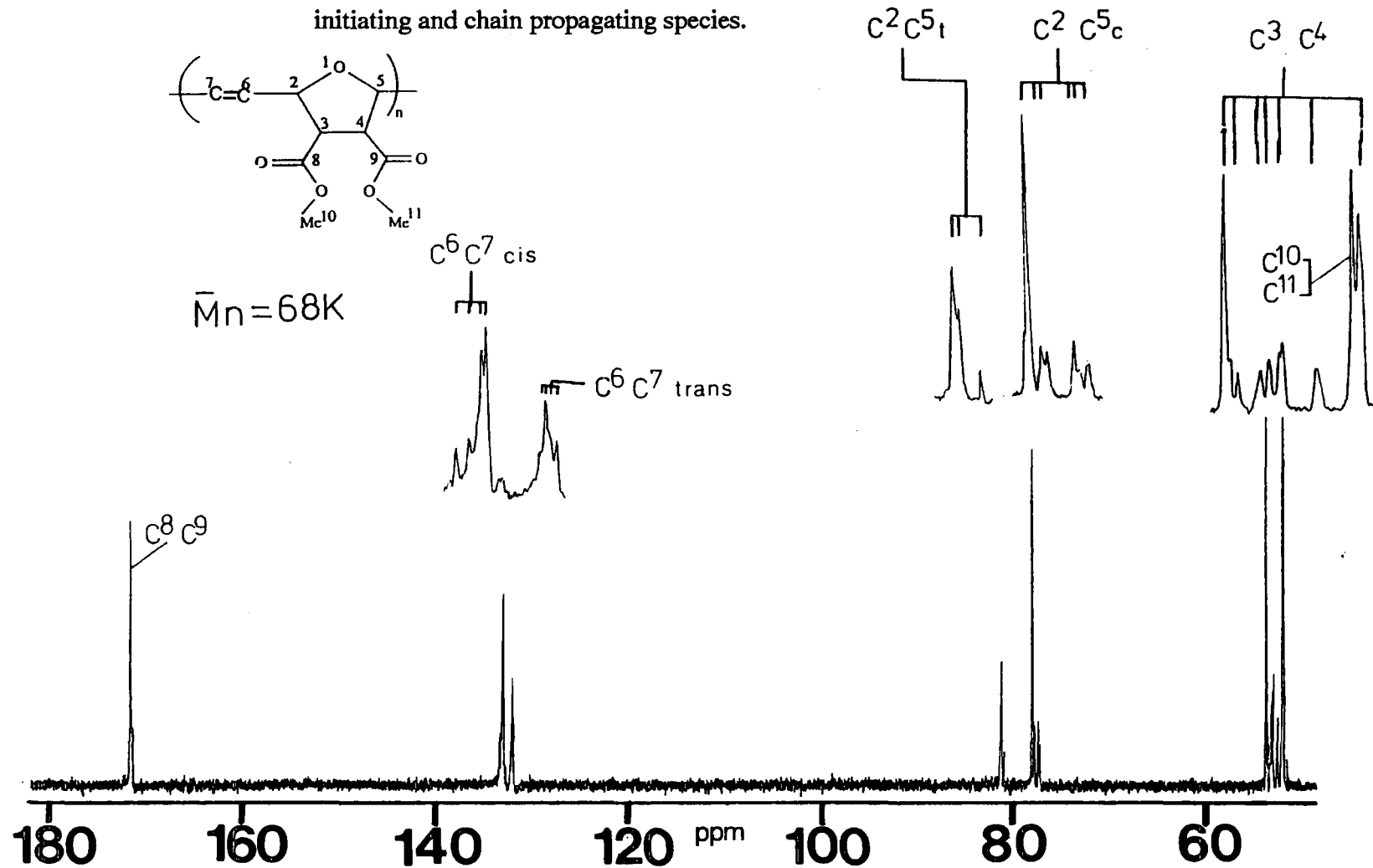
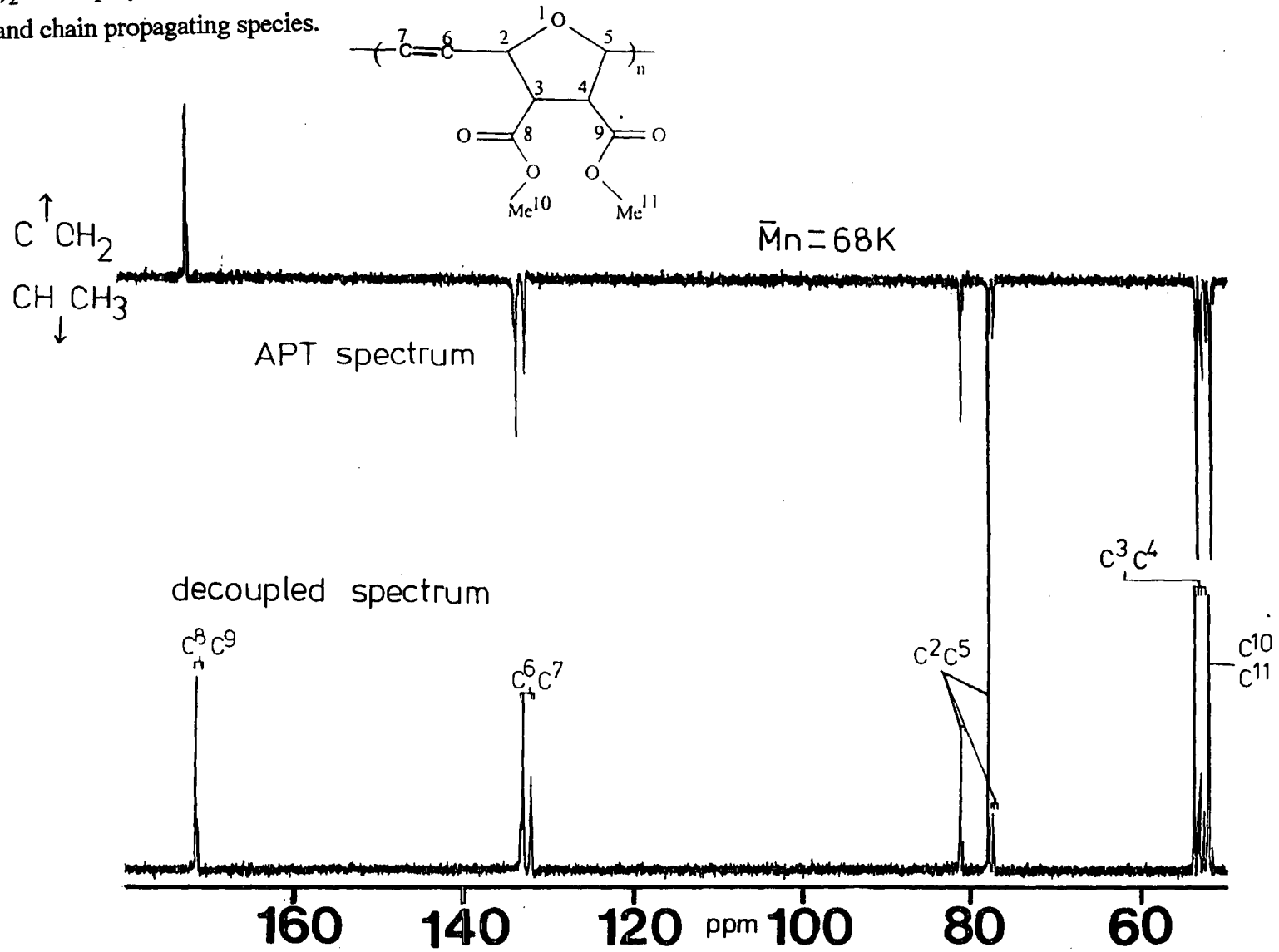


Figure 3.20: APT and proton decoupled  $^{13}\text{C}$  NMR spectra recorded at 100.577 MHz in  $(\text{CD}_3)_2\text{CO}$  of polymer **PV** prepared using  $\text{RuCl}_3 \cdot 3\text{H}_2\text{O}$  as the precursor to the initiating and chain propagating species.



Multiple resonances are observed for each of the backbone carbon atoms in the  $^{13}\text{C}$  NMR spectrum of polymer **PV** (Figure 3.19). The principal resonance of the *trans* vinylic carbons is at 132.13 ppm, although a total of four resonances are observed. Similarly, there are at least four resonances associated with *cis* vinylic carbons, with principal resonances at 133.06 and 133.00 ppm. Using the arguments developed in section 3.3 it is clear that the polymer is atactic.

The  $^{13}\text{C}$  NMR spectrum of the allylic carbons 3 and 4 contains multiple resonances for both *cis*- and *trans*-allylic carbons, whereas the  $^1\text{H}$  NMR spectrum of the same region contains only two broad resonances, one *cis*- and one *trans*-allylic, with a shoulder on the *cis*-allylic resonance. This can be compared to the  $^1\text{H}$  NMR spectrum of **PIII-Ru** (Figure 3.4a) contained two *cis*-allylic resonances, one of which was provisionally assigned as resulting from *cis*-isotactic blocks. Multiple resonances are also observed for the methine carbons 3 and 4, and again sequence and/or tacticity effects must be present.

#### 3.4.3 Conclusions on the microstructure of polymer **PV**:

Detailed assignment of the spectra of ROMP polymers is impossible unless several samples of different microstructure are compared, which was not possible in this case. The spectra of a single sample led to the conclusion that polymer **PV**, prepared using  $\text{RuCl}_3 \cdot 3\text{H}_2\text{O}$  as the precursor to the initiator, contains predominantly *cis* double bonds ( $\sigma^c = 0.6$ ), and is probably atactic.

**3.5: Synthesis and characterisation of  
poly(2,5-(3,4-bis(carboxylic acid)furanylene)vinylene) (PIV).**

**3.5.1 Polymer syntheses:**

The ROMP process is outlined in Figure 3.21, which also records the numbering system employed.

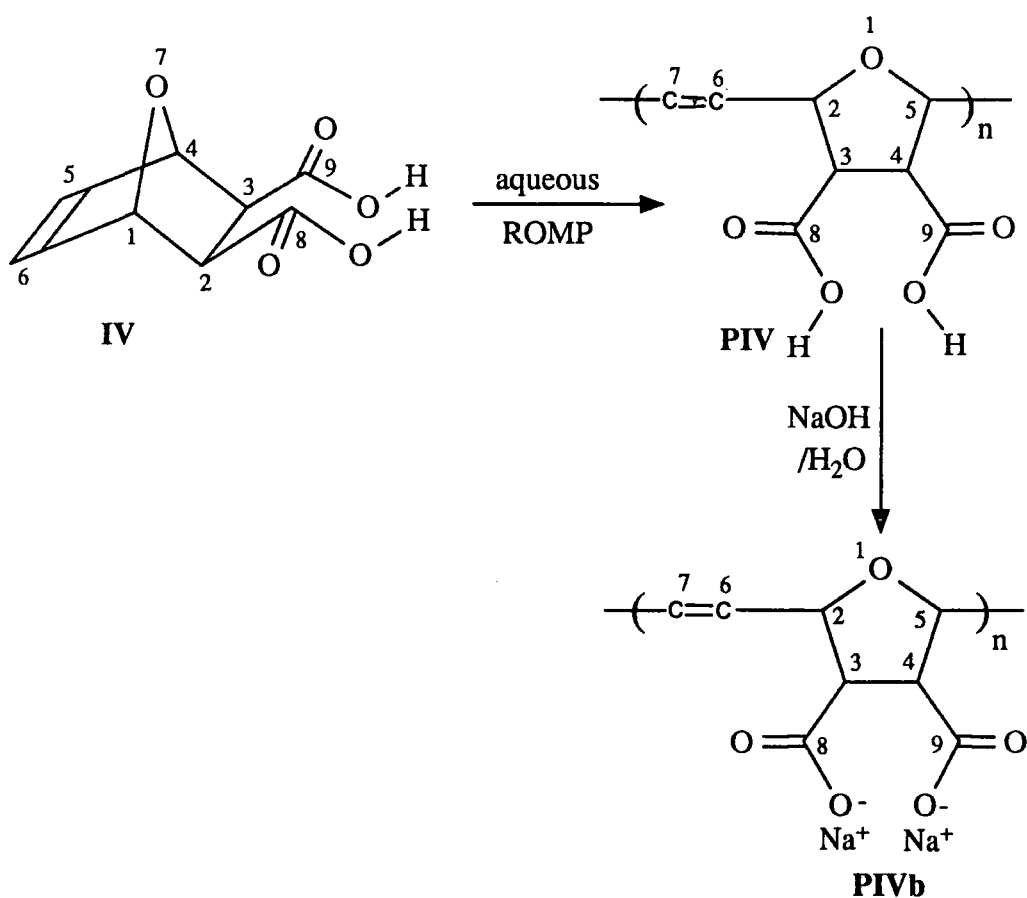


**Figure 3.21: Aqueous ROMP of monomer IV to yield polymer PIV: conversion of polymer PIV to polymer PIVb.**

The aqueous ROMP of monomer IV was attempted using various transition metal chlorides as the precursors to the initiating and chain propagating species (Table 3.6). In each case, monomer IV (1g, 5.4 mmol) was placed in a test tube

(13mm I.D.) containing water (3.0 ml), and equipped with a magnetic stirring bar. The resulting solution was stirred at  $55\pm 0.1^\circ\text{C}$  under a normal laboratory atmosphere for 10 minutes prior to the addition of an aqueous solution of the metal chloride (3.5 ml of a 0.02g/ml solution).

TABLE 3.6: Aqueous ROMP<sup>1</sup> of monomer IV using various transition metal chlorides as the precursors to the initiating and chain propagating species.

	Transition metal compounds used as precursors to the initiating and chain propagating species				
	$\text{RuCl}_3 \cdot 3\text{H}_2\text{O}$	$\text{OsCl}_3 \cdot 3\text{H}_2\text{O}$	$\text{IrCl}_3 \cdot 3\text{H}_2\text{O}$	$\text{RhCl}_3 \cdot 3\text{H}_2\text{O}$	$\text{PdCl}_2$
monomer	1.0g	1.0g	1.0g	1.0g	1.0g
catalyst	0.07g	0.07g	0.07g	0.07g	0.07g
water	6.5ml	6.5ml	6.5ml	6.5ml	6.5ml
temp.	$55^\circ\text{C}$	$55^\circ\text{C}$	$55^\circ\text{C}$	$55^\circ\text{C}$	$55^\circ\text{C}$
yield	95%	80%	0% <sup>2</sup>	0% <sup>2</sup>	0% <sup>2</sup>
Mn	$>100\text{K}^3$	$>100\text{K}^3$	---	---	---
$\sigma^c$ <sup>3</sup>	0.60 <sup>4</sup>	0.60 -0.90 <sup>4,5</sup>	---	---	---

- 1) duration of polymerisation was two days unless stated.
- 2) no polymer formed after one week.
- 3) polymers were partially excluded from the GPC column.
- 4) determined by  $^1\text{H}$  NMR spectroscopy.
- 5) polymerisations were irreproducible.

The reaction was allowed to proceed for two days at  $55^\circ\text{C}$ , during which time several colour changes were observed. When  $\text{RuCl}_3 \cdot 3\text{H}_2\text{O}$  was used as the precursor to the initiator, the initial brown colour of the solution turned crimson red three hours after its addition to the monomer solution, and dark green after six

hours; a polymeric hydrogel was formed after twelve hours. When  $\text{OsCl}_3 \cdot 3\text{H}_2\text{O}$  was used in a similar manner, the initial green colour of the solution turned brown after one hour, with polymer hydrogel formed after 36 hours. No colour changes were observed in any of the other reactions, and no polymers were formed.

The product polymers, poly(2,5-(3,4-bis(carboxylic acid)furanylene)-vinylene)s, **PIV**, were recovered by filtration, and thoroughly washed with dilute hydrochloric acid (10% w/w). The disodium salts of the polymers, **PIVb**, were recovered by addition of the solid diacid polymers **PIV** (1.0g) to aqueous sodium hydroxide (10 ml, 30 wt%) followed by filtration and precipitation into methanol (100 ml). Polymers **PIVb** were purified by three successive reprecipitations into methanol from water then recovered by filtration and finally dried and stored under vacuum to afford 95% ( $\text{RuCl}_3 \cdot 3\text{H}_2\text{O}$ ), 80% ( $\text{OsCl}_3 \cdot 3\text{H}_2\text{O}$ ) conversions.

The elemental analyses (appendix D) of the polymers **PIVb** were consistent with ROMP polymer salts containing dibasic repeat unit.

### 3.5.2 Catalyst choice:

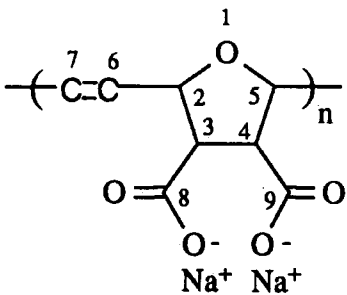
The aqueous ROMP of monomer **IV** was accomplished using both  $\text{RuCl}_3 \cdot 3\text{H}_2\text{O}$  and  $\text{OsCl}_3 \cdot 3\text{H}_2\text{O}$  as the precursors to the initiating and chain propagating species, although in the latter case the polymerisation was irreproducible (Table 3.6). Generally, ROMP using  $\text{OsCl}_3 \cdot 3\text{H}_2\text{O}$  as the precursor to the initiating and chain propagating species produced polymer with 60% *cis* vinylenes (Figure 3.22c), but once a polymer containing 90% *cis* vinylenes was produced (Figure 3.22b), and frequently the reactions failed. This result is surprising, since  $\text{OsCl}_3 \cdot 3\text{H}_2\text{O}$  has been successfully employed in ethanol for the polymerisation of acid functionalised norbornenes.<sup>75</sup> Previous studies with osmium initiators also reported ether ring opening as a competitive reaction,<sup>74</sup> although no evidence for this was observed in the spectra of polymers prepared here.

It is surprising that  $\text{IrCl}_3 \cdot 3\text{H}_2\text{O}$  failed to initiate the polymerisation of monomer **IV** in view of previous successful polymerisations of other acid functionalised monomers in ethanol,<sup>105</sup> although Rooney also reported failure for the attempted aqueous ROMP of some 7-oxanorbornadiene derivatives.<sup>74</sup> Similarly, rhodium and palladium chlorides have so far failed to initiate the aqueous ROMP of monomer **IV**, although very little success with such systems has been reported (cf. ROMP of monomer **III** in section 3.3.2).<sup>79,63,71</sup>

### 3.5.3 Polymer microstructure:

The  $^1\text{H}$  NMR spectra are shown in Figure 3.22 and their assignments, which follow in a straight forward way from the shifts and integrations, are recorded in Table 3.7.

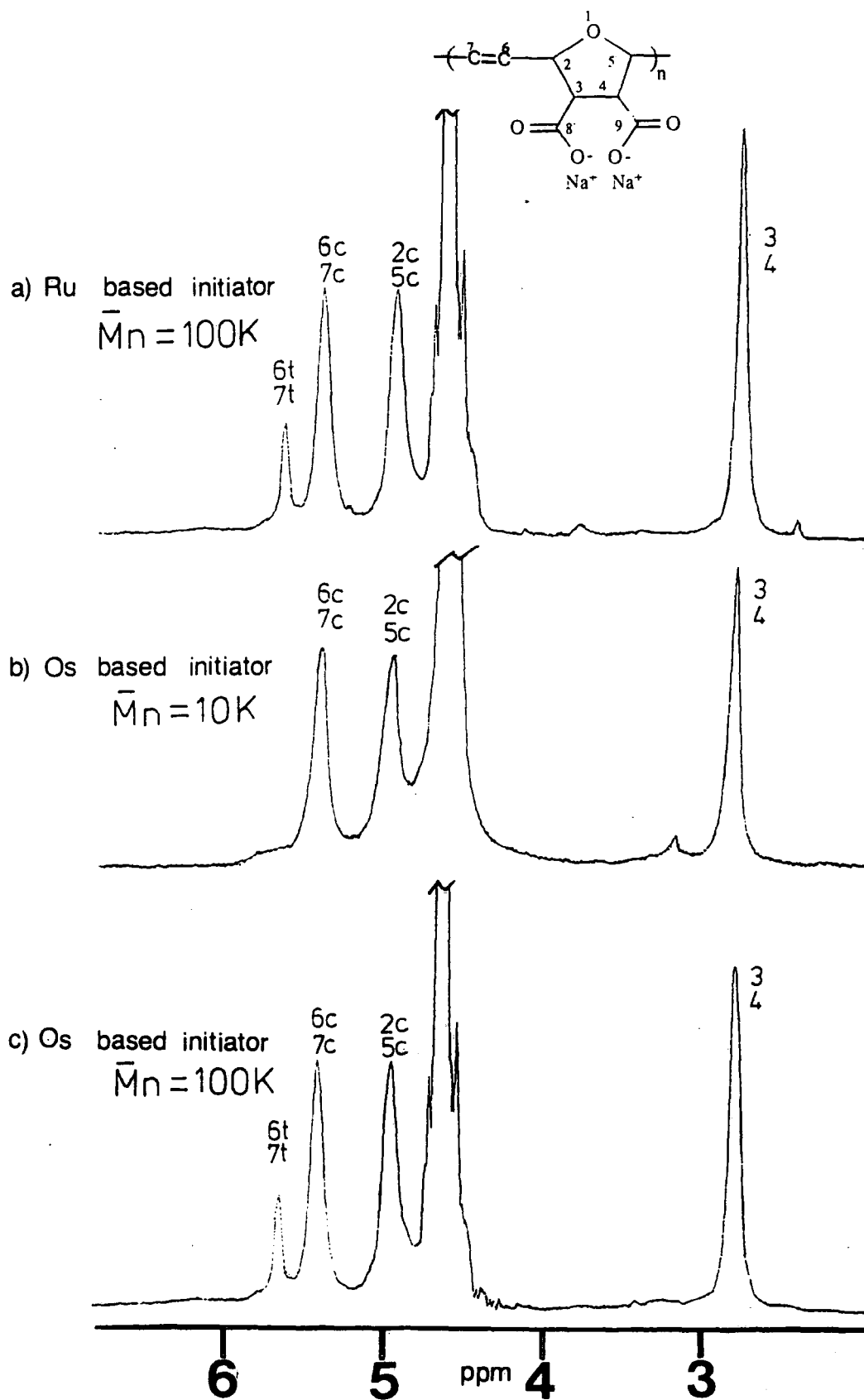
TABLE 3.7: Principal  $^1\text{H}$  NMR spectral parameters<sup>1</sup> of polymer **PIVb** (disodium salt) (399.952 MHz,  $\text{D}_2\text{O}$ ).

polymer <b>PIVb</b>	H at position	chemical shifts (ppm)
	6 and 7	5.70 (trans) 5.44 (cis)
	2 and 5	4.99 (c) <sup>2</sup> 4.57 (t) <sup>3</sup>
	3 and 4	2.85

- 1) with respect to water at 4.67 ppm.
- 2) "c" refers to a position  $\alpha$  to a *cis* vinylene.
- 3) "t" refers to a position  $\alpha$  to a *trans* vinylene.



Figure 3.22:  $^1\text{H}$  NMR spectra recorded at 399.952 MHz in  $\text{D}_2\text{O}$  of polymers PIVb 101 prepared using; a)  $\text{RuCl}_3 \cdot 3\text{H}_2\text{O}$ ; b)  $\text{OsCl}_3 \cdot 3\text{H}_2\text{O}$ ; and c)  $\text{OsCl}_3 \cdot 3\text{H}_2\text{O}$  as the precursors to the initiating and chain propagating species.



The microstructural analysis of the high polymers **PIVb** was made with reference to their analogues, polymers **PIII**, and the assumptions made in section 3.3 were applied here.

The vinylic protons (6 and 7) resonate at 5.70ppm (*trans*) and 5.44ppm (*cis*), both as broad signals. The allylic protons on positions 2 and 5 resonate at 4.99ppm (adjacent to *cis*) and 4.57ppm (adjacent to *trans*), although the latter resonance is partially concealed by the solvent resonances; the integration of this region is consistent with the integration of the vinylic region. Finally, methine protons on positions 3 and 4 resonate together at 2.85ppm. From this analysis, the polymers **PIVb** have predominantly *cis* double bonds,  $\sigma^c = 0.6$  for  $\text{RuCl}_3 \cdot 3\text{H}_2\text{O}$  (Figure 3.22a), and  $\sigma^c = 0.9$  or  $0.6$  for  $\text{OsCl}_3 \cdot 3\text{H}_2\text{O}$  (Figures 3.22b and 3.22c respectively).

Only the  $^{13}\text{C}$  NMR spectrum of the polymer prepared using  $\text{RuCl}_3 \cdot 3\text{H}_2\text{O}$  as the precursor to the initiating and chain propagating species is discussed (Figure 3.23). The assignment of the spectrum is recorded in Table 3.8.

All the resonances in the spectrum of **PIVb** are broader than those observed in the spectra of other related polymers (see sections 3.3 and 3.4), and little fine structure can be resolved. The carbonyl carbons (8 and 9) resonate as a multiplet centred at 182.28 ppm; the observation of multiple carbonyl resonances was also reported in the  $^{13}\text{C}$  NMR spectra of related ester functionalised polymers.<sup>75</sup> These multiple resonances result from carbons with different stereochemical environments, and are manifestations of sequence and/or tacticity effects in the main chain being transmitted into the pendant groups.

The allylic carbons at positions 2 and 5 allow unambiguous assignment of the vinylene content since *cis*-allylic resonances occur approximately 5 ppm upfield of *trans*-allylic resonances.<sup>23</sup> Allylic carbons adjacent to *trans* vinylenes are observed at 85.95 and 85.65 ppm, and those adjacent to *cis* at 81.60 and 81.13 ppm. Following the arguments developed in section 3.3.3, tacticity and/or sequence effects are present.

Figure 3.23: Proton decoupled  $^{13}\text{C}$  NMR spectrum recorded at 100.577 MHz in  $\text{D}_2\text{O}$  of polymer PIVb prepared using  $\text{RuCl}_3 \cdot 3\text{H}_2\text{O}$  as the precursor to the initiating and chain propagating species.

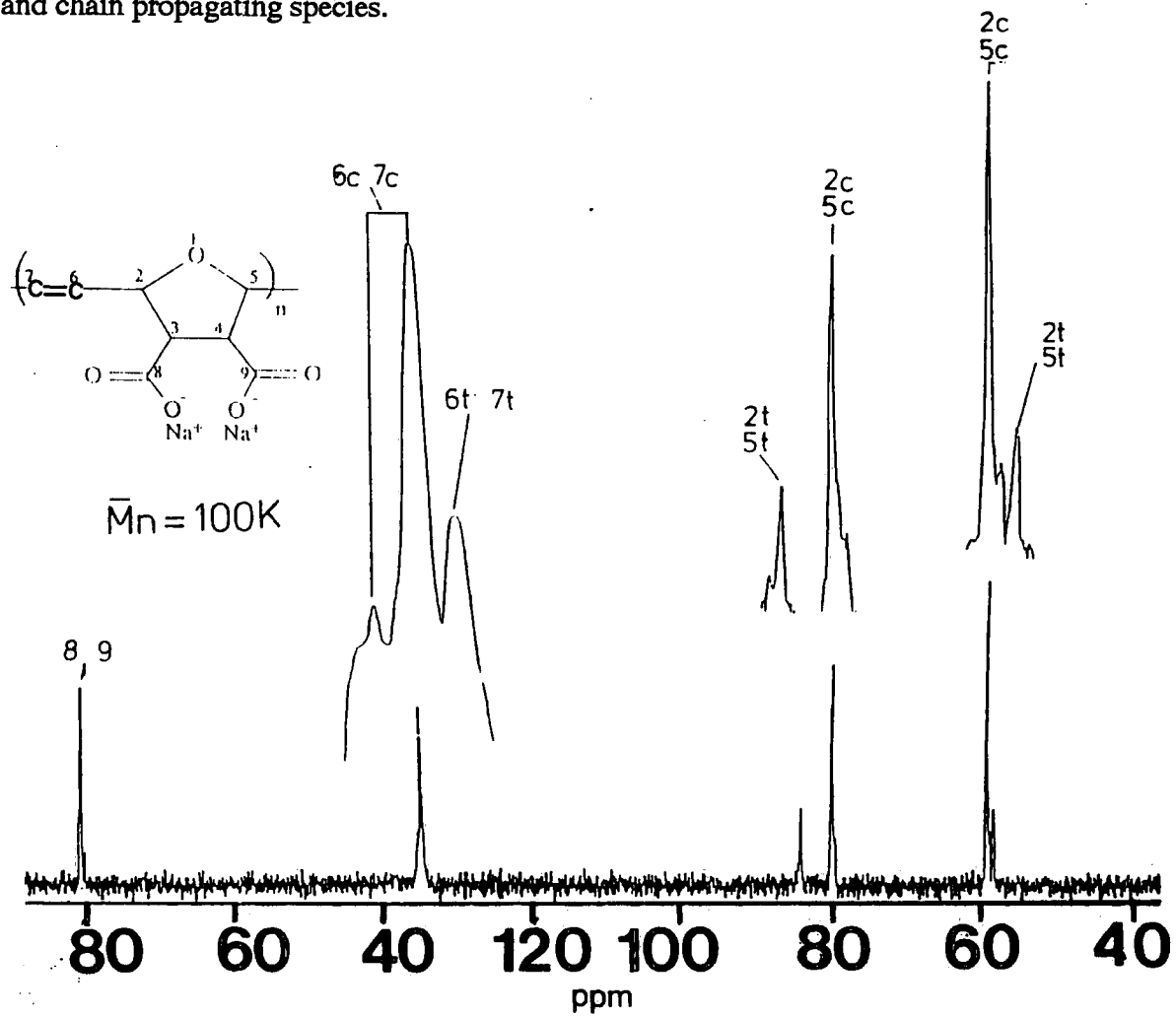
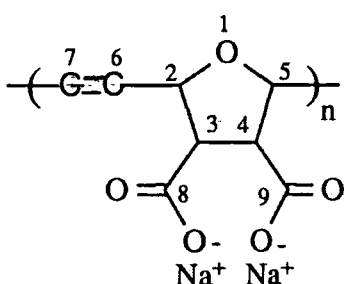


TABLE 3.8: Principal  $^{13}\text{C}$  NMR spectral parameters<sup>1</sup> of polymer PIVb (disodium salt) (100.577 MHz,  $\text{D}_2\text{O}$ ).

polymer PIVb	C at position	chemical shifts (ppm)
	8 and 9	182.44, 182.28
	6 and 7	136.78, 136.44 (cis) 136.18 (trans)
	2 and 5	85.95, 85.65 (t) <sup>2</sup> 81.56, 81.13 (c) <sup>3</sup>
	3 and 4	60.56 (c), 60.34 59.83 (t)

1) with respect to  $(\text{Me}_3\text{Si})\text{CD}_2\text{CD}_2\text{CO}_2\text{Na}$  at 1.70 ppm.

2) "t" refers to a position  $\alpha$  or  $\beta$  to a *trans* vinylene.

3) "c" refers to a position  $\alpha$  or  $\beta$  to a *cis* vinylene.

The fine structure observed in the allylic region is consistent with the multiple resonances observed in the vinylic region (C-6 and 7): *cis* signals at 136.78ppm and 136.44ppm and *trans* at 136.18ppm. Finally, the methine carbons at positions 3 and 4 are observed as a group of three resonances, the low field resonances (60.56 ppm) resulting from carbons  $\beta$  to *cis* vinylenes and the high field resonance from a carbon  $\beta$  to a *trans* vinylene. The central resonance at 60.33 ppm cannot be unambiguously assigned.

**3.6: Attempted aqueous ROMP of poly(2,5-(3,4-bis(carboxylic acid)pentylene)vinylene) (PVII).**

**3.6.1 *Attempted polymer synthesis:***

The ROMP process attempted is shown in Figure 3.24, which also records the numbering system employed for these polymers.

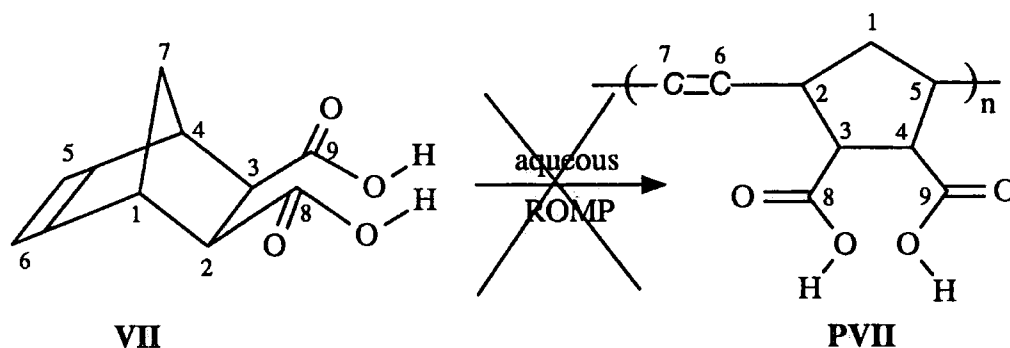


Figure 3.24: Attempted aqueous ROMP of monomer VII.

The polymerisation of monomer VII via aqueous ROMP was attempted using  $\text{RuCl}_3 \cdot 3\text{H}_2\text{O}$  as the precursor to the initiating and chain propagating species. In the first series of experiments, the monomer and transition metal concentrations were constant, and the temperature was altered (Table 3.9).

In each case, monomer VII (1g, 5.4 mmol) was placed in a test tube (13mm I.D.) containing water (3.0 ml), and equipped with a magnetic stirring bar. The resulting solution was stirred at the required temperature under a normal laboratory atmosphere for 10 minutes prior to the addition of an aqueous solution of  $\text{RuCl}_3 \cdot 3\text{H}_2\text{O}$  (3.5 ml of a 0.02g/ml solution). The solution was stirred for two days at the same temperature, during which time no colour change was observed in the reaction solution, and no polymer was formed. The disodium salt of the monomer, VIIb, was recovered by addition of the contents of the reaction vessel to aqueous

sodium hydroxide (10 ml, 30 wt%) followed by filtration and precipitation into methanol (100 ml). In all cases approximately 90-95% of the monomer was recovered as its disodium salt.

TABLE 3.9: Attempted aqueous ROMP<sup>1</sup> of monomer VII.

monomer	1.0g	1.0g	1.0g	1.0g	1.0g
catalyst	0.07g	0.07g	0.0.7g	0.07g	0.07g
water	6.5 ml	6.5 ml	6.5 ml	6.5 ml	6.5 ml
temp.	35°C	45°C	55°C	65°C	75°C
yield	0%	0%	0%	0%	0%

1) duration of experiment was two days.

The polymerisation of monomer VII by aqueous ROMP was also attempted by altering the concentration of  $\text{RuCl}_3 \cdot 3\text{H}_2\text{O}$ , and in some cases the temperature (Table 3.10). In each case, monomer VII (1g, 5.4 mmol) was placed in a test tube (13mm I.D.) containing water (3.0 ml), and equipped with a magnetic stirring bar. The resulting solution was stirred at the required temperature under a normal laboratory atmosphere for 10 minutes prior to the addition of an aqueous solution of  $\text{RuCl}_3 \cdot 3\text{H}_2\text{O}$  (3.5 ml of various concentrations). The solution was stirred for two days at the initial temperature, during which no colour change was observed in the reaction solution, and no polymer was formed. The disodium salt of the monomer, VIIb, was recovered by addition of the contents of the reaction vessel to aqueous sodium hydroxide (10 ml, 30 wt%) followed by filtration and precipitation into methanol (100 ml). In all cases approximately 90-95% of the monomer was recovered as its disodium salt.

TABLE 3.10: Attempted aqueous ROMP<sup>1</sup> of monomer VII.

monomer	1.0g	1.0g	1.0g	1.0g	1.0g
catalyst	0.04g	0.07g	0.14g	0.04g	0.14g
water	6.5 ml	6.5 ml	6.5 ml	6.5 ml	6.5 ml
temp.	55°C	55°C	55°C	75°C	75°C
yield	0%	0%	0%	0%	0%

1) duration of experiment was two days.

### 3.6.2 Discussion:

In this study, monomer VII could not be polymerised via aqueous ROMP using  $\text{RuCl}_3 \cdot 3\text{H}_2\text{O}$  as the precursor to the initiating and chain propagating species. However, these preliminary experiments do not rule out the possibility of the aqueous ROMP of monomer VII, since early publications have reported that  $\text{IrCl}_3 \cdot 3\text{H}_2\text{O}$  in water<sup>105</sup>, and both  $\text{RuCl}_3 \cdot 3\text{H}_2\text{O}$  and  $\text{OsCl}_3 \cdot 3\text{H}_2\text{O}$  in ethanol<sup>75</sup> were effective for the ROMP of *exo*-bicyclo[2.2.1]hept-5-ene-2-carboxylic acid. The aqueous ROMP of monomer VII may be possible with other catalyst precursors, or at different temperatures and concentrations, since the initiating species must be generated *in situ*.

Polymer PVIIb can be prepared by the non-aqueous ROMP of monomer VI,<sup>84</sup> followed by caustic hydrolysis of the product. As an example, the <sup>13</sup>C NMR spectrum (Figure 3.25) and infrared spectrum (Appendix B9) of polymer PVIIb are displayed; <sup>13</sup>C NMR assignments are recorded in Table 3.11.

Figure 3.25: Proton decoupled  $^{13}\text{C}$  NMR spectrum recorded at 100.577 MHz in  $\text{D}_2\text{O}$  of polymer **PVIIb** prepared using  $\text{WCl}_6$  as the precursor to the initiating and chain propagating species.

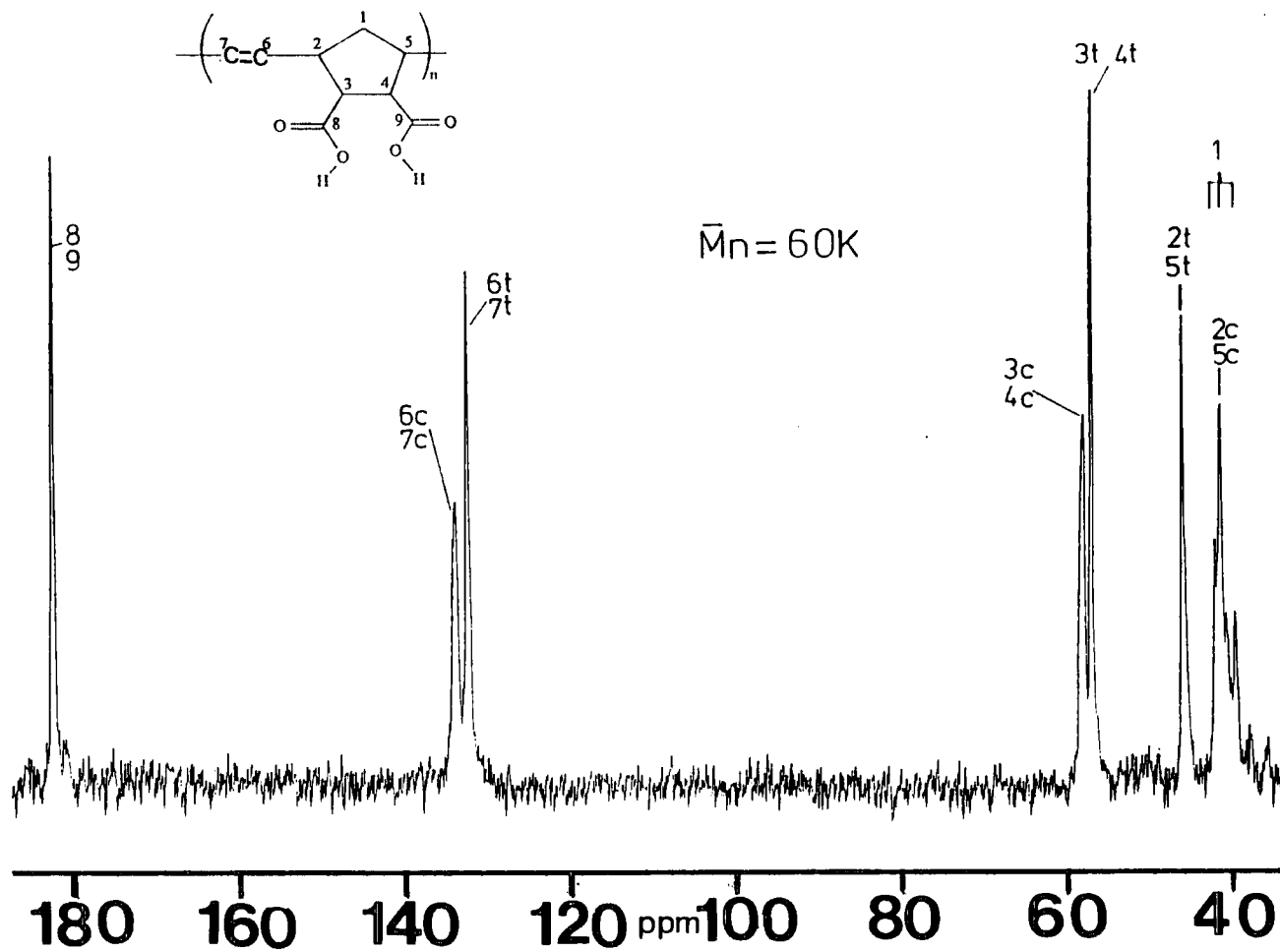
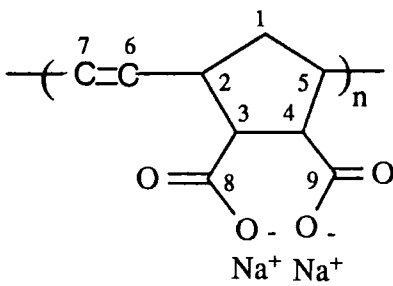




TABLE 3.11: Principal  $^{13}\text{C}$  NMR spectral parameters<sup>1</sup> of polymer PVIIb (disodium salt) (62.89 MHz,  $\text{D}_2\text{O}$ ).

polymer PVIIb	C at position	chemical shifts (ppm)
	8 and 9	182.38
	6 and 7	133.93 (cis), 133.89(cis) 132.50(trans)
	3 and 4	57.78(c) <sup>2</sup> , 56.79(t) <sup>3</sup>
	2 and 5	45.84(t), 41.25(c)
	1	41.45(cc) <sup>4</sup> , 41.05(ct) <sup>5</sup> 40.60(tt) <sup>6</sup>

- 1) with respect to  $(\text{Me}_3\text{Si})\text{CD}_2\text{CD}_2\text{CO}_2\text{Na}$  at 1.70 ppm.
- 2) "c" refers to a position  $\alpha$  to a *cis* vinylene.
- 3) "t" refers to a position  $\alpha$  to a *trans* vinylene.
- 4) "cc" refers to a position  $\beta$  to two *cis* vinylenes.
- 5) "ct" refers to a position  $\beta$  to a *cis* vinylene and a *trans* vinylene.
- 6) "tt" refers to a position  $\beta$  to two *trans* vinylenes.

### 3.7: Synthesis and characterisation of poly(2,5-(3,4-bis(hydroxymethyl)furanylene)vinylene) (PII).

#### 3.7.1 Polymer synthesis:

The ROMP process attempted is shown in Figure 3.26, which also records the numbering system employed.

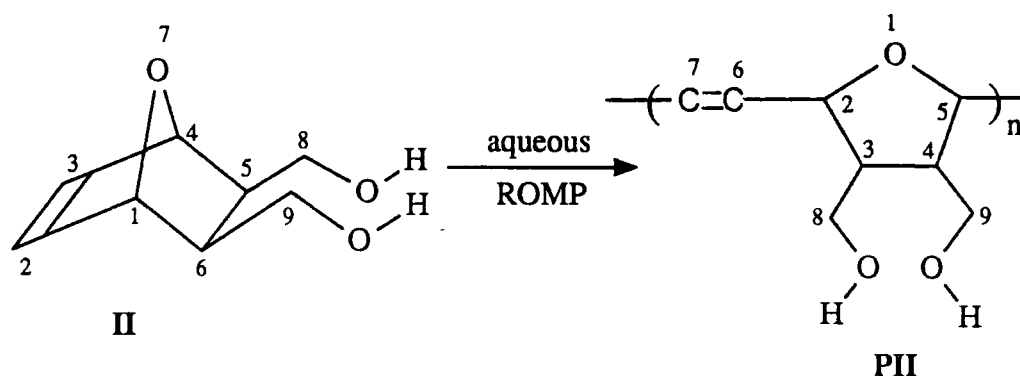
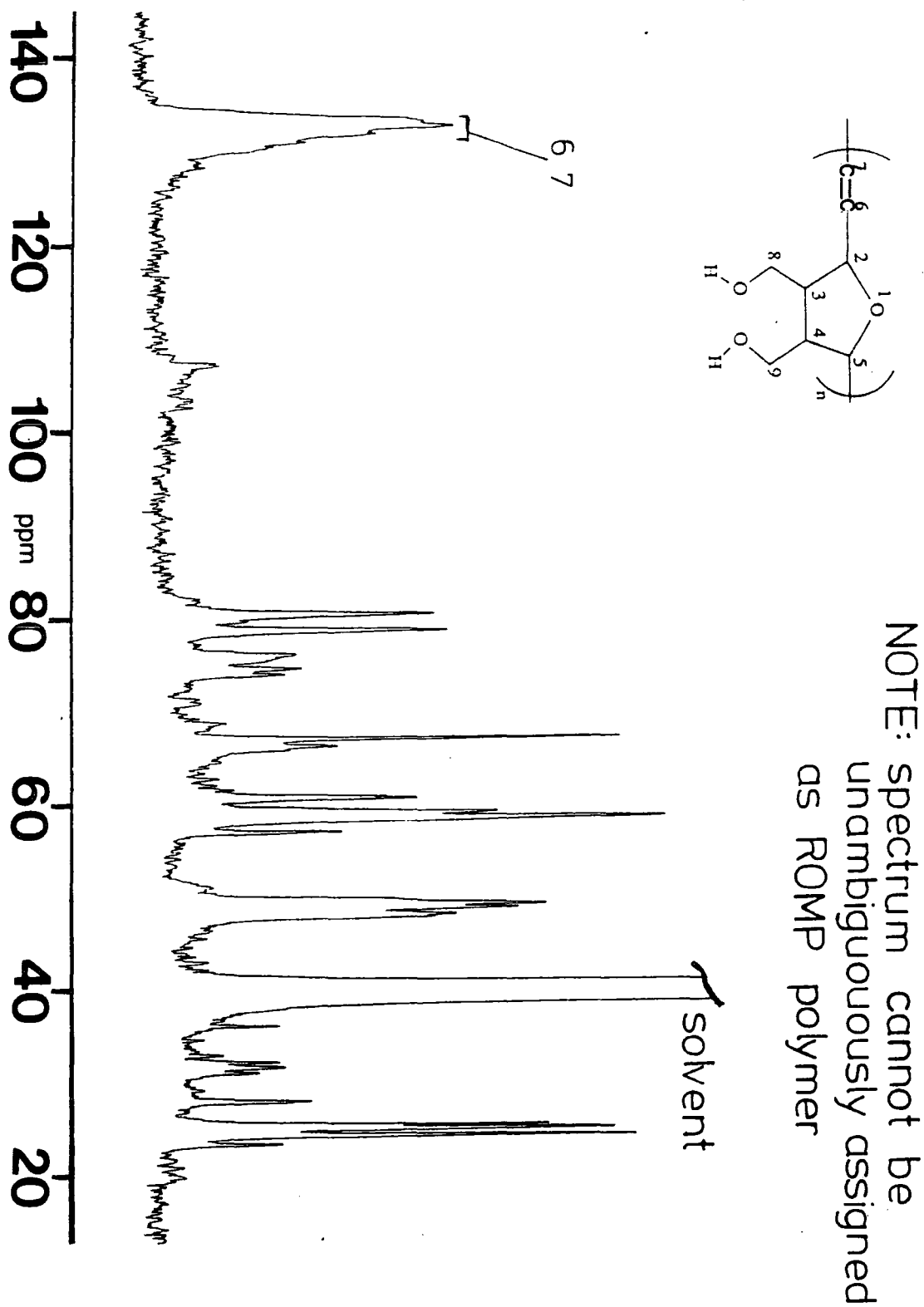


Figure 3.26: Aqueous ROMP of monomer II to yield polymer PII.

The aqueous ROMP of monomer **II** was attempted using  $\text{RuCl}_3 \cdot 3\text{H}_2\text{O}$  as the precursor to the initiating and chain propagating species. Monomer **II** (1.0g, 5.43 mmol) was placed in a test tube (13mm I.D.) equipped with a magnetic stirring bar. The resulting solution was stirred at  $55 \pm 0.1^\circ\text{C}$  for 30 minutes prior to the addition of an aqueous solution of  $\text{RuCl}_3 \cdot 3\text{H}_2\text{O}$  (3.5 ml of a 0.02g/ml solution). The reaction was allowed to proceed for two days at  $55^\circ\text{C}$ , during which time the colour of the reaction solution turned from its initial brown, to a dark green colour. Polymeric gel was precipitated after 5 hours, as the supernatant solution changed from dark green to pale green/brown.

The product polymer, obtained in 80% yield, was analysed by  $^{13}\text{C}$  NMR spectroscopy (Figure 3.27), but did not appear to be a pure ROMP polymer. This was an unexpected result since other workers have reported the aqueous ROMP of **II**.<sup>72</sup> The polymer was slightly swellable in THF but not soluble, which implies that cross-linking has occurred, and consequently no molecular weight analysis has been performed. A study of the purity of the transition metal chlorides used in this work has not been undertaken, but is clearly important with respect to future development of this field.

Figure 3.27: Proton decoupled  $^{13}\text{C}$  NMR spectrum recorded at 100.577 MHz in  $(\text{CD}_3)_2\text{SO}$  of polymer **PII** prepared using  $\text{RuCl}_3 \cdot 3\text{H}_2\text{O}$  as the precursor to the initiating and chain propagating species.



CHAPTER 4:  
SYNTHESIS AND  
CHARACTERISATION  
OF OLIGOMERS.

#### 4.1: Introduction.

The objectives of this chapter are the synthesis of oligomers by aqueous ROMP, and their characterisation. Oligomers can be formed by cross-metathesis of a chain propagating species with an acyclic olefin, termed a Chain Transfer Agent (CTA) (Figure 1.8): in this chapter, *cis*-but-2-ene-1,4-diol (VIII), *cis*-1,4-dimethoxybut-2-ene (IX), acrylic acid (X), and maleic acid (XI) are all employed as potential CTA's.

In chapter 3 it was observed that the aqueous ROMP reaction proceeded to high yield using  $\text{RuCl}_3 \cdot 3\text{H}_2\text{O}$  as the precursor to the initiating and chain propagating species; with other initiators the reactions were either irreproducible, or proceeded to low yield. In view of these findings, the ROMP of monomers III, IV, and VII were attempted in the presence of the various acyclic olefins, using  $\text{RuCl}_3 \cdot 3\text{H}_2\text{O}$  as the precursor to the initiating and chain propagating species.

#### 4.2: General Details.

##### 4.2.1 *Reactants:*

The water for the polymerisations was doubly distilled. *Cis*-but-2-ene-1,4-diol (VIII) (Aldrich, 95% *cis*) was doubly distilled under nitrogen (b.pt.<sup>15</sup> = 131.0°C, lit.<sup>106</sup> b.pt.<sup>16</sup> = 132.0°C) , and isolated as 99.7% pure (assessed by <sup>1</sup>H NMR spectroscopy). *Cis*-1,4-dimethoxybut-2-ene (IX) was synthesised by methylation of *cis*-but-2-ene-1,4-diol, doubly distilled under nitrogen (b.pt.<sup>760</sup> = 138.1 °C, lit.<sup>107</sup> b.pt.<sup>760</sup> = 138.0-138.5°C), and isolated as 99.5% pure (assessed by <sup>1</sup>H NMR spectroscopy).  $\text{RuCl}_3 \cdot 3\text{H}_2\text{O}$  (Aldrich Chemical Co. Ltd.), acrylic acid (X) (Aldrich, 99%), maleic acid (XI) (Aldrich, 99%), and the solvents (BDH) for the polymer recovery stages, were all used as supplied.

#### 4.2.2 Polymer characterisation:

All NMR spectra of polymers and oligomers were recorded using either a Varian VXR-400-S NMR spectrometer, operating at 399.952 MHz for  $^1\text{H}$  NMR, and 100.577 MHz for  $^{13}\text{C}$  NMR, or a Bruker AC 250 NMR spectrometer, operating at 250.133 MHz for  $^1\text{H}$  NMR, and 62.896 MHz for  $^{13}\text{C}$  NMR. Infrared spectra were recorded using either a Nicolet 730 FTIR or a Perkin Elmer 577 infrared spectrometer.

The molecular weights of water soluble polymers, **PIVb**, were assessed by aqueous Gel Permeation Chromatography (GPC) in saline buffer (pH. 6) of composition 0.141 M sodium chloride, 0.008 M sodium phosphate (monobasic) and 0.003 M sodium phosphate (dibasic). The equipment comprised of a Knauer HPLC 64 pump, Rheodyne 7125 injector with 100 $\mu\text{l}$  loop, Knauer refractive index detector and PLaquagel P3 30cm column (Polymer Laboratories Ltd.). Molecular weight calculations were made with a Chromatocorder 12 integrator (Quadrant Scientific) calibrated with polyethylene oxide standards (Polymer Laboratories Ltd.). All molecular weight data for polymers **PIVb** are expressed in polyethylene oxide equivalent molecular weights.

The molecular weight of THF soluble polymers, **PIII**, were assessed by non-aqueous GPC using THF as eluent. The equipment comprised of a Waters model 590 HPLC pump, Waters R401 Refractive Index (RI) detector, Waters U6K injection valve with 200 $\mu\text{l}$  injection loop, and a three column set: 5 $\mu$  10 $^5\text{\AA}$  30cm + 5 $\mu$  10 $^3\text{\AA}$  30cm + 5 $\mu$  100 $\text{\AA}$  30cm (Polymer Laboratories Ltd.). Molecular weight calculations were made with a Chromatocorder 12 integrator (Quadrant Scientific) calibrated with polystyrene standards (Polymer Laboratories Ltd.). All molecular weight data for polymers **PIII** are expressed in polystyrene equivalents.

**4.3: Oligomerisation of monomer III by aqueous ROMP using *cis*-but-2-ene-1,4-diol (VIII) as a chain transfer agent.**

**4.3.1 General considerations:**

The ROMP process is outlined in Figure 4.1, which also records the numbering and notation systems used; the **mid-chain units** are the repeat units in the polymer main chain; the **chain-end units** are the first and last addition units of the polymer or oligomer chain; and the **end groups** are the actual ends of the polymer or oligomer. When *cis*-but-2-ene-1,4-diol (VIII) was used as a chain transfer agent, vinyl hydroxymethyl end groups were formed (see later for proof).

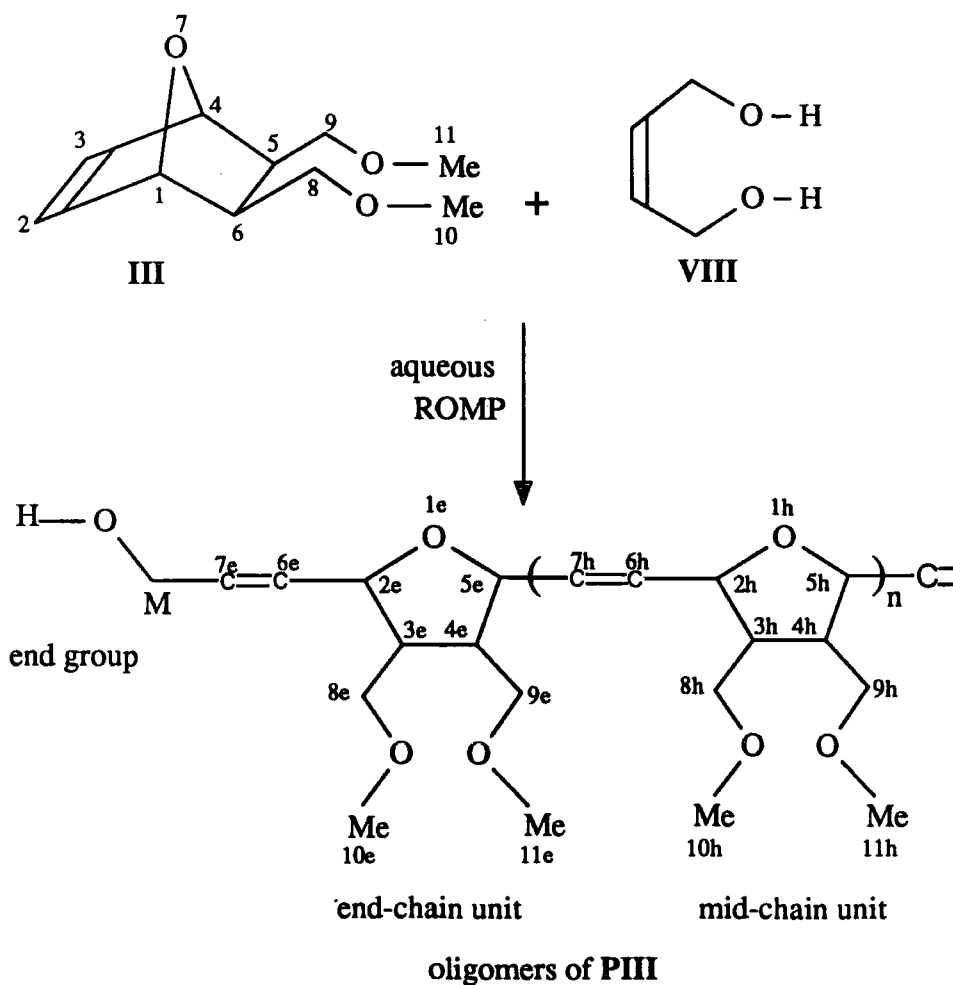


Figure 4.1: ROMP of monomer III to yield oligomers of PIII.

A number of characteristic colour changes are observed during the ROMP of monomer **III**. The solution of  $\text{RuCl}_3 \cdot 3\text{H}_2\text{O}$  changes from dark brown to crimson after its addition to the monomer, and eventually turns green; polymer/oligomers precipitated after the solution turned green. The timescale of the colour changes was found to be dependant on the concentration of **VIII** used in the reaction. The  $\text{RuCl}_3 \cdot 3\text{H}_2\text{O}$  was unpurified, and therefore it was impossible to associate the observed colour changes with specific events in the polymerisation such as the formation of the active initiator. The factors influencing the observed colours and their duration are discussed in chapter 5.

#### 4.3.2 ROMP of monomer **III** in the presence of low concentrations of *cis-but-2-ene-1,4-diol* (**VIII**):

The ROMP of monomer **III** was attempted in the presence of low concentrations of *cis-but-2-ene-1,4-diol*, which acted as a chain transfer agent (CTA) (molar ratio  $[\text{III}]:[\text{VIII}] > 10:1$ ) (Table 4.1). In these experiments, the concentration of **VIII** was not high enough to be a major component of the diluent mixture. In each case, monomer **III** (1g, 5.4 mmol) was placed in a test tube (13mm I.D.) containing mixtures of water and **VIII** (total volume, 3.0 ml), and equipped with a magnetic stirring bar. The resulting suspensions were stirred at  $55 \pm 0.1^\circ\text{C}$  under a normal laboratory atmosphere for 30 minutes prior to the addition of an aqueous solution of  $\text{RuCl}_3 \cdot 3\text{H}_2\text{O}$  (3.5 ml of a 0.02g/ml solution).

The reaction was allowed to proceed for two days at  $55^\circ\text{C}$ , after which the products, poly(2,5-(3,4-bis(methoxymethyl)furanylene)vinylene)s (**PIII**), were recovered by extraction into chloroform followed by precipitation into methanol. The polymers/oligomers were purified by reprecipitation of a magnesium sulphate dried, chloroform solution of each product into pentane. After filtration under a nitrogen atmosphere, the products were dried and stored under vacuum in the dark.



Elemental analyses of the products of these reactions are consistent with that of polymer PIII, and are recorded in appendix D.

TABLE 4.1: ROMP<sup>1</sup> of monomer III using RuCl<sub>3</sub>.3H<sub>2</sub>O as the precursor to the initiating and chain propagating species, and *cis*-but-2-ene-1,4-diol as a chain transfer agent (CTA).

molar ratio <sup>2</sup> of reactants		Time to ppt of polymer <sup>3</sup> /min	yield / %	Mn	Mw/Mn	σ <sup>c 4</sup>
RuCl <sub>3</sub> .3H <sub>2</sub> O	CTA					
1	---	1200	95	122K	2.5	0.35
1	1.2	950	95	99K	2.6	0.31
1	1.8	900	90	58K	3.2	0.40
1	2.4	800	92	62K	2.8	0.39
1	4.9	600	89	46K	2.6	0.35
1	7.3	360	87	18K	4.5	0.31
1	1.2	900	90	45K	2.9	0.40
1	2.4	860	83	53K	3.2	0.37
1	3.6	700	89	65K	2.8	0.34
1	2.9	810	93	81K	2.3	0.38
1	1.2	870	80	53K	4.8	0.35
1	2.4	760	91	59K	2.9	0.40
1	3.6	710	82	63K	2.6	0.35
1	4.9	560	86	17K	6.8	0.37

1) all polymerisations were run for two days at 55°C.

2) molar ratio of monomer : RuCl<sub>3</sub>.3H<sub>2</sub>O = 22:1 and [M] = 0.81 molar: this is a heterogeneous reaction.

3) time between the addition of RuCl<sub>3</sub>.3H<sub>2</sub>O and the precipitation of polymer: the solution colour was green.

4) determined by <sup>1</sup>H NMR spectroscopy.

### 4.3.3 ROMP of monomer **III** in the presence of high concentrations of *cis-but-2-ene-1,4-diol* (**VIII**):

The ROMP of monomer **III** was attempted in the presence of high concentrations of *cis-but-2-ene-1,4-diol*, which acted as a chain transfer agent (CTA) (molar ratio [**III**]:[**VIII**] < 10:1) (Table 4.2): the volume of **VIII** was a major component of the diluent mixture.

TABLE 4.2: ROMP<sup>1</sup> of monomer **III** using RuCl<sub>3</sub>.3H<sub>2</sub>O as the precursor to the initiating and chain propagating species, and *cis-but-2-ene-1,4-diol* as a co-diluent and a chain transfer agent (CTA).

molar ratio <sup>2</sup> of reactants		time to ppt of polymer <sup>3</sup> /min	yield / %	Mn	Mw/Mn	σ <sup>c 4</sup>
RuCl <sub>3</sub> .3H <sub>2</sub> O	CTA					
1	47	15	90	8.0K	2.2	0.42
1	93	3	87	3.1K	1.8	0.39
1	23	45	93	9.4K	2.7	0.40
1	47	10	88	5.0K	2.4	0.37
1	70	7	86	3.8K	2.1	0.39
1	93	5	74	2.9K	1.8	0.39
1	81	5	79	4.0K	2.0	0.40
1	93	4	75	3.5K	2.3	0.41
1	170	2	80	500	2.0	0.22

- 1) all polymerisations were run for two days at 55°C.
- 2) molar ratio of monomer : RuCl<sub>3</sub>.3H<sub>2</sub>O = 21:1 and [M] = 0.81 molar: this is a heterogeneous reaction.
- 3) time between the addition of RuCl<sub>3</sub>.3H<sub>2</sub>O and the precipitation of polymer: solution colour was green.
- 4) determined by <sup>1</sup>H NMR spectroscopy.

In each case, monomer **III** (1g, 5.4 mmol) was placed in a test tube (13mm

I.D.) containing mixtures of water and VIII (total volume, 3.0 ml), and equipped with a magnetic stirring bar. The resulting suspensions were stirred at  $55\pm 0.1^\circ\text{C}$  under a normal laboratory atmosphere for 30 minutes prior to the addition of an aqueous solution of  $\text{RuCl}_3\cdot 3\text{H}_2\text{O}$  (3.5 ml of a 0.02g/ml solution). The reaction was allowed to proceed for two days at  $55^\circ\text{C}$ , after which the product polymers/oligomers, poly(2,5-(3,4-bis-(methoxymethyl)furanylene)vinylene)s (PIII), were recovered by extraction into chloroform and precipitation into methanol. The polymers/oligomers were purified by reprecipitation of a magnesium sulphate dried, chloroform solution of each product into pentane. After filtration under a nitrogen atmosphere, the products were dried and stored under vacuum in the dark.

Elemental analyses of the products are consistent with polymer PIII, and are recorded in appendix D.

#### 4.3.4 Oligomer microstructure:

ROMP of monomer III in the presence of low concentrations of *cis*-but-2-ene-1,4-diol (section 4.3.2) produced high molecular weight polymers, PIII, with  $^1\text{H}$  NMR spectra identical to that shown in section 3.5.3: no end group resonances were observed (spectra not shown). By contrast, ROMP of monomer III in the presence of high concentrations of *cis*-but-2-ene-1,4-diol (section 4.3.3) produced a series of low molecular weight polymers and oligomers (Figure 4.2). In these materials the resonances of the mid-chain units at 5.72, 5.52, 4.63, 4.54, 4.20, 3.44, 3.29 and 2.29 ppm, were visible in the  $^1\text{H}$  NMR spectra, which also displayed resonances of the chain-end units and end groups (Figure 4.3 and Table 4.3).

Figure 4.2: GPC chromatograms recorded in THF of oligomers of **PIII** prepared using  $\text{RuCl}_3 \cdot 3\text{H}_2\text{O}$  as the precursor to the initiating and chain propagating species, and *cis*-but-2-ene-1,4-diol (**VIII**) as chain transfer agent (CTA).

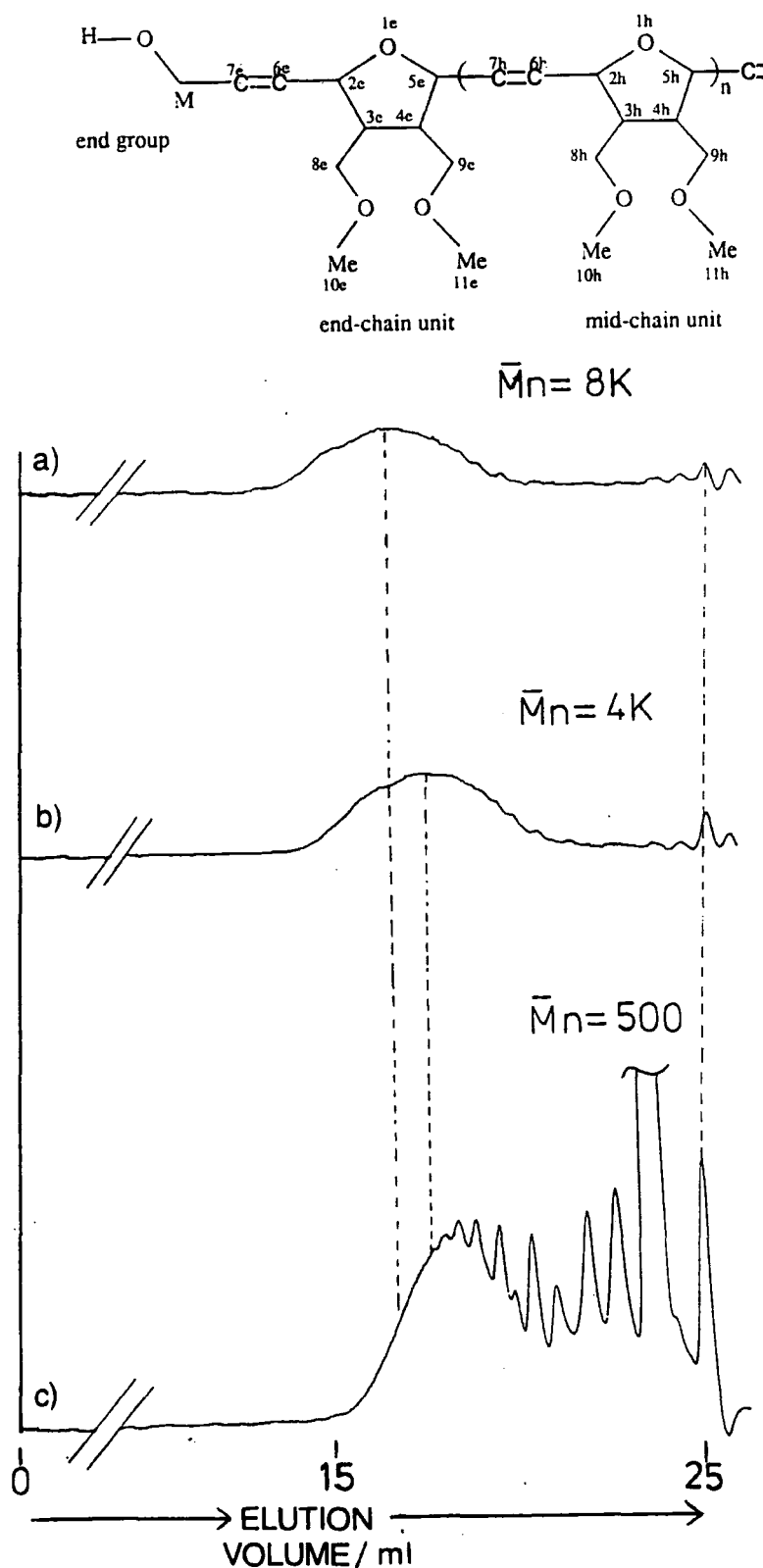
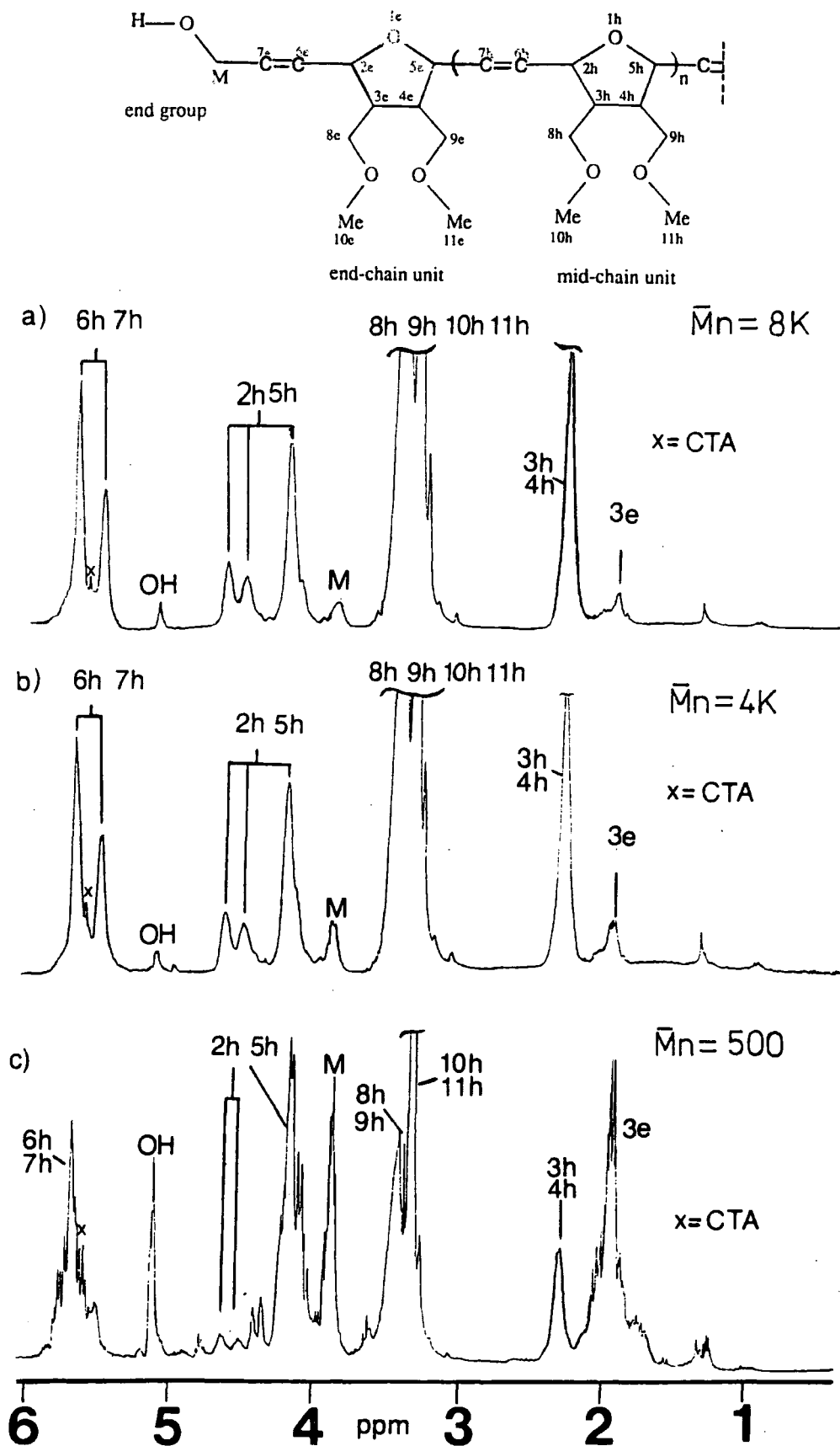


Figure 4.3:  $^1\text{HMR}$  spectra recorded at 250.133 MHz in  $\text{CDCl}_3$  of oligomers of **PIII** prepared using  $\text{RuCl}_3 \cdot 3\text{H}_2\text{O}$  as the precursor to the initiating and chain propagating species, and *cis*-but-2-ene-1,4-diol (**VIII**) as chain transfer agent (CTA). 121



Protons in units at the ends of the polymer/oligomer chain resonate with different chemical shifts compared with protons in the main body of the chain. Thus the methine protons at position 3 and 4 resonate at 2.29 ppm in a mid-chain unit (3h, 4h) and at 1.91 ppm in a chain end unit (3e) (Figures 4.1 and 4.3). The total integration of this region matches the total integration of the vinylic region, and the relative intensities of these two methine resonances correlate with the decrease in molecular weight calculated by GPC (Figure 4.2).

TABLE 4.3:  $^1\text{H}$  NMR spectral parameters<sup>1</sup> for the end groups of polymer PIII prepared using *cis*-but-2-ene-1,4-diol as a chain transfer agent (250.133 MHz,  $\text{CDCl}_3$ ).

PIII end groups	H at position	chemical shifts / ppm
	6e and 7e	masked
	methylene M	3.87
	hydroxyl H	5.10 <sup>2</sup>
	8e	masked
	10e	masked
	3e	1.91

1) with respect to chloroform at 7.26 ppm.

2) overlap with signals from *cis*-but-2-ene-1,4-diol impurity.

The  $^1\text{H}$  NMR spectra of the oligomers contain resonances of vinylene protons of the mid-chain units at 5.72 ppm (*cis*) and 5.52 ppm (*trans*), which are broader

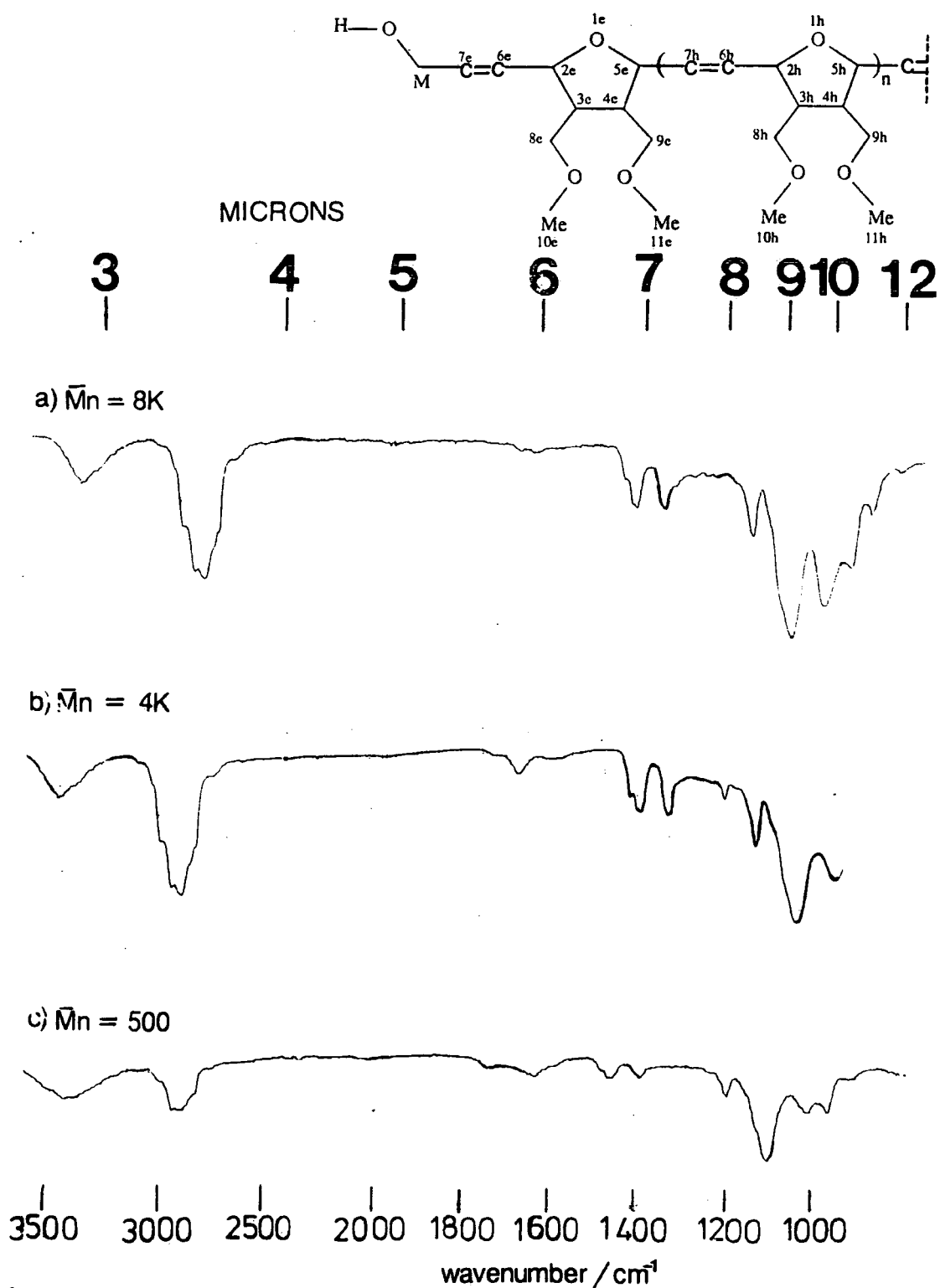
than those in the spectra of the high polymer (Figure 3.22), although no new resonances are observed. The ratio of *cis:trans* double bonds is generally consistent with the high polymer ( $\sigma^c = 0.4$ ) (Figures 4.3a and 4.3b), except for the lowest molecular weight oligomer (Figure 4.3c), which has a greater *trans* content ( $\sigma^c = 0.22$ ). This change in the microstructure is also observed in the allylic region ( $H_2$  and  $H_5$ ), where the relative intensity of the *trans*-allylic resonance at 4.20 ppm has greatly increased with respect to the *cis*-allylic resonances at 4.63 and 4.54 ppm (Figure 4.3c).

Additional proton resonances are observed principally at 3.9 ppm and 5.1 ppm, and are assigned as end-group resonances, methylene (M), and hydroxyl respectively (Figure 4.1). Their chemical shifts are similar to those of *cis*-but-2-ene-1,4-diol,<sup>108</sup> although their intensities are too large to result solely from residual chain transfer agent.

Infrared spectra were recorded for films of these oligomers cast from acetone solution, and contain all the absorptions of the high polymer, and additional absorptions in the region 1680-1640  $\text{cm}^{-1}$  and at 3400  $\text{cm}^{-1}$  (Figure 4.4). The relative intensity of these additional absorptions with respect to the high polymer absorptions show a qualitative increase as the molecular weight decreases, and it is possible that they arise from vinylenes in the polymer end groups. The absorption at 3400  $\text{cm}^{-1}$  results from the hydroxyl O-H stretch of the oligomer end groups.

Overall, the oligomers have a similar main chain microstructure to the high polymer ( $\sigma^c = 0.4$ ), although the *trans* content of very low molecular weight oligomers is greater ( $\sigma^c = 0.22$ ). It therefore appears that the terminal vinylene units are predominantly *trans*, suggesting that chain transfer preferentially yields *trans* products. The actual end groups are vinyl hydroxymethyl groups, and are observed in both infrared and  $^1\text{H}$  NMR spectra.

Figure 4.4: Infrared spectra recorded from films cast from acetone of oligomers of **PIII** prepared using  $\text{RuCl}_3 \cdot 3\text{H}_2\text{O}$  as the precursor to the initiating and chain propagating species, and *cis*-but-2-ene-1,4-diol (**VIII**) as chain transfer agent (CTA).





**4.4: Oligomerisation of monomer III by aqueous ROMP using *cis*-1,4-dimethoxybut-2-ene (IX) as a chain transfer agent.**

**4.4.1 Oligomer synthesis:**

The ROMP process is outlined in Figure 4.5, which also records the numbering and notation systems used; the **mid-chain units** are the repeat units in the polymer main chain; the **chain-end units** are the first and last addition units of the polymer or oligomer chain; and the **end groups** are the actual ends of the polymer or oligomer. When *cis*-1,4-dimethoxybut-2-ene is used as a chain transfer agent, vinyl methoxymethyl end groups are formed (see below).

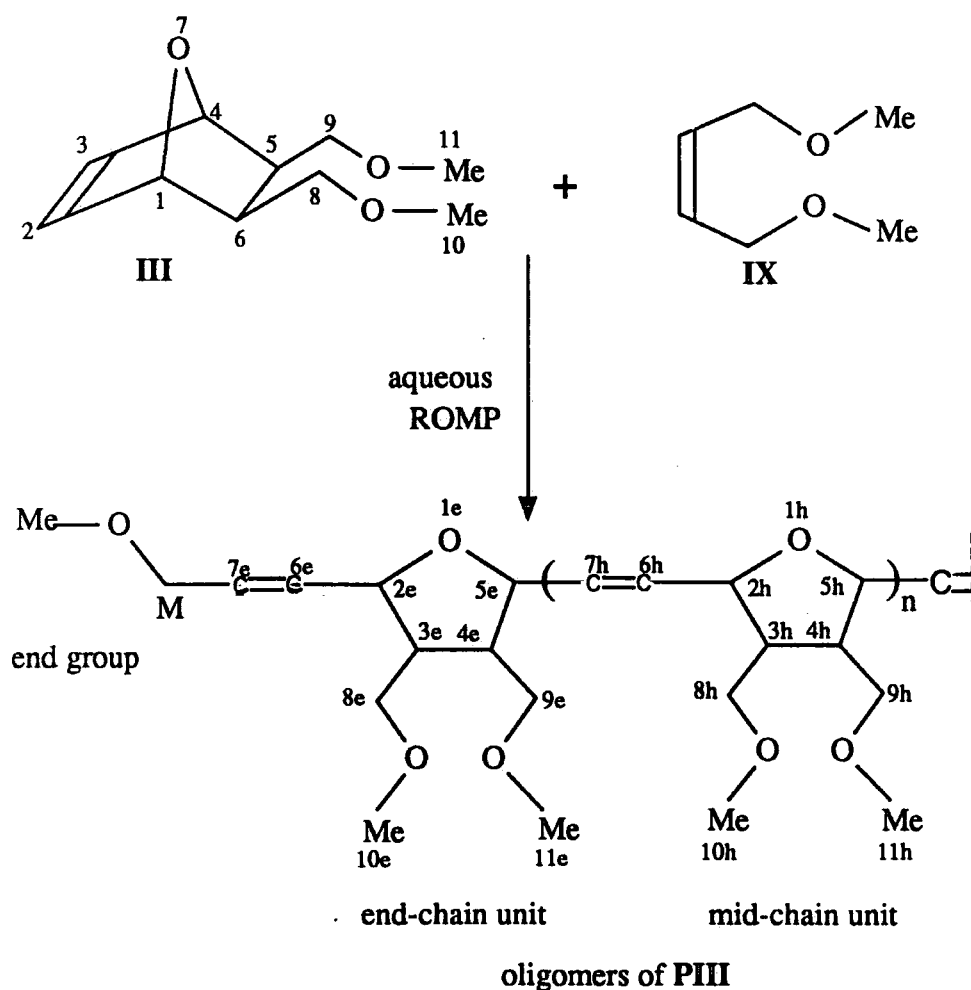


Figure 4.5: ROMP of monomer III to yield oligomers of PIII.

The ROMP of monomer **III** was performed in the presence of high concentrations of *cis*-1,4-dimethoxybut-2-ene (**IX**), which acted as a chain transfer agent (CTA) (molar ratio [**III**]: [**IX**] < 10:1) (Table 4.4): the volume of **IX** was a major component of the diluent mixture, although it was not water soluble.

TABLE 4.4: ROMP<sup>1</sup> of monomer **III** using RuCl<sub>3</sub>.3H<sub>2</sub>O as the precursor to the initiating and chain propagating species, and *cis*-1,4-dimethoxybut-2-ene as a co-diluent and a chain transfer agent (CTA).

molar ratio <sup>2</sup> of reactants		Time to ppt of polymer <sup>3</sup> /min	yield / %	Mn	Mw/Mn	σ <sup>c 4</sup>
RuCl <sub>3</sub> .3H <sub>2</sub> O	CTA					
1	18	860	80	41K	2.1	0.40
1	35	500	76	29K	2.0	0.39
1	71	420	69	13K	2.9	0.43
1	0	1200	95	155K	2.6	0.39
1	7	1100	94	26K	2.7	0.40
1	18	800	87	27K	2.8	0.40
1	29	600	79	25K	2.6	0.40
1	43	480	70	19K	2.5	0.37
1	85	360	64	7K	2.2	0.41
1	95	300	57	4K	2.1	0.42

- 1) all polymerisations were run for two days at 55°C.
- 2) molar ratio of monomer : RuCl<sub>3</sub>.3H<sub>2</sub>O = 21:1 and [M] = 0.81 molar: this is a heterogeneous reaction.
- 3) time between the addition of RuCl<sub>3</sub>.3H<sub>2</sub>O and the precipitation of polymer: solution colour was green.
- 4) determined by <sup>1</sup>H NMR spectroscopy.

In a typical experiment monomer **III** (1.0g, 5.43 mmol) was placed in a test

tube (13mm I.D.) equipped with a magnetic stirring bar. Appropriate quantities of distilled water and **IX** were added (total volume of diluent, 3.0 ml), and the resulting suspension was stirred at  $55\pm 0.1^\circ\text{C}$  under a normal laboratory atmosphere for 30 minutes prior to the addition of an aqueous solution of  $\text{RuCl}_3\cdot 3\text{H}_2\text{O}$  (3.5 ml of a 0.02g/ml solution).

As with previous experiments, the colour changes accompanying the reaction were brown-red-green, and were used as an empirical indication of the progress of the reaction; the time scale of the changes were dependant on the concentration of **IX** (see chapter 6). The reaction was allowed to proceed for two days at  $55^\circ\text{C}$ , after which the product polymers poly(2,5-(3,4-bis(methoxymethyl)furanylene)-vinylene)s (**PIII**), were recovered by extraction into chloroform and precipitation into methanol. The polymers were purified by reprecipitation of a magnesium sulphate dried, chloroform solution of the polymer into pentane, filtered, and finally dried under and stored under vacuum in the dark.

Elemental analyses of the products are consistent with that of polymer **PIII**, and are recorded in appendix D.

#### 4.4.2 *Oligomer microstructure:*

The ROMP of monomer **III** in the presence of high concentrations of *cis*-1,4-dimethoxybut-2-ene produced a series of low molecular weight polymers and oligomers (Figure 4.6). The resonances of the high polymer are clearly observed at 5.72, 5.52, 4.63, 4.54, 4.20, 3.44, 3.29 and 2.29 ppm, and in addition, resonances resulting from the end groups (Figure 4.7 and Table 4.5).

Figure 4.6: GPC chromatograms recorded in THF of oligomers of **PIII** prepared using  $\text{RuCl}_3 \cdot 3\text{H}_2\text{O}$  as the precursor to the initiating and chain propagating species, and *cis*-1,4-dimethoxybut-2-ene (**IX**) as chain transfer agent (CTA). 128

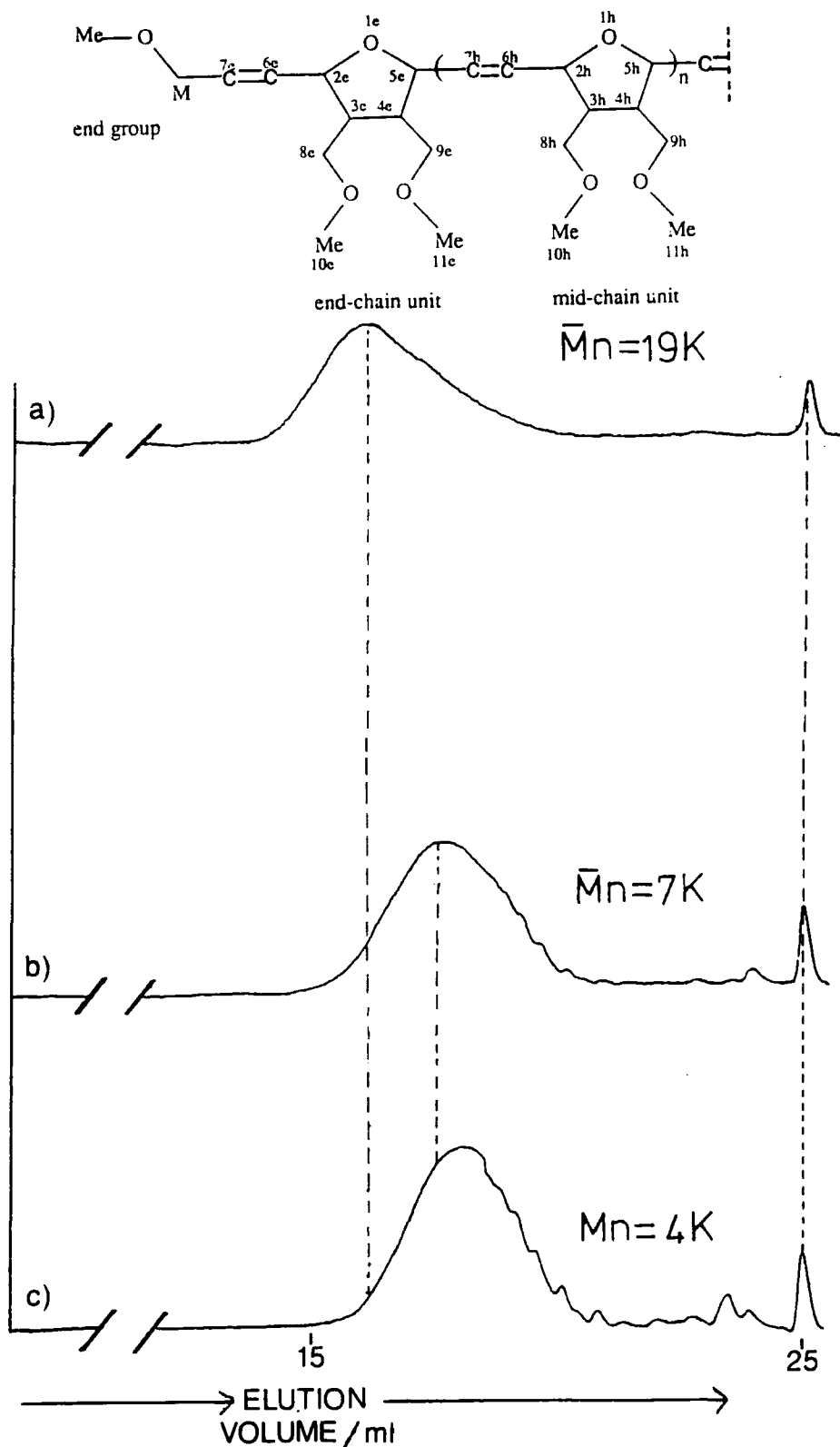
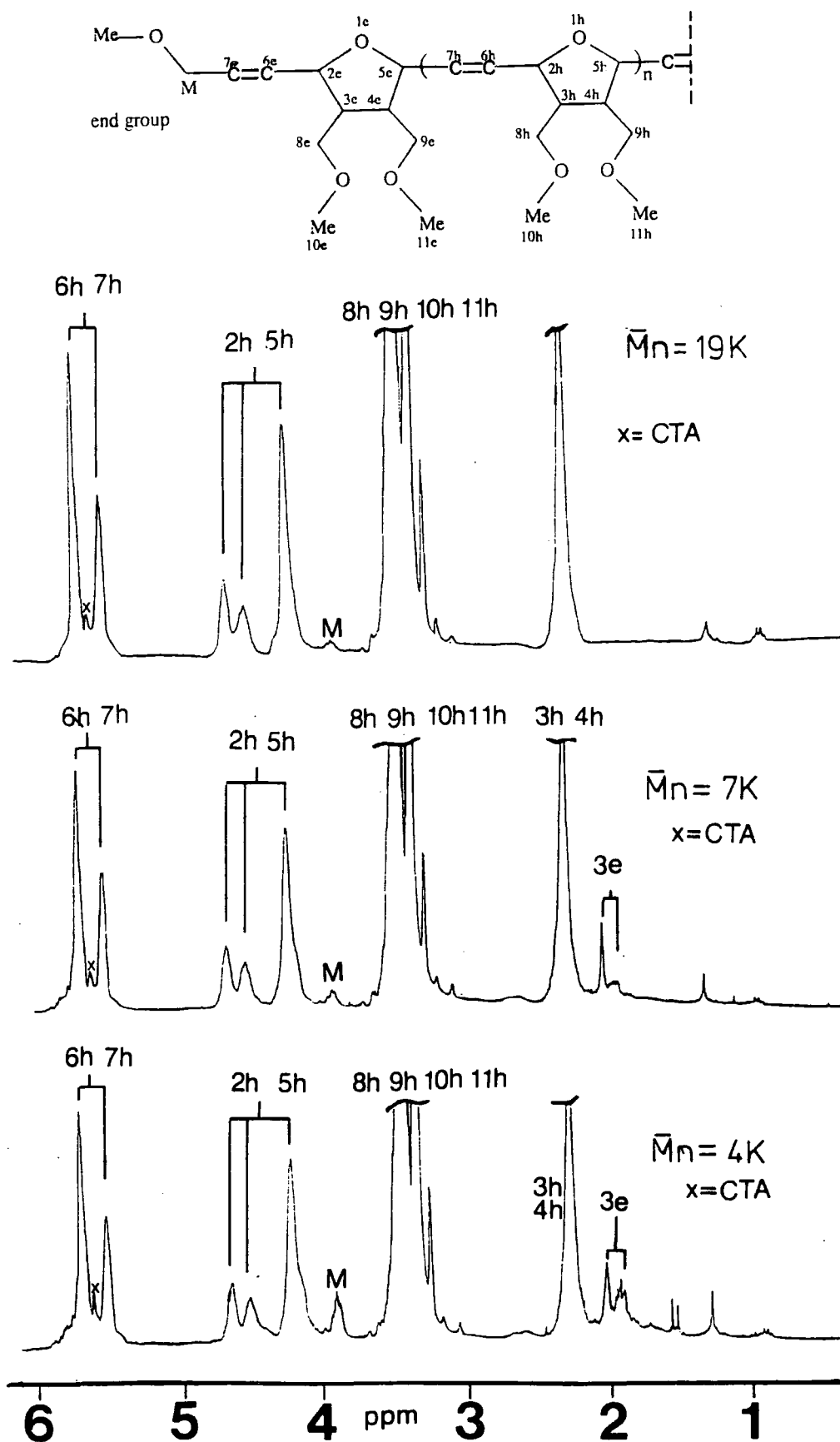


Figure 4.7:  $^1\text{HMR}$  spectra recorded at 250.133 MHz in  $\text{CDCl}_3$  of oligomers of **PIII** <sup>129</sup> prepared using  $\text{RuCl}_3 \cdot 3\text{H}_2\text{O}$  as the precursor to the initiating and chain propagating species, and *cis*-1,4-dimethoxybut-2-ene (**IX**) as chain transfer agent (CTA).



The methine protons on positions 3 and 4 resonate at 2.29 ppm in a mid-chain unit (3h, 4h) and at 2.03 and 1.91 ppm in a chain-end unit (3e) (Figure 4.7). The total integration of this region matches the total integration of the vinylic region: the combined intensities of these two additional methine resonances correlate with the decrease in molecular weight calculated by GPC (Figure 4.6). For oligomers prepared with *cis*-but-2-ene-1,4-diol as CTA, one high field resonance was observed at 1.91 ppm (section 4.3.4), and the end groups appeared to be predominantly *trans*. It is therefore possible that in these oligomers both *cis* and *trans* end groups are present.

TABLE 4.5:  $^1\text{H}$  NMR spectral parameters<sup>1</sup> for the end groups of polymer **PIII** prepared using *cis*-1,4-dimethoxybut-2-ene as a chain transfer agent (250.133 MHz,  $\text{CDCl}_3$ ).

PIII end groups	H at position	chemical shifts / ppm
	6e and 7e	masked
	methylene M	3.80
	methoxy end	masked
	8e	masked
	10e	masked
	3e	2.03, 1.91

1) with respect to chloroform at 7.26 ppm.

The resonances of the vinylic protons in the  $^1\text{H}$  NMR spectra (Figure 4.7) are broader than those in the high polymer (Figure 3.4a), although no new resonances

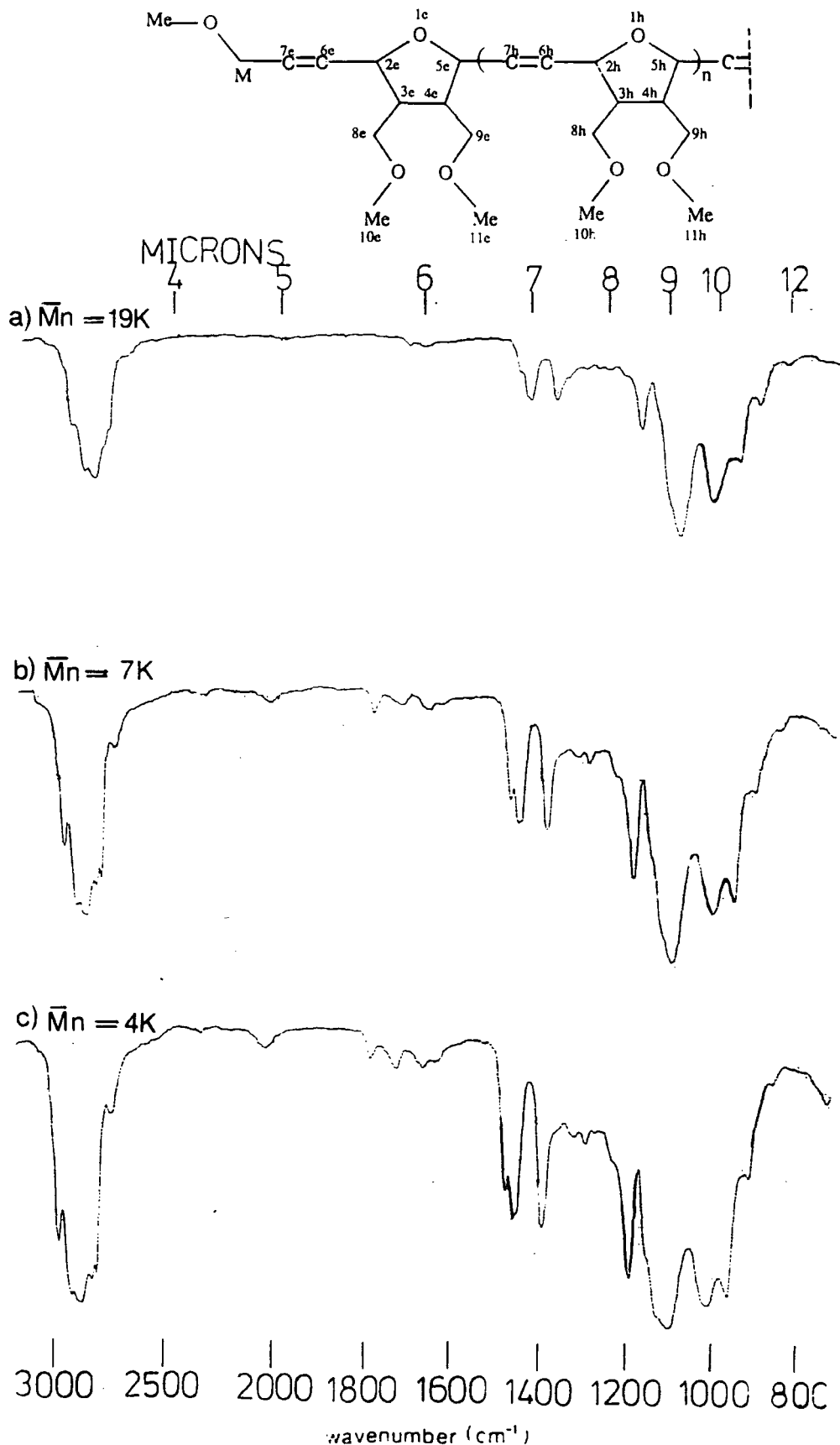
are observed. The ratio of *cis:trans* double bonds is consistent with the high polymer ( $\sigma^c = 0.4$ ) regardless of molecular weight. This could indicate that both *cis* and *trans* terminal vinylic bonds are formed, although the molecular weight of these oligomers is probably too high to allow such fine distinctions to be made (cf. section 4.3.4 where no change in *cis/trans* ratio was observed for  $M_n = 4K$  oligomers).

An additional resonance is observed in all the spectra at 3.80 ppm, and is assigned as the methylene end group (M), since the methylene group of *cis*-1,4-dimethoxybut-2-ene resonates at 3.80 ppm in  $CDCl_3$  (Figure 4.7);<sup>109</sup> the relative intensity of this signal increases as molecular weight decreases. The methyl group of the chain end is not observed, and is presumably masked by the resonances of the methoxy pendant groups of the polymer ( $H_{10}, H_{11}$ ).

Infrared spectra were recorded for films of these oligomers cast from acetone solution, and contain all the absorptions of the high polymer, and additional absorptions in the region 1680-1640  $cm^{-1}$  (Figure 4.8). The relative intensity of these additional absorptions with respect to those of the high polymer increase as the oligomer molecular weight decreases. The high polymer spectra (Figures 4.8a and 3.3a) contain little or no C=C stretching absorptions, and it is possible that the additional absorptions observed here result from vinylene bonds in the polymer end groups.

Overall the oligomers have a similar backbone structure to the high polymers, and there appears to be no strong preference for *cis/trans* initiation or termination. The actual end groups appear to be vinyl methoxymethyl groups derived from the chain transfer agent.

Figure 4.8: Infrared spectra recorded from films cast from acetone of oligomers of **PIII** prepared using  $\text{RuCl}_3 \cdot 3\text{H}_2\text{O}$  as the precursor to the initiating and chain propagating species, and *cis*-1,4-dimethoxybut-2-ene (**IX**) as chain transfer agent (CTA).





#### 4.5: Oligomerisation of monomer IV by aqueous ROMP using *cis*-but-2-ene-1,4-diol (VIII) as a chain transfer agent.

##### 4.5.1 Oligomer syntheses:

The ROMP process is outlined in Figure 4.9, which also records the numbering and notation systems used. The **mid-chain units** are the repeat units in the polymer main chain; the **chain-end units** are the first and last addition units of the polymer or oligomer chain; and the **end groups** are the actual ends of the polymer or oligomer. Oligomers are formed by cross metathesis of the chain carrying species with the chain transfer agent. Thus when *cis*-but-2-ene-1,4-diol is used as a chain transfer agent, vinyl hydroxymethyl end groups are formed (see below).

The ROMP of monomer IV was attempted in the presence of high concentrations of *cis*-but-2-ene-1,4-diol (VIII), which acted as a chain transfer agent (CTA) (molar ratio [IV]:[VIII] < 10:1) (Table 4.6): the volume of VIII was a major component of the solvent mixture.

In each case, monomer IV (1g, 5.4 mmol) was placed in a test tube (13mm I.D.) containing mixtures of water and VIII (total volume 3.0 ml), and equipped with a magnetic stirring bar. The resulting solutions were stirred at  $55 \pm 0.1^\circ\text{C}$  under a normal laboratory atmosphere for 30 minutes prior to the addition of an aqueous solution of  $\text{RuCl}_3 \cdot 3\text{H}_2\text{O}$  (3.5 ml of a 0.02g/ml solution).

The colour of the solution changed during the reaction, brown-red-green, and was used as an indication of the progress of the reaction; precipitation of polymer was observed when the reaction solution was green. The reaction was allowed to proceed for two days at  $55^\circ\text{C}$ , after which the products, poly(2,5-(3,4-bis(carboxylic acid)furanylene)vinylene)s (PIV) were recovered by filtration and thoroughly washed with dilute hydrochloric acid. The disodium salts of the polymer/oligomers (PVIb) were recovered by addition of the solid diacid

polymer/oligomers, **PIV** (0.5g), to aqueous sodium hydroxide (30 wt%), followed by filtration and precipitation into methanol (100 ml).

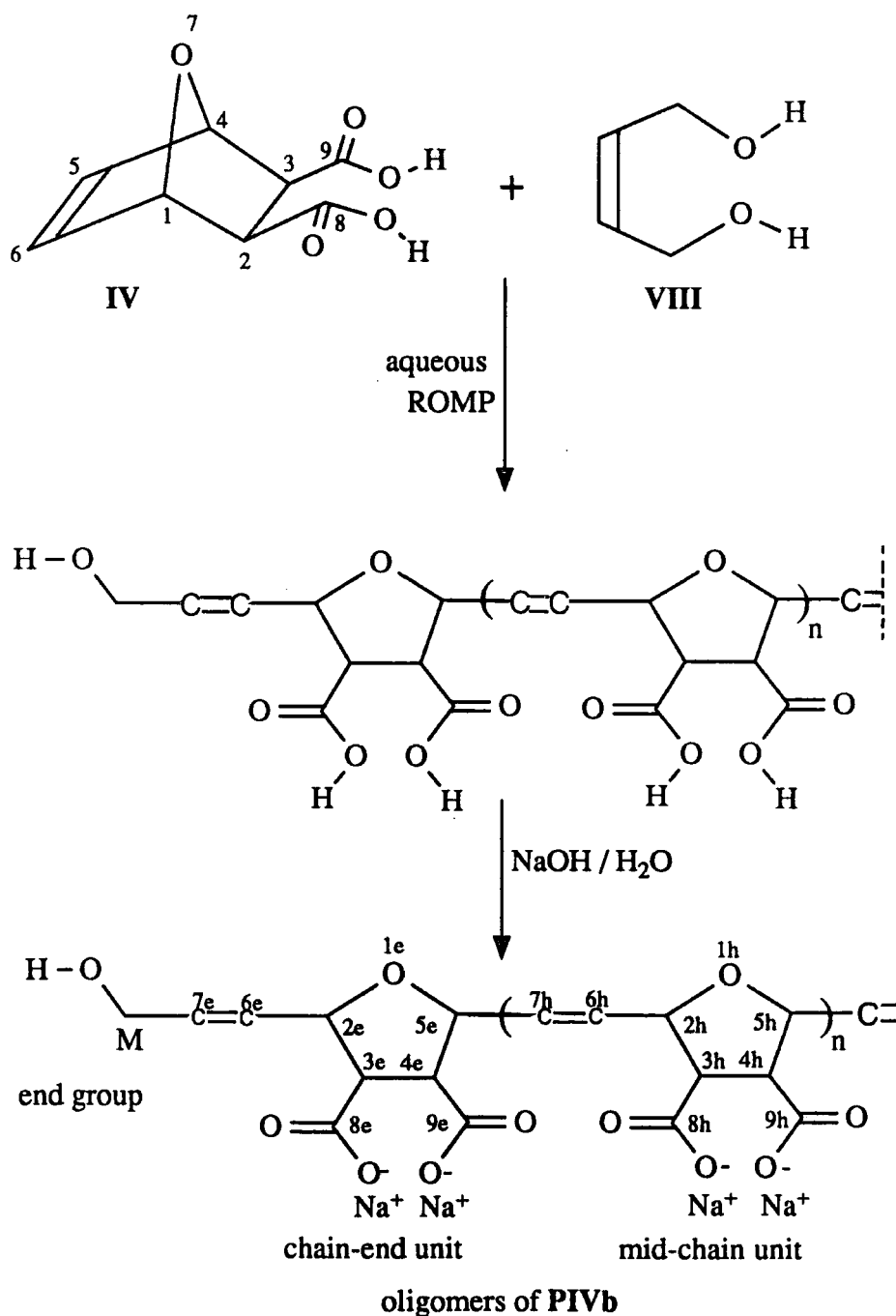


Figure 4.9: ROMP of monomer IV to yield oligomers of PIV: conversion of oligomers PIV into oligomers PIVb.

TABLE 4.6: ROMP<sup>1</sup> of monomer **IV** using RuCl<sub>3</sub>.3H<sub>2</sub>O as the precursor to the initiating and chain propagating species, and *cis*-but-2-ene-1,4-diol as a co-solvent and a chain transfer agent (CTA).

molar ratio <sup>2</sup> of reactants		Time to ppt of polymer <sup>3</sup> /min	yield / %	Mn	Mw/ Mn	σ <sup>c4</sup>
RuCl <sub>3</sub> .3H <sub>2</sub> O	CTA					
1	0	1200	95	>100K <sup>5</sup>	---	0.65
1	22	200	93	5.9K	2.4	0.64
1	54	100	92	4.0K	2.4	0.62
1	72	15	90	2.9K	2.0	0.65
1	81	15	85	2.3K	2.0	0.62
1	108	7	87	1.9K	2.4	0.58
1	210	5	90	700	2.1	0.40

- 1) all polymerisations were run for two days at 55°C.
- 2) molar ratio of monomer:RuCl<sub>3</sub>.3H<sub>2</sub>O = 16:1, and [M]= 0.84 molar: this is a homogeneous reaction.
- 3) time between the addition of RuCl<sub>3</sub>.3H<sub>2</sub>O and the precipitation of polymer: solution colour was green.
- 4) determined by <sup>1</sup>H NMR spectroscopy.
- 5) polymer was partially excluded from the GPC column.

Polymer/oligomers **PIVb** were purified by three successive reprecipitations into methanol from water, then recovered by filtration and finally dried and stored under vacuum. The polymer/oligomers, **PVIb**, formed by this method were pale green/brown solids, the colour being due to the presence of 0.1-0.3% by weight transition metal contamination, which was difficult, but not impossible to remove.

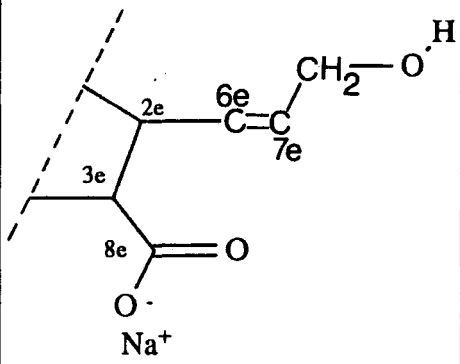
Elemental analyses of polymers **PIVb** are consistent with ROMP polymers of

IV containing dibasic repeat units, and are found in appendix D.

#### 4.5.2 Oligomer characterisation:

The reduction of molecular weight of the oligomers, **PIVb**, can be observed using aqueous GPC (Figure 4.10), and correlated to the observation of new end group resonances in the  $^{13}\text{C}$  NMR spectra (Figures 4.11, 4.12 and 4.13). The  $^{13}\text{C}$  NMR spectrum of the high polymer (Figure 3.23) was discussed in great depth in section 3.5.3, and contains resonances at: 182.44, 182.28 ppm (8h, 9h); 136.78, 136.44, 136.18 ppm (6h, 7h); 85.95, 85.65, 81.56, 81.13 ppm (2h, 5h); and 60.56, 60.34, 59.83 ppm (3h, 4h) (Table 3.9). New resonances are observed in the  $^{13}\text{C}$  NMR spectra of the oligomers (Figures 4.12 and 4.13, Table 4.7).

TABLE 4.7:  $^{13}\text{C}$  NMR spectral parameters<sup>1</sup> for the end groups of polymer **PIVb** (disodium salt) prepared using *cis*-but-2-ene-1,4-diol as a chain transfer agent (100.577 MHz,  $\text{D}_2\text{O}$ ).

PIVa end group	C at position	chemical shifts/ ppm
	8e	185.30
	7e	134.52, 134.14
	2e	86.79 (t) <sup>2</sup> 83.87 (c) <sup>3</sup> , 83.55 (c)
	3e	59.60 (c), 59.51 (c) 59.45 (t)
	methylene M	65.50 (t)

1) with respect to  $(\text{Me}_3\text{Si})\text{CD}_2\text{CD}_2\text{CO}_2\text{Na}$  at 1.70 ppm.

2) "t" refers to a position  $\alpha$  or  $\beta$  to a *trans* vinylene.

3) "c" refers to a position  $\alpha$  or  $\beta$  to a *cis* vinylene.

Figure 4.10: GPC chromatograms recorded in saline buffer of oligomers of **PIVb** prepared using  $\text{RuCl}_3 \cdot 3\text{H}_2\text{O}$  as the precursor to the initiating and chain propagating species, and *cis*-but-2-ene-1,4-diol (**VIII**) as chain transfer agent (CTA).

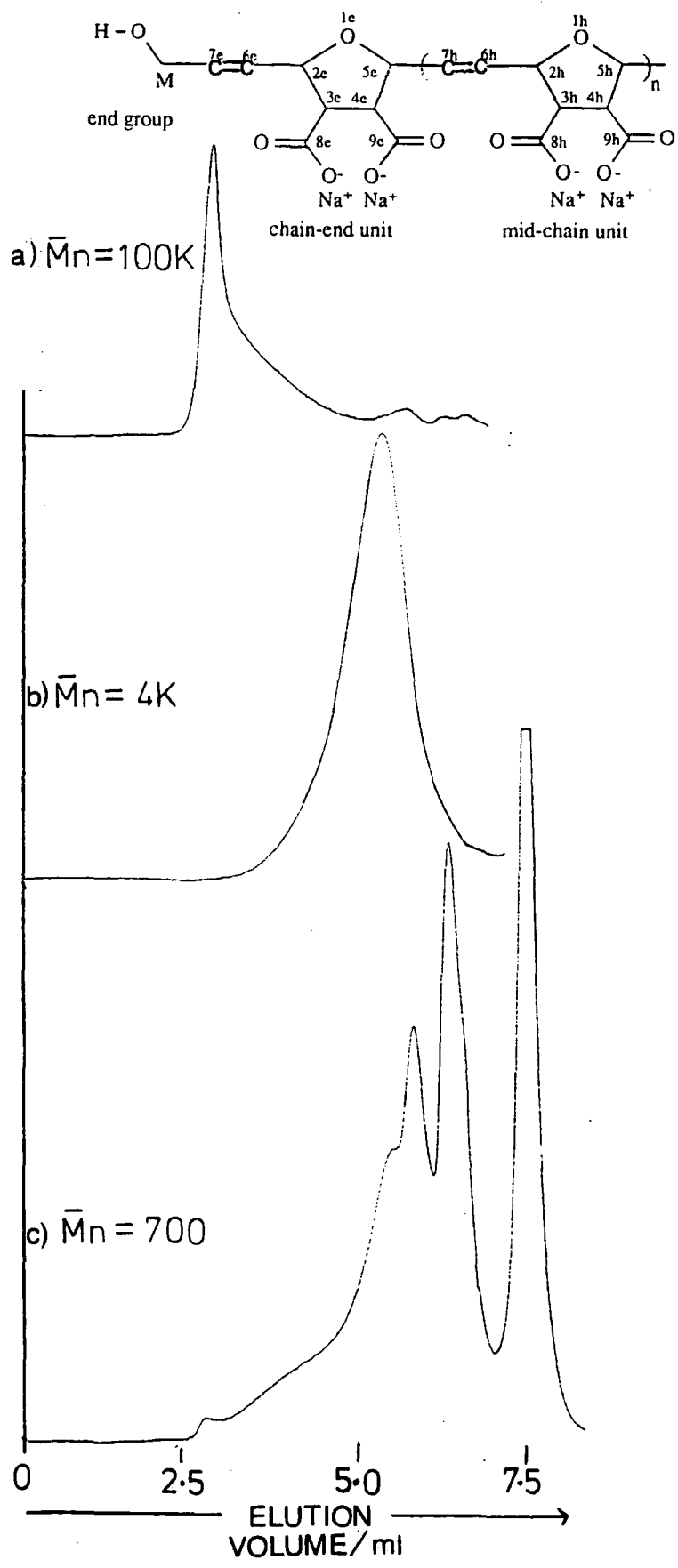


Figure 4.11: APT and proton decoupled  $^{13}\text{C}$  NMR spectra recorded at 100.577 MHz in  $\text{D}_2\text{O}$  of polymer PIVb prepared using  $\text{RuCl}_3 \cdot 3\text{H}_2\text{O}$  as the precursor to the initiating and chain propagating species.

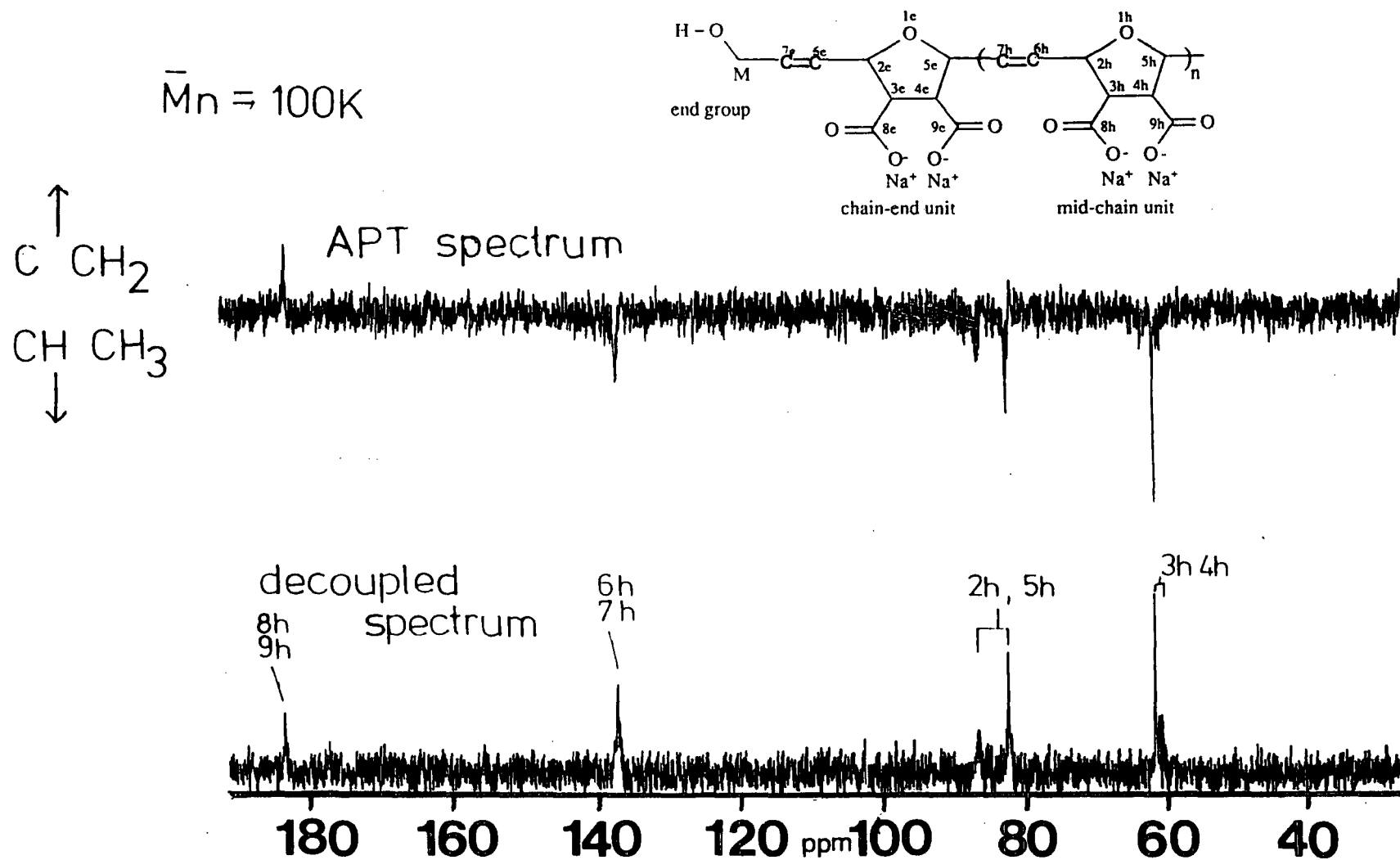


Figure 4.12: APT and proton decoupled  $^{13}\text{C}$  NMR spectra recorded at 100.577 MHz in  $\text{D}_2\text{O}$  of oligomers of PIVb prepared using  $\text{RuCl}_3 \cdot 3\text{H}_2\text{O}$  as the precursor to the initiating and chain propagating species, and *cis*-but-2-ene-1,4-diol (VIII) as chain transfer agent (CTA).

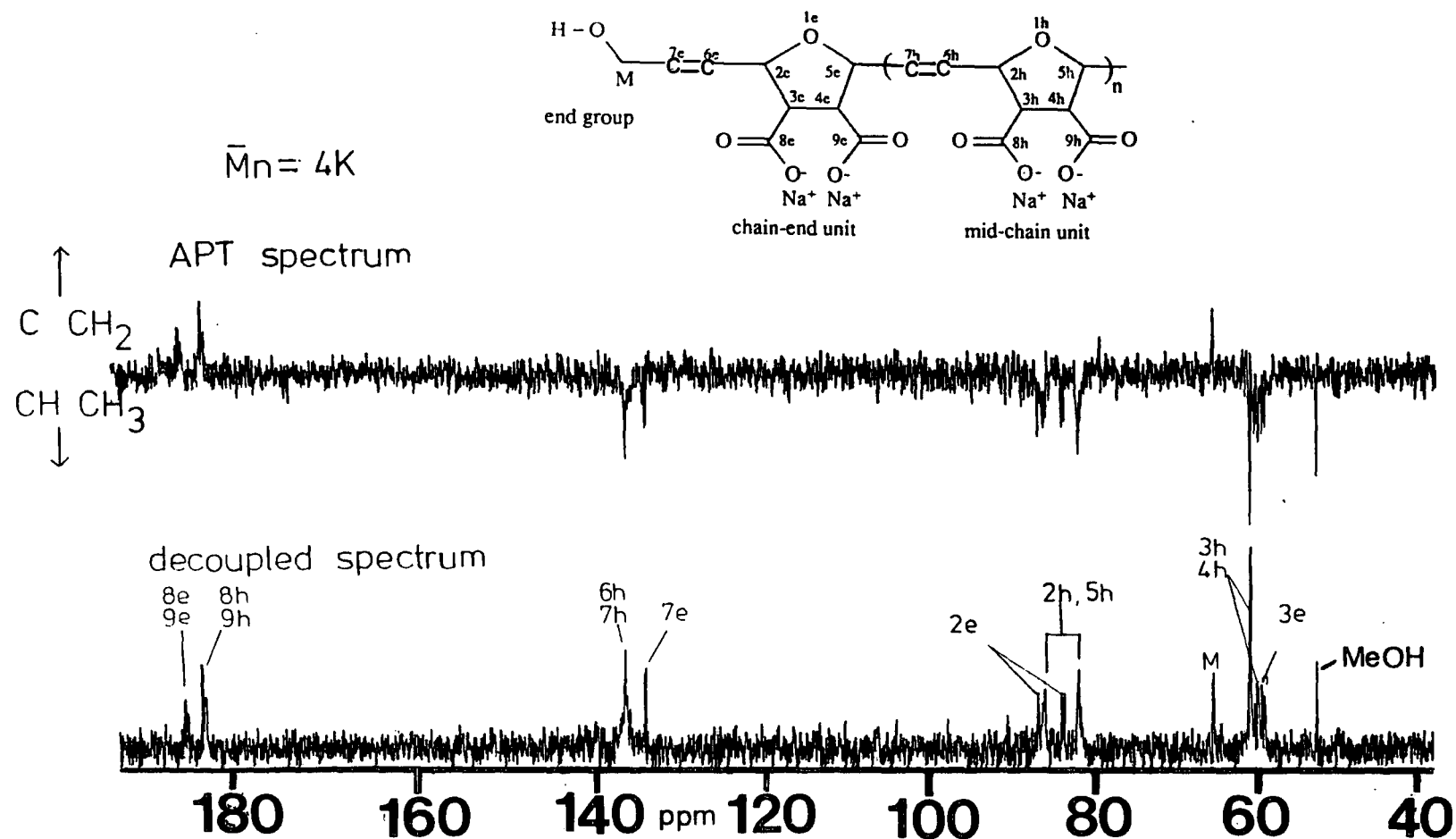
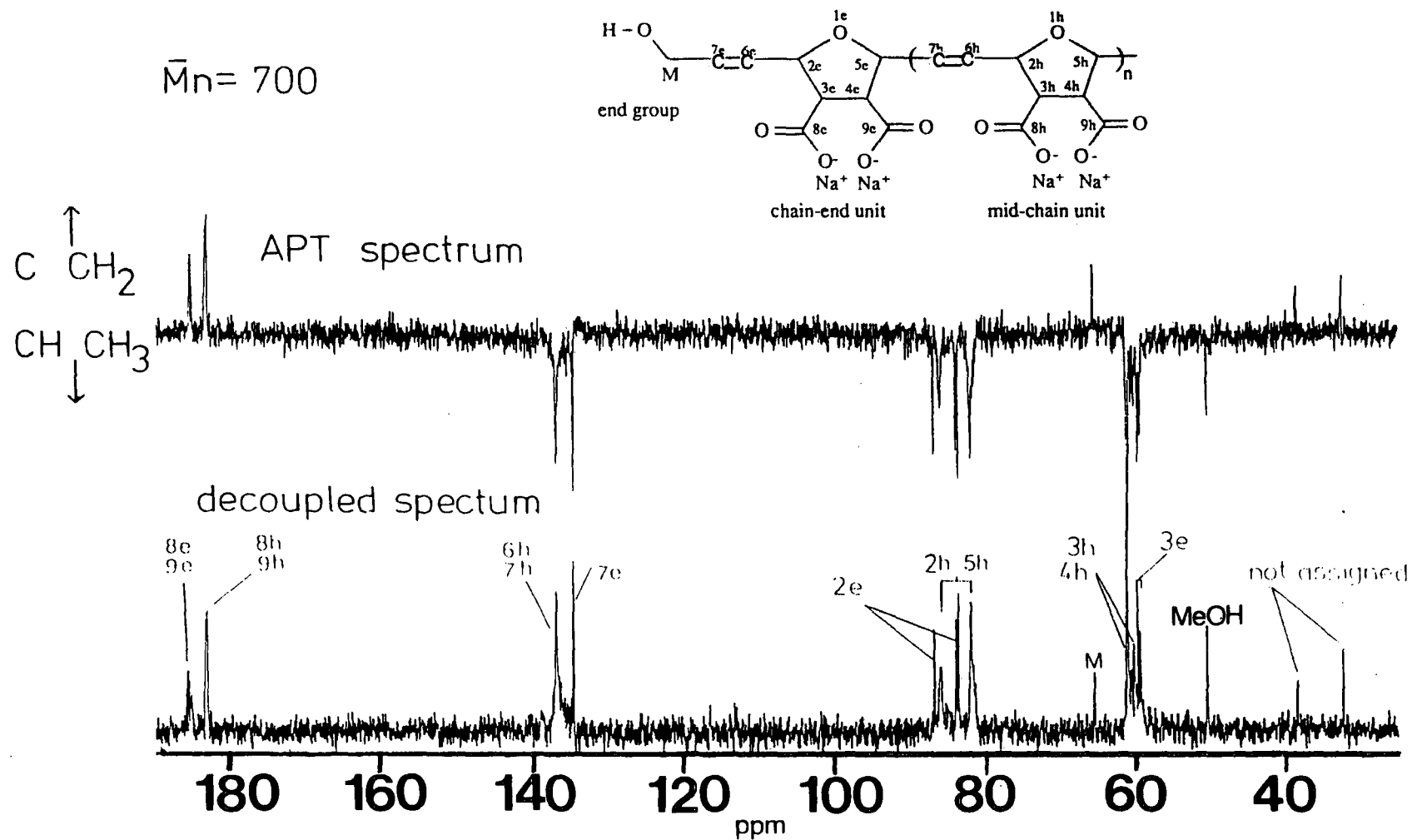


Figure 4.13: APT and proton decoupled  $^{13}\text{C}$  NMR spectra recorded at 100.577 MHz in  $\text{D}_2\text{O}$  of oligomers of PIVb prepared using  $\text{RuCl}_3 \cdot 3\text{H}_2\text{O}$  as the precursor to the initiating and chain propagating species, and *cis*-but-2-ene-1,4-diol (VIII) as chain transfer agent (CTA).





The carbonyl groups in mid-chain units (8h, 9h) resonate at 182.44 and 182.28 ppm (Figure 4.11), and at 185.30 ppm on chain-end units (8e) (Figures 4.12 and 4.13). A shift to lower field is also observed for both *cis*-allylic (83.87, 83.55 ppm), and *trans*-allylic (87.79 ppm) chain-end carbons (2e); the observation of both these resonances suggests that there is no strong preference for *cis/trans* chain transfer.

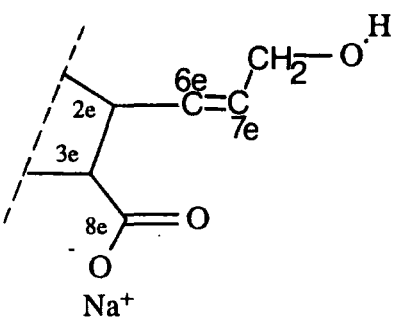
The vinylic carbons (7e) are observed as two narrow resonances at 134.52 and 134.14 ppm, of similar intensity (Figures 4.12 and 4.13), and approximately two ppm upfield of the corresponding resonances of the high polymer (Table 3.8). These resonances are provisionally assigned as *trans* and *cis* vinylic chain-ends respectively (7e), since inspection of the allylic regions of these spectra revealed that both *cis* and *trans* chain-end units were present. As expected from their structure, the vinylene carbon 7e group appears to have similar chemical shifts to the vinylic carbons of *cis*-but-2-ene-1,4-diol (134.38 ppm)<sup>108</sup> and *trans*-but-2-ene-1,4-diol (134.18 ppm).<sup>108</sup> Comparison of these spectra with those of oligomers of poly(norbornene) reveals the absence of the resonance of carbon 6e.<sup>110</sup> This resonance is expected to be slightly downfield of the vinylene resonances of the mid-chain units, and is presumably obscured.

The resonance of the methylene end group (M) adjacent to a *trans*-vinylene is observed at 65.50 ppm (Figures 4.12 and 4.13) and confirmed as a methylene in the APT spectra; its chemical shift is similar to the methylene carbons of *trans*-but-2-ene-1,4-diol (65.78 ppm in D<sub>2</sub>O), as expected.<sup>108</sup> The chemical shift of the methylene end group (M) adjacent to a *cis*-vinylene is therefore expected to be similar to the methylene resonance of *cis*-but-2-ene-1,4-diol (61.15 ppm in D<sub>2</sub>O).<sup>108</sup> Several new resonances are observed in this region, which also coincide with the mid-chain and chain-end resonances of carbons 3 and 4, although the APT spectra suggest that none of them are methylene carbons, although any signal may have been swamped by the strong main chain methine signals.

The methyl resonance at 50.54 ppm corresponds to the resonance of methanol impurities which can also be detected in the  $^1\text{H}$  NMR spectra (Figure 4.14) at 3.45 ppm; other resonances at 38.55 and 32.51 ppm correspond to methylene groups, the presence of which are again confirmed by resonances in the  $^1\text{H}$  NMR spectra between 2.1 and 1.0 ppm. These cannot be assigned as resonances of the ROMP polymer, or the cross-metathesis end groups, and may therefore correspond to the end groups of oligomers terminated by other mechanisms.

Proton resonances at 5.70ppm, 5.44ppm, 4.99ppm, 4.57ppm and 2.85ppm are observed in the  $^1\text{H}$  NMR spectra of the oligomers (Figures 4.14b and 4.14c), and correspond to those of the high polymer **PIVb** (Figure 4.14a). In addition, new resonances are observed in the  $^1\text{H}$  NMR spectra of the oligomers (Table 4.8).

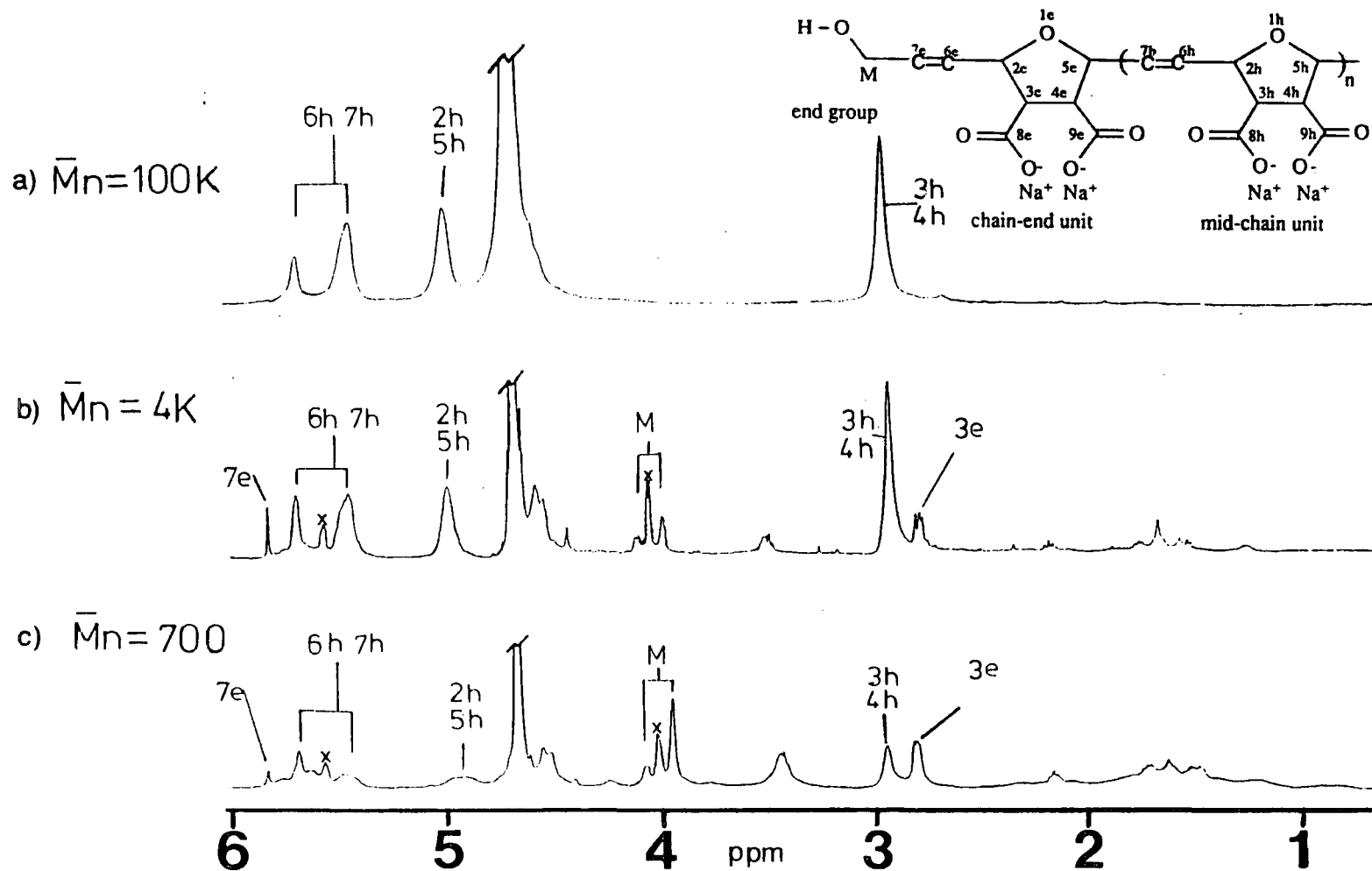
TABLE 4.8:  $^1\text{H}$  NMR spectral parameters<sup>1</sup> for the end groups of polymer **PIVb** (disodium salt) prepared using *cis*-but-2-ene-1,4-diol as a chain transfer agent (399.952 MHz,  $\text{D}_2\text{O}$ ).

PIVa end group	H at position	chemical shifts /ppm
	6e /7e	5.83 ( <i>trans</i> )
	2e	masked
	3e	2.70
	methylene M	4.08 ( <i>trans</i> )
		3.95 ( <i>cis</i> )

1) with respect to water at 4.67 ppm.

2) *cis* and *trans* methylene end groups.

Figure 4.14:  $^1\text{H}$  NMR spectra recorded at 399.952 MHz in  $\text{D}_2\text{O}$  of oligomers of **PIVb** prepared using  $\text{RuCl}_3 \cdot 3\text{H}_2\text{O}$  as the precursor to the initiating and chain propagating species, and *cis*-but-2-ene-1,4-diol (**VIII**) as chain transfer agent (CTA).



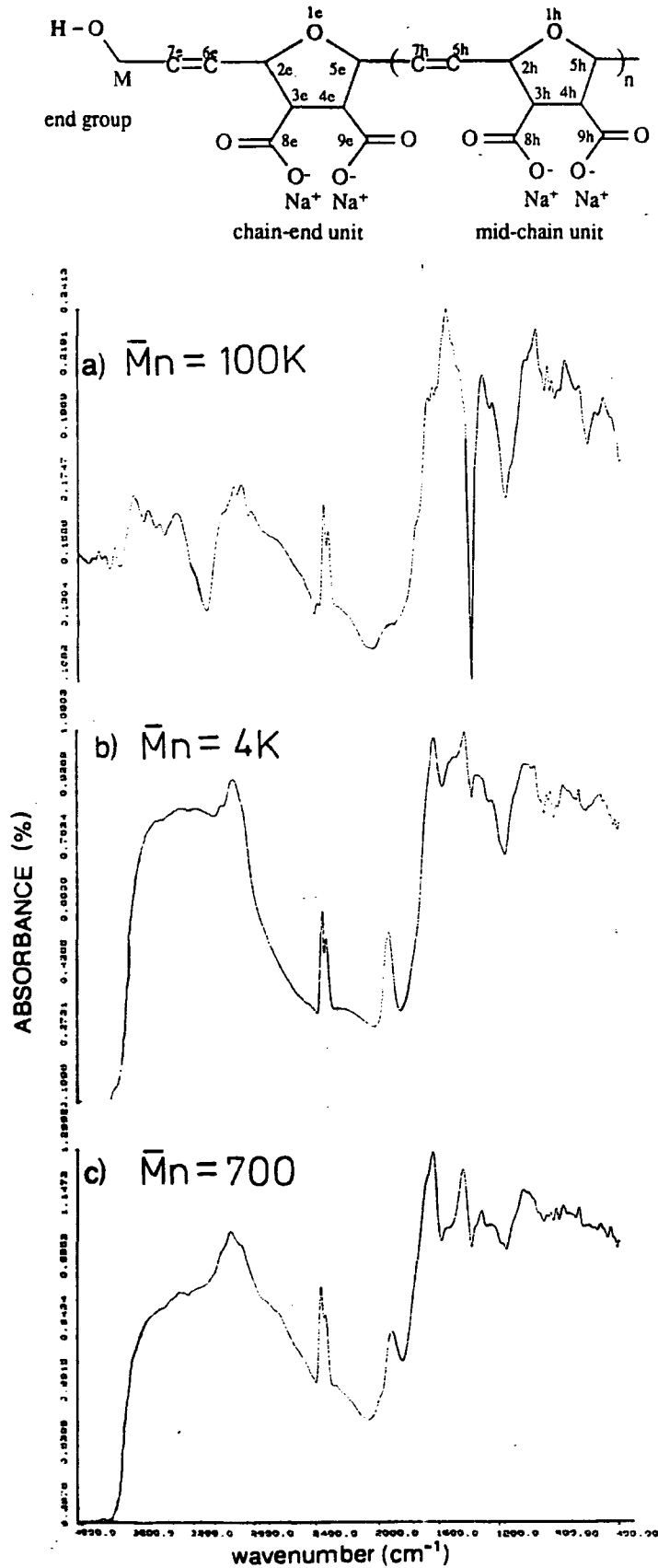
The end group and chain-end resonances that are observed in the  $^{13}\text{C}$  NMR spectra of these oligomers can also be seen in the  $^1\text{H}$  NMR spectra (Figure 4.14). The methine protons at position 3 and 4 resonate at 2.85 ppm in a mid-chain unit (3h, 4h), but at 2.70 ppm in a chain-end unit (3e). The relative intensity of these two resonances allows an approximation of the average oligomer length to be made. Thus in Figure 4.14c, where both resonances are of equal intensity, the "average" oligomer appears to be a dimer. This calculation is in good agreement with the GPC data (Figure 4.10c).

Analysis of the  $^{13}\text{C}$  NMR spectra suggested that the oligomers contained vinyl hydroxymethyl end groups. Resonances of methylene protons (M) adjacent to *trans* and *cis* vinylenes are observed at 4.08 ppm and 3.95 ppm respectively; these compare with the methylene resonance of *cis*-but-2-ene-1,4-diol at 4.02 ppm, which can be seen in some of the spectra as a residual impurity (Table 4.8 and Figure 4.14). The vinylenes resonances of mid-chain units at 5.70 ppm (*trans*) and 5.44 ppm (*cis*) are generally broader than corresponding resonances of the high polymer (Figure 4.14a). The *trans*-vinylic and *cis*-vinylic chain-end resonances (6e, 7e) are observed at 5.83 ppm and 5.57 ppm respectively, although since the latter appears to coincide with vinylenes resonances of the *cis*-but-2-ene-1,4-diol impurity there is some uncertainty about this.

The  $^{13}\text{C}$  NMR spectra of methine carbons 2 and 5 contained well resolved resonances of both *cis*-allylic and *trans*-allylic carbons. Surprisingly, no significant changes are observed in  $^1\text{H}$  NMR spectra of this region (4.99 *cis*-allylic and 4.57 *trans*-allylic), although the resonances are generally broader than the corresponding resonances in the high polymer. Additional resonances are observed principally at 3.45 ppm (methanol impurity), and between 2.1 ppm and 1 ppm as discussed above.

Infrared spectra were recorded for solid polymers and oligomers PIVb (Figure 4.15).

Figure 4.15: Infrared spectra recorded from solid samples of oligomers of **PIVb** prepared using  $\text{RuCl}_3 \cdot 3\text{H}_2\text{O}$  as the precursor to the initiating and chain propagating species, and *cis*-but-2-ene-1,4-diol (**VIII**) as chain transfer agent (CTA).



The spectra of the oligomers (Figures 4.15b and 4.15c) contain all the absorptions of the high polymer, and an additional absorption at  $3400\text{ cm}^{-1}$ , which can be assigned to the hydroxyl O-H stretch of the end group. The absorptions of carbonyl groups in mid chain units at  $1750\text{ cm}^{-1}$  are supplemented by an additional absorption of carbonyls in the chain ends at  $1780\text{ cm}^{-1}$ ; new carbonyl resonances were also observed in the  $^1\text{H}$  NMR spectra (Figures 4.14b and 4.14c).

Overall the oligomers have a similar backbone structure to the high polymers, and there appears to be no strong preference for the formation of *cis* or *trans* vinylene end groups by chain transfer. The actual end groups appear to be vinyl hydroxymethyl groups derived from the chain transfer agent.

#### **4.6: Oligomerisation of monomer IV by aqueous ROMP using acrylic acid (X) as a chain transfer agent.**

##### *4.6.1 Oligomer syntheses:*

The ROMP of monomer IV, outlined in Figure 4.16, was attempted in the presence of acrylic acid (X) as a chain transfer agent (CTA) (Table 4.9). In each case, monomer IV (1g, 5.4 mmol) was placed in a test tube (13mm I.D.) containing mixtures of water (3.0 ml) and X, and equipped with a magnetic stirring bar. The resulting solutions were stirred at  $55\pm 0.1^\circ\text{C}$  under a normal laboratory atmosphere for 30 minutes prior to the addition of an aqueous solution of  $\text{RuCl}_3\cdot 3\text{H}_2\text{O}$  (3.5 ml of a 0.02g/ml solution). During the course of the reaction, colour changes were observed, brown-red-green, and precipitation of polymer/oligomer was observed after the reaction solution became green.

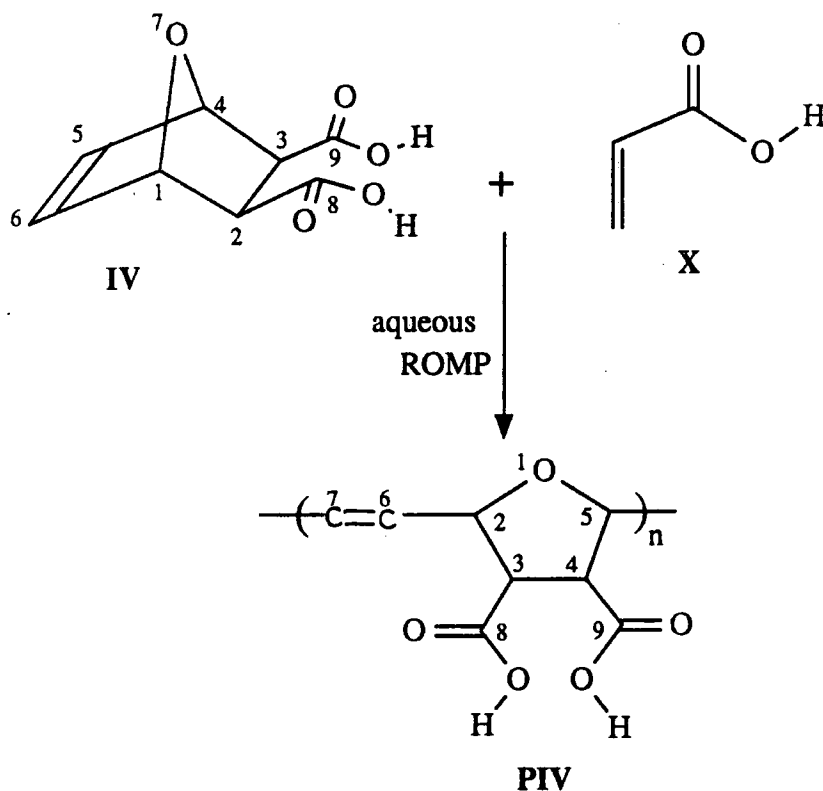


Figure 4.16: ROMP of monomer IV to yield polymers PIV.

The reaction was allowed to proceed for two days at 55°C, after which the product polymers/oligomers, poly(2,5-(3,4-bis(carboxylic acid)furanylene)-vinylene)s (PIV) were recovered by filtration and thoroughly washed with dilute hydrochloric acid. The disodium salt of the polymer/oligomers (PVIb) was recovered by addition of the solid polymer/oligomer, PIV (0.5g), to aqueous sodium hydroxide (30 wt%) followed by filtration and precipitation into methanol (100 ml). Product PVIb was purified by three successive reprecipitations into methanol from water then recovered by filtration and finally dried and stored under vacuum.

The polymers PVIb were pale green/brown solids, the colour being due to the presence of 0.1-0.3% by weight transition metal contamination. Elemental analyses of polymers PIVb are consistent with a polymer containing dibasic repeat units, and are recorded in appendix D.

TABLE 4.9: ROMP<sup>1</sup> of monomer IV using RuCl<sub>3</sub>.3H<sub>2</sub>O as the precursor to the initiating and chain propagating species, and acrylic acid (X) as a chain transfer agent (CTA).

molar ratio of reactants <sup>2</sup>		time for solution to turn red <sup>3</sup> /min	polymerisation		
CTA	RuCl <sub>3</sub> .3H <sub>2</sub> O		time to ppt of polymer <sup>4</sup>	yield/%	Mn
0	1	300	1200	80	>100K
2	1	100	800	65	10K
4	1	60	500	44	8K
6	1	45	240	28	6K
8	1	25	100	10	5K
10	1	10	50	0	--
12	1	5	10	0	--
20	1	5	10	0	--
40	1	5	10	0	--

Note: <sup>1</sup>H NMR shows that  $\sigma^c = 0.6$  for all polymers.

- 1) all polymerisations were run for two days at 55°C.
- 2) molar ratio of monomer : RuCl<sub>3</sub>.3H<sub>2</sub>O = 14:1, and [M]= 0.78 molar: this is a homogeneous reaction.
- 3) time between the addition of RuCl<sub>3</sub>.3H<sub>2</sub>O and change of solution colour to red.
- 4) time between the addition of RuCl<sub>3</sub>.3H<sub>2</sub>O and the onset of precipitation of polymer.

#### 4.6.2 Oligomer microstructure:

The polymers/oligomers PIVb prepared by aqueous ROMP in the presence of acrylic acid all have microstructures identical with those of the high polymers



prepared in section 3.5.3; no oligomer end groups were observed (spectra not shown). The ultimate yield of the reaction is substantially reduced by inclusion of acrylic acid in the reaction mixture, which suggests that any carbenes formed by cross metathesis with the acrylic acid do not initiate further metathesis.

**4.7: Attempted oligomerisation of monomer IV by aqueous ROMP using maleic acid (XI) as a chain transfer agents.**

**4.7.1 Polymer syntheses:**

The ROMP process is outlined in Figure 4.17, which also records the numbering system used.

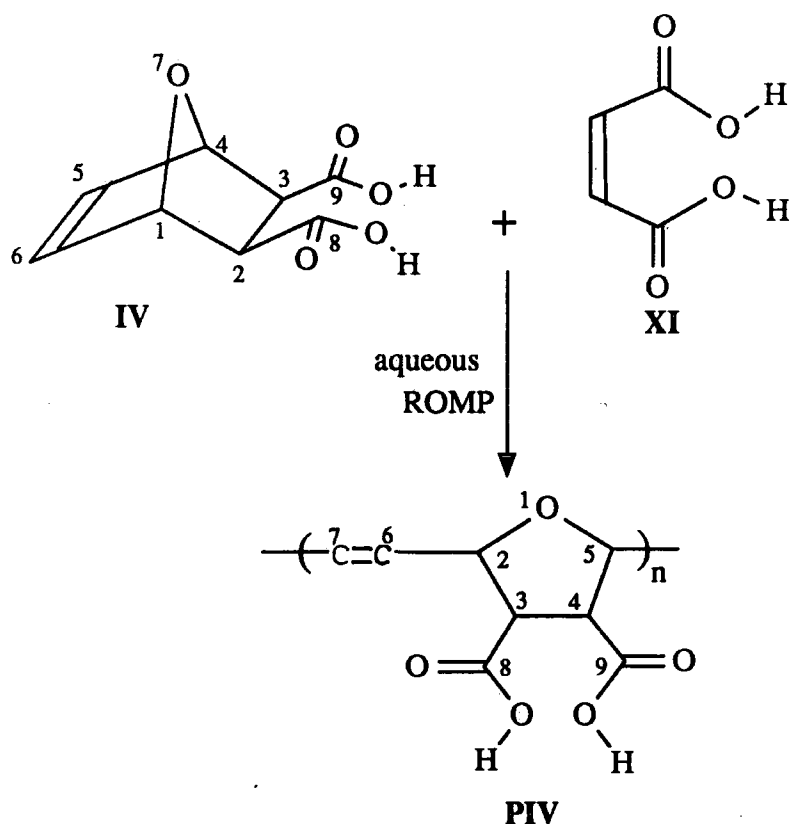


Figure 4.17: ROMP of monomer IV to yield polymers PIV.

The ROMP of monomer **IV** was attempted in the presence of maleic acid (**XI**) (Table 4.10).

TABLE 4.10: ROMP<sup>1</sup> of monomer **IV** using RuCl<sub>3</sub>.3H<sub>2</sub>O as the precursor to the initiating and chain propagating species, and maleic acid as a chain transfer agent (CTA).

molar ratio of reactants <sup>2</sup>		Primary precipitation <sup>3</sup>		Secondary precipitation <sup>4</sup>	
CTA	RuCl <sub>3</sub> .3H <sub>2</sub> O	time to ppt of polymer/ min	yield / %	time to ppt of polymer/ min	yield / %
0	1	300	0	1200	95
1	1	120	5	700	87
2	1	90	14	300	79
3	1	60	23	200	69
4	1	45	35	160	57
5	1	35	30	140	55
6	1	25	19	100	44
7	1	20	9	90	37
8	1	10	4	60	30
10	1	10	0	45	20
15	1	10	0	30	0

Note: <sup>1</sup>H NMR shows that  $\sigma^c = 0.6$  for all polymer; aqueous GPC shows that all polymers have Mn > 100K.

1) all polymerisations were run for two days at 55°C.

2) molar ratio of monomer : RuCl<sub>3</sub>.3H<sub>2</sub>O = 19:1, and [M]= 0.78 molar: this is a homogeneous reaction.

3) time between the addition of RuCl<sub>3</sub>.3H<sub>2</sub>O and the precipitation of polymer: solution colour was red.

4) time between the addition of RuCl<sub>3</sub>.3H<sub>2</sub>O and the precipitation of polymer: solution colour was green.

In each case, monomer **IV** (1g, 5.4 mmol) was placed in a test tube (13mm I.D.) containing mixtures of water (3.0 ml) and **XI**, and equipped with a magnetic stirring bar. The resulting solutions were stirred at  $55\pm 0.1^\circ\text{C}$  under a normal laboratory atmosphere for 30 minutes prior to the addition of an aqueous solution of  $\text{RuCl}_3 \cdot 3\text{H}_2\text{O}$  (3.5 ml of a 0.02g/ml solution). The colour of the reaction solution changed during the reaction, brown-red-green; the precipitation of polymer occurred both when the reaction solution was red (primary precipitation) and green (secondary precipitation).

The reaction was allowed to proceed for two days at  $55^\circ\text{C}$ , after which the product polymers, poly(2,5-(3,4-bis(carboxylic acid)furanylene)vinylene)s (**PIV**) were recovered by filtration and thoroughly washed with dilute hydrochloric acid. The disodium salt of the polymer (**PVIb**) was recovered by addition of the solid diacid polymer **PIV** (0.5g) to aqueous sodium hydroxide (30 wt%) followed by filtration and precipitation into methanol (100 ml). Polymer **PIVb** was purified by three successive reprecipitations into methanol from water then recovered by filtration and finally dried and stored under vacuum. The polymers **PVIb** were pale green/brown solids, the colour being due to the presence of 0.1-0.3% by weight transition metal contamination.

Elemental analyses of polymers **PIVb** are consistent with a polymer with dibasic repeat units, and are recorded in appendix D

#### 4.7.2 Polymer microstructure:

The polymers/oligomers **PIVb** prepared by aqueous ROMP in the presence of maleic acid all have microstructures identical with the high polymers prepared in chapter 3, and all had number average molecular weights in excess of 100K; no oligomer end groups were observed (spectra not shown), and no chain transfer occurred.

#### 4.8: Attempted ROMP of monomer VII in the presence of maleic acid (XI).

##### 4.8.1 *Polymer synthesis:*

In view of the apparent effect of maleic acid on the induction period of the ROMP reaction (section 4.7), the aqueous ROMP of monomer VII was attempted in the presence of maleic acid (note the failure to polymerise from section 3.6.1) (Figure 4.18). Experimental conditions for the reaction are recorded in Table 4.11.

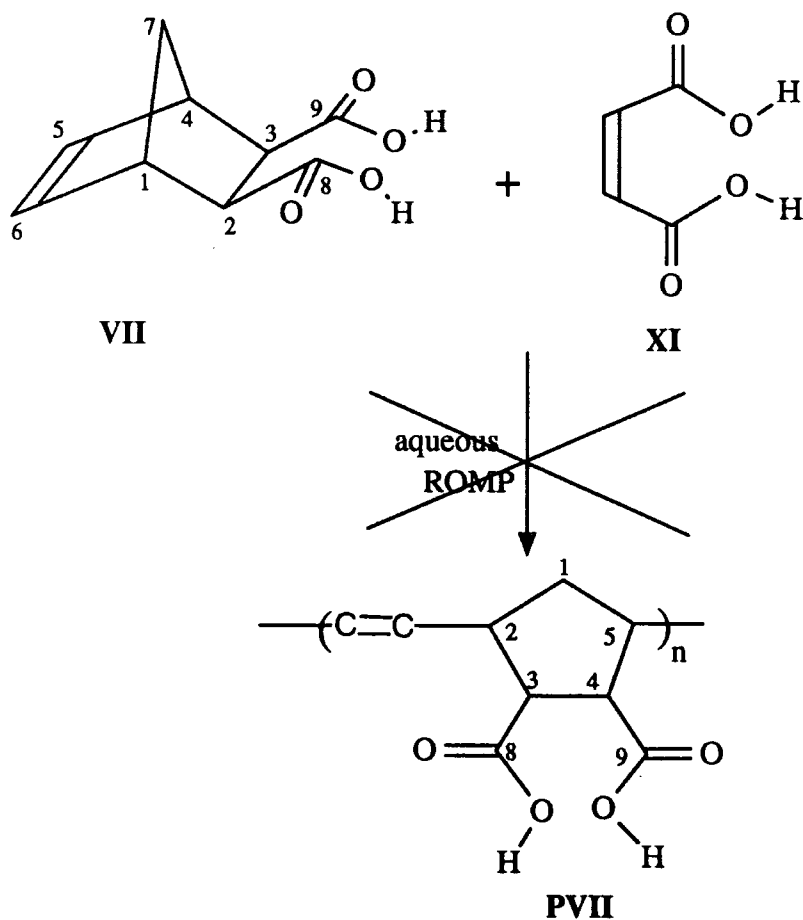


Figure 4.18: Attempted ROMP of monomer VII.

In each case, monomer VII (1g, 5.4 mmol) was placed in a test tube (13mm I.D.) containing water (3.0 ml), maleic acid (X), and equipped with a magnetic

stirring bar. The resulting solutions were stirred at  $55\pm 0.1^\circ\text{C}$  under a normal laboratory atmosphere for 10 minutes prior to the addition of an aqueous solution of  $\text{RuCl}_3\cdot 3\text{H}_2\text{O}$  (3.5 ml of a 0.02g/ml solution). The colour of the reaction solution changed during the reaction, brown-red-green, although no polymer was formed after two days. The disodium salt of the monomer **VIIb** was recovered by addition of the contents of the reaction vessel to aqueous sodium hydroxide (10 ml, 30 wt%) followed by filtration and precipitation into methanol (100 ml). In all cases approximately 90-95% of the monomer was recovered as its disodium salt.

TABLE 4.11: Attempted ROMP<sup>1</sup> of monomer **VII** initiated by  $\text{RuCl}_3\cdot 3\text{H}_2\text{O}$  in the presence of maleic acid.

molar ratio of reactants <sup>2</sup>		first colour change <sup>3</sup>		second colour change <sup>4</sup>	
		time to turn red / min	yield / %	time to turn green / min	yield / %
CTA	$\text{RuCl}_3\cdot 3\text{H}_2\text{O}$				
0	1	300	0	1200	0
1	1	140	0	800	0
2	1	100	0	340	0
3	1	70	0	180	0
4	1	60	0	140	0
5	1	35	0	100	0
6	1	30	0	90	0
7	1	20	0	80	0
8	1	10	0	60	0
10	1	10	0	20	0

1) all experiments were run for two days at  $55^\circ\text{C}$ .

2) molar ratio of monomer: $\text{RuCl}_3\cdot 3\text{H}_2\text{O}$  = 19:1, and  $[\text{M}] = 0.78 \text{ M}$ .

3) reaction solution was red.

4) reaction solution was green.

**CHAPTER 5:  
DISCUSSION**

## **5.1: Introduction.**

The preparation of various high molecular weight polymers and oligomers by aqueous ROMP was described in Chapters 3 and 4. Each ROMP reaction proceeded after an induction period that appeared to be dependant on the transition metal chloride used as the precursor of the initiator, the monomer, and the presence of acyclic olefins. An attempt to correlate and rationalise these observations is presented in this chapter.

Metathesis initiators are assumed to be formed *in situ* by reaction of the transition metal chlorides with the monomers, and/or decomposition products of the monomers, and/or acyclic chain transfer agents. The exact nature of each initiator is not known, although it is assumed to contain a metal carbene, since the reaction products are consistent with ROMP having occurred.<sup>22</sup> The induction periods referred to in this chapter refer to the time taken for colour changes to be observed in the reaction solution; no kinetic experiments were made. The actual colour of the reaction solution is a combination of the colours of the assumed metal carbene initiator, the original transition metal halide, and any other transition metal compounds that may be formed. Therefore, the prominent solution colour is not necessarily that of the metathesis initiator, and consequently, observations of colour changes only give an empirical indication of the progress of the reaction.

## **5.2: Synthesis of high molecular weight polymers.**

### **5.2.1 Catalyst choice for aqueous ROMP reactions:**

The yield of polymers prepared by aqueous ROMP using various transition metal chlorides as the precursors to the initiating and chain propagating species are

recorded in Table 5.1.

TABLE 5.1: Yields of polymers prepared with various monomers and initiators.<sup>1</sup>

initiators derived from:	Yield of polymer from monomer				
	II	III	IV	V	VII
RuCl <sub>3</sub> .3H <sub>2</sub> O	95%	95%	95%	60%	0%
OsCl <sub>3</sub> .3H <sub>2</sub> O	N/A	95%	80%	N/A	N/A
IrCl <sub>3</sub> .3H <sub>2</sub> O	N/A	2%	0%	N/A	N/A
RhCl <sub>3</sub> .3H <sub>2</sub> O	N/A	0%	0%	N/A	N/A
PdCl <sub>2</sub>	N/A	0%	0%	N/A	N/A

- 1) Full experimental conditions for these polymerisations are recorded in chapter 3.
- 2) N/A: this polymerisation was not attempted.

The transition metal compounds investigated as precursors to the initiating species are not simple pure compounds but complex mixtures of metal chlorides and oxychlorides.<sup>111</sup> Consequently, the initiating carbenes which are probably formed are the products of reaction of an ill-defined metal compound with the monomer and/or a decomposition product of the monomer; it is impossible to determine which actual species react to form the carbene, or indeed the nature of the other ligands in the carbene complex using the experimental methods described in this thesis, and the author has not engaged in a detailed investigation of these transition metal species.

The induction period for the formation of the initiating species, and the rate of the reaction are dependant on many other factors, including temperature, monomer



and solvent. For example, the aqueous ROMP of monomer III proceeded most rapidly with osmium initiators, and most slowly with iridium initiators. In contrast, Michelotti reported that the ROMP of norbornene in ethanol proceeded faster for initiators derived from iridium salts, and slowest for those derived from ruthenium salts, with osmium salts intermediate.<sup>62</sup> However, changes in solvent and/or monomer are well known to have marked effects on metathesis activity.<sup>22</sup>

No solution colour changes were observed in any of the attempted aqueous ROMP reactions using rhodium or palladium salts as precursors to the initiating species, and no polymers of any kind were produced. These observations suggest that no reactions of any type occurred between these transition metals and monomers III or IV in water. Previous studies of the polymerisation of norbornene with initiators derived from rhodium and palladium salts reported the occurrence of vinyl type polymerisation, and/or copolymerisation with carbon monoxide.<sup>63,64,79</sup> In these cases, the involvement of the monomer with the transition metal compound is presumably critical.

In summary, ruthenium, osmium and iridium salts all have the potential to form aqueous ROMP initiators, although whether the reaction actually proceeds will depend on other parameters such as temperature and/or monomer. Rhodium and palladium salts appear to have little or no potential for aqueous ROMP.

### *5.2.2 Monomer choice for aqueous ROMP reactions:*

The aqueous ROMP of monomer III has been successfully conducted using initiators derived from ruthenium, osmium, and iridium compounds, although in the latter case, the yield of the reaction was low (Table 5.1),<sup>73</sup> and confirmed previous reports in the cases of  $\text{RuCl}_3 \cdot 3\text{H}_2\text{O}$  and  $\text{OsCl}_3 \cdot 3\text{H}_2\text{O}$ .<sup>71,72</sup> In contrast, the ROMP of monomer IV using an osmium based initiator was irreproducible, and under the same reaction conditions, the attempted ROMP using  $\text{IrCl}_3 \cdot 3\text{H}_2\text{O}$  was

unsuccessful (section 3.5). This observation is surprising, since *exo*-bicyclo[2.2.1]hept-5-ene-2-carboxylic acid has been successfully polymerised by aqueous ROMP using an iridium salt as the precursor to the initiator.<sup>105, 112</sup> A rationalisation of these observations is that the interaction of the monomer and/or its decomposition products are crucial in the production of the initiating carbene, and/or in the propagation step of the reaction.

a) monomer involvement:

It seems reasonable to postulate that the production of an initiator requires both the formation of a transition metal carbene, and other associated ligands. Functionalised monomers that are able to co-ordinate to the transition metal through their side groups may alter the rate of production and subsequent reactivity of a carbene, and hence the apparent induction period of the ROMP reaction. This postulate could partially explain the difference in metathesis activity of  $\text{RuCl}_3 \cdot 3\text{H}_2\text{O}$  with monomers **II**, **III**, **IV** and **V** (Table 5.2), but cannot account for its lack of activity with monomer **VII**, which is similar to monomer **IV** in the respect of its carboxylic acid side groups.

TABLE 5.2: Induction periods<sup>1</sup> for some aqueous ROMP reactions using  $\text{RuCl}_3 \cdot 3\text{H}_2\text{O}$  as the precursor to the initiating and chain propagating species.

	monomer			
	<b>II</b>	<b>III</b>	<b>IV</b>	<b>V</b>
induction period <sup>1</sup> / hours	2	4	6	4

1) Estimated induction period based on the brown to red colour change in the reaction solutions.

The major difference between these monomers is the ether bridge in monomer IV, and therefore it is possible that this ether bridge is in some manner crucial in the reaction. However this argument does not explain the lack of metathesis activity of  $\text{IrCl}_3 \cdot 3\text{H}_2\text{O}$  with monomer IV, and literature reports of the aqueous ROMP of similar monomers using the same conditions.<sup>112</sup>

b) decomposition of monomer:

The derivatives of 7-oxabicyclo[2.2.1]hept-2-ene that have been used as monomers in the work reported in this thesis are reported to undergo retro Diels-Alder reactions at 55°C.<sup>92</sup> As an example, monomer IV undergoes 4% decomposition, based on  $^1\text{H}$  NMR analysis, after eight hours at 55°C, to yield furan and maleic acid.<sup>113</sup> The initiator may be produced by reaction between the monomer decomposition products and the transition metal compound. This hypothesis could account for the lack of metathesis activity of  $\text{RuCl}_3 \cdot 3\text{H}_2\text{O}$  with monomer VII, since monomer VII does not readily decompose at 55°C.<sup>106</sup>

It is possible that monomer decomposition is an important factor in the aqueous metathesis reactions performed in this thesis. However, it is impossible to assess the effect of one variable when the others are changed at the same time.

### 5.2.3 Conclusions:

Ruthenium, osmium and iridium salts all have the potential to form aqueous ROMP initiators that can polymerise methoxymethyl, carbomethoxy and carboxylic acid functionalised 7-oxanorbornenes. Extensive speculation as to the factors involved in the production of the carbene is not warranted at this stage because there are too many variables in the type of experiment performed in this thesis to allow unambiguous deductions to be made.

### **5.3: The effect of acyclic olefins on aqueous ROMP reactions.**

#### **5.3.1 Introduction:**

In the section 5.2, it was suspected that the monomers, or some of their decomposition products, were able to co-ordinate to the transition metal species in solution to aid the formation of the initiating carbene and the other ligands in the transition metal complex. Various acyclic olefins were used as chain transfer agents in chapter 4, some of which appeared to affect the induction period of the reaction.

#### **5.3.2 *The effect of cis-but-2-ene-1,4-diol (VIII) on the induction period of ROMP reactions:***

The ROMP reactions of monomer **III** in the presence of *cis-but-2-ene-1,4-diol* (**VIII**) using initiators derived from  $\text{RuCl}_3 \cdot 3\text{H}_2\text{O}$  were found to proceed after shorter induction periods than similar reactions in the absence of **VIII** (Tables 4.1 and 4.2). The induction period of each reaction refers to the time taken for the reaction solution to turn to a green colour, and was found to be dependant on the concentration of **VIII** in the reaction mixture (Figure 5.1); the shortest induction periods were recorded for reactions in the presence of the highest concentrations of **VIII**. For example, the induction period was reduced from 1200 min to 15 min by using *cis-but-2-ene-1,4-diol* in molar proportions 47:1 with respect to  $\text{RuCl}_3 \cdot 3\text{H}_2\text{O}$ .

GPC examination has demonstrated that the molecular weights of the polymers and oligomers prepared by this method were related to the concentration of **VIII** in the reaction mixture (Figure 5.2); products of lowest molecular weight were produced from reactions in the presence of the highest concentrations of **VIII**.

Figure 5.1: Graph of induction period against the ratio  $[\text{VIII}]/[\text{RuCl}_3 \cdot 3\text{H}_2\text{O}]$  for the ROMP of a) monomer III, and b) monomer IV, in the presence of 161 *cis*-but-2-ene-1,4-diol (VIII), and using  $\text{RuCl}_3 \cdot 3\text{H}_2\text{O}$  as the precursor to the initiating and chain propagating species.

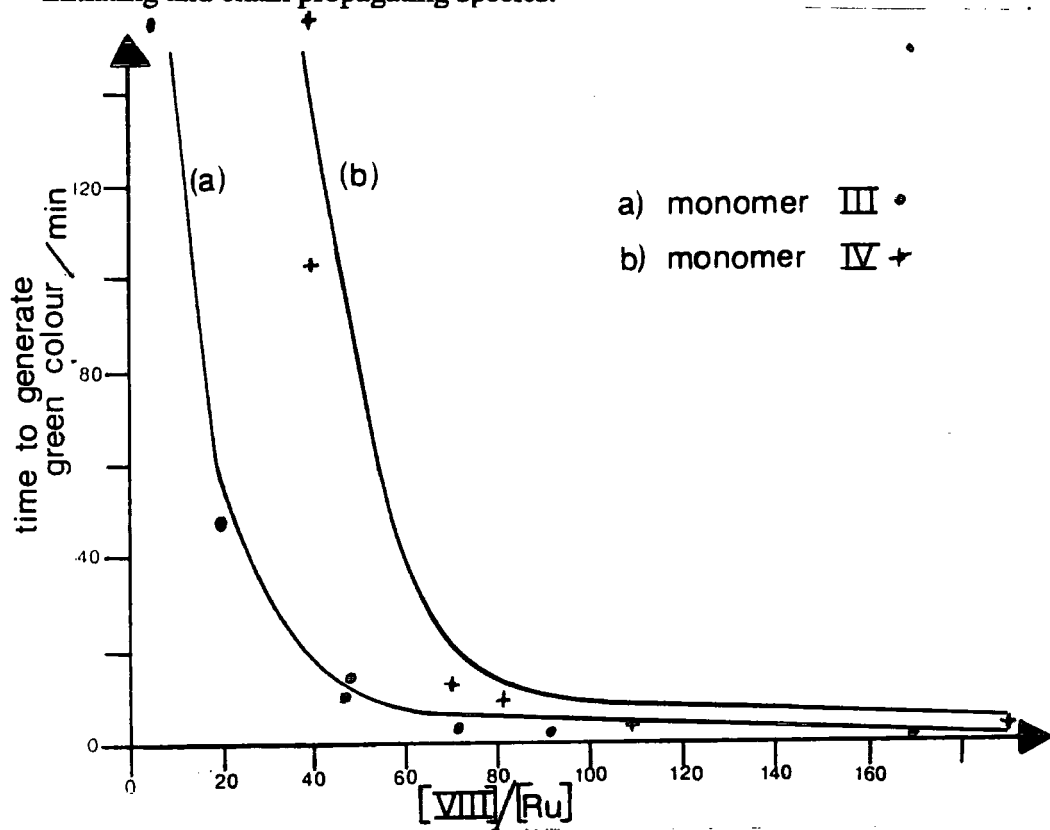
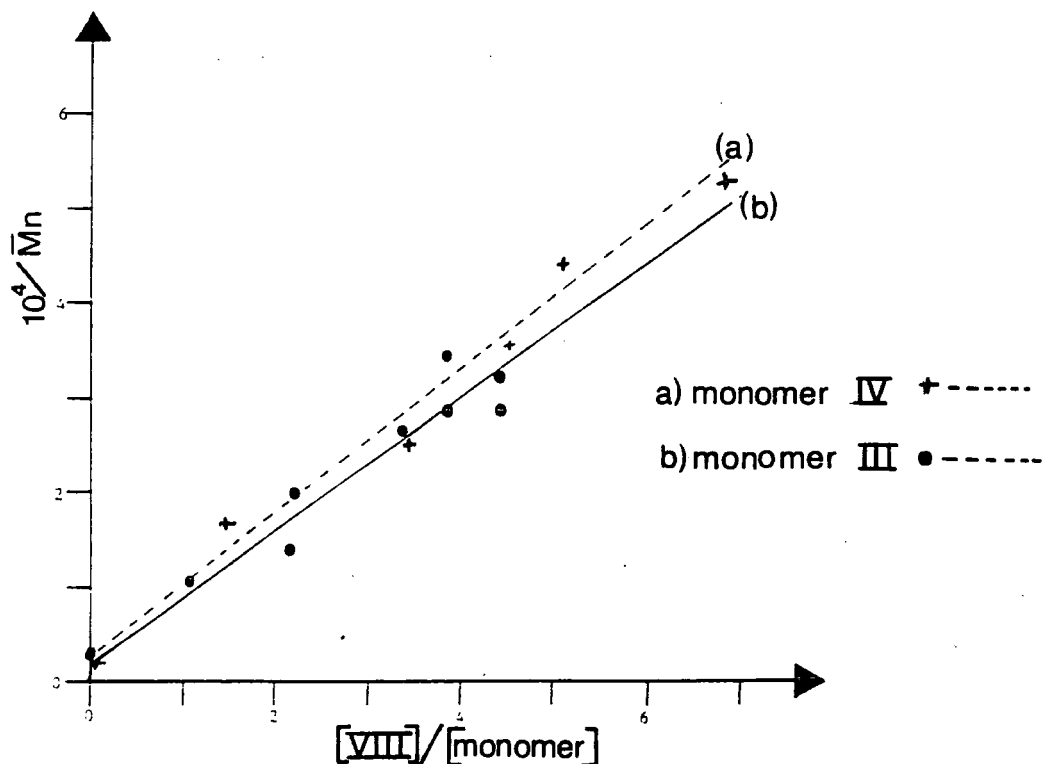


Figure 5.2: Graph of reciprocal number average degree of polymerisation against  $[\text{VIII}]/[\text{Monomer}]$  for the ROMP of a) monomer III, and b) monomer IV, in the presence of *cis*-but-2-ene-1,4-diol (VIII), and using  $\text{RuCl}_3 \cdot 3\text{H}_2\text{O}$  as the precursor to the initiating and chain propagating species.



The yield of each reaction was not significantly affected by the presence of VIII, which suggests that the carbene formed by cross metathesis with the chain transfer agent can initiate further metathesis:  $^1\text{H}$  NMR analysis of the oligomers suggested that the end groups are vinyl hydroxymethyl groups (section 4.3).

The induction period for the ROMP of monomer IV using initiators derived from  $\text{RuCl}_3 \cdot 3\text{H}_2\text{O}$  was also reduced by the presence of *cis*-but-2-ene-1,4-diol (VIII) in the reaction mixture (Figure 5.1, Table 4.6). Again, the yield of the reaction was approximately constant, regardless of the molecular weight of the products, and  $^1\text{H}$  NMR examination suggested that the oligomer end groups were vinyl hydroxymethyl groups formed by cross metathesis of the chain propagating species with VIII (section 4.5).

Plots of reciprocal  $M_n$  against the ratio of VIII concentration to monomer concentration allow the Chain Transfer Constant to be determined;<sup>22</sup> such plots for this system are shown in Figure 5.2. Although the plots give reasonably good straight lines, the chain transfer constants for the cross metathesis of *cis*-but-2-ene-1,4-diol with monomer III, and monomer IV are very small,  $7.3 \times 10^{-5}$  and  $7.6 \times 10^{-5}$  respectively,\* implying that the rate of propagation is very fast with respect to chain transfer.

The apparent reduction of the induction period of each reaction in the presence of VIII suggests that the initiating carbene is being generated more rapidly. However, it is important to note that we are dealing with a heterogeneous polymerisation for the ROMP of monomer III, and a homogeneous polymerisation for the ROMP of monomer IV. Any increase in the concentration of VIII in the reaction mixture changes the polarity of the medium, and hence could account for the apparent change in induction period.

The polymerisation of monomer II was found to proceed after a shorter induction period than the polymerisation of III under the same reaction conditions (section 3.7). This could be rationalised by suggesting that monomer II is partially

\* accuracy  $\pm 10^5$

decomposed in the reaction to yield furan and *cis*-but-2-ene-1,4-diol, the latter being able to aid the production of the initiator. However the polymerisation of **II** did not yield pure ROMP polymers, and monomer **II** is water soluble, hence cannot be directly compared to the heterogeneous polymerisation of **III**.

If the initiating species prepared in the presence of **VIII** was different to that produced in the absence of **VIII**, then one might expect the backbone microstructure to be different. However,  $^1\text{H}$  and  $^{13}\text{C}$  NMR analysis of the oligomers of **PIII** and **PIVb** has demonstrated that each oligomer has a similar backbone microstructure to the corresponding high polymer (sections 4.3 and 4.5).

### 5.3.3 The effect of *cis*-1,4-dimethoxybut-2-ene (**IX**) on the induction period of ROMP reactions:

The aqueous ROMP of monomer **III** in the presence of *cis*-1,4-dimethoxybut-2-ene (**IX**) as a chain transfer agent using initiators derived from  $\text{RuCl}_3 \cdot 3\text{H}_2\text{O}$  was found to proceed after a shorter induction period than similar reactions performed in its absence (Figure 5.3, Table 4.4): the induction period refers to the time taken for the reaction solution to turn to a green colour. The molecular weight of the product polymers were found to be dependant on the concentration of **IX** in the reaction mixture: the lowest molecular weight products were produced when the polymerisation was performed in the presence of the highest concentration of chain transfer agent. The plot of reciprocal  $M_n$  against the ratio of **IX** concentration to monomer concentration allows the chain transfer constant to be determined,<sup>22</sup> in this case it is  $2.0 \times 10^{-5}$ \* (Figure 5.4), which is smaller than the chain transfer constant for the same reaction using **VIII** as chain transfer agent,  $7.3 \times 10^{-5}$ \*, although the reactions are not directly comparable since **VIII** is water soluble and **IX** is not.

\* accuracy  $\pm 10^5$

Figure 5.3: Graph of induction period against the ratio  $[CTA]/[RuCl_3 \cdot 3H_2O]$  for the ROMP of monomer **III** using a) **VIII**, and b) **IX** as chain transfer agents (CTA), and  $RuCl_3 \cdot 3H_2O$  as the precursor to the initiating and chain propagating species.

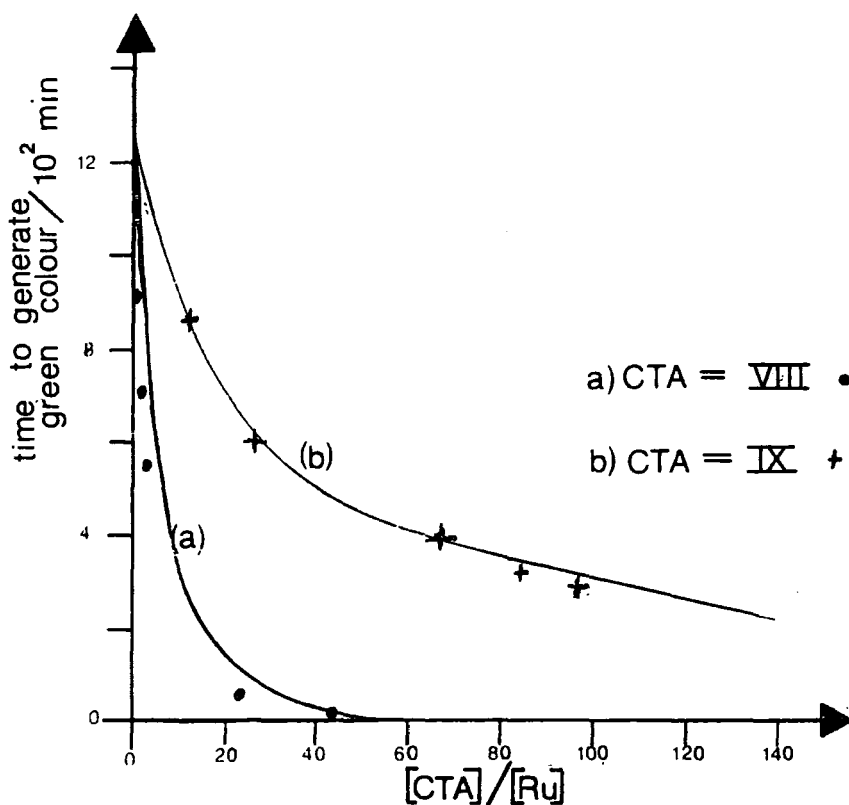
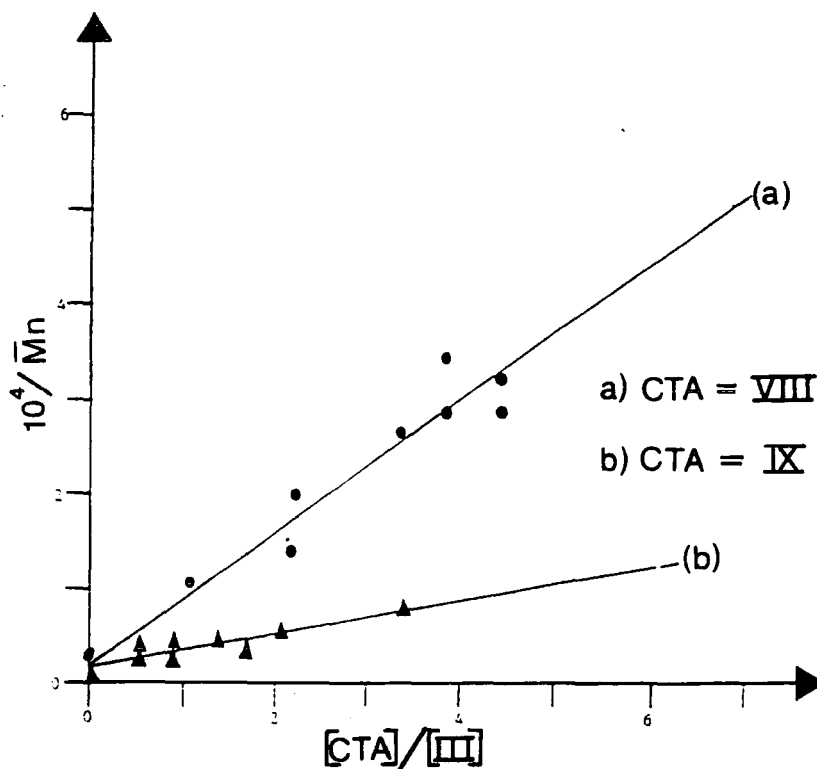


Figure 5.4: Graph of reciprocal number average degree of polymerisation against  $[CTA]/[III]$  for the ROMP of monomer **III** using a) **VIII**, and b) **IX** as chain transfer agents (CTA), and  $RuCl_3 \cdot 3H_2O$  as the precursor to the initiating and chain propagating species.





The yields of these reactions were found to decrease slightly as the concentration of IX in the reaction mixture was increased. This suggests that the carbenes formed by cross metathesis of the chain propagating species and the chain transfer agent were not efficient initiators of further metathesis.  $^1\text{H}$  NMR analysis of the polymers revealed that they all had similar microstructures to the high polymers PIII, and to the oligomers prepared by ROMP of monomer III in the presence of *cis*-but-2-ene-1,4-diol. The end groups of the polymers were found to be vinyl methoxymethyl groups, which is consistent with a cross metathesis reaction.

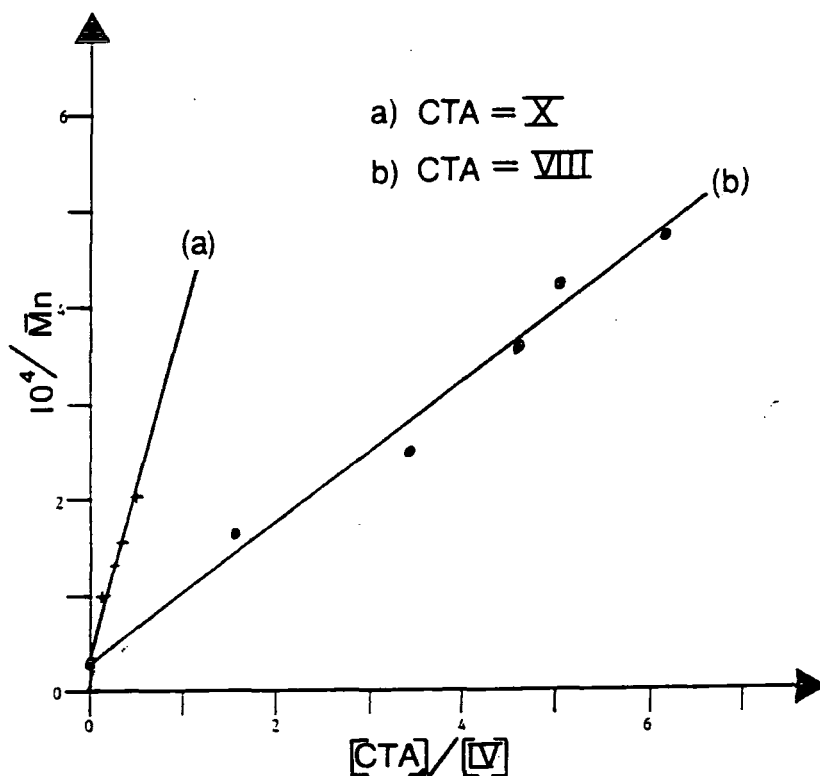
It has been demonstrated that IX can act as a chain transfer agent for the ROMP of monomer III. The apparent reduction in the induction period could be rationalised by suggesting that the change in the polarity and homogeneity of the reaction mixture affects the induction period, or that IX may help in forming the initiating carbene: too many uncontrolled variables are involved for a decision to be made concerning the dominant factors.

#### 5.3.4 The effect of acrylic acid (X) on the induction period of ROMP reactions:

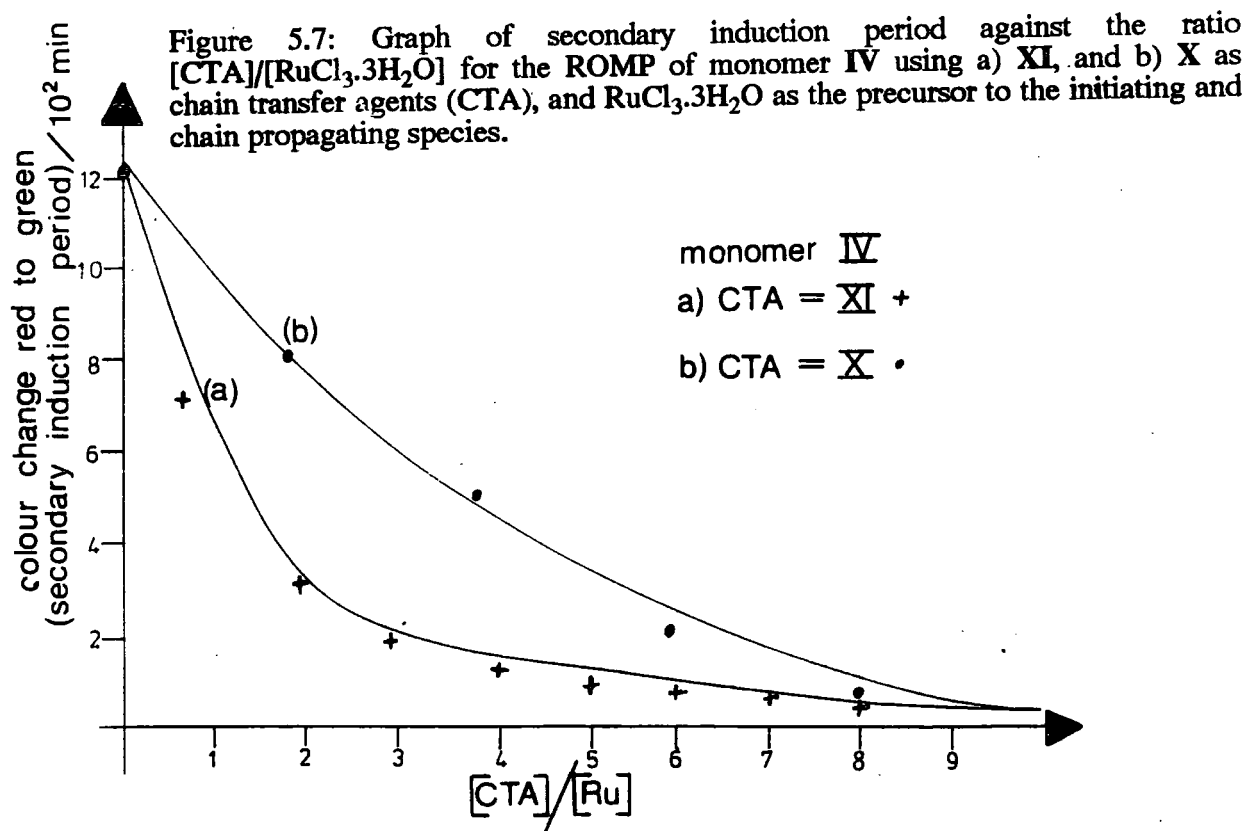
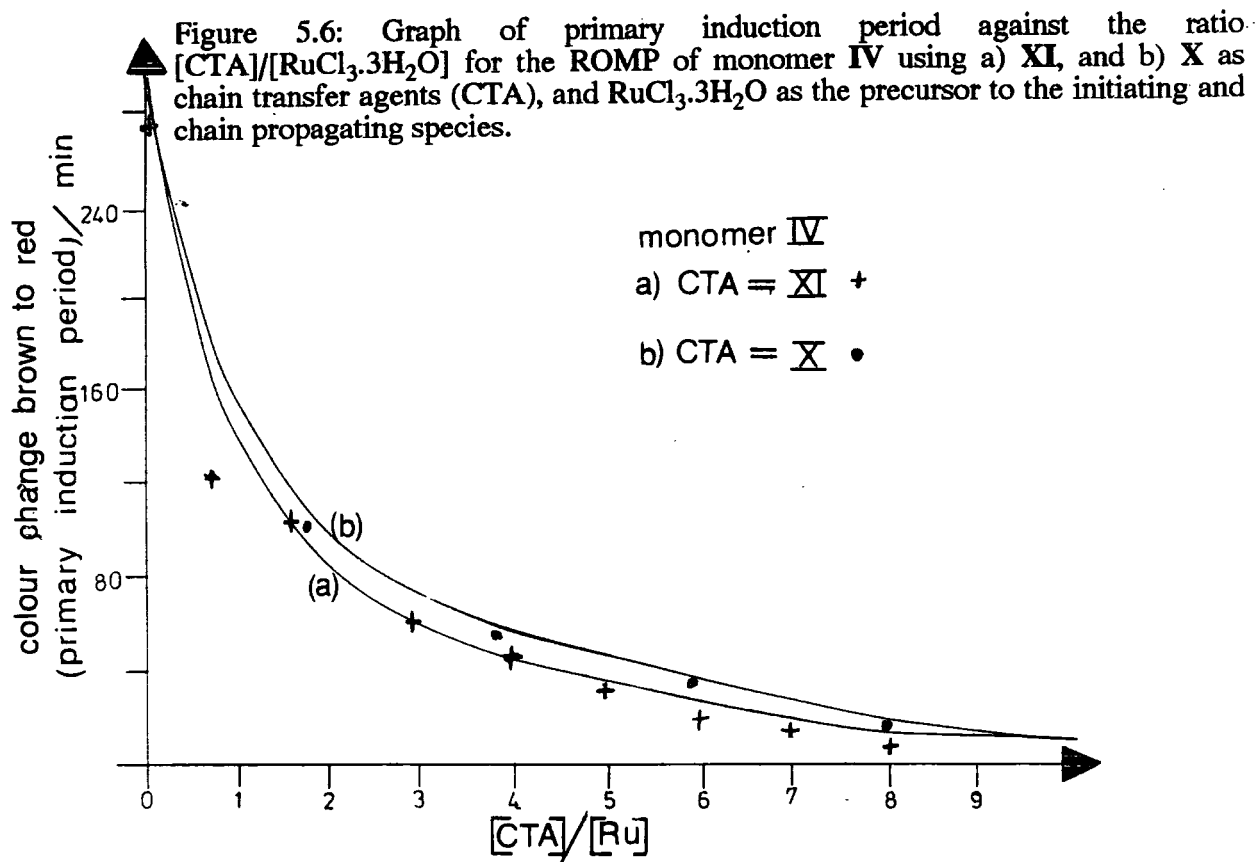
The experiments in section 4.6 demonstrate that acrylic acid (X) can be used as a chain transfer agent in the ROMP of monomer IV using initiators derived from  $\text{RuCl}_3 \cdot 3\text{H}_2\text{O}$ . The chain transfer efficiency of X is higher than that of VIII,  $2.2 \times 10^{-4}$  and  $7.3 \times 10^{-5}$  respectively (Figure 5.5), although both CTA's are water soluble. The yield of the reaction was decreased as the concentration of X in the reaction mixture was increased (Table 4.9), which suggests that the carbene formed by cross metathesis with the chain propagating species is an inefficient initiator of further metathesis. In concentrations greater than 8:1 [X]:[ $\text{RuCl}_3 \cdot 3\text{H}_2\text{O}$ ] no polymer or oligomer was formed. Presumably above this concentration other competitive reactions are dominant.

\* accuracy  $\pm 10^5$

Figure 5.5: Graph of reciprocal number average degree of polymerisation against  $[CTA]/[IV]$  for the ROMP of monomer IV using a) X, and b) VIII as chain transfer agents (CTA), and  $RuCl_3 \cdot 3H_2O$  as the precursor to the initiating and chain propagating species



The induction period of the reaction is reduced by the presence of X in the reaction mixture (Figure 5.6 and 5.7). The primary induction period refers to the time taken for the reaction solution to change to a red colour, and the secondary induction period refers to the time taken for the reaction solution to turn to a green colour: polymer was precipitated after the reaction solution was green. The reduction of the induction period of the reaction is unlikely to result solely from co-ordination of the ruthenium salts with the carboxylic acid group in X, since the monomer is also acid functionalised, and would presumably also react in a similar manner. Interactions of this type may be a contributory factor in conjunction with interactions of the double bond in X with the ruthenium salts in solution, although, on the basis of the evidence in this thesis alone, no firm conclusions can be drawn.



### 5.3.5 *The effect of maleic acid (XI) on the induction period of ROMP reactions:*

The results from section 4.7 demonstrate that the ROMP of monomer IV can be accomplished in the presence of XI using  $\text{RuCl}_3 \cdot 3\text{H}_2\text{O}$  as the precursor to the initiating and chain propagating species, although no chain transfer appears to occur (Table 4.10). The precipitation of polymer proceeds during two successive solution colour changes. The primary precipitation period refers to precipitation while the reaction solution is red, and the secondary precipitation period refers to precipitation while the reaction solution is green. High molecular weight polymer PIV was formed during both stages, and the total yield was constant for reactions where  $[\text{XI}]:[\text{RuCl}_3 \cdot 3\text{H}_2\text{O}]$  was less than 4:1.

Both primary and secondary precipitation periods for the ROMP of IV in the presence of XI depend on the concentration of XI: as the concentration of XI in the reaction solution is increased, the induction period is decreased (Figure 5.6 and 5.7). Comparison between ROMP of IV in the presence of X and XI reveals that the initial reaction periods are similar (colour change brown to red), and that the secondary reaction stage (colour change red to green) is much shorter for ROMP in the presence of XI. The presence of maleic acid in the reaction solution appears to aid the formation of the initiating carbene without loss of polymer yield when used in concentrations less than 4:1  $[\text{XI}]:[\text{RuCl}_3 \cdot 3\text{H}_2\text{O}]$ ; ROMP in the presence of greater than 4:1  $[\text{XI}]:[\text{RuCl}_3 \cdot 3\text{H}_2\text{O}]$  proceeds to lower yield, although the induction period is even shorter.

Any involvement of XI in the formation of an initiator is presumably similar to the involvement of X, ie. complexation via carboxylic acid groups and/or co-ordination with the double bond. Comparison of the ROMP of IV in the presence of XI (section 4.7), and the attempted ROMP of VII in the presence of XI (section 4.8) demonstrates that the involvement of the monomer is also critical in the reaction. Monomer IV contains an oxygen at ring position 7, whereas monomer VII has a methylene. Therefore, it is possible that an active initiator was

produced during the attempted ROMP of VII, but the monomer was unable to undergo the reaction.

#### 5.4 Conclusions.

Aqueous ROMP using  $\text{RuCl}_3 \cdot 3\text{H}_2\text{O}$  as the precursor to the initiating and chain propagating species can be accomplished in the presence of VIII, IX, X and XI. All these acyclic olefins appear to reduce the time to precipitation of the polymer, the timescale of the solution colour changes, and all except XI appear to act as chain transfer agents. The rationalisation of these observations is difficult since the presence of high concentrations of CTA alters the polarity of the reaction medium. As a consequence, no firm conclusions concerning the formation of initiators in the presence of CTA's can be made, although this work demonstrates a useful method for regulating the molecular weight of polymers synthesised by aqueous ROMP.

**CHAPTER 6:  
APPLICATIONS  
TESTING OF THE  
OLIGOMERS PIVb**

## 6.1: Introduction.

Some of the low molecular weight polymers and oligomers, **PIVb**, synthesised by aqueous ROMP of monomer **IV** in section 4.5, were assessed for their ability to prevent the precipitation of calcium carbonate from aqueous solution. The theoretical change in potential energy resulting from the interaction of each oligomer with an aragonite surface was calculated, and the results correlated to the microstructure and molecular weight of the oligomers, and their observed efficiency in preventing the precipitation of aragonite.

## 6.2: Experimental details.

### 6.2.1 *Synthesis and characterisation of oligomers:*

The synthesis and characterisation of oligomers, **PIVb**, was described in section 4.5.

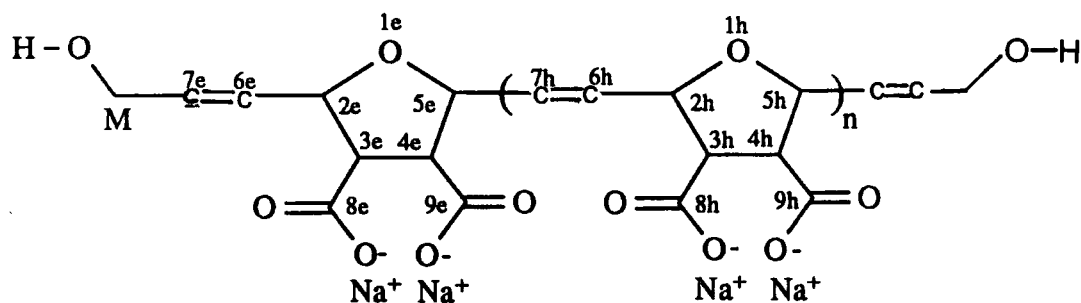


Figure 6.1: Oligomers of PIVb used for applications tests.

Based on the analysis of <sup>1</sup>H and <sup>13</sup>C NMR spectra, the oligomers appear to contain approximately 60% *cis* double bonds ( $\sigma^c = 0.6$ ), and vinyl hydroxymethyl end groups (Figure 6.1).

### 6.2.2 Applications test:

The oligomers synthesised in section 4.5 were assessed in an aragonite "threshold" test, which measured the ability of each oligomer to inhibit the precipitation of aragonite from an aqueous solution containing calcium and carbonate ions at 70°C. Air was bubbled through the test solution (Figure 6.2) in order to simulate the operating conditions found close to an industrial heat exchanger; due to its simplicity, this test is used only as a preliminary evaluation for aragonite anti-scalent products.

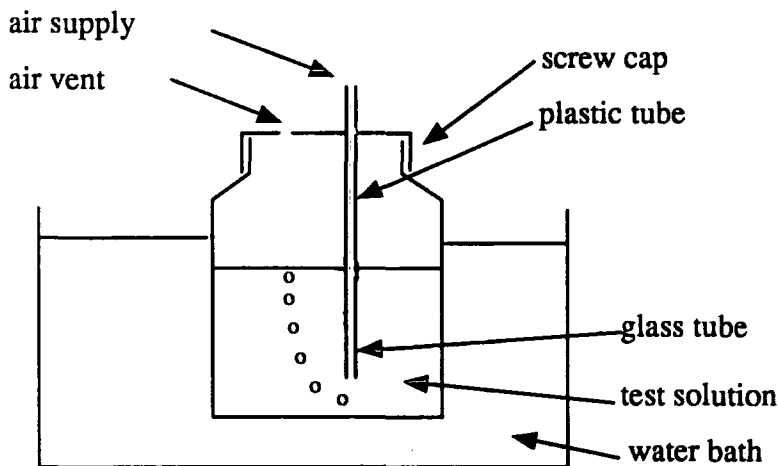


Figure 6.2: Apparatus for an aragonite "threshold" test.

50.0 ml of an aqueous solution containing sodium carbonate (0.009g, 0.08 mmol) and sodium bicarbonate (0.037g, 0.44 mmol) were added to a 150 ml capacity glass jar containing water (50.2 ml), calcium chloride dihydrate (0.055g, 0.37 mmol), magnesium chloride hexahydrate (0.038g, 0.19 mmol), and an oligomer of PIVb (variable dose level) at room temperature. The resulting test solution, through which air was bubbled at 0.5 litres/minute, was heated at  $70 \pm 0.1^\circ\text{C}$  for 30 minutes, and then filtered to remove any aragonite formed. Hydrochloric acid (0.2 ml, 50 wt%) was added to the filtrate (40 ml), and the



resulting solution stirred for one minute, during which time the remaining carbonate ions reacted to form carbon dioxide, which was evolved. The acidity of the solution was adjusted to pH 12 with solid sodium hydroxide and titrated with aqueous EDTA solution (0.01 M),<sup>114</sup> using Patton and Reeders indicator solution.<sup>115</sup> The solution colour changes from reddish-violet to blue at the end point.

A blank test was performed by repeating the experimental procedure described above in the absence of an oligomer of PIVb, and a standard test was performed by repeating the experimental procedure in the absence of both carbonate ions and PIVb. The standard test determined the actual concentration of calcium ions in solution, and the blank test determined the concentration of calcium ions remaining in solution after 30 minutes at 70°C in the presence of carbonate ions. A test solution containing an oligomer that inhibits the formation of aragonite will contain a higher calcium ion concentration than the blank test.

The efficiency of each oligomer to inhibit the formation of aragonite is measured in its "% CaCO<sub>3</sub> inhibition", given by the formula:

$$\% \text{ CaCO}_3 \text{ inhibition} = 100 \times \frac{((\text{test titre}) - (\text{blank titre}))}{(\text{standard titre}) - (\text{blank titre})}$$

Oligomers whose threshold test results have a high "% CaCO<sub>3</sub> inhibition" are potentially better aragonite anti-scalent products than those with a low "% CaCO<sub>3</sub> inhibition".

### 6.2.3 Computer modelling:

Theoretical calculations of the energy of interaction of various oligomers with an aragonite surface were made using a transputer based computer modelling

system custom built for Ciba-Geigy Industrial Chemicals. The hardware comprised of 16 INMOS floating point transputers in network with an IBM 80 personal computer, and DIGISOLE BGP64 graphics processing unit. The software, based on the commercial CHEMMOD package, was written for Ciba-Geigy by Dr. D.N.J. White at the University of Glasgow,<sup>86</sup> and used Newton-Raphson equations for the energy minimisation calculations.<sup>87</sup>

Models of ionic oligomers **PIVb** of various chain lengths and backbone microstructures were produced, and the lowest energy conformation for each model calculated in the absence of imbibed water and sodium ions. The minimum energy conformation of each model was found by moving the atoms of the model and calculating the sum of the Van der Waals, bond, and bond strain energies. Each oligomer model was fitted to a model of an aragonite crystal surface by removing carbonate ions from the model of the surface to leave "holes", and coordinating some of the carboxylate groups of the oligomer model to calcium ions exposed by these "holes".

The minimum energy of the new oligomer/aragonite model was calculated in a similar manner to the calculation of the minimum energy of the uncoordinated oligomer. The change in potential energy resulting from the formation of an oligomer/aragonite interaction was calculated as the difference in energy between each oligomer/aragonite model and models of the uncoordinated oligomer and aragonite surface. The presence of imbibed water and sodium ions was not taken into account in these models, so the calculated potential energies can only be used comparatively.

### 6.3: Results.

#### 6.3.1 *Inhibition of aragonite formation:*

The percentage  $\text{CaCO}_3$  inhibition of various oligomers of **PIVb** in the "threshold" test are recorded in Table 6.1.

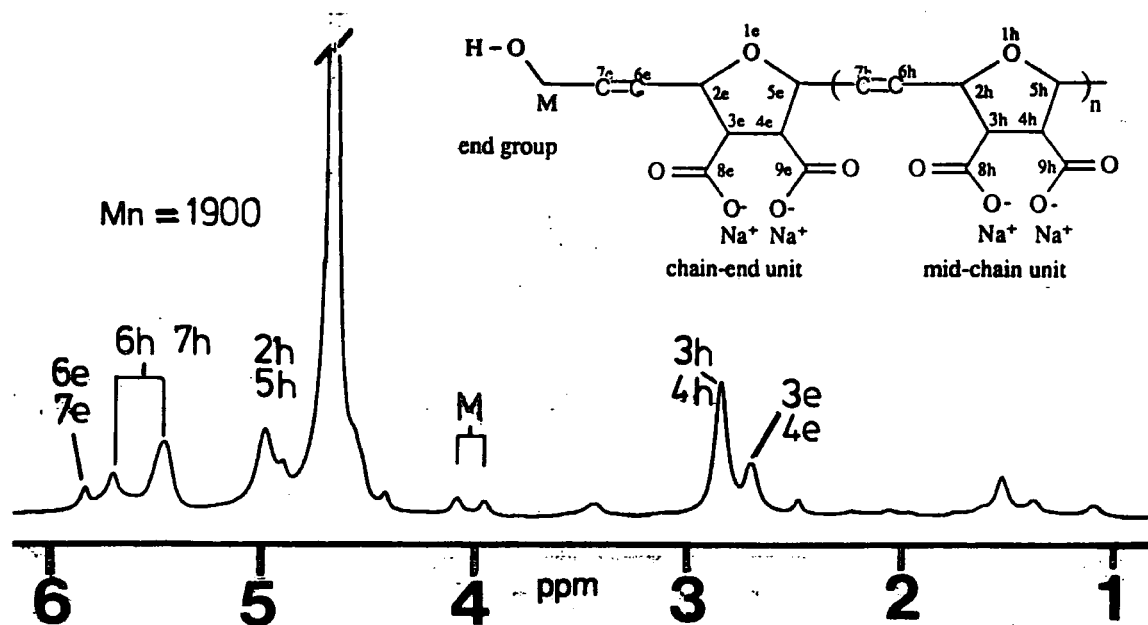
TABLE 6.1: Efficiency of various materials for the inhibition of aragonite formation in a "threshold" test.

Material	dose level	percentage inhibition
oligomer Mn 700	2 ppm	32%
oligomer Mn 1900	2 ppm	79%
oligomer Mn 2300	2 ppm	66%
oligomer Mn 2900	2 ppm	64%
oligomer Mn 4000	2 ppm	10%
oligomer Mn 5900	2 ppm	0%
$\text{RuCl}_3 \cdot 3\text{H}_2\text{O}$	0.01 ppm	0%
monomer IV	2 ppm	0%
NaOH	0.4 ppm	0%

**NOTE:** The oligomer samples are contaminated with 0.1-0.3 wt% ruthenium impurity. Thus the test using  $\text{RuCl}_3 \cdot 3\text{H}_2\text{O}$  in a 0.01 ppm dose instead of an oligomer sample simulated the effect of ruthenium impurities on the threshold test result, and corresponded to a impurity concentration of 0.5 wt%. The test using monomer IV instead of oligomer **PIVb** was purely for comparative purposes, and the test using NaOH simulated the concentration of sodium ions present in each oligomer sample. The results in Table 6.1 suggest that  $\text{RuCl}_3 \cdot 3\text{H}_2\text{O}$  impurities of less than 0.5% by weight of the samples do not affect the threshold test result, and that monomer IV does not inhibit aragonite formation.

The most effective oligomer tested for the prevention of aragonite formation has  $M_n = 1900$  (Table 6.1). Analysis of the  $^1\text{H}$  NMR spectrum of this particular oligomer using the methods described in section 4.5.2 suggests that the *average* oligomer is a trimer or tetramer containing 60% *cis* double bonds, and vinyl hydroxymethyl end groups (Figure 6.3). The *average* oligomer length is calculated by comparison of the integration of the resonances of protons on chain end units (3e) with the resonances of protons on mid chain units (3h, 4h) in the  $^1\text{H}$  NMR spectra of the oligomers (Figure 6.1 and section 4.5).

Figure 6.3:  $^1\text{H}$  NMR spectrum recorded at 399.952 MHz in  $\text{D}_2\text{O}$  of oligomers of **PIVb** prepared using  $\text{RuCl}_3 \cdot 3\text{H}_2\text{O}$  as the precursor to the initiating and chain propagating species, and *cis*-but-2-ene-1,4-diol (**VIII**) as chain transfer agent (CTA).



The oligomer which has a  $M_n = 700$  (Table 6.1) appears to have a much lower %  $\text{CaCO}_3$  inhibition than the oligomer with  $M_n = 1900$ . The  $^1\text{H}$  NMR spectrum of this sample shows that the *average* oligomer length is a dimer (Figure 4.14c), which suggests that dimers are not as effective for aragonite scale control as trimers or tetramers. Similarly, the sample which has  $M_n = 4000$ , and an *average*

oligomer length of eight (Figure 4.14b) appeared to have a very low %  $\text{CaCO}_3$  inhibition, which suggests that octamers are not as effective for aragonite scale control as dimers and tetramers.

### 6.3.2 Computer modelling:

The theoretical change in potential energy upon interaction of an oligomer with an aragonite surface for various dimers, trimers and tetramers ( $n = 1,2,3$  in Figure 6.1 respectively) are recorded in Tables 6.2, 6.3, 6.4, and 6.5. An increase in potential energy in the total system is unfavourable, therefore the energy change for the interaction must be small, or negative, if the interaction is to occur.

TABLE 6.2: Change in potential energy resulting from the coordination of a dimer of PIVb by its first or both addition units to an aragonite surface.

change in potential energy / Kcal.mol <sup>-1</sup>				
unit bound to surface	configuration of dimer.			
	C iso	C syn	T iso	T syn
first unit	0.4	0.1	1.2	0.8
both unit	7.9	0.4	27.8	3.2

Note: C iso = isotactic *cis*, T iso = isotactic *trans* etc.

The theoretically calculated change in potential energy resulting from the formation of an oligomer/aragonite interaction was found to be positive for all

models, and is therefore unfavourable. Furthermore, it can be seen that the configuration of the unbound units affects the energetics of the overall binding.

TABLE 6.3: Change in potential energy resulting from the coordination of a trimer of PIVb by its first addition unit to an aragonite surface.

change in potential energy / Kcal.mol <sup>-1</sup>				
configuration of first unit.	configuration of second unit.			
	C iso	C syn	T iso	T syn
<i>cis</i> isotactic	7.9	0.2	29.0	16.9
<i>cis</i> syndiotactic	6.5	0.4	23.1	17.0
<i>trans</i> isotactic	32.4	29.2	27.9	28.7
<i>trans</i> syndiotactic	15.1	13.8	6.8	3.2

Note: C iso = isotactic *cis*, T iso = isotactic *trans* etc.

TABLE 6.4: Change in potential energy resulting from the coordination of a trimer of PIVb by its first or middle addition unit to an aragonite surface.

change of potential energy / Kcal.mol <sup>-1</sup>				
unit bound to surface	configuration of trimer.			
	C iso	C syn	T iso	T syn
first unit	7.9	0.4	27.9	3.2
middle unit	26.5	26.5	27.1	31.3

Note: C iso = isotactic *cis*, T iso = isotactic *trans* etc.

TABLE 6.5: Change in potential energy resulting from the coordination of a tetramer of PIVb by its first or middle addition unit to an aragonite surface.

change in potential energy / Kcal.mol <sup>-1</sup>				
unit bound to surface	configuration of tetramer.			
	C iso	C syn	T iso	T syn
first unit	22.5	37.5	31.7	32.1
middle unit	42.3	42.5	43.0	41.0

Note: C iso = isotactic *cis*, T iso = isotactic *trans* etc.

The lowest change in energy was found to result from the interaction of the first unit of dimers containing either an isotactic or syndiotactic *cis* double bond with the aragonite surface (Table 6.2, Figures 6.4 and 6.5), 0.4 Kcal.mol<sup>-1</sup> and 0.1 Kcal.mol<sup>-1</sup> respectively; the interaction of dimers containing a *trans* double bond were marginally less favoured (Figure 6.6): 1.2 Kcal.mol<sup>-1</sup> and 0.8 Kcal.mol<sup>-1</sup> for isotactic and syndiotactic *trans* dimers respectively (Table 6.2).

The calculations for the energy of interaction of oligomers with the aragonite surface can be compared with the interaction of a monomer with the surface (24.1 Kcal.mol<sup>-1</sup>). The monomer proved to have no inhibition ability in the threshold test (section 6.3.1), so it is unlikely that oligomers whose interaction with an aragonite surface increases the total potential energy of the system by more than 24.1 Kcal.mol<sup>-1</sup> will have any effect. Based on this deduction, tetramers of PIVb, or trimers bonded by their middle repeat unit, appear unlikely aragonite anti scalent products (Figure 6.7, Tables 6.4 and 6.5).

Figure 6.4: Theoretical interaction of a *cis* isotactic dimer of **PIVb** with an aragonite surface.

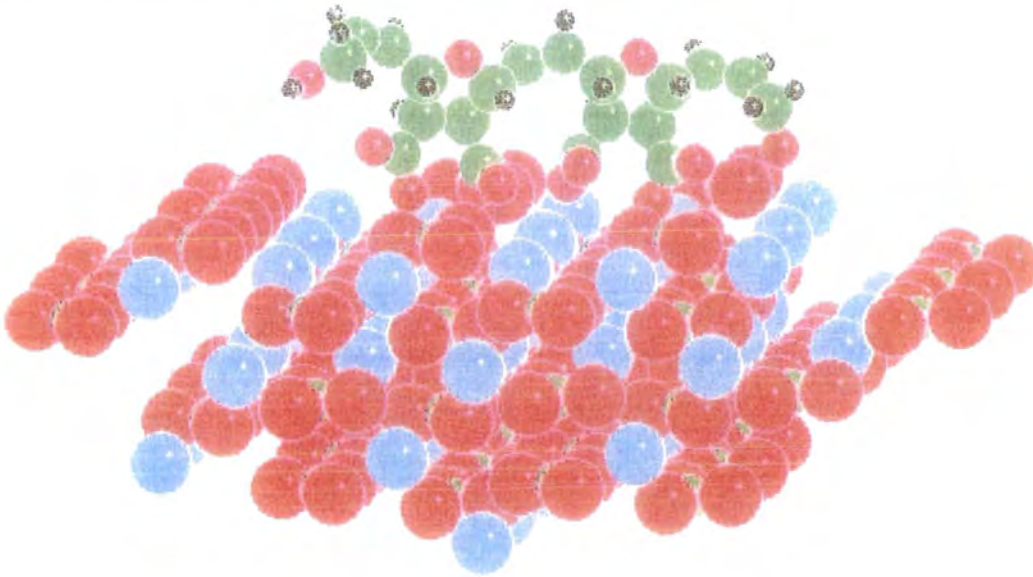


Figure 6.5: Theoretical interaction of a *cis* syndiotactic dimer of **PIVb** with an aragonite surface.

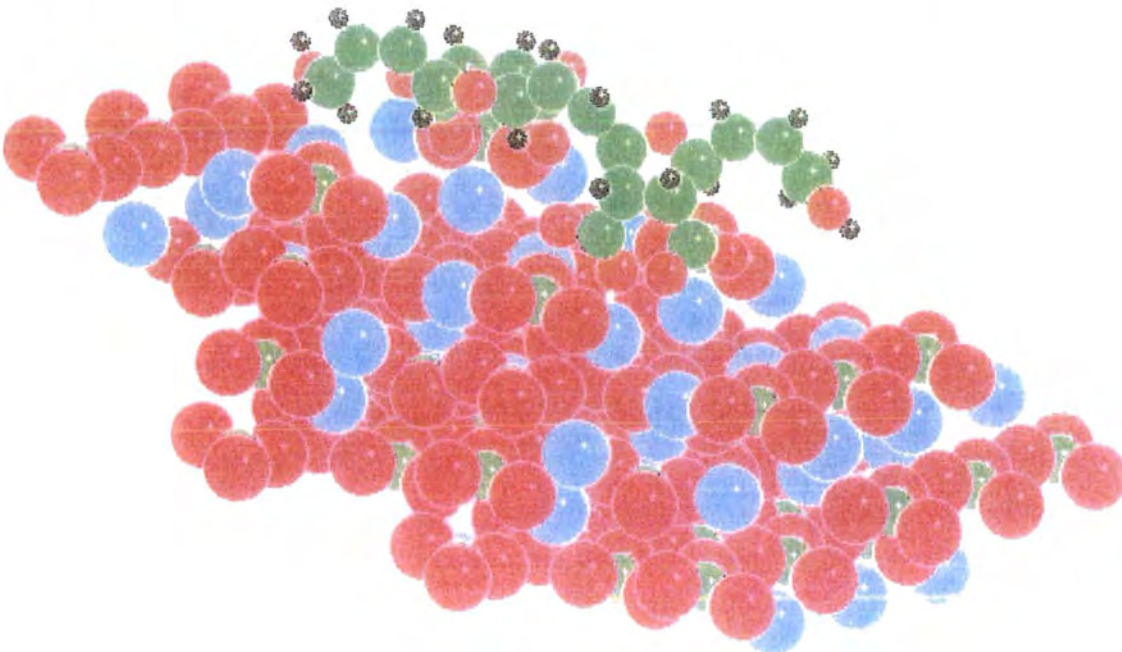




Figure 6.6: Theoretical interaction of a *trans* isotactic dimer of **PIVb** with an aragonite surface.

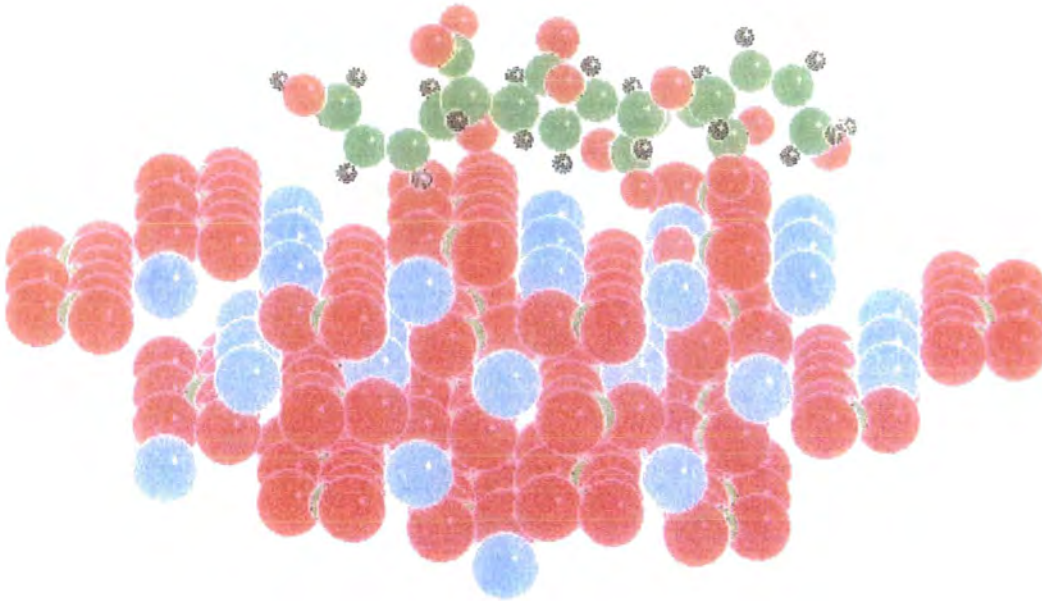
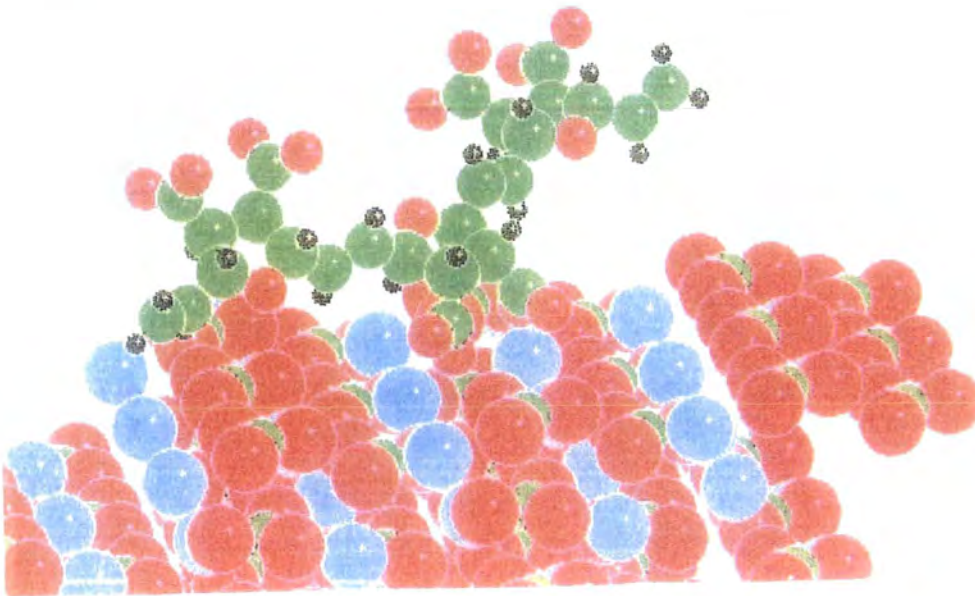
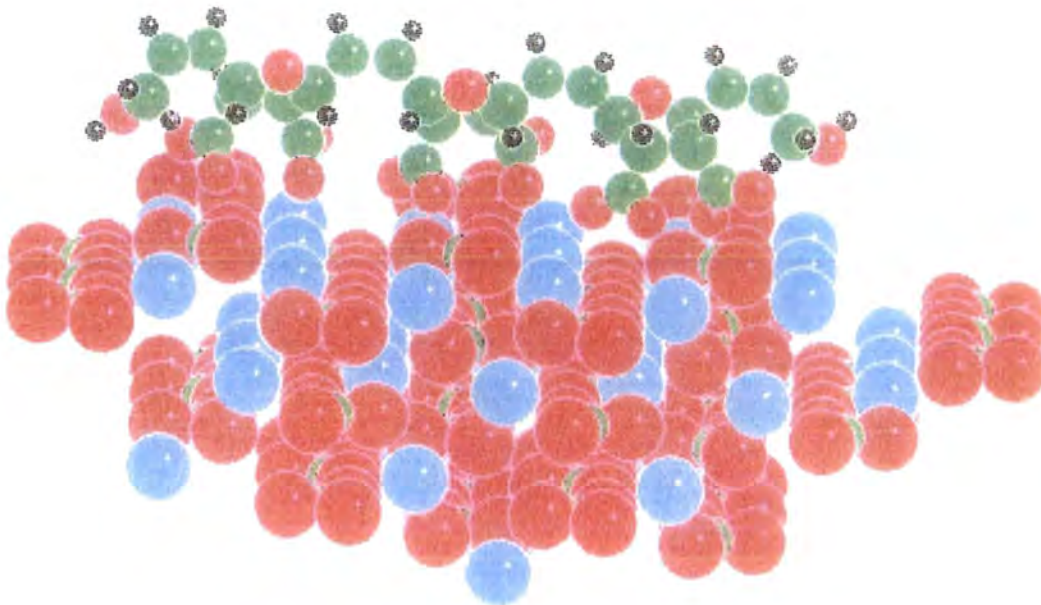


Figure 6.7: Theoretical interaction of a *trans* isotactic trimer of **PIVb** with an aragonite surface.



Trimers containing a *cis* syndiotactic bond between the second (middle) and third (last) repeat units appear to have a favourable interaction with the surface through the first repeat unit only when the bond between the first and second repeat unit is *cis* isotactic ( $0.2 \text{ Kcal.mol}^{-1}$ , Table 6.3, Figure 6.8) or *cis* syndiotactic ( $0.4 \text{ Kcal.mol}^{-1}$ ) (Table 6.3). The only favourable interactions of trimers containing *trans* double bonds occurs through the first addition unit when the double bond between the first and second unit is syndiotactic, and the double bond between the second (middle) and third (last) addition units is either *trans* isotactic ( $6.8 \text{ Kcal.mol}^{-1}$ ) or *trans* syndiotactic ( $3.2 \text{ Kcal.mol}^{-1}$ , Table 6.3). No other trimer conformation or interaction appears energetically favourable for aragonite scale control.

Figure 6.8: Theoretical interaction of a *cis* isotactic, *cis* syndiotactic trimer of **PIVb** with an aragonite surface.



#### 6.4 Discussion.

There is an apparent difference between the practical threshold test results (section 6.3.1) and the computer modelling (section 6.3.2). The threshold test results suggested that oligomers **PIVb** containing between three and four addition units are the most effective for aragonite scale control when the oligomer backbone contains 60% *cis* double bonds. Dimers and oligomers containing more than eight addition units were comparatively ineffective. Molecular modelling calculations suggested that only dimers of any microstructure, and trimers containing two syndiotactic double bonds, either both *cis* or both *trans* but not a mixture, are the most effective aragonite anti-scalent products. However the computer modelling was based on the coordination of the oligomer to a preformed aragonite crystal (section 1.3.3c), whereas in reality many other anti-scalent mechanisms may be involved. Furthermore, the computer models did not account for imbibed water or sodium ions, or imperfections in the aragonite surface.

#### 6.5 Conclusions.

Comparison of the results of the threshold test (section 6.4.1) and the theoretical calculations (section 6.4.2) conclude that trimers containing at least one *cis* double bond between repeat units are the most effective oligomers of **PIVb** for aragonite scale control. The highest percentage CaCO<sub>3</sub> inhibition (79%) for any of the oligomers tested was recorded using an oligomer of Mn = 1900 and  $\sigma^c = 0.6$  (Table 6.1), and this compares favourably with commercially available products.<sup>17</sup>

CHAPTER 7:  
CONCLUSIONS  
AND PROPOSALS  
FOR FUTURE WORK.

## 7.1: Introduction.

Three main research themes were investigated during the course of the work described in this thesis: a) assessing the range of monomers and transition metal compounds available for the aqueous ROMP reaction; b) characterisation of ROMP polymer and oligomer microstructure; and c) investigation of the application of oligomers of **PIVb** to aragonite scale control. All three areas yielded promising results, and now need to be investigated further.

## 7.2: Conclusions.

The work described in this thesis illustrates that ether, ester and carboxylic acid functionalised derivatives of 7-oxabicyclo[2.2.1]hept-2-ene can be polymerised via aqueous Ring Opening Metathesis Polymerisation (ROMP). The ROMP initiators can be prepared *in situ* using  $\text{RuCl}_3 \cdot 3\text{H}_2\text{O}$ ,  $\text{OsCl}_3 \cdot 3\text{H}_2\text{O}$ , or  $\text{IrCl}_3 \cdot 3\text{H}_2\text{O}$  as the precursors to the initiating and chain propagating species, and the molecular weight of the product polymers can be regulated by including *cis*-but-2-ene-1,4-diol, *cis*-1,4-dimethoxybut-2-ene, or acrylic acid in the reaction mixture. The induction period of the ROMP reaction was also dependant on the presence of these acyclic olefins, and strongly dependant on the presence of maleic acid in the reaction solution.

Oligomers prepared by aqueous ROMP of *exo,exo*-7-oxabicyclo[2.2.1]hept-5-ene-2,3-bis(carboxylic acid) (**IV**) in the presence of *cis*-but-2-ene-1,4-diol using commercially available  $\text{RuCl}_3 \cdot 3\text{H}_2\text{O}$  as the precursor to the initiating and chain propagating species were found to be particularly effective for the prevention of

aragonite precipitation from salt water. The most effective oligomer of this type had a number average molecular weight of 1900 with respect to polyethylene oxide standards, and 60% of the backbone double bond in the *cis* conformation. The test result for this material compared well with test results of current commercial products.<sup>17</sup>

### **7.3: Proposals for future work.**

The nature of the initiating and chain propagating species formed in these aqueous ROMP reactions was not investigated, although they were assumed to contain a metal carbene since the reaction products were all consistent with ROMP polymers.<sup>22</sup> The transition metal chlorides used as the precursors to the initiating and chain propagating species were not purified or characterised, and therefore little information concerning mechanism was found. Future developments in the study of aqueous metathesis require the synthesis of well defined transition metal carbenes; such a study was out of the scope of the work described in this thesis.

The polymer characterisation is soundly based in this work, but it is clear that none of the materials made are homostructural and consequently the scale inhibition/modelling correlation is not on particularly firm ground. The studies did however indicate that dimers, trimers or tetramers of **PIVb** may have potential as aragonite antiscalent products, and these materials could possibly be prepared by classical organic synthesis rather than ROMP in the presence of chain transfer agents.

## REFERENCES.

- 1) J.C. Cowan, D.J. Weintritt, "Water-formed scale deposits", Gulf Publishing Company, Houston, 1976.
- 2) Skeist Laboratories INC, "Water-soluble polymers", 1983.
- 3) A. Reeckman, G.M. Friedman, "Exploration for carbonate petroleum reservoirs", Wiley, New York, 1982.
- 4) A.G. Collins, "Geochemistry of oilfield waters", Elsevier, Amsterdam, 1975.
- 5) P. Nigeli, R.L. Parker, "Rock and mineral deposits", Freeman, San Fransisco, 1954.
- 6) Y. Ohno, J.Ceram. Assoc. Japan, 60, 548, 1952.
- 7) G.L. Frear, J. Johnston, J. Am. Chem. Soc., 79, 2031, 1929.
- 8) L. Bragg, G.F. Claringbull, "Crystal strutures of minerals" vol IV, Bell, London, 1965.
- 9) J.D.C. McConnel, Min. Mag., 32, 535, 1960.
- 10) Y.Kitano, Bull. Chem. Soc. Jpn., 35, 1973, 1959.
- 11) J.L. Wray, F. Daniels, J. Am. Chem. Soc., 79, 2031, 1957.
- 12) U.M. Oxburgh, R.E. Segnit, H.D. Holland, Bull. Geol. Soc. Amer., 70, 1653, 1959.
- 13) G.R. Fonda, J. Phys. Chem., 44, 435 1940.
- 14) J. Sinkankas, "Mineralogy: A first course", Van Nostrand, Princeton, 1964.
- 15) J.R. Smith, D.L. Bish, "Crystal structures and cation sites of the rock-forming minerals", Allen and Unwin, Wellington, 1988.
- 16) G. Allen, J.C. Bevington, "Comprehensive polymer science", Vol. 3, Pergamon, Oxford, 1989.
- 17) Ciba-Giegy Industrial Chemicals, Private Communication.
- 18) G. Wilkinson, "Comprehensive co-ordination chemistry", Vol. 3, Pergamon, Oxford, 1987.



- 19) P. Hartman, "Crystal Growth: an introduction", North-Holland, Amsterdam, 1973.
- 20) R.M. Garrels, "Mineral Equilibria", Harpers, New York, 1960.
- 21) R.F. Stickland-Constable, "Crystallisation", Academic Press, London, 1968.
- 22) K.J. Ivin, "Olefin Metathesis", Academic Press, London, 1983.
- 23) G. Allen, J.C. Bevington, "Comprehensive polymer science", Vol. 4, Pergamon, Oxford, 1989.
- 24) K.J. Ivin, Sagussa, "Ring opening Polymerisation" Elsevier 1984
- 25) A.W. Anderson, N.G. Merckling, Chem. Abs. 50, 3008, 1955.
- 26) R.L. Banks and G.C. Bailey, Ind. Eng. Chem. Prod. Res. Div., 3, 170, 1964.
- 27) N. Calderon *et al.*, Chem. Eng. News., 45, 51, 1967.
- 28) R.R. Schrock, Acc. Chem. Res., 23, 158 1990.
- 29) E. Ceausescu, A. Cornilescu, E. Nicolescu, M. Popescu, S. Coca, M. Dimonie, M. Gherorghui, V. Dragutan, M. Chipara, J. Mol. Cat., 28, 337, 1985.
- 30) E. Thorn-Csanyi and M. Kessler, J. Mol. Cat., 36, 31, 1986.
- 31) E. Thorn-Csanyi and H. Timm, J. Mol. Cat., 28, 37, 1985.
- 32) E. Ceausescu, A. Cornilescu, E. Nicolescu, M. Popescu, S. Coca, M. Cuzmici, C. Oprescu, J. Mol. Cat., 36, 163, 1986.
- 33) K.J. Ivin, D.T. Lavery, J.J. Rooney, Makromol. Chem., 178, 1545, 1977.
- 34) E.A. Ofstead, N. Calderon, Makromol. Chem., 154, 21, 1972.
- 35) K.C. Wallace, R.R. Schrock, Macromolecules, 20, 448, 1987.
- 36) R.R. Schrock, Acc. Chem. Res., 19, 342, 1986.
- 37) R.R. Schrock, I.A. Wienstock, A.D. Horton, A.H. Liu, M.H. Schofield, J. Am. Chem. Soc., 110, 2686, 1988.
- 38) L.F. Cannizzo, R.H. Grubbs, J. Org. Chem., 50, 2386, 1985.

- 39) M.T. Youinou, J. Kress, J. Fischer, A. Agero, J.A. Osborne,  
J. Am. Chem. Soc., 110, 1488, 1988.
- 40) J.L. Herisson and Y. Chauvin, Makromol. Chem., 141, 161, 1970.
- 41) E.O. Fischer, and A. Maasbol, Angew. Chem., Inter. Ed. 3, 580, 1964.
- 42) H.T. Ho, K.J. Ivin, and J.J. Rooney, J. Mol. Cat., 15, 245, 1982.
- 43) C.P. Casey and T.J. Burkhart, J. Am. Chem. Soc., 95, 5833, 1973.
- 44) C.P. Casey and T.J. Burkhart, J. Am. Chem. Soc., 96, 7808, 1974.
- 45) T.J. Katz, S.J. Lee, N. Acton, Tet. Lett., 4247, 1976.
- 46) F.N. Tebbe, G.W. Parshall, G. Reddy, J. Am. Chem. Soc., 100, 3611, 1978.
- 47) L.R. Gilliom and R.H. Grubbs, J. Am. Chem. Soc., 108, 733, 1986.
- 48) J. Kress, J.A. Osborn, R.M.E. Greene, K.J. Ivin, J.J. Rooney,  
J. Am. Chem. Soc., 109, 899, 1987.
- 49) R.R. Schrock, R.T. DePue, J. Feldman, C.J. Schaverien, J.C. Dewan,  
A.H. Liu, J. Am. Chem. Soc., 110, 1423, 1988.
- 50) C.J. Schaverien, J.C. Dewan, R.R. Schrock, J. Am. Chem. Soc., 108,  
2771, 1986.
- 51) R.R. Schrock, J. Feldman, L.F. Cannizzo, R.H. Grubbs, Macromolecules,  
20, 1169, 1987.
- 52) J.G. Hamilton, K.J. Ivin, M. McCann, J.J. Rooney, J. Chem. Soc., Chem.  
Commun., 1379, 1984.
- 53) G. Bazan, R.R. Schrock, E. Khosravi -Babadi, W.J. Feast, V.C. Gibson,  
Polymer Commun, 30, 258, 1989.
- 54) J. Kress, J.A. Osborn, R.M.E. Greene, K.J. Ivin, J.J. Rooney,  
J. Chem. Soc., Chem. Commun., 874 1985.
- 55) K.C. Wallace, A.H. Liu, J.C. Dewan, R.R. Schrock, J. Am. Chem. Soc.,  
110, 4964, 1988.
- 56) J.S. Murdzek, R.R. Schrock, Macromolecules, 20, 2640, 1987.

- 57) W.C. Finch, E.V. Anslyn, R.H. Grubbs, *J. Am. Chem. Soc.*, **110**, 2406, 1988.
- 58) J. Feldman, W.M. Davis, R.R. Schrock, *Organometallics*, **8**, 2266, 1989.
- 59) R.R. Schrock, J.S. Murdzek, G. C. Bazan, J. Robbins, M. DiMare, M. O'Regan, *J. Am. Chem. Soc.*, **112**, 3875, 1990.
- 60) J. Feldman, J.S. Murdzek, W.M. Davis, R.R. Schrock, *Organometallics*, **8**, 2260, 1989.
- 61) L. Porri, R. Rossi, P. Diversi, A. Lucherini, *Makromol. Chem.*, **175**, 3097, 1974.
- 62) F.W. Michelotti, W.P. Keaveney, *J. Pol. Sci.*, **A3**, 895, 1965.
- 63) C. Tanielian, A. Kiennemann, T. Osparpucu, *Can. J Chem.*, **57**, 2022, 1979.
- 64) G. Dall'Asta, *J. Pol. Sci.*, **A6**, 2407, 1968.
- 65) US PATENT 1983, 4,412,044.
- 66) British Patent 1977, 1,487,185.
- 67) Uniroyal Inc. British Patent 1968, 1,131,160.
- 68) R.E. Rinehart, U.S. Patent 1968, 3,367,924.
- 69) R.E. Rinehart, H.P. Smith, *J. Pol. Sci.*, **B3**, 1049, 1965.
- 70) M. Lautens, A.S. Adb-El-Aziz, J. Reibel, *Macromolecules*, **22**, 4132 1989.
- 71) B.M. Novak, R.H. Grubbs, *J. Am. Chem. Soc.*, **110**, 960, 1988.
- 72) B.M. Novak, R.H. Grubbs, *J. Am. Chem. Soc.*, **110**, 7542, 1988.
- 73) W.J. Feast, D.B. Harrison, In Press, *J. Mol. Cat.*
- 74) J.G. Hamilton, D.G. Marquess, T.J. O'Neill, J.J. Rooney, *J. Chem. Soc., Chem. Commun.*, 119, 1990.
- 75) H.T. Ho, K.J. Ivin, B.S.R. Reddy, J.J. Rooney, *Eur. Poly. J.*, **25**, 805, 1989.
- 76) K.J. Ivin, J.J. Rooney, L. Bencze, J.G. Hamilton, L.M. Lam, G. Lapienis, B.S.R. Reddy, H.T. Ho, *Pure Appl. Chem*, **54**, 447, 1982.
- 77) W.J. Feast, D.B. Harrison, submitted to *Polymer*.
- 78) H. Lammens, G. Sartori, J. Siffert, N. Specher, *J. Pol. Sci.*, **C9**, 341, 1971.

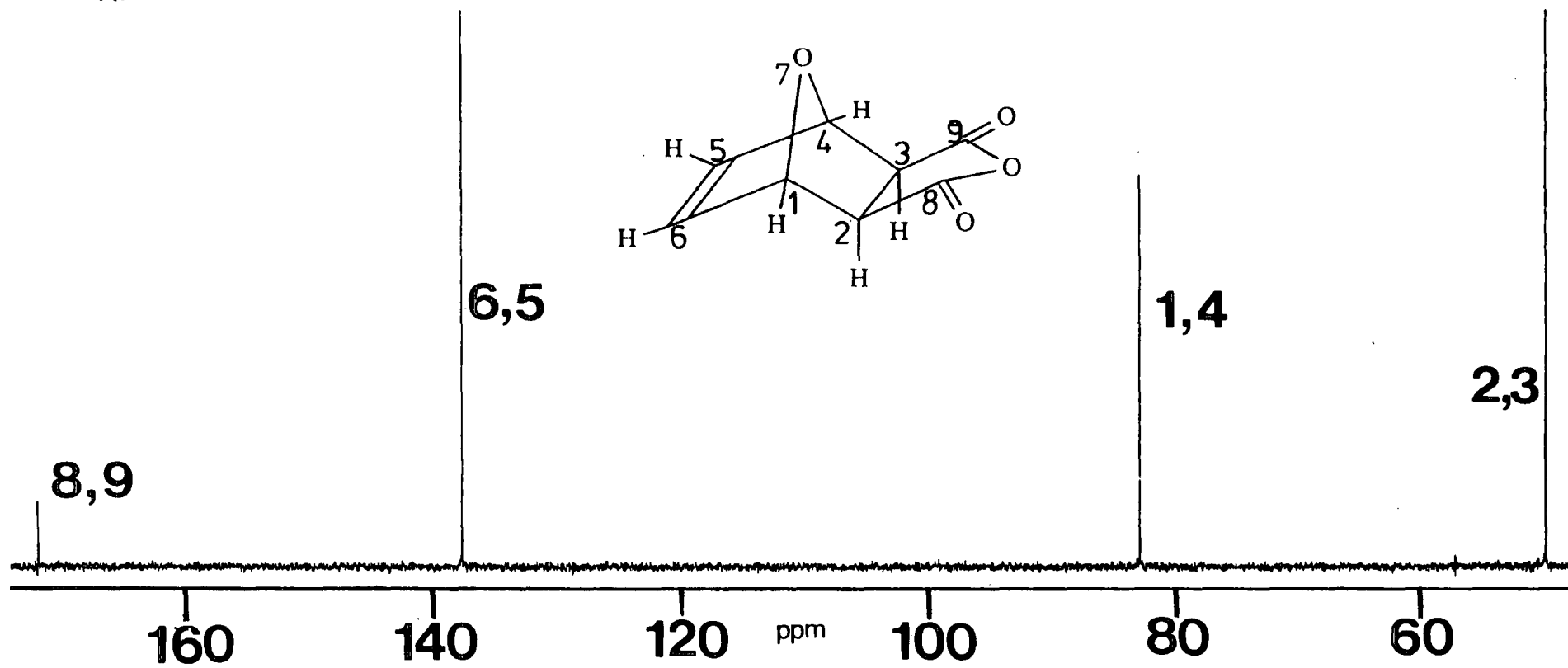
- 79) R.E. Rinehart, *J. Pol. Sci.*, **C27**, 7, 1969.
- 80) H.T. Ho, K.J. Ivin, J.J. Rooney, *J. Mol. Cat.*, **15**, 245, 1982.
- 81) A. Steitweiser, C.H. Heathcock, "Introduction to organic chemistry", 2<sup>nd</sup> Ed., MacMillan, New York, 1981.
- 82) W.G. Dauben, H.O. Krabbenhoft, *J. Am. Chem. Soc.*, **98**, 1992, 1976.
- 83) P.V. Bonnesen, C.L. Puckett, R.V. Honeychuck, W.H. Hersh, *J. Am. Chem. Soc.*, **111**, 6070, 1989.
- 84) K.F. Castner, N. Calderon, *J. Mol. Cat.*, **15**, 47, 1982.
- 85) D. Craig, *J. Am. Chem. Soc.*, **73**, 4889, 1951.
- 86) D.N.J. White/ Ciba-Geigy Collaboration.
- 87) R.L. Burden, J.D. Faires, A.C. Reynolds, "Numerical Analysis", 2<sup>nd</sup> Ed., Prindle, Weber, Schmidt, Boston, 1981.
- 88) M.W. Lee, W.C. Herndon, *J. Org. Chem.*, **43**, 518, 1978.
- 89) R.B. Woodward, H. Baer, *J. Am. Chem. Soc.*, **70**, 1161, 1948.
- 90) H. Stockman, *J. Org. Chem.*, **26**, 2025, 1961.
- 91) E.W. Garbisch, *J. Am. Chem. Soc.*, **80**, 5561, 1964.
- 92) J. Das, US Patent 1986, 4,611,006.
- 93) J.C. Grandguillot, F. Rouessac, *Synthesis*, **8**, 607, 1979.
- 94) S. Takano, K. Ogasawa, *Synthesis*, **3**, 42, 1974.
- 95) V.M. Micovic, M.L.J. Milhailovic, *J. Org. Chem.*, **18**, 1190, 1953.
- 96) B.A. Stoochnoff, N.L. Benoiton, *Tet. Lett.*, **1**, 961, 1973.
- 97) J. Jean, *Ann. Chim.*, **5**, 1165, 1960.
- 98) R.M. Acheson, "An introduction to the chemistry of heterocyclic compounds", Interscience, New York, 1960.
- 99) H. Kotsuki, H. Nishizawa, M. Ochi, K. Matsuoka, *Bull. Chem. Soc. Jpn.*, **55**, 496, 1982.
- 100) F. Brion, *Tet. Lett.*, **23**, 5299, 1982
- 101) Dictionary of organic compounds, Vol 1.

- 102) B.M. Novak, R.H. Grubbs, Proc. Am. Chem. Soc. PMSE, 57, 651, 1987.
- 103) S.L. Patt, J.N. Shoolery, J. Mag. Resonance, 46, 535, 1982.
- 104) J.G. Hamilton, K.J. Ivin, J.J. Rooney, British Polymer Journal, 16, 21 1984.
- 105) F.W. Michelotti, J.H. Carter, Am. Chem. Soc. Poly. Pre., 6, 224, 1965.
- 106) R.C. Weast, "Handbook of chemistry and Physics", 68<sup>th</sup> Edition, CRC Press Inc.
- 107) D.S. Tarbell, J.F. Burnett, J. Am. Chem. Soc., 70, 1290, 1948.
- 108) J.V. Schloss, F.C. Hartman, Bio-org. Chem., 9, 217, 1980.
- 109) H. Baltes, E. Streckham, H.J. Schafer; Chem. Berichte, 111, 1294, 1978.
- 110) H. Cramail, M. Fontanille, A. Soum, J. Mol. Cat. In Press.
- 111) E.A. Seddon, K.R. Seddon, "The Chemistry of Ruthenium", Elsevier, Amsterdam, 1984.
- 112) U.S. Patent, 1,131,160.
- 113) NMR experimental result.
- 114) H.A. Flaschka, "EDTA titrations", Pergamon, Oxford, 1967.
- 115) 2-hydroxy-1-(2-hydroxy-4-sulpho-1-naphthylazo)-3-naphthoic acid.

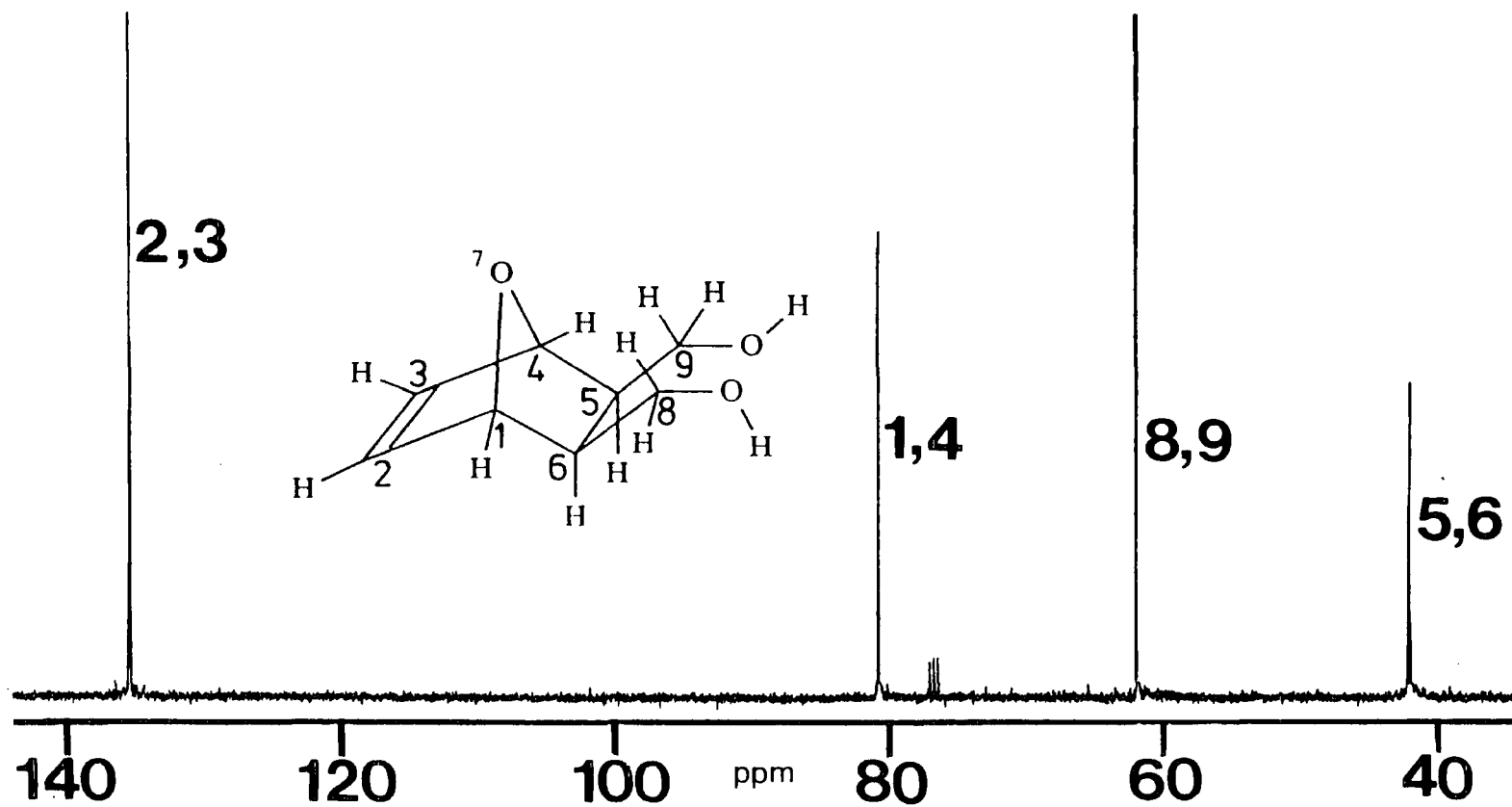
APPENDIX A:  
<sup>13</sup>C NMR SPECTRA

Appendix A1:  $^{13}\text{C}$  NMR spectrum of *exo*-7-oxabicyclo[2.2.1]hept-5-ene-2,3-dicarboxy anhydride (monomer **I**) recorded at 100.577 MHz in  $(\text{CD}_3)_2\text{CO}$ .

A1

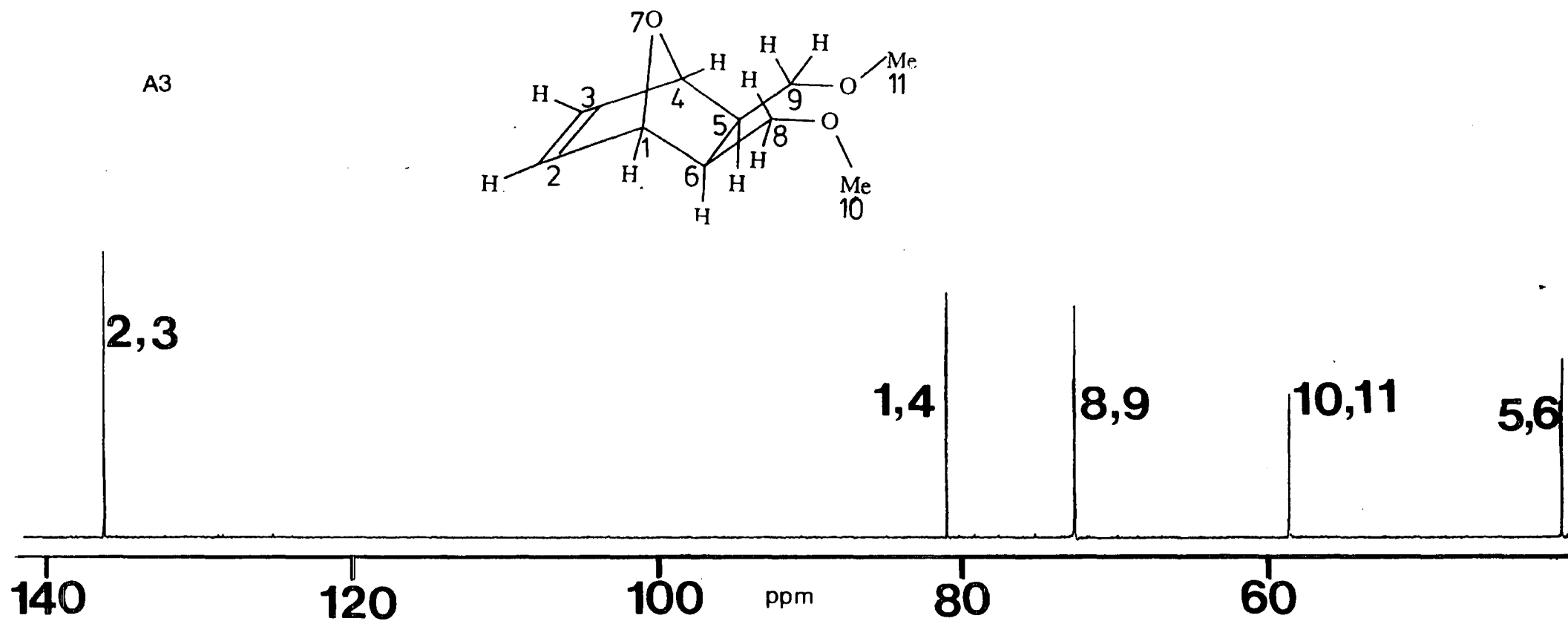


A2 Appendix A2:  $^{13}\text{C}$  NMR spectrum of *exo,exo*-5,6-bis(hydroxymethyl)-7-oxabicyclo[2.2.1]hept-2-ene (monomer **II**) recorded at 100.577 MHz in  $\text{CDCl}_3$ .

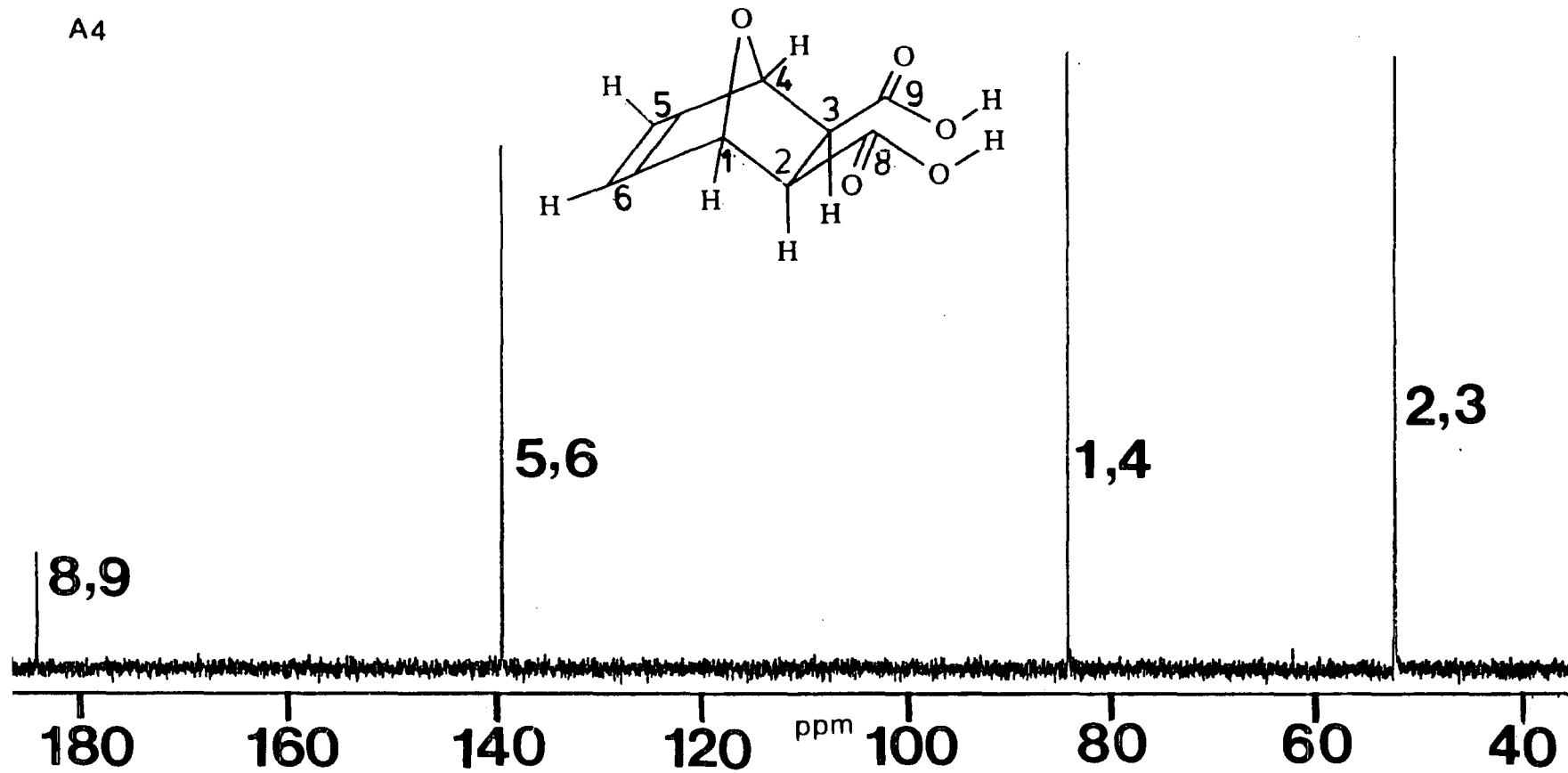




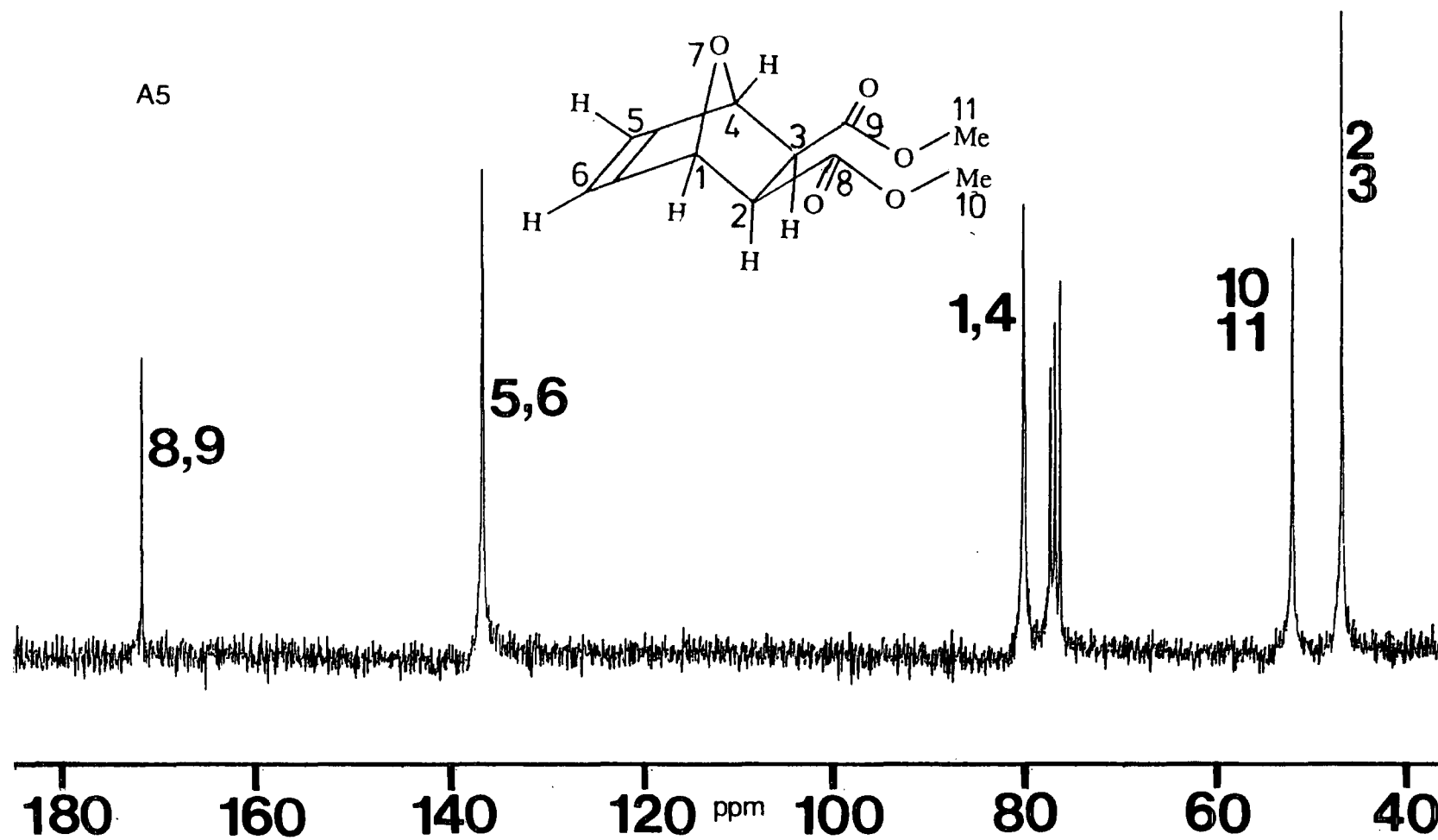
Appendix A3:  $^{13}\text{C}$  NMR spectrum of *exo,exo*-5,6-bis(methoxymethyl)-7-oxa-bicyclo[2.2.1]hept-2-ene (monomer **III**) recorded at 100.577 MHz in  $(\text{CD}_3)_2\text{CO}$ .



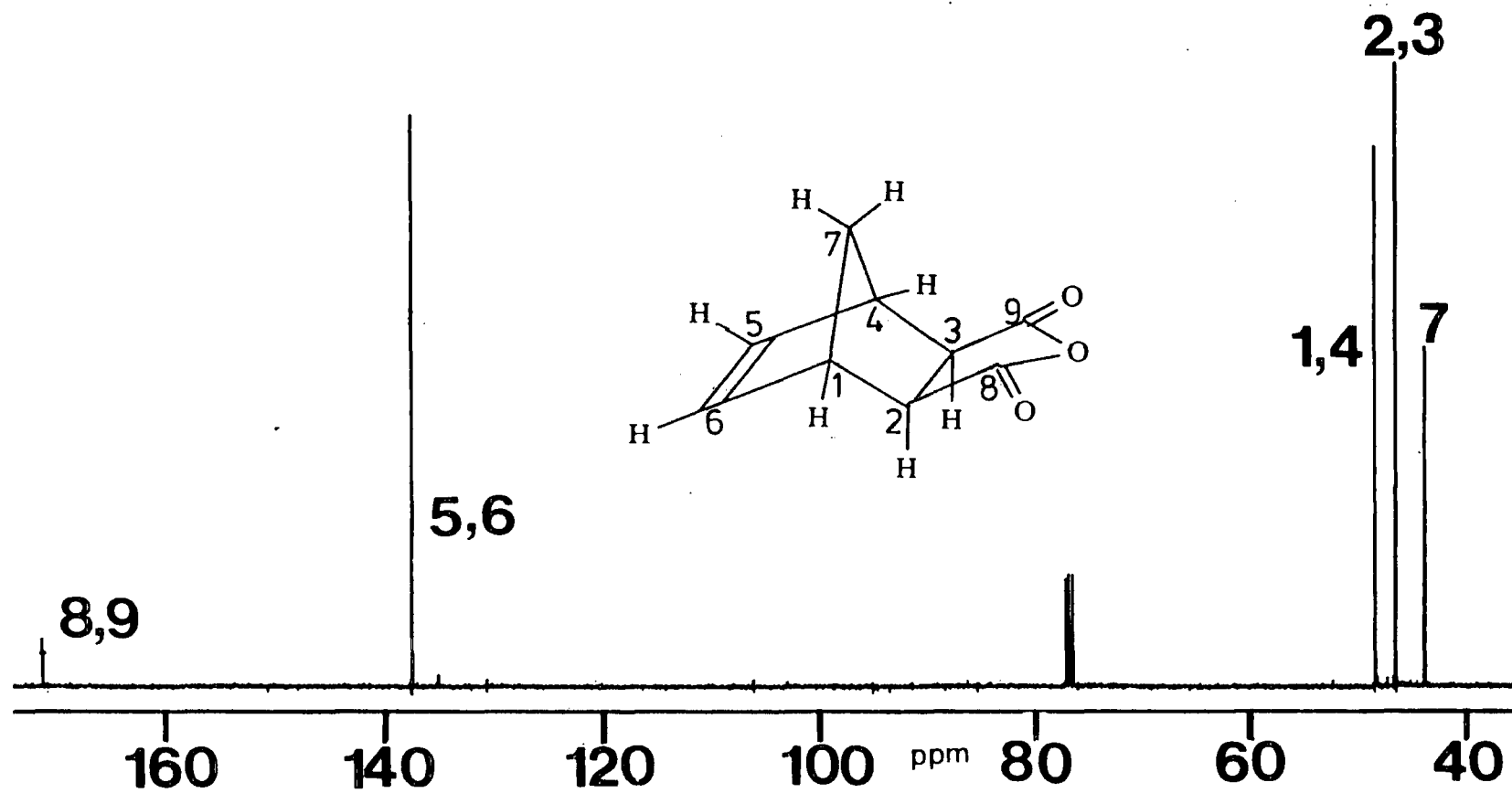
Appendix A4:  $^{13}\text{C}$  NMR spectrum of *exo,exo*-7-oxabicyclo[2.2.1]hept-5-ene-2,3-bis(carboxylic acid) (monomer **IV**) recorded at 100.577 MHz in  $\text{D}_2\text{O}$ .



Appendix A5:  $^{13}\text{C}$  NMR spectrum of *exo,exo*-7-oxabicyclo[2.2.1]hept-5-ene-2,3-bis(carboxymethyl ester) (monomer V) recorded at 62.896 MHz in  $\text{CDCl}_3$ .

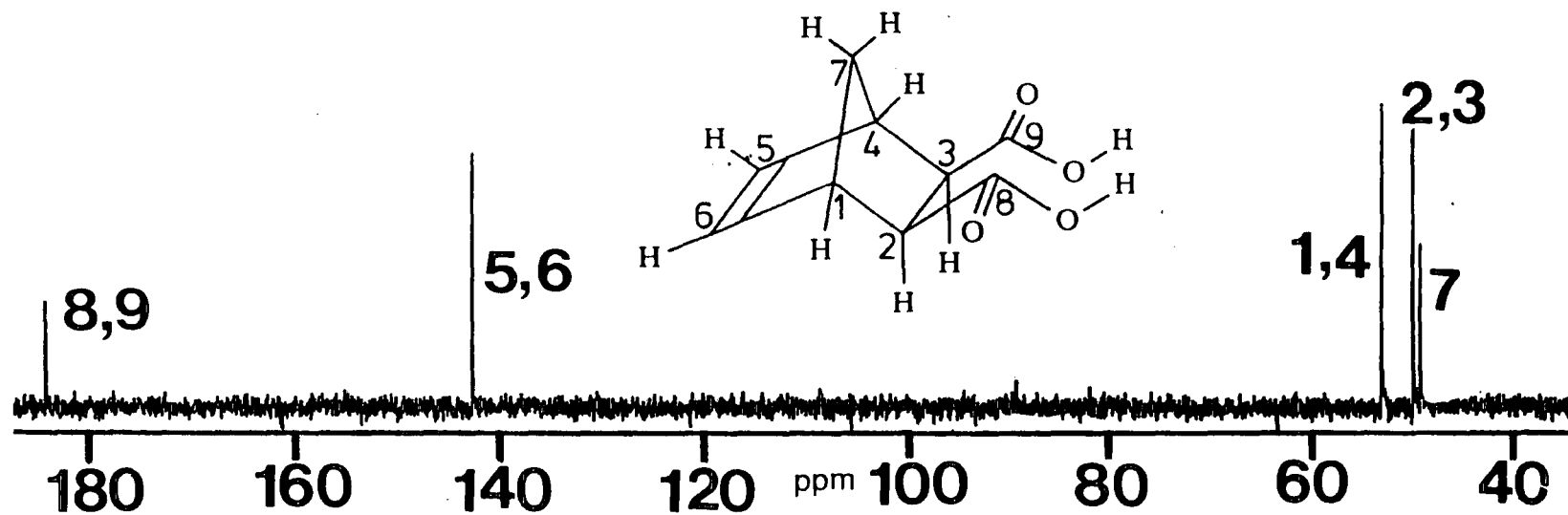


A6 Appendix A6:  $^{13}\text{C}$  NMR spectrum of *exo*-bicyclo[2.2.1]hept-5-ene-2,3-dicarboxy anhydride (monomer VI) recorded at 100.577 MHz in  $\text{CDCl}_3$ .



Appendix A7:  $^{13}\text{C}$  NMR spectrum of *exo,exo*-bicyclo[2.2.1]hept-5-ene-2,3-bis(carboxylic acid) (monomer VII) recorded at 100.577 MHz in  $\text{D}_2\text{O}$ .

A7



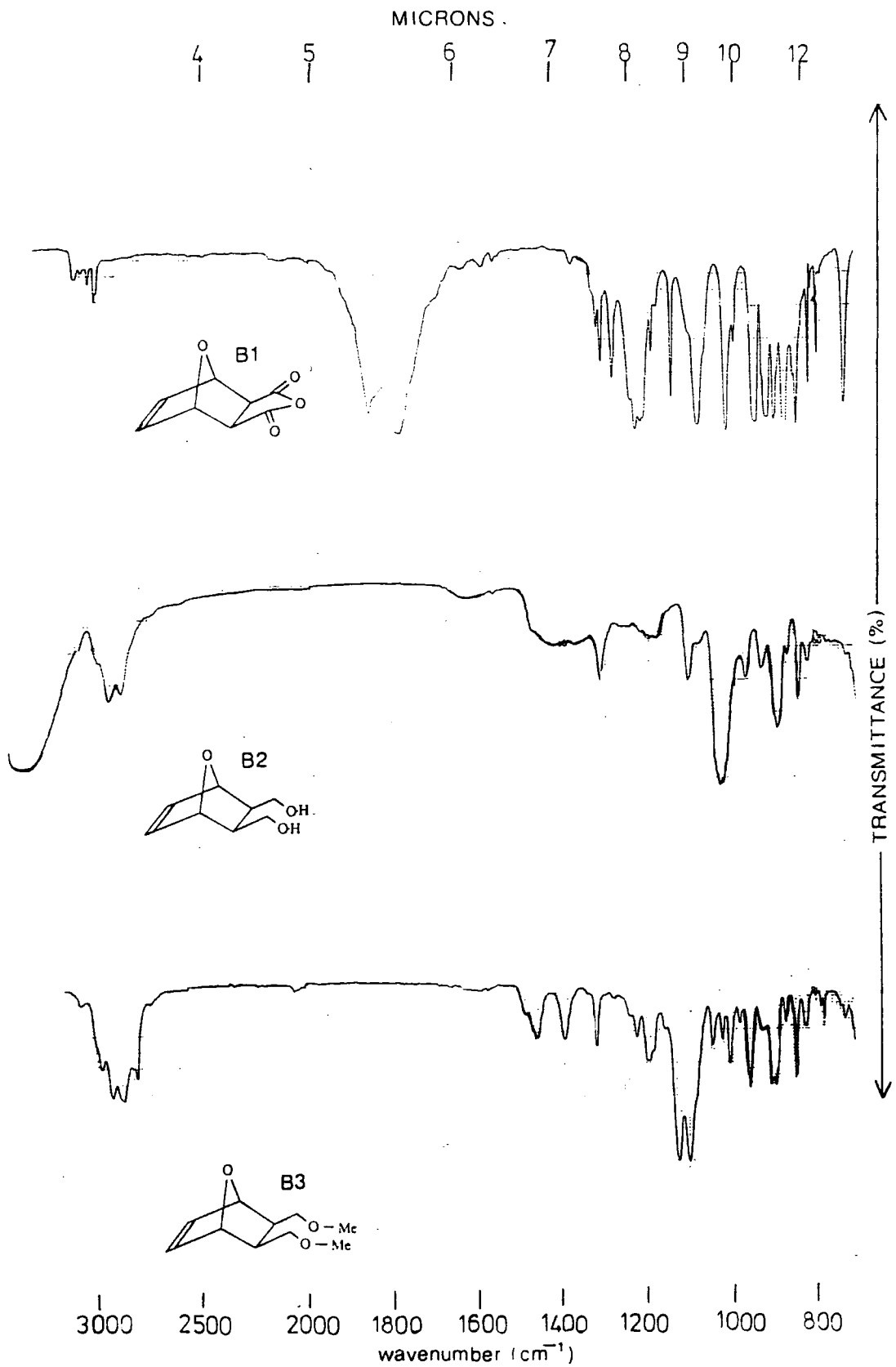
**APPENDIX B:  
INFRARED SPECTRA**

Infrared spectra are given below. All spectra were recorded using KBr plates of discs, and were run under the conditions designated by:

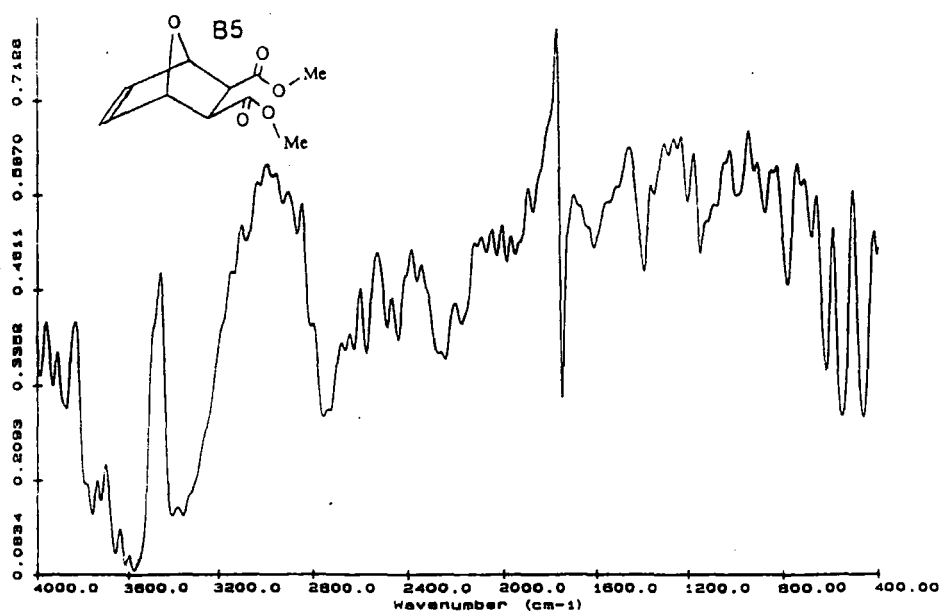
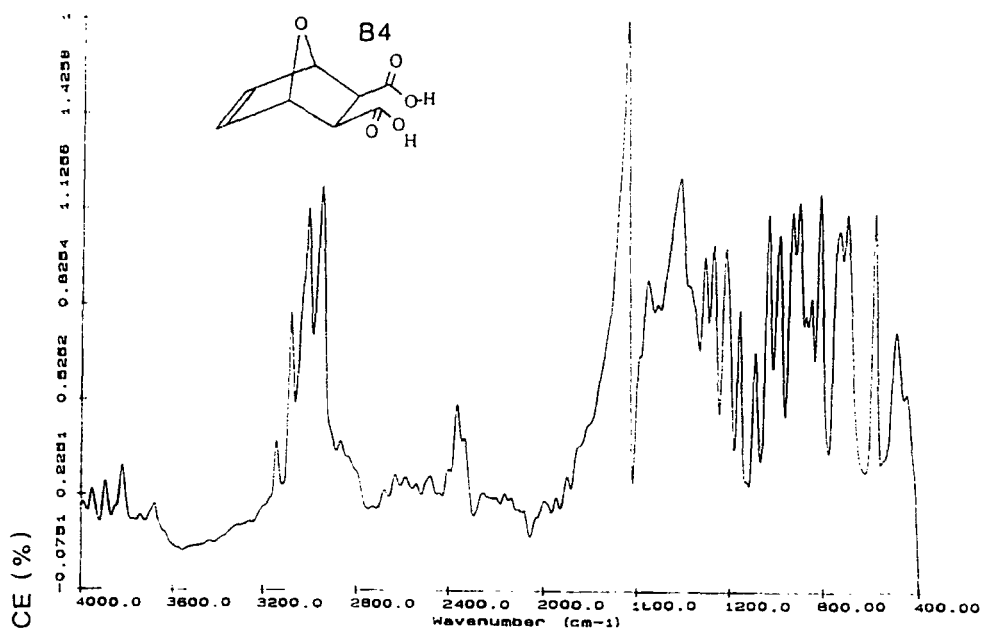
(A)- KBr disc

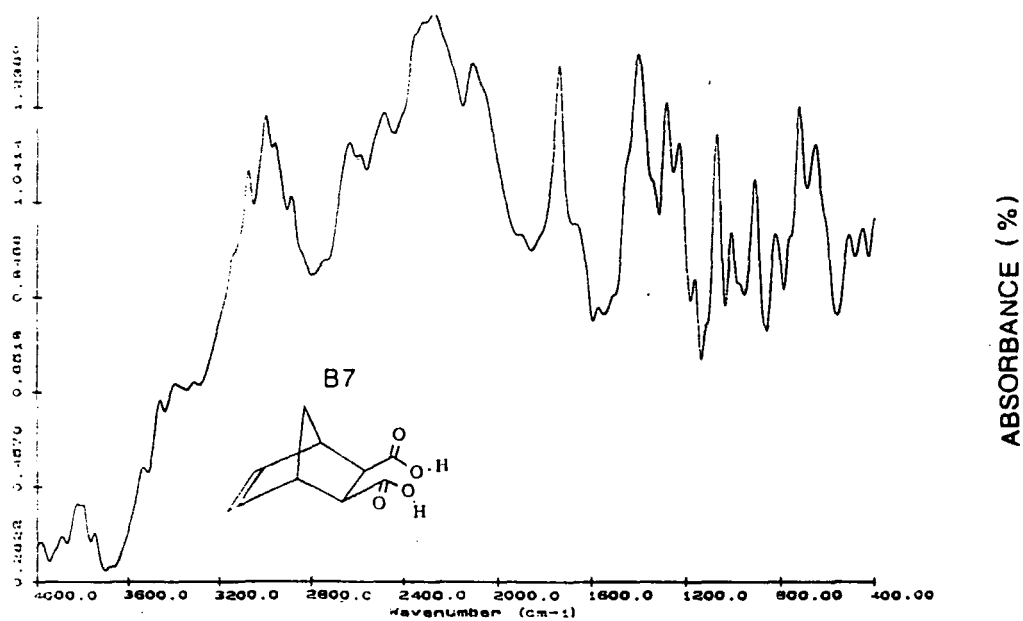
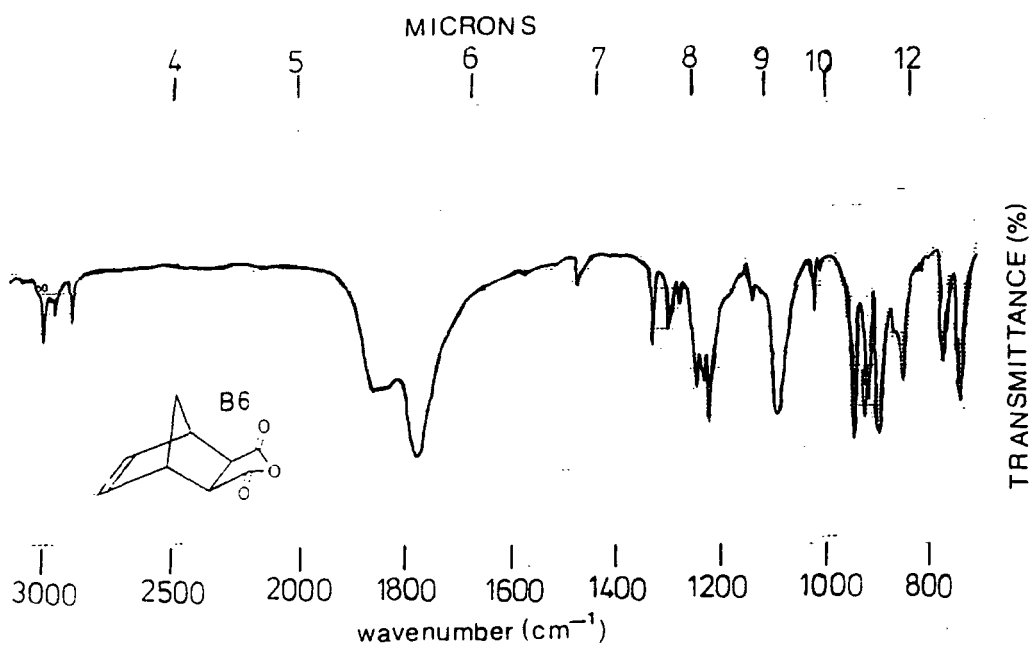
(B)- film cast from acetone

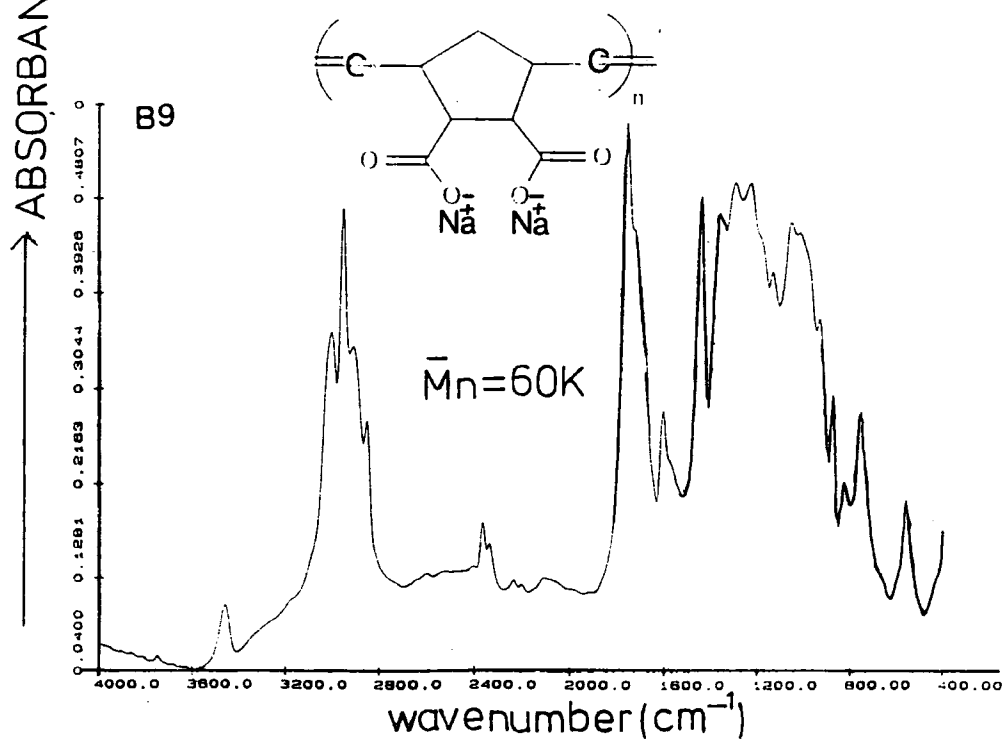
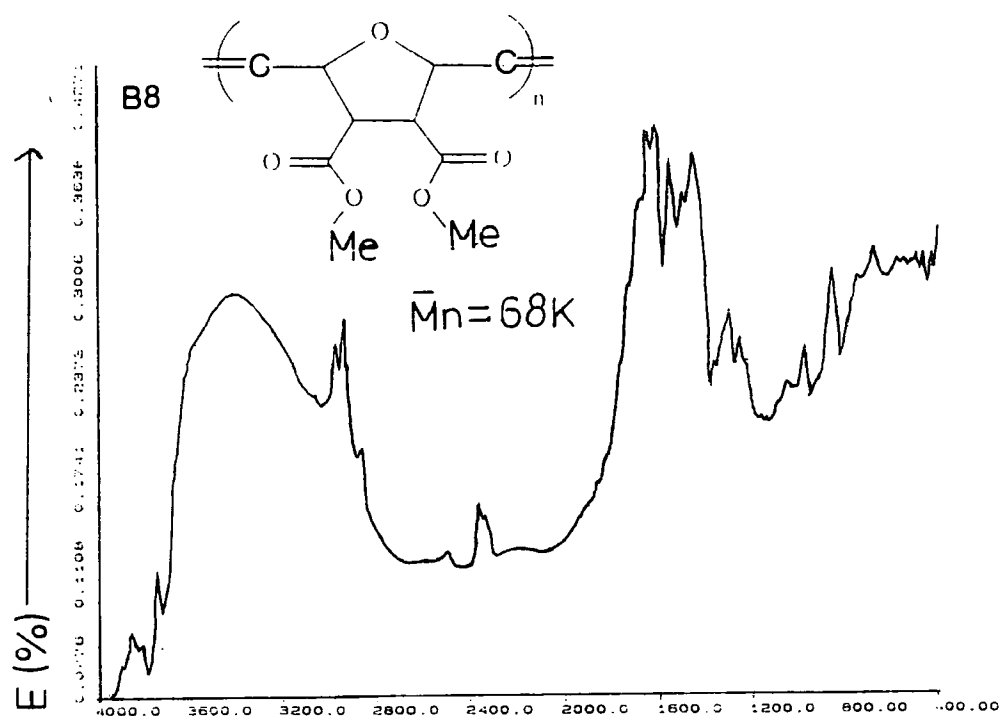
- 1) *exo*-7-oxabicyclo[2.2.1]hept-5-ene-2,3-dicarboxy anhydride (A).
- 2) *exo,exo*-5,6-bis(hydroxymethyl)-7-oxabicyclo[2.2.1]hept-2-ene (A).
- 3) *exo,exo*-5,6-bis(methoxymethyl)-7-oxabicyclo[2.2.1]hept-2-ene (A).
- 4) *exo,exo*-7-oxabicyclo[2.2.1]hept-5-ene-2,3-bis(carboxylic acid) (A).
- 5) *exo,exo*-7-oxabicyclo[2.2.1]hept-5-ene-2,3-bis(carboxymethyl ester) (A).
- 6) *exo*-bicyclo[2.2.1]hept-5-ene-2,3-dicarboxy anhydride (A).
- 7) *exo,exo*-bicyclo[2.2.1]hept-5-ene-2,3-bis(carboxylic acid) (A).
- 8) poly(2,5-(3,4-bis(carboxymethyl)furanylene)vinylene) (B).
- 9) poly(2,5-(3,4-bis(carboxylic acid)pentylene)vinylene) (A).











**APPENDIX C:  
MASS SPECTRA**

The mass spectra of monomers obtained during this work are recorded below.

Ions are tabulated in the form:

113 (15%,  $C_5H_5O_3$ , B-MeOH)

In this example the ion has mass 113, its intensity is 15% of the base peak (B), and its origin is the loss of MeOH from the base peak. The monomer is denoted by M, and therefore the molecular ion is either  $MNH_4^+$  or  $MH^+$ . Peaks of intensity below 3% of the base peak intensity are not recorded, except for the molecular ion.

(1) exo-7-oxabicyclo[2.2.1]hept-5-ene-2,3-dicarboxy anhydride(I). (M =  $C_8H_6O_4$ )

184 (1%,  $C_8H_{10}NO_4$ ,  $MNH_4^+$ ) : 68 (100%,  $C_4H_4O$ , B)

(2) exo,exo-5,6-bis(hydroxymethyl)-7-oxabicyclo[2.2.1] hept-2-ene(II). (M =  $C_8H_{12}O_3$ )

174 (19%,  $C_8H_{16}NO_3$ ,  $MNH_4^+$ ) : 157 (84%,  $C_8H_{13}O_3$ ,  $MH^+$ )

139 (27%,  $C_8H_{11}O_2$ ,  $MH^+ - H_2O$ ) : 121 (25%,  $C_8H_9O$ ,  $139 - H_2O$ )

108 (41%,  $C_7H_8O$ ,  $139 - MeO$ ) : 91 (59%,  $C_7H_7$ ,  $121 - CH_2=O$ )

68 (100%,  $C_4H_4O$ , B)

(3) exo,exo-5,6-bis(methoxymethyl)-7-oxabicyclo[2.2.1]

hept-2-ene(III). (M =  $C_{10}H_{16}O_3$ )

202 (2%,  $C_{10}H_{20}NO_3$ ,  $MNH_4^+$ ) : 117 (100%,  $C_6H_{13}O_2^+$ , B)

85 (58%,  $C_5H_9O$ , B-MeOH) : 84 (22%,  $C_5H_8O$ , B-Me- $H_2O$ )

71 (10%,  $C_4H_7O$ , B- $Me_2O$ ) : 68 100%,  $C_4H_4O$ , B)

(4) exo,exo-7-oxabicyclo[2.2.1]hept-5-ene-2,3-bis

(carboxylic acid) (IV). (M = C<sub>8</sub>H<sub>8</sub>O<sub>5</sub>)

202 (2%, C<sub>8</sub>H<sub>12</sub>NO<sub>5</sub>, MNH<sub>4</sub><sup>+</sup>) : 134 (100%, C<sub>4</sub>H<sub>4</sub>O<sub>4</sub>+NH<sub>4</sub><sup>+</sup>, B)

(5) exo,exo-7-oxabicyclo[2.2.1]hept-5-ene-2,3-bis

(carboxymethylester) (V). (M = C<sub>10</sub>H<sub>12</sub>O<sub>5</sub>)

230 (1%, C<sub>8</sub>H<sub>16</sub>NO<sub>5</sub>, MNH<sub>4</sub><sup>+</sup>) : 145 (100%, C<sub>6</sub>H<sub>9</sub>O<sub>4</sub>, B)

130 (9%, C<sub>5</sub>H<sub>6</sub>O<sub>4</sub>, B-CH<sub>3</sub>) : 113 (18%, C<sub>5</sub>H<sub>6</sub>O<sub>3</sub>, B-MeOH)

68 (6%, C<sub>4</sub>H<sub>4</sub>O, M-B)

(6) exo-bicyclo[2.2.1]hept-5-ene-2,3-dicarboxy

anhydride (VI). (M = C<sub>9</sub>H<sub>8</sub>O<sub>3</sub>)

182 (100%, MNH<sub>4</sub><sup>+</sup>, B) : 120 (18%, C<sub>8</sub>H<sub>8</sub>O, M-CO<sub>2</sub>)

91 (39%, C<sub>7</sub>H<sub>7</sub>, MH<sup>+</sup>-CO<sub>2</sub>-H<sub>2</sub>O) : 66 (10%, C<sub>5</sub>H<sub>6</sub>, M-C<sub>4</sub>H<sub>2</sub>O<sub>3</sub>)

(7) exo,exo-bicyclo[2.2.1]hept-5-ene-2,3-bis

(carboxylic acid)(VII). (M = C<sub>9</sub>H<sub>10</sub>O<sub>4</sub>·H<sub>2</sub>O)

200 (100%, MNH<sub>4</sub><sup>+</sup>-H<sub>2</sub>O) : 91 (52%, C<sub>7</sub>H<sub>7</sub>, MH<sup>+</sup>-2CO-2H<sub>2</sub>O)

**APPENDIX D**  
**ELEMENTAL ANALYSIS**

## CHAPTER 3:

**PIII** (Ru) Found C,65.0%, H,8.7%; calculated for  $(C_{10}H_{16}O_3)_n$ : C,65.2%, H,8.7%

**PIII** (Os) Found C,63.8%, H,8.9%; calculated for  $(C_{10}H_{16}O_3)_n$ : C,65.2%, H,8.7%

**PIII** (Ir) Found C,64.9%, H,8.9%; calculated for  $(C_{10}H_{16}O_3)_n$ : C,65.2%, H,8.7%

**PIVb** (Ru) Found C,42.0%, H,2.4%, Na,19.7; calculated for  $(C_8H_6O_5Na_2)_n$ :  
C,42.1%, H,2.6%, Na,20.1%

**PIVb** (Os) Found C,41.8%, H,2.5%, Na,19.5; calculated for  $(C_8H_6O_5Na_2)_n$ :  
C,42.1%, H,2.6%, Na,20.1%

## CHAPTER 4:

**PIII** with **VIII** as CTA; (calculated for  $(C_{10}H_{16}O_3)_n$ : C,65.2%, H,8.7%)

Found C,65.1%, H,8.6%; Mn = 150K

Found C,62.0%, H,8.8%; Mn = 8K

Found C,60.3%, H,8.9%; Mn = 4K

Found C,59.1%, H,8.9%; Mn = 500

**PIII** with **IX** as CTA; (calculated for  $(C_{10}H_{16}O_3)_n$ : C,65.2%, H,8.7%)

Found C,65.1%, H,8.6%; Mn = 150K

Found C,64.9%, H,8.9%; Mn = 19K

Found C,64.5%, H,9.4%; Mn = 7K

Found C,63.8%, H,9.6%; Mn = 4K

**PIVb** with **VIII** as CTA; (calculated for  $(C_8H_6O_5Na_2)_n$ : C,42.1%, H,2.6%,  
Na,20.1%)

Found C,42.0%, H,2.4%, Na,19.7%; Mn = 100K

Found C,42.5%, H,2.9%, Na,19.4%; Mn = 4K

Found C,43.0%, H,3.4%, Na,17.2%; Mn = 700



**PIVb** with **X** as CTA; (calculated for  $(C_8H_6O_5Na_2)_n$ : C,42.1%, H,2.6%, Na,20.1%)

Found C,42.0%, H,2.4%, Na,19.7%; Mn = 100K

Found C,42.3%, H,2.7%, Na,19.9%; Mn = 10K

Found C,42.4%, H,2.8%, Na,19.7%; Mn = 5K

**PIVb** with **XI** as CTA; (calculated for  $(C_8H_6O_5Na_2)_n$ : C,42.1%, H,2.6%, Na,20.1%)

ALL polymers had Mn =100K

Found C,42.0%, H,2.4%, Na,19.7%; Mn = 100K

APPENDIX E  
LECTURES/ CONFERENCES

The author has attended the following conferences during the course of his Post-Graduate study:

- 1) One Day NMR conference, University of York, 2/12/87
- 2) Macro Group Annual Meeting, University of Lancaster, 16/3/88
- 3) Macro Group Annual Meeting, University of Lancaster, 15/3/89
- 4) First International Conference on Molecular Characterisation of polymers,  
University of Bradford, 20-23/3/89
- 5) Industrial Water Soluble and Water Swellable Polymers, UMIST, 17-19/4/90
- 6) High Polymer Research Group, 29<sup>th</sup> Moretonhampstead conference, 24-28/4/89
- 7) 8<sup>th</sup> International Symposium on Olefin Metathesis, University of Bayreuth,  
4-8/9/89

Lectures given in the chemistry department by external Speakers during the course of the author's Post-Graduate study:

UNIVERSITY OF DURHAM

Board of Studies in Chemistry

COLLOQUIA, LECTURES AND SEMINARS GIVEN BY INVITED SPEAKERS  
1ST AUGUST 1987 to 31st JULY 1988

<u>BIRCHALL</u> , Prof. D. (I.C.I. Advanced Materials) Environmental Chemistry of Aluminium	25th April 1988
<u>BORER</u> , Dr. K. (University of Durham Industrial Research Labs.) The Brighton Bomb - A Forensic Science View	18th February 1988
<u>BOSSONS</u> , L. (Durham Chemistry Teachers' Centre) GCSE Practical Assessment	16th March 1988
<u>BUTLER</u> , Dr. A.R. (University of St. Andrews) Chinese Alchemy	5th November 1987
<u>CAIRNS-SMITH</u> , Dr. A. (Glasgow University) Clay Minerals and the Origin of Life	28th January 1988
<u>DAVIDSON</u> , Dr. J. (Herriot-Watt University) Metal Promoted Oligomerisation Reactions of Alkynes	November 1987
<u>GRADUATE CHEMISTS</u> (Northeast Polytechnics and Universities) R.S.C. Graduate Symposium	19th April 1988
<u>GRAHAM</u> , Prof. W.A.G. (University of Alberta, Canada) Rhodium and Iridium Complexes in the Activation of Carbon-Hydrogen Bonds	3rd March 1988
<u>GRAY</u> , Prof. G.W. (University of Hull) Liquid Crystals and their Applications	22nd October 1987
<u>HARTSHORN</u> , Prof. M.P. (University of Canterbury, New Zealand) Aspects of Ipsso-Nitration	7th April 1988
<u>HOWARD</u> , Dr. J. (I.C.I. Wilton) Chemistry of Non-Equilibrium Processes	3rd December 1987
<u>JONES</u> , Dr. M.E. (Durham Chemistry Teachers' Centre) GCSE Chemistry Post-mortem	29th June 1988
<u>JONES</u> , Dr. M.E. (Durham Chemistry Teachers' Centre) GCE Chemistry A Level Post-mortem	6th July 1988
<u>KOCH</u> , Prof. H.F. (Ithaca College, U.S.A.) Does the E2 Mechanism Occur in Solution?	7th March 1988
<u>LACEY</u> , Mr. (Durham Chemistry Teachers' Centre) Double Award Science	9th February 1988

<u>OLAH</u> , Prof. G.A. (University of Southern California) New Aspects of Hydrocarbon Chemistry)	29th June, 1988
<u>PALMER</u> , Dr. F. (University of Nottingham) Luminescence (Demonstration Lecture)	21st January 1988
<u>PINES</u> , Prof. A. (University of California, Berkeley, U.S.A.) Some Magnetic Moments	28th April 1988
<u>RICHARDSON</u> , Dr. R. (University of Bristol) X-Ray Diffraction from Spread Monolayers	27th April 1988
<u>ROBERTS</u> , Mrs. E. (SATRO Officer for Sunderland) Talk - Durham Chemistry Teachers' Centre - "Links Between Industry and Schools"	13th April 1988
<u>ROBINSON</u> , Dr. J.A. (University of Southampton) Aspects of Antibiotic Biosynthesis	27th April 1988
<u>ROSE</u> van Mrs. S. (Geological Museum) Chemistry of Volcanoes	29th October 1987
<u>SAMMES</u> , Prof. P.G. (Smith, Kline and French) Chemical Aspects of Drug Development	19th December 1987
<u>SEEBACH</u> , Prof. D. (E.T.H. Zurich) From Synthetic Methods to Mechanistic Insight	12th November 1987
<u>SODEAU</u> , Dr. J. (University of East Anglia) Durham Chemistry Teachers' Centre Lecture: "Spray Cans, Smog and Society"	11th May 1988
<u>SWART</u> , Mr. R.M. (I.C.I.) The Interaction of Chemicals with Lipid Bilayers	16th December 1987
<u>TURNER</u> , Prof. J.J. (University of Nottingham) Catching Organometallic Intermediates	11th February 1988
<u>UNDERHILL</u> , Prof. A. (University of Bangor) Molecular Electronics	<del>25th February 1988</del>
<u>WILLIAMS</u> , Dr. D.H. (University of Cambridge) Molecular Recognition	26th November 1987
<u>WINTER</u> , Dr. M.J. (University of Sheffield) Pyrotechnics (Demonstration Lecture)	15th October 1987

UNIVERSITY OF DURHAM

Board of Studies in Chemistry

COLLOQUIA, LECTURES AND SEMINARS GIVEN BY INVITED SPEAKERS  
1ST AUGUST 1988 to 31st JULY 1989

- ASHMAN, Mr. A. (Durham Chemistry Teachers' Centre) 3rd May, 1989  
The Chemical Aspects of the National Curriculum
- AVEYARD, Dr. R. (University of Hull) 15th March, 1989  
Surfactants at your Surface
- AYLETT, Prof. B.J. (Queen Mary College, London) 16th February, 1989  
Silicon-Based Chips:- The Chemist's Contribution
- BALDWIN, Prof. J.E. (Oxford University) 9th February, 1989  
Recent Advances in the Bioorganic Chemistry of Penicillin Biosynthesis
- BALDWIN & WALKER, Drs. R.R. & R.W. (Hull University) 24th November, 1988  
Combustion: Some Burning Problems
- BOLLEN, Mr. F. (Durham Chemistry Teachers' Centre) 18th October, 1988  
Lecture about the use of SATIS in the classroom
- BUTLER, Dr. A.R. (St. Andrews University) 15th February, 1989  
Cancer in Linxiam: The Chemical Dimension
- CADOGAN, Prof. J.I.G. (British Petroleum) 10th November, 1988  
From Pure Science to Profit
- CASEY, Dr. M. (University of Salford) 20th April, 1989  
Sulphoxides in Stereoselective Synthesis
- CRESSEY & WATERS, Mr. D. & T. (Durham Chemistry Teachers' Centre) 1st February, 1989  
GCSE Chemistry 1988: "A Coroner's Report"
- CRICH, Dr. D. (University College London) 27th April, 1989  
Some Novel Uses of Free Radicals in Organic Synthesis
- DINGWALL, Dr. J. (Ciba Geigy) 18th October, 1988  
Phosphorus-containing Amino Acids: Biologically Active Natural and Unnatural Products
- ERRINGTON, Dr. R.J. (University of Newcastle-upon-Tyne) 1st March, 1989  
Polymetalate Assembly in Organic Solvents
- FREY, Dr. J. (Southampton University) 11th May, 1989  
Spectroscopy of the Reaction Path: Photodissociation Raman Spectra of NOCl
- GRADUATE CHEMISTS, (Polytechs and Universities in North East England) 12th April, 1989  
R.S.C. Symposium for presentation of papers by postgraduate students

- HALL, Prof. L.D. (Addenbrooke's Hospital, Cambridge) 2nd February, 1989  
NMR - A Window to the Human Body
- HARDGROVE, Dr. G. (St. Olaf College, U.S.A.) December, 1988  
Polymers in the Physical Chemistry Laboratory
- HARWOOD, Dr. L. (Oxford University) 25th January, 1988  
Synthetic Approaches to Phorbols Via Intramolecular  
Furan Diels-Alder Reactions: Chemistry under Pressure
- JÄGER, Dr. C. (Friedrich-Schiller University GDR) 9th December, 1988  
NMR Investigations of Fast Ion Conductors of the  
NASICON Type
- JENNINGS, Prof. R.R. (Warwick University) 26th January, 1989  
Chemistry of the Masses
- JOHNSON, Dr. B.F.G. (Cambridge University) 23rd February, 1989  
The Binary Carbonyls
- JONES, Dr. M.E. (Durham Chemistry Teachers' Centre) 14th June, 1989  
Discussion Session on the National Curriculum
- JONES, Dr. M.E. (Durham Chemistry Teachers' Centre) 28th June, 1989  
GCSE and A Level Chemistry 1989
- LUDMAN, Dr. C.J. (Durham University) 18th October, 1988  
The Energetics of Explosives
- MACDOUGALL, Dr. G. (Edinburgh University) 22nd February, 1989  
Vibrational Spectroscopy of Model Catalytic Systems
- MARKO, Dr. I. (Sheffield University) 9th March, 1989  
Catalytic Asymmetric Osmylation of Olefins
- McLAUCHLAN, Dr. K.A. (University of Oxford) 16th November, 1988  
The Effect of Magnetic Fields on Chemical Reactions
- MOODY, Dr. C.J. (Imperial College) 17th May, 1989  
Reactive Intermediates in Heterocyclic Synthesis
- MORTIMER, Dr. C. (Durham Chemistry Teachers' Centre) 14th December, 1988  
The Hindenberg Disaster - an Excuse for Some Experiments
- NICHOLLS, Dr. D. (Durham Chemistry Teachers' Centre) 11th July, 1989  
Demo. "Liquid Air"
- PAETZOLD, Prof. P. (Aachen) 23rd May, 1989  
Iminoboranes  $\text{XB}\equiv\text{NR}$ : Inorganic Acetylenes?
- PAGE, Dr. P.C.B. (University of Liverpool) 3rd May, 1989  
Stereocontrol of Organic Reactions Using 1,3-dithiane-  
1-oxides

- POLA, Prof. J. (Czechoslovak Academy of Sciences) 15th June, 1989  
Carbon Dioxide Laser Induced Chemical Reactions -  
New Pathways in Gas-Phase Chemistry
- REES, Prof. C.W. (Imperial College London) 27th October, 1988  
Some Very Heterocyclic Compounds
- REVELL, Mr. P. (Durham Chemistry Teachers' Centre) 14th March, 1989  
Implementing Broad and Balanced Science 11-16
- SCHMUTZLER, Prof. R. (Technische Universitat Braunschweig) 6th October, 1988  
Fluorophosphines Revisited - New Contributions to an  
Old Theme
- SCHROCK, Prof. R.R. (M.I.T.) 13th February, 1989  
Recent Advances in Living Metathesis
- SINGH, Dr. G. (Teesside Polytechnic) 9th November, 1988  
Towards Third Generation Anti-Leukaemics
- SNAITH, Dr. R. (Cambridge University) 1st December, 1988  
Egyptian Mummies: What, Where, Why and How?
- STIBER, Dr. R. (Czechoslovak Academy of Sciences) 16th May, 1989  
Recent Developments in the Chemistry of Intermediate-  
Sited Carboranes
- VON RAGUE SCHLEYER, Prof. P. (Universitat Erlangen Nurnberg) 21st October, 1988  
The Fruitful Interplay Between Computational and  
Experimental Chemistry
- WELLS, Prof. P.B. (Hull University) 10th May, 1989  
Catalyst Characterisation and Activity



UNIVERSITY OF DURHAM

Board of Studies in Chemistry

COLLOQUIA, LECTURES AND SEMINARS GIVEN BY INVITED SPEAKERS  
1ST AUGUST 1989 TO 31ST JULY 1990

- ASHMAN, Mr. A. (Durham Chemistry Teachers' Centre) 11th October, 1989  
The National Curriculum - an update
- BADYAL, Dr. J.P.S. (Durham University) 1st November, 1989  
Breakthroughs in Heterogeneous Catalysis
- BECHER, Dr. J. (Odense University) 13th November, 1989  
Synthesis of New Macrocyclic Systems using  
Heterocyclic Building Blocks
- BERCAW, Prof. J.E. (California Institute of Technology) 10th November, 1989  
Synthetic and Mechanistic Approaches to  
Ziegler-natta Polymerization of Olefins
- BLEASDALE, Dr. C. (Newcastle University) 21st February, 1990  
The Mode of Action of some Anti-tumour Agents
- BOLLEN, Mr. F. (Formerly Science Advisor, Newcastle LEA) 27th March, 1990  
Whats's New in Satis, 16-19
- BOWMAN, Prof. J.M. (Emory University) 23rd March, 1990  
Fitting Experiment with Theory in Ar-OH
- BUTLER, Dr. A. (St. Andrews University) 7th December, 1989  
The Discovery of Penicillin: Facts and Fancies
- CAMPBELL, Mr. W.A. (Durham Chemistry Teachers' Centre) 12th September, 1989  
Industrial catalysis - some ideas for the  
National Curriculum
- CHADWICK, Dr. P. (Dept. of Physics, Durham University) 24th January, 1990  
Recent Theories of the Universe (with Reference  
to National Curriculum Attainment Target 16)
- CHEETHAM, Dr. A.K. (Oxford University) 8th March, 1990  
Chemistry of Zeolite Cages
- CLARK, Prof. D.T. (ICI Wilton) 22nd February, 1990  
Spatially Resolved Chemistry (using Natures's  
Paradigm in the Advanced Materials Arena)
- COLE-HAMILTON, Prof. D.J. (St. Andrews University) 29th November, 1989  
New Polymers from Homogeneous Catalysis

- CROMBIE, Prof. L. (Nottingham University) 15th February, 1990  
The Chemistry of Cannabis and Khat
- DYER, Dr. U. (Glaxo) 31st January, 1990  
Synthesis and Conformation of C-Glycosides
- FLORIANI, Prof. C. (University of Lausanne, Switzerland) 25th October, 1989  
Molecular Aggregates - A Bridge between homogeneous and Heterogeneous Systems
- GERMAN, Prof. L.S. (USSR Academy of Sciences - Moscow) 9th July, 1990  
New Syntheses in Fluoroaliphatic Chemistry: Recent Advances in the Chemistry of Fluorinated Oxiranes
- GRAHAM, Dr. D. (B.P. Reserch Centre) 4th December, 1989  
How Proteins Absorb to Interfaces
- GREENWOOD, Prof. N.N. (University of Leeds) 9th November, 1989  
Novel Cluster Geometries in Metalloborane Chemistry
- HOLLOWAY, Prof. J.H. (University of Leicester) 1st February, 1990  
Noble Gas Chemistry
- HUGHES, Dr. M.N. (King's College, London) 30th November, 1989  
A Bug's Eye View of the Periodic Table
- HUISGEN, Prof. R. (Universität München) 15th December, 1989  
Recent Mechanistic Studies of [2+2] Additions
- IDDON, Dr. B. (Univeristy of Salford) 15th December, 1989  
Schools' Christmas Lecture - The Magic of Chemistry
- JONES, Dr. M.E. (Durham Chemistry Teachers' Centre) 3rd July, 1990  
The Chemistry A Level 1990
- JONES, Dr. M.E. (Durham Chemistry Teachers' Centre) 21st November 1989  
GCSE and Dual Award Science as a starting point for A level Chemistry - how suitable are they?
- JOHNSON, Dr. G.A.L. (Durham Chemistry Teachers' Centre) 8th February, 1990  
Some aspects of local Geology in the National Science Curriculum (attainment target 9)
- KLINOWSKI, Dr. J. (Cambridge University) 13th December 1989  
Solid State NMR Studies of Zeolite Catalysts
- LANCASTER, Rev. R. (Kimbolton Fireworks) 8th February, 1990  
Fireworks - Principles and Practice
- LUNAZZI, Prof. L. (University of Bologna) 12th February, 1990  
Application of Dynamic NMR to the Study of Conformational Enantiomerism
- PALMER, Dr. F. (Nottingham University) 17th October, 1989  
Thunder and Lightning

- PARKER, Dr. D. (Durham University) 16th November, 1989  
Macrocycles, Drugs and Rock 'n' roll
- PERUTZ, Dr. R.N. (York University) 24th January, 1990  
Plotting the Course of C-H Activations with  
Organometallics
- PLATONOV, Prof. V.E. (USSR Academy of Sciences - 9th July, 1990  
Novosibirsk)  
Polyfluoroindanes: Synthesis and Transformation
- POWELL, Dr. R.L. (ICI) 6th December, 1989  
The Development of CFC Replacements
- POWIS, Dr. I. (Nottingham University) 21st March, 1990  
Spinning off in a huff: Photodissociation of  
Methyl Iodide
- RICHARDS, Mr. C. (Health and Safety Executive, 28th February, 1990  
Newcastle)  
Safety in School Science Laboratories and COSHH
- ROZHKOVA, Prof. I.N. (USSR Academy of Sciences - 9th July, 1990  
Moscow)  
Reactivity of Perfluoroalkyl Bromides
- STODDART, Dr. J.F. (Sheffield University) 1st March, 1990  
Molecular Lego
- SUTTON, Prof. D. (Simon Fraser University, 14th February, 1990  
Vancouver B.C.)  
Synthesis and Applications of Dinitrogen and Diazo  
Compounds of Rhenium and Iridium
- THOMAS, Dr. R.K. (Oxford University) 28th February, 1990  
Neutron Reflectometry from Surfaces
- THOMPSON, Dr. D.P. (Newcastle University) 7th February, 1990  
The role of Nitrogen in Extending Silicate  
Crystal Chemistry

